

27869

NORGES GEOLOGISKE UNDERSØKELSE NR. 219

GRANITE STUDIES: II.
THE PRECAMBRIAN FLÅ GRANITE,
A GEOLOGICAL AND
GEOPHYSICAL INVESTIGATION

By

SCOTT B. SMITHSON

OSLO 1963

UNIVERSITETSFORLAGET



63
798

55(481)

*Editor for
the Publications of the Geological Survey of Norway:*

*Fredrik Hagemann
State Geologist*

Table of Contents

Abstract	5
Introduction	7
General Statement	7
Location and Accessibility	7
Physiography	9
Exposures	9
Purpose and Method of Approach	9
Geologic Setting	10
Acknowledgements	11
Previous Investigations	11
Petrography	12
Introduction	12
Gneiss	15
Granite	36
Inclusions	50
Pegmatites	57
Eocambrian and Cambro-Silurian Rocks	61
Permian Dikes	61
Tectonics	62
Regional Tectonics	62
Granite Tectonics	78
Deformation Associated with the Granite Emplacement	85
Regional Synthesis and Conclusions	91
Contact Relations	96
General Statement	96
Hedal Granite	96
Adal Granite	106
The Origin of the Contact Features	111
Gravimetry	112
General Statement	112
Density Determinations	112
The Bouguer Anomaly Map	113
The Regional and Residual Anomaly Maps	114
Interpretation	115
The Feldspars	123
General Statement	123
Interpretation of Textural Features	123
Composition of the Feldspars	130
The Symmetry Relations of K-feldspar	136

Metamorphism and Metasomatism	152
Metamorphic Facies	152
Metasomatism	154
Origin of the Metamorphosed Rocks	156
Petrogenesis	157
Introduction	157
Comparison of Magmatic and Metasomatic Hypotheses with the Field Evidence	158
The Magmatic Hypothesis	167
The Metasomatic Hypothesis	172
Conclusions	174
Age of the Flå Granite and Comparison with Other Southern Norwegian Granites	177
General remarks	177
Sammendrag	180
Appendix	183
References	207

Abstract.

The Flå granite is composed of two adjacent elliptical granite bodies, the larger northern Hedal granite and the Adal granite. The granites are surrounded by banded granodioritic gneisses. Migmatites and augen gneisses are common just outside the granite contacts. Banded quartz-monzonitic gneisses are found on the east side. Telemark supracrustal rocks composed of inter-layered quartzites and amphibolites are found on the west side and banded quartz-dioritic gneisses are found on the north side of the area. The varieties of the granite are limited to porphyric granite, which comprises most of the outcrops, and to fine-grained granite which comprises the center of the Hedal granite. The porphyric granite appears to be younger than the fine-grained granite; K-feldspar megacrysts in the porphyric granite are probably porphyroblasts. The composition of the granite falls within the range of quartz monzonites and corresponds fairly closely to the minimum-melting composition in the granite system.

Foliation, linear structures, and β axes in the gneiss generally strike between north and northwest. The plunge of linear fabric elements ranges from low to moderate; the overall symmetry of the megascopic fabric is triclinic. Steeply plunging β axes near the granites are attributed to deformation that accompanied the granite emplacement. Foliation is commonly found in the granite and parallels the granite contacts; lineation in the granite is observed sparingly. Granite that exhibits oriented structures is always sheared. This shearing represents late diapiric movements in a predominantly solid granite. The shape and position of the granites is largely determined by the regional structural geometry, which has, in turn, been locally deformed by the granite emplacement. The granites are generally concordant, conformable late-kinematic plutons that show some features of synkinematic plutons.

The contacts of the granite are marked by a gradation from granite enclosing numerous fragments of gneiss to gneiss transected by numerous granitic dikes and sills. The fragments of gneiss are not displaced in some places and are definitely rotated in others; the border zone is a large scale agmatite.

Gravity measurements reveal residual Bouguer anomalies of 4 to 6 mgal over the granites; these anomalies correspond to thickness of 1.7 to 2.5 km. A -6-mgal anomaly southeast of the Adal granite occurs over a zone of granitized gneiss and is interpreted to be a buried 2.5-km-thick extension of the Adal granite. The maximum thickness of the granites is postulated to be about 2.5 km.

Antiperthite, which is common in augen gneisses, is interpreted as a replacement phenomenon. Oriented plagioclase grains in K-feldspar megacrysts occur in inclusions as well as in granite; this development probably indicates

porphyroblastic growth of the K-feldspar. The composition of plagioclase and K-feldspar from the granite shows a moderate range within a single hand specimen; therefore, feldspar thermometry cannot be applied to this granite. An investigation of K-feldspar obliquities shows that K-feldspars from the granite, gneiss, and pegmatites are near maximum microcline while those from augen gneisses, migmatites, inclusions, and the granite contact exhibit low and/or variable obliquity are associated with rocks undergoing a recrystallization or a chemical change; K-feldspar in these latter rocks has probably formed metastably as orthoclase and has been "frozen" at different stages in the orthoclase-microcline inversion.

The gneisses are in the middle part of the amphibolite facies. The mineral assemblages of the granite are the same as those of the granitic gneisses.

The petrogenesis of the granite is considered in terms of anatectic and metasomatic hypotheses. The behavior of inclusions indicates that considerable volume-for-volume replacement has taken place. This observation coupled with the metamorphic (or endometamorphic) texture of the granite leads to the conclusion that the minimum-melting composition of the granite is not definitive for an origin by fractional crystallization or fusion. Although both the anatectic and metasomatic hypotheses explain certain features of the granite and fail to explain others, the system must have been open irregardless of the main process; *i. e.*, metasomatism has been an active agent.

Introduction.

General Statement.

A problem as controversial and complicated as the origin of a granitic body cannot hope to be solved by the application of just one method of approach with the possible exception of detailed mapping. With this in mind, the writer has attempted to treat the Precambrian Flå granite in broader aspects by the application of structural, petrographic, feldspar, and geophysical studies in order to gain insight into its origin.

The name, Flå granite, actually designates two adjacent granite bodies, which are approximately elliptical in plan. The larger northern body will hereafter be called the Hedal granite, and the southern body will be called the Ådal granite. The term Flå granite will designate the two granites as a whole. The Hedal granite covers *ca.* 650 sq km, and the Ådal granite covers *ca.* 90 sq km.

Location and Accessibility.

The area studied is located between 60° 10' and 60° 50' N. Lat. and 0° 20' and 1° 40' Long. West of Oslo. The area is bounded on the east side by the valleys of Ådal and Begndal and bounded on the west side by the valley of Hallingdal. The southern boundary is Soknadalen and the northern boundary is a line between the towns of Gol and Bagn. The center of the area is *ca.* 90 km north-northwest of Oslo. Fig. 1 shows the location of the area studied.

The region immediately outside the granite outcrops is traversed by the two major roads, highways 20 and 60, that run through Hallingdal and Ådal-Begndal. Highway 60 crosses the "tail" of the Ådal granite whose contact is beautifully exposed in a roadcut just south of Sperillen. The county road to Hedalen passes over the eastern border of the Hedal granite and continues to the center of the granite. The

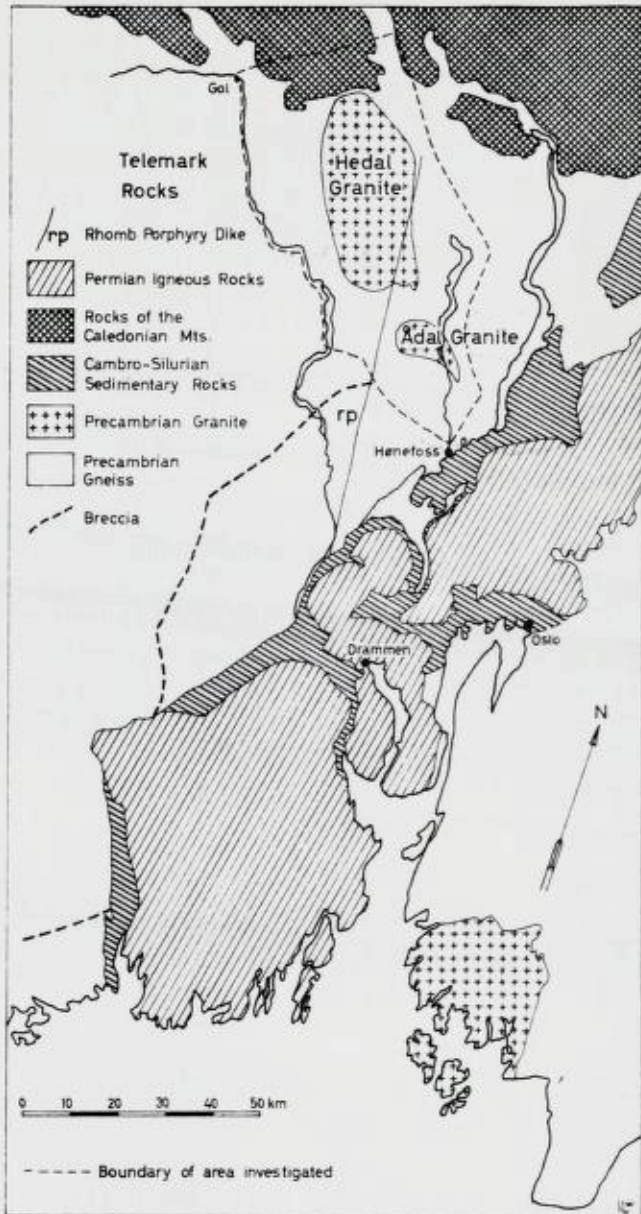


Fig. 1. Map showing the general geology around the Flå granite. The area studied is outlined by the broken line. Adapted from Holtedahl and Dons, 1953.

Kart som viser alminnelig geologi rundt Flå-granitten. Det undersøkte område er vist med stiplet linje.

majority of the area would be accessible only on foot if it were not for the numerous private logging and access roads that have been built recently and that continue to be built. Since only the older of these roads appear on the topographic maps, local inquiry is recommended before proceeding to any particular district.

Physiography.

Most of the area is represented by a rolling upland surface. This surface is the pre-Cambrian peneplane, which is dissected by steep-walled, ice-carved valleys. The major roads follow these subparallel valleys which are undoubtedly subsequent valleys following tectonic lines of weakness. The highest parts of the area which lie at 1000 to 1200 m are underlain by granite. Since the two major valleys are at *ca.* 150 m, the maximum relief which occurs in Hallingdal is about 850 m. More commonly the relief is in the order of 300—500 m from the valley bottom to the top of the valley wall. The average elevation of a smaller district is conditioned by the underlying rock type. The ascent from the valley floor to the 1000-m level occurs in two steps, the first from the valley to about 600 m in the gneiss and the second from the gneiss to about 1100 m in the granite. The high mountain tops are found in the granite and in the quartzites, which are located to the north and west of the granite.

Exposures.

The rock exposure in the areas studied varies considerably. Much of the upland area has been swept clean by the Pleistocene glaciers so that exposures here may be fairly good. The northern end of the Heddal granite, however, which is largely covered by glacial drift at an elevation of about 900 m, provides an exception to the rule. The valleys are filled with alluvium; however, good exposures may be found even in the valleys, particularly in roadcuts. The worst exposures are generally in the valley slopes, which are almost completely covered with glacial drift and thick forests.

Purpose and Method of Approach.

The purpose of this investigation is to determine the mode of emplacement and the genesis of these two Precambrian granites. Since

no single discipline provides adequate information to properly discuss the origin and emplacement of a granite, a number of methods which complement each other was applied.

The petrography of the rocks is described and textural interpretations are attempted with the realization that textural interpretations are inherently ambiguous. Enough modal and chemical analyses were undertaken to indicate the general composition of the granite, but they have not been stressed because recent opinion (Whitten, 1961) indicates that a tremendous number of analyses are required to adequately describe the mean composition and the variability of so large a granite. Accordingly, more emphasis was placed on structural and geophysical studies as being the most rewarding.

Mapping of the granite and the surrounding gneiss was undertaken to describe the field relationships and geometry of the granite and its surroundings gneisses. The geometry of the gneissic country rocks removed from the granite is particularly important in order to describe the changes brought about by the emplacement of the granite. A total of 203 days were spent on the field work during the summers of 1959, 1960, 1961 and 1962.

Because the evolution of the granite is locked up within the feldspars, they were analyzed for both composition and obliquity. Correlations are proposed among the texture, composition, and obliquity of the alkali feldspar.

A gravity survey was undertaken in order to reveal the shape and thickness of the granite bodies. Since the discussion of a granite only on the basis of its surface outcrop represents considerable speculation, a gravity survey complements the structural studies and furnishes the necessary 3-dimensional picture. The present study provides a striking example of the dangers in interpreting the form of a granite from surface information only. A total of 36 days was spent on the gravity survey in the summers of 1960 and 1961.

Geologic Setting.

The broad geologic relationships can be seen in Fig. 1. The Flå granite is part of the southern Norwegian Precambrian shield. The Flå granite is composed of two spatially related granite bodies, the Hedal granite and the Ådal granite. These granites are surrounded on the north, south, and west by Precambrian gneisses and schists whose

derivation is uncertain. A few kilometers west of the Hedal granite, lie the Telemark supracrustal rocks, interlayered quartzites and amphibolites. The probable northern border of the Hedal granite coincides with the Caledonian thrust front. The Hedal granite is cut by a rhomb porphyry dike from the Oslo igneous province.

Acknowledgements.

The writer is greatly indebted to Professor Tom. F. W. Barth for critically discussing the project and reading the manuscript. Dr. H. Björlykke of the Geological Survey of Norway granted the writer field expenses and offered to publish this manuscript. Professor T. Strand, Professor I. Th. Rosenqvist, Dr. F. Dickson, Dr. F. M. Vokes, Conservator J. A. Dons, and Mr. I. Bryhni receive thanks for reading parts of the manuscript and offering criticism. The writer thanks Dr. H. Neumann for placing the facilities of the Geological Museum at the writer's disposal, for providing field expenses and the rental of a gravity meter for the gravity survey, and for critically reading part of the manuscript.

The gravity survey would not have been possible without the excellent cooperation of Messrs. O. Trovaag and G. Jelstrup of the Geodetic Division and Mr. G. Hagene of the Topographic Division of the Geographical Survey of Norway. Messrs. T. Nordby and A. Grønhaug were of invaluable help with the gravity measurements.

Mr. S. Bergstöl, Mrs. J. Morton, and Mrs. H. Ugland receive thanks for the many samples that they X-rayed for the writer. Miss I. Lowzow is thanked for all the drafting and Miss B. Mauritz is thanked for the photography. Mr. and Mrs. Ola Elsrud in Hedalen and Mr. and Mrs. P. P. Hagen in Gol receive sincere thanks for their hospitality during field work. The study was performed with financial support from a Postgraduate Fellowship of the U.S. National Science Foundation.

Previous Investigations.

The Flå granite was first mapped as the Sperillen granite by H. Mohns, who mapped the Ådal granite along the lake Sperillen in 1859 and noted the swarms of granite dikes that surround the contacts of the granite. Kjerulf (1879) mentioned the Sperillen granite, printed Mohns' field sketches, and later gave a petrographic description of the

Sperillen (Ådal) granite. Holtedahl and Schetelig (1923) mapped the eastern tail of the Ådal granite. Andersen (1921), who had undertaken a geological reconnaissance of the area, mentioned a "huge eruptive breccia" that surrounds the Flå granite. The northern part of the Heddal granite was mapped by Strand (1954) as part of his investigation of the Aurdal map sheet. Strand reported a similar breccia zone around the northern borders of the granite. A. Bugge (1928) mentions the Flå (Ådal) granite in connection with the northern extension of a fault zone, the "great friction breccia". He postulated that the granite was emplaced in a period between the recurrent movements along the fault zone because the fault zone was less conspicuous within the granite.

Strand (1943) has subdivided the Precambrian surrounding the Heddal granite in the Aurdal quadrangle into two general types, quartz-dioritic gneiss and granodioritic gneiss. These two general units can be distinguished further south, also; however, in detail the units are much more variable.

Probably more has been written regarding the Permian dikes than any other aspect of the area. Brögger (1933 a, 1933 b) has mentioned the essexite and rhomb-porphry dikes from Sperillen and Vidalen. Isachsen (1942) discussed the fractures and Permian dikes of the Begndal—Sperillen section of the area and the importance of these features to the development of landforms.

Petrography.

Introduction.

For the purpose of this study, the rocks of the Flå area can be subdivided into two broad groups, the granite and the gneisses that both surround the granite and occur as inclusions within it. Four general classes of rock are recognized for the petrographic descriptions; these include gneiss, granite, inclusions, and pegmatites.

Terminology.

Since the purpose of petrography is primarily to describe the occurrence and composition of rocks, the terminology should be de-

scriptive, not genetic. Unfortunately many useful and necessary terms possess a genetic as well as descriptive meaning, and the writer finds it necessary to employ many such words. The descriptive meaning only is intended.

Some common terms are taken mostly from Howell (1957) and Dietrich and Mehnert (1961); others are defined here for clarity as follows:

Inclusion. A rock fragment that is foreign to the rock body in which it occurs (used in place of both skialith and xenolith).

Granite. Is used in the conventional general sense to mean a phaneritic rock in which quartz and feldspar predominate. Granite is used in this general sense throughout the text with the understanding that the rock is a quartz monzonite for classification purposes.

Quartz-monzonitic gneiss, etc. Used in place of quartz-microcline-plagioclase biotite gneiss for the sake of brevity in the text. The term has only a descriptive meaning although the color index may be higher than for a normal plutonic quartz monzonite, etc.

Foliated Quartz Monzonite. A quartz monzonite that is foliated (commonly but not necessarily a border facies). The rock exhibits a megascopic granitic texture and is not layered.

Megacryst. A large crystal that occurs in a finer-grained ground-mass (used in place of phenocryst or porphyroblast when the origin is doubtful).

Porphyric. Adjective applied to a rock containing megacrysts.

Magma. The most difficult term to define acceptably is to mean rock-forming fluid although only a small part need be liquid (Shand, 1950 a).

Dike and sill. These words are applied to describe the geometric relations between a planar granitic body and the country rocks without genetic implications.

Modal Analyses.

Modal analyses by point counting have been carried out on the rocks rich in quartz and feldspar as a means of determining their chemical composition. Chayes (1956) and Heier (1961) have pointed out that, for granitic rocks, a modal analysis is almost as accurate as a chemical analysis and much more economical.

Errors in modal analyses are due to two factors, the counting error and the sampling error. Theoretical discussions of these errors

are found in Chayes (*op. cit.*) and Bayly (1960). If the mineral identification is assumed to be perfect, the counting error will be the expected result of the probability distribution of the points among the different minerals. As the number of points is increased this error diminishes rapidly. A sampling error occurs when the sample counted differs from the country rock, and the coarser grained rocks present a difficulty in obtaining a representative sample. Coarse-grained rocks and porphyritic rocks necessitate large count areas for the results to be quantitatively useful.

Rock slabs were utilized almost exclusively for the modal analyses in order to count large areas. K-feldspar in the slabs was stained yellow by the method of Bailey and Stevens (1960); quartz and plagioclase were easily distinguished by their etch so that a plagioclase stain was unnecessary. The slabs were counted on a mechanical stage under a binocular microscope, equipped with a cross hair. As suggested by Chayes (*op. cit.*), banded (and foliated) rocks were placed so that their foliation made an angle of 40° with the traverse direction.

Chayes (1956, p. 72) has designated the IC number (mineral identity changes) as a measure of the index of coarseness of a rock. The writer has followed the modification of Bayly (1960, p. 127) in which

$$IC = 1250/L$$

where L equals the count length in mm for 50 mineral identity changes. The count area necessary to maintain a given sampling precision is a function of the IC number (Chayes, 1956, p. 72; Bayly, 1960, p. 127).

In order to determine an estimate of the counting precision (counting standard deviation), the writer has counted 5 replications of a rock slab of fine-grained granite. The precision of the 5 replications (Table I) is better for each mineral than the expected theoretical precisions (calculated from Chayes, 1956, p. 39). This is rather common occurrence that probably results from a lack of complete independence for the replications.

The greatest problem encountered is the modal analysis of the porphyritic granite. Lafitte (1953) has noted that a large error may arise in a chemical analysis if porphyritic rocks are sampled. Bayly (1960, p. 127) gives tables that show the count area necessary for a given precision in granitic rocks. This table was followed by the writer to determine the count area of the porphyritic rocks. When necessary, several slabs were cut from the same rock in order to obtain a sufficiently large count area. The accuracy of the modal analyses of por-

Table 1.

Replications for modal analysis of fine-grained granite, Sp 595 c.

	Plagioclase %	Microcline %	Quartz %	Biotite %	Accessories %
Trial 1	31.3	33.6	31.1	3.6	0.4
Trial 2	30.9	31.4	32.5	4.6	0.5
Trial 3	29.1	32.7	34.0	3.6	0.5
Trial 4	28.8	34.8	32.1	3.6	0.7
Trial 5	28.4	34.4	32.5	4.4	0.4
Mean Value	29.7	33.4	32.4	4.0	0.5
Sample Standard Deviation, <i>s</i>	1.34	1.50	1.04	0.50	0.12
Theoretical Stan- dard Deviation, σ	1.93	1.99	1.97	0.83	0.30

for 560 counts over 14 cm², IC=35.

phyric granite may be obtained from the comparison of the modes and mesonorms (Barth, 1959) of the two chemically analyzed granites, which are both foliated rocks. The agreement is good for most minerals of the porphyric granites and just exceeds the expected precision; the mode of the fine-grained granite shows good agreement with the mesonorm.

Modal analyses of the rocks appear in Tables X—XIII in the Appendix. The expected precision for minerals of the granite whose proportions lie in the range from 20 to 40 per cent is ± 2.0 per cent.

Gneiss.

The Precambrian gneisses in the Flå area range all the way from amphibolites to quartz-monzonitic gneisses to orthoquartzites. For mapping, four types of gneiss are recognized:

1. The Telemark supracrustal rocks principally composed of alternating amphibolites and orthoquartzites.
2. Banded quartz-dioritic gneiss.
3. Banded granodioritic gneiss.
4. Banded quartz-monzonitic gneiss.

The geologic map (Plate 1) shows the areal extent of these rock types. In detail, the rocks are highly variable.

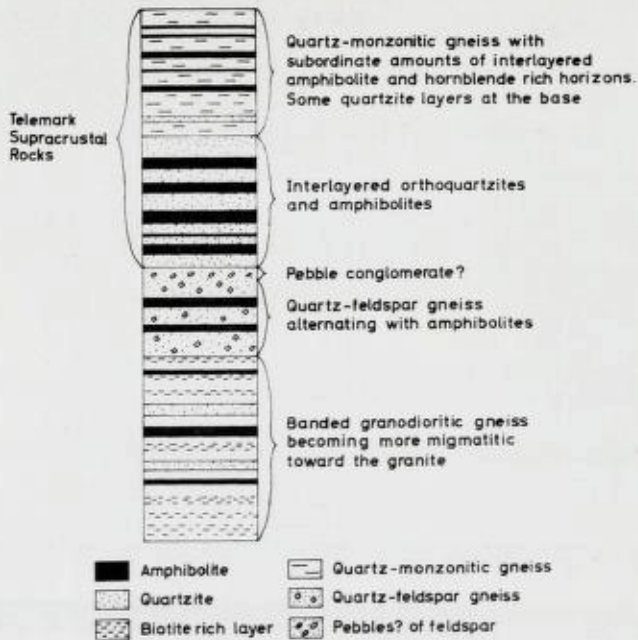


Fig. 2. Columnar section showing the stratigraphy proposed for the gneisses on the east side of Hallingdal.

Kolonneseksjon som viser den foreslåtte stratigrafi for gneis på østsidan av Hallingdal.

Telemark Supracrustal Gneisses.

The Telemark supracrustal series, whose base is placed at the lowest orthoquartzite, is represented by alternating amphibolites and orthoquartzites on the western side of the Flå area. Banded quartz-monzonitic gneiss overlies the interlayered amphibolites and orthoquartzites. This succession easily constitutes the most distinctive map unit in the area.

In central Telemark, the Telemark gneisses have been described and subdivided into the Rjukan, Seljord, and Bandak groups by Dons (1960). Dons tentatively equates the quartzites between Tinnsjö and Gol with the Seljord quartzite. In this case, the quartzites and amphibolites on the west side of the Flå area could be in the Seljord group.

The rocks along the east side of Hallingdal are tentatively divided into the following stratigraphic succession (Fig. 2) from youngest to oldest:

1. Banded quartz-monzonitic gneiss.
2. Interlayered orthoquartzites and amphibolites.
3. A transition zone of quartz-feldspar gneiss interlayered with amphibolites.
4. Banded granodioritic gneiss.

Although the contact of the Telemark rocks is placed at the base of the lowest orthoquartzite for mapping purposes, no unconformity has been found between the orthoquartzites and the underlying quartz-feldspar gneiss. Indeed, the quartz-rich nature of the underlying gneiss suggests a transition zone between the banded granodioritic gneiss and the interlayered orthoquartzites and amphibolites.

Tectonic, intrusive, and gradational contacts are described from southern Telemark between the Telemark supracrustal rocks and the underlying granitic gneisses (Dons, 1960). The transition between recognizable supracrustal rocks and the rather monotonous biotite gneisses, amphibolites, and migmatites that surround the Flå granite is gradational over a width of several kilometers.

The rocks of the area will be introduced in petrographic descriptions which follow. The salient features of the rocks are discussed after each petrographic description.

Quartzite (Sp 528 A)¹

The rock is found 5 km northeast of Nesbyen (36.8, 1-32.6)² where it forms layers of massive light gray quartzite from 2 to 20 m thick (Fig. 3) that

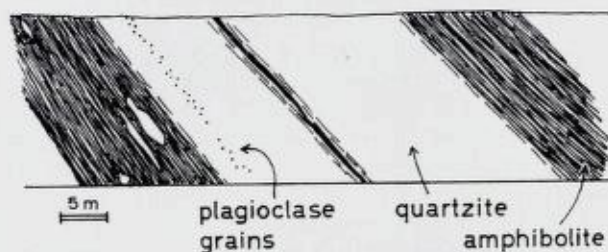


Fig. 3. *Interlayered Telemark orthoquartzites and amphibolites.*

Vekslende lag av Telemark ortokvartsit og amfibolit.

¹ Sp signifies specimen and the number 528A signifies the station number in the writer's field notes.

² The coordinates indicate the latitudes and longitudes of the locality; e.g., 36.8 means 60° 36.8' N. and 1-32.6 means 1° 32.6' W. of Oslo.

are interlayered with amphibolites (described in following section). The rock appears glassy in hand specimen. Oriented muscovite imparts a faint foliation to the rock. Quartz grains from 1-8 mm long are flattened along the foliation. Small (1 mm) white grains of feldspar are scattered along horizons in the rock. The rock is cut by closely spaced joints which are normal to the foliation. In thin section, the rock is chiefly composed of quartz. Muscovite, plagioclase, biotite, chlorite, zircon, and apatite occur in accessory amounts. The texture is homeoclastic. The rock is almost entirely quartz which occurs in grains 3—4 mm long. The quartz is strongly elongated along the foliation. Some of the smaller grains are unstrained but the large grains are always crushed almost to the point of disintegration into numerous smaller grains. Serrate edges are common. Most bubble trains in quartz are perpendicular to the foliation. Plagioclase (An_{65}) occurs in subhedral 0.3—0.9 mm grains with bent twins, and is only slightly sericitized. Muscovite occurs in ragged bent laths, but some muscovite is fresh appearing and transects the foliation. Altered biotite occurs in grains together with fresh chlorite and muscovite. Apatite occurs in equant euhedral grains and in laths. Zircon occurs in rounded to euhedral grains. One zircon grain appeared to have growth layers enclosing a rounded core. The rock mode appears in Table X.

Amphibolite (Sp 528B)

The rock occurs interlayered with the quartzite described previously (Fig. 3). The layers range from 30 cm to several tens of meters in thickness. Boudinage of the amphibolite is common. Oriented hornblende crystals 2—3 mm long produce a lineation in the amphibolite. At the margins of the layers, biotite is more abundant and the amphibolite is well foliated across a 10-cm zone. In thin section, the rock is chiefly composed of plagioclase, hornblende, and biotite. Opaque minerals (ilmenite), apatite, quartz, calcite, zircon, chlorite, and sphene occur in accessory amounts. The texture is nematoblastic. Plagioclase occurs in 1 mm grains and is heavily sericitized. Hornblende ($Z, Y = \text{green}, X = \text{pale greenish yellow}, Z \wedge c = 18^\circ$) occurs in 1—3 mm crystals with irregular outlines and may be twinned. Biotite ($Z, Y = \text{brown}, X = \text{tan}$) occurs in 1—2.5 mm laths and is commonly slightly chloritized along its cleavage. Quartz shows a weak undulatory extinction. Apatite and opaque minerals comprise most of the accessory minerals. Apatite occurs in euhedral to subhedral grains closely associated with opaque minerals. Zircon mostly occurs in subrounded grains, but some are euhedral. Sphene occurs in widely scattered oval grains. The rock mode appears in Table X.

The quartzite (Sp 528A) shows signs of strong shearing and recrystallization which probably recurred continuously. The bubble trains probably follow high-angle joints which have formed and subsequently healed. Muscovite and chlorite have replaced biotite and recrystallized syn- to postkinematically.

The mica-rich quartzites usually exhibit a smaller grain size than the orthoquartzites. Although this fact may be due to sedimentation, deformation has probably played an important role. Movement in the mica-rich quartzites could be largely accommodated by intergranular gliding. Movement in the orthoquartzites must be accommodated by intragranular translation and recrystallization which has caused a coarsening of the grain size.

Quartzites are remarkably restricted in their occurrence. Except for the Telemark orthoquartzites, only three occurrences of quartzite are found in the entire area. The most widespread occurrence is as thin, 10—30-cm layers in the banded granodioritic gneiss underlying the Telemark supracrustal rocks in Hallingdal. The other occurrences are in a thin layer in striped supracrustal gneisses (Strand, 1954) near Bagn and as a 40-cm-thick layer near Haugland on the west side of Adalselv. This rock type is certainly rare in these gneisses if its common occurrence in sedimentary rocks is considered.

In the amphibolites (Sp 528 B), differential movements have been stronger at the borders of the layers than throughout the entire unit. A greater proportion of the accessory minerals in the amphibolite seems to be rounded than in the quartzite. The amphibolites have very likely undergone less repeated crystallization than the quartzites during the deformation. This fact may account for the better rounded accessory minerals of possible sedimentary origin in the amphibolite.

The silica content of these two specimens has been calculated from the mode (Heier, 1961). The orthoquartzite contains 98 per cent silica; the amphibolite contains *ca.* 36 per cent silica.

Granitic gneiss (Sp 612B)

The rock is found 1.5 km E of Austvoll (25.8, 1-19.8) and occurs inter-layered with an arkosic conglomerate, which is described in the following paragraph. These rocks are intensely smallfolded so that the original geometrical relations may be obscured. The pink fine-grained dominantly granitic rock contains dark 4-mm layers that are rich in biotite and plagioclase. Quartz and K-feldspar, which are flattened to impart a foliation, are megascopically identifiable in the granitic part. In thin section, the granitic part is chiefly composed of microcline perthite and quartz. Plagioclase, muscovite, chlorite, sphene, apatite, and zircon occur in accessory amounts. The texture is granoblastic. The grain size ranges from 0.5 to 1 mm. Quartz is strongly elongated but shows only weak undulatory extinction. Microcline usually appears nonperthitic and exhibits grid twinning. Some scattered microcline grains contain patch perthite

and may have dusty alteration zones around the grain margin. Microcline is concentrated in 1-mm-wide zones next to the plagioclase-biotite layers. Plagioclase (An₁₀) occurs in widely scattered anhedral grains. Chlorite (pennine) occurs in ragged laths that may contain strips of biotite. Muscovite occurs in small laths that transect the foliation. Sphene occurs in subhedral crystals but may be rounded. Zircon occurs in sub-to well rounded grains. In thin section, the dark layers are chiefly composed of plagioclase and biotite; chlorite, sphene, zircon, and clinozoisite occur in accessory amounts. Plagioclase (An₃₀) is highly sericitized in contrast to plagioclase from the granitic part. Biotite (Z, Y = reddish brown, X = tan) is partially chloritized to pennine. Sphene is much more abundant than in the granitic part. Zircon is common as rounded grains. Biotite in the plagioclase-rich layer occurs almost in contact with chlorite in the granitic layer. The modes for both parts appear in Table X.

Meta-conglomerate (Sp 612 A)

The rock occurs in 20-cm-thick layers intercalated with the granitic gneiss described previously. Rounded grains of pink K-feldspar from 1 to 6 mm in diameter are subordinate to quartz in 2 to 3 mm grains. Although they are flattened somewhat, the K-feldspar grains appear to be clastic pebbles. Biotite-rich layers border on the arkosic conglomerate. In thin section, the rock is chiefly composed of quartz and microcline perthite. Plagioclase (An₀₇), muscovite, zircon, and clinozoisite occur in accessory amounts. The texture formed by rounded grains of microcline perthite in xenoblastic sutured quartz in blastosammitic. The microcline perthite grains are sub-to well rounded and fringed by a dusty marginal zone (Fig. 1, Plate 2). This dusty marginal zone follows the outline of the individual microcline crystals in composite grains and does not occur in plagioclase. The microcline contains plagioclase interpositions that form patch perthite and vein perthite, which are reminiscent of pegmatitic perthites. Some polysynthetic twinning is visible in the plagioclase veins of the perthite. Plagioclase occurs very rarely as discreet grains; more commonly it forms composite grains with microcline (Fig. 1, Plate 2) in which the plagioclase is subhedral and the microcline is rounded. Quartz occurs in 1—4 mm crystals that are flattened parallel to the foliation and may show highly undulatory extinction. Quartz comprises the major portion of the rock. Zircon, which usually occurs within feldspar grains, is sub-to euhedral.

The layers in the granitic gneiss (Sp 612 B) exhibit a sharp contrast in mineralogy; *i. e.*, plagioclase and biotite in the one layer and microcline and quartz in the other; moreover, the contact between the two layers sharply marks the boundary for the occurrence of biotite in the former and chlorite in the latter.

The meta-conglomerate shows some contradictory features. These are the subhedral plagioclase in composite grains with well rounded microcline and the dusty "alteration" zone around the edges of micro-

cline crystals. This dusty zone follows the individual mineral outlines in composite grains. The subhedral habit and lack of alteration of plagioclase may be due to recrystallization, but then the "relict sedimentary" features in the microcline become even more puzzling.

The rounded microcline grains should also be diagnostic, but incipient pegmatization and feldspathization in the quartzites indicates a certain mobility for K-feldspar, controlled by potential low pressure areas. A medium-grained quartzite in which no feldspar is megascopically visible becomes coarse grained and contains subrounded pink K-feldspar crystals within the 10 to 20 cm adjacent to a vertical joint. This K-feldspar was similar megascopically to the rounded microcline grains in the meta-conglomerate. The occurrence of composite feldspar grains together with the high percentage of quartz (Fig. 1, Plate 2) is the feature most indicative of a sedimentary origin for the meta-conglomerate.

The meta-conglomerate and the granite gneiss occur near the base of the Telemark rocks, an interlayered series of quartzites and amphibolites. Some feldspar-and biotite-rich layers are also intercalated, but the typical rock units are orthoquartzite and amphibolite, which is either quartz poor or quartz free. The sphene and the more common zircon may occur in fairly well rounded grains or may exhibit a euhedral habit. Rounded zircons are suggestive of a sedimentary origin (Poldervaart, 1955); however, quantitative data on their habit are required before worthwhile conclusions can be drawn. The high quartz content of all the rocks except the amphibolites is best evidence for a sedimentary origin. No sedimentary structures have been observed nor are they likely to be observed. These rocks are so strongly tectonized and recrystallized that all primary structures have probably been obliterated.

Banded Granodioritic Gneiss.

The base of the lowest quartzite marks the end of the well defined stratigraphy and of compositions highly indicative for a sedimentary origin. The underlying gneiss complex, composed of quartz-feldspar gneisses interlayered with amphibolites and banded granodioritic gneiss, lacks distinctive marker horizons. The transition from the Telemark quartzites into the banded granodioritic gneisses, however, is not perfectly abrupt because of the underlying quartz-feldspar gneiss which grades into the banded granodioritic gneiss.

These banded gneisses are largely composed of 5-to-50-cm-thick layers of granodioritic or quartz dioritic composition intercalated with amphibolites (Figs. 21 a and c) and are exposed south of Flå in Hallingdal. The amphibolite layers range from 5 cm to 5 m in thickness but are intensely boudinaged. A few 10-to-30-cm-wide quartzitic layers have been observed. This succession that has distinct and rapidly alternating banding passes into gneisses with less pronounced banding, migmatites, and augen gneisses toward the granite.

Quartz-Plagioclase Gneiss (Sp 145E)

The rock is found 0.5 km north of Tjernsetsaeter (37.8, 1-30.0) where it forms a gray resistant unit interlayered with amphibolites. The rock is dominantly fine grained (1 mm) but contains coarser grained layers that may have a grain size of 5 mm or 1 cm. The coarsest layers look like conformable pegmatitic veins. Most of the K-feldspar found in the rock is restricted to these coarse veins. All the minerals, particularly quartz, are elongated to give the rock a pronounced foliation. Tight minor folds are common in the rock. In thin section, the rock is principally composed of plagioclase, quartz, microcline perthite, chlorite, and biotite. Muscovite, zircon, opaque minerals, and apatite are accessory minerals. The texture is lepidoblastic. The average grain size is 1 mm. Plagioclase (An_{24}) is polysynthetically twinned and commonly sericitized. Sericitization is heavier adjacent to the pegmatic vein containing microcline. Plagioclase is elongated along the foliation. Some larger plagioclase grains are antiperthitic and contain patches of indistinctly twinned K-feldspar along twin lamellae (similar to Fig. 2, Plate 2). Bubble trains in the quartz are perpendicular to the foliation. Most of the microcline occurs as large crystals within the pegmatitic vein. Some microcline-perthite porphyroblasts may contain oriented plagioclase inclusions that extinguish simultaneously with each other and with the perthite films. Microcline also occurs in micro-to non-perthitic grains in the groundmass and shows a hazy twinning. Myrmekite occurs sporadically between microcline and plagioclase. Some microcline perthite contains the plagioclase interpositions in both patches and films that are normal to each other. Randomly disordered K-feldspar occurs in the vein. Biotite (Z, Y = reddish brown, X = tan) occurs in ragged scattered crystals together with chlorite and muscovite. Some opaque minerals occur along horizons parallel to the foliation. Zircon is a common accessory and is usually rounded but may exhibit crystal faces. The rock mode appears in Table X.

This rock has an interesting modal composition because it is a quartz-rich rock that contains considerable sodium and calcium in the form of plagioclase and is poor in potassium. A high quartz content is indicative of a clastic rock, but the high sodium and calcium content

is not (Pettijohn, 1957). If the microcline in the pegmatitic vein is taken into account, the proportion of potassium becomes somewhat higher. Randomly disordered K-feldspar occurs in this vein. This rock occurs below the Telemark quartzites and amphibolites from which it is separated by additional quartz-rich gneisses interlayered with amphibolites.

Quartz-dioritic Gneiss (Sp 219A)

The rock is found just north of Gulsvik (23.0, 1-17.1) and forms the part of the banded gneiss that occurs commonly between the western contact of the Heddal granite and the Telemark supra-crustal rocks. The variable concentration of biotite and, to a lesser extent, hornblende, imparts a comparatively weak banding to the rock. The rock is given a foliation and a lineation by the orientation of biotite. Pegmatites and granitic dikes cut the gneiss at this outcrop (Fig. 21). Biotite, plagioclase, and quartz, having a grain size of 1 mm are visible megascopically. In thin section, the rock is chiefly composed of plagioclase (An₃₈), quartz, and biotite. Hornblende, microcline, chlorite, epidote, sphene, opaque minerals, apatite, and zircon occur in accessory amounts. The texture is lepidoblastic. Plagioclase occurs in xenoblastic grains from 0.5 to 1.7 mm in diameter. Plagioclase is sericitized in widely scattered patches and is polysynthetically twinned. Subrectangular patches of indistinctly twinned K-feldspar occur in a very few of the plagioclase crystals. K-feldspar is concentrated along a healed fracture normal to the foliation and along a felsic horizon parallel to the foliation. Quartz occurs in xenoblastic grains from 0.3 to 1.7 mm long and shows a very weak undulatory extinction. Fractures in quartz are approximately parallel to the foliation and extend through plagioclase grains also. Biotite (Z, Y = brown, X = tan) occurs in idioblastic laths up to 2 mm long. Biotite is commonly very slightly chloritized along its cleavage. In a limited area along the healed fracture, biotite is completely altered to anhedral chlorite, and the associated plagioclase is heavily sericitized. Epidote occurs along the cleavage in chloritized biotite. Hornblende occurs sparsely in small equant grains. Sphene occurs in both rounded and euhedral grains and is usually closely associated with biotite. Zircon occurs in well rounded grains. The rock mode appears in Table X.

This rock type (Sp 219A) occurs commonly with varying proportions of hornblende and K-feldspar between the west contact of the Heddal granite and the Telemark rocks. The proportion of K-feldspar ranges from accessory amounts to considerable amounts along certain horizons. The quartz-dioritic gneiss also exhibits some quartz-rich layers in which biotite and feldspar occur in subordinate amounts. Pegmatitic veins parallel the foliation. Plagioclase forms the common felsic mineral in veins and eyes. The effect of fractures normal to the

foliation resembles that in the Telemark quartzite because these fractures have localized sericitization, chloritization, and K-feldspathization along their course.

Veined Amphibolitic Gneiss (Sp 545)

The rock is found 1 km northwest of Halvasbu near Soknavatn (17.6, 1-18.2) where it constitutes part of an extensive outcrop of amphibolites. The rock has a poor flat-lying foliation, but a lineation is distinct. The rock is permeated by 2-cm-wide white plagioclase veins which contain red garnets 1 to 2 cm in diameter. This undulating veining imparts the foliation to the rock. A green amphibole occurs in needles up to 4 mm long. In thin section, the rock is chiefly composed of plagioclase (An_{47}), hornblende, garnet, and diopside; quartz occurs in accessory amounts. The texture is nematoblastic. Plagioclase occurs in 0.5 to 1 mm grains and is sericitized in a very few places, particularly in grains enclosed by garnet. Hornblende ($X =$ light greenish yellow, $Y, Z =$ olive green, $Z \wedge c = 20^\circ$) occurs in 2 mm grains. Hornblende may be intergrown with diopside. Diopside ($Z \wedge c = 41^\circ$) occurs in 1.5 mm grains. Pink garnet occurs in amoeboid poikiloblasts that enclose numerous small grains of plagioclase, hornblende, and quartz. Fractures in the garnet contain microgranular hornblende. Quartz occurs in xenoblasts up to 3 mm in diameter and is slightly strained.

This rock (Sp 545) is one of the numerous amphibolites that are scattered throughout this map unit. The width of the amphibolites ranges from 1 to 20 m. Amphibolites are most common in the area between the south side of the Ådal granite and Soknadalen. This is the only one investigated that contains diopside; most of the amphibolites resemble Sp 528 B petrographically. Quartz constitutes a very few scattered grains in most of the amphibolites, and biotite occurs commonly up to *ca.* 10 per cent.

Most of the amphibolites occur as concordant layers within the banded gneisses. A small number of amphibolites that cut across the foliation of the gneisses have been observed, especially in the area south of the Ådal granite. These amphibolites, which are usually highly deformed, must represent basic dikes. Two generations of Precambrian dikes can be distinguished on the basis of their deformation and metamorphism.

Quartz-dioritic Gneiss (Sp 10)

The rock is found 1 km south of Simensrud farm (28.8, 0-41.4) where it occurs adjacent to an area of granitic gneiss and pegmatite that encloses undisturbed septa of biotite gneiss. Hornblende, which gives the rock a lineation,

biotite, and plagioclase in 1–2 mm crystals constitute most of the rock megascopically. In thin section, the rock is chiefly composed of hornblende, plagioclase, biotite, and quartz; microcline and sphene occur in accessory amounts. The texture is nematoblastic and the grain size ranges from 0.5 to 1 mm. Hornblende ($Z = \text{deep green}$, $Y = \text{green}$, $X = \text{pale greenish yellow}$, $Z \wedge c = 18^\circ$) occurs in crystals that are embayed by plagioclase and quartz and encloses grains of sphene. Plagioclase (An_{40}) is polysynthetically twinned and is heavily sericitized in scattered patches. Myrmekite is formed where plagioclase touches microcline. The larger xenoblasts of plagioclase are antiperthitic and contain patches of K-feldspar (Fig. 2, Plate 2), which exhibit optical continuity within a single plagioclase grain. The patches in some plagioclase crystals are grid twinned; those in others show a splotchy, undulating extinction. Microcline occurs as widely separated intergranular films and as patches in some plagioclase crystals. Microcline in both occurrences is nonperthitic. Microcline ($2V_x = 60^\circ, 64^\circ, 72^\circ, \text{ and } 82^\circ$) exhibits variable obliquity as shown by its optical properties and X-ray pattern. The microcline patches in plagioclase commonly have a trapezoidal shape formed by the plagioclase twin planes on two sides (Fig. 2, Plate 2). Biotite ($Z, Y = \text{greenish brown}$, $Z = \text{tan}$) occurs in ragged slightly bent laths. Quartz occurs interstitially. Quartz shows moderate undulatory extinction and some crushing; it is elongated along the foliation. Sphene is very common in accessory amounts; opaque minerals are rare. The rock mode appears in Table X.

The occurrence of indistinctly twinned antiperthitic K-feldspar in the quartz-dioritic gneiss (Sp 10) is the presumed initial stage of a feature which is widely developed in the Flå area. This phenomenon is characteristic of gneisses that fall in the general classification of augen gneisses and migmatites. These rocks are presumed to have undergone at least a local mobilization and metasomatism of the K-feldspar. The K-feldspar in the hornblende gneiss is present as intergranular films that are associated with myrmekite and as trapezoidal interpositions in the antiperthitic plagioclase (Fig. 2, Plate 2). This antiperthite shows a distinct tendency to occur in the larger plagioclase xenoblasts and is present only in relatively few grains in this rock. The K-feldspar is characterized by variable obliquity and partial development of grid twinning.

Augen Gneiss (Sp 420B)

The rock is found 0.5 km southwest of Bagn church (49.1, 1-19.6). The augen occur in zones which die out laterally (Fig. 4) within a biotite-hornblende gneiss. Zones of felsic streaks and lenses, which may be crushed augen, occur also. These zones of K-feldspar augen or streaks occur sporadically in what appears to be a uniform gneiss. The K-feldspar augen are elongated parallel to a strong lineation in the biotite and hornblende. The augen commonly consist

of a single K-feldspar porphyroblast with drawn-out tails of crushed K-feldspar. The augen range from 1 to 3 cm in diameter. In thin section, the rock is chiefly composed of microcline perthite, plagioclase (An_{35}), quartz, biotite, and hornblende. Chlorite, sphene, opaque minerals, and apatite occur in accessory amounts. The texture is blastomylonitic. The rock is strongly sheared along certain horizons rather than uniformly sheared. All minerals are elongated parallel to the foliation. Microcline occurs in xenoblasts and porphyroclasts up to 2 mm in diameter. Microcline forms heavy flame perthite in which the plagioclase lamellae are unevenly distributed. The plagioclase lamellae are particularly common where the microcline touches a plagioclase crystal. The plagioclase lamellae of the flame perthite appear to be contiguous with the plagioclase. Film perthite is also common. Screens and pockets of corroded plagioclase occur plastered along the interface where two microcline porphyroclasts are in contact. Flame perthite commonly occurs in microcline adjacent to these plagioclase screens. Some pockets of granulated groundmass are enclosed by microcline porphyroclasts. Some microcline of lower obliquity occurs in this rock (see feldspar chapter). Plagioclase is sericitized sporadically. Myrmekite is common. Patches of hazy microcline are found in plagioclase (similar to those in Fig. 2, Plate 2). Plagioclase is polysynthetically twinned, and the twin lamellae are bent. Quartz is completely granulated in some places and drawn out in leaves in others. Scattered quartz granules are strung out in trains through larger strained quartz porphyroblasts. Some quartz grains show no sign of strain. Hornblende ($Z = \text{blue green}$, $Y = \text{yellow green}$, $X = \text{pale greenish yellow}$, $Z \wedge c = 15^\circ$) occurs in a few patches scattered through the rock. Hornblende crystals are fractured and strung out. Hornblende poikilitically encloses many grains of sphene, plagioclase, and quartz and is itself highly indented. Biotite ($Z, Y = \text{brown}$, $X = \text{tan}$) occurs in ragged bent laths. Biotite that is shredded and drawn out into slip planes occurs together with fresh appearing 1 to 2-mm-long biotite laths. Sphene, which is euhedral to anhedral, occurs clustered with hornblende and biotite. The rock mode appears in Table X.

Quartz-dioritic Gneiss (Sp 420C)

This rock occurs in the zone without augen immediately adjacent to and north of the zone with augen (Fig. 4). The rock is even grained and distinctly lineated. Pegmatitic pods of plagioclase, quartz, and hornblende are found in this zone. In thin section, the rock is chiefly composed of plagioclase (An_{35}), quartz, biotite, and hornblende. Microcline, sphene, chlorite, and opaque minerals occur in accessory amounts. Most of the minerals are preferentially oriented and slightly layered to impart a foliation (S). Biotite laths are drawn out into a second foliation (S') that cuts S obliquely; the rock is slightly sheared along S' . Quartz is commonly somewhat strained and is granulated in places. Some trails of granulated quartz run through large quartz crystals. Biotite occurs in ragged laths. K-feldspar occurs in some discrete crystals but mostly as antiperthitic patches (similar to Fig. 2, Plate 2) in plagioclase. The rock mode appears in Table X.

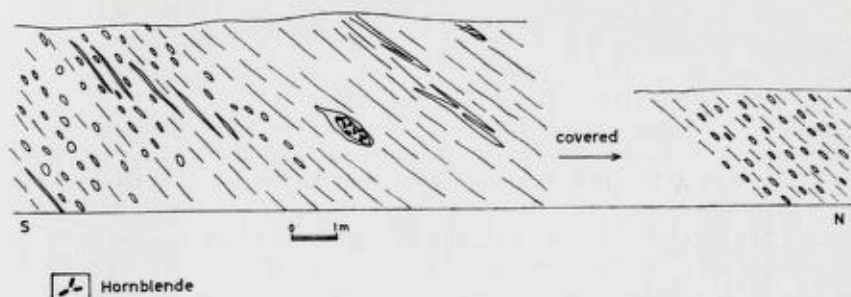


Fig. 4. *Augen gneiss in the shear zone at Bagn. Augen gneiss grades laterally into quartz-dioritic gneiss.*

Øyegneis i bevegelsessonen i Bagn. Øyegneisen går gradvis over i kvartsdioritisk gneis.

Most of the K-feldspar in the quartz-dioritic gneiss (Sp 420 C) is found in antiperthitic patches. In the augen gneiss (Sp 420), however, K-feldspar occurs both in antiperthite patches in plagioclase and in large porphyroclasts. The marginal pockets and screens of plagioclase together with the inclusions of plagioclase from the groundmass demonstrate that the K-feldspar augen have grown porphyroblastically in zones that disappear laterally. Furthermore, pockets of granulated groundmass in the K-feldspar indicate that growth proceeded simultaneously (or recurrently) with shearing, and some quartz and biotite recrystallized postkinematically. Both flame perthite and antiperthite are typical textural features of these rocks. Disordered K-feldspar structures are also common in augen gneisses and will be considered in more detail in a later section. This augen gneiss occurs in a shear zone that separates the quartz-dioritic gneiss to the north (Strand, 1943) from the migmatitic and granodioritic gneisses to the south.

Augen Gneiss (224 A)

The rock is found 3 km east of Gulsvik (23.2, 1-04.0). The zone of augen gneiss is about 2 km wide; layers of coarse-grained granitic gneiss and of amphibolite are interlayered with the augen gneiss. The felsic part of the rock varies from augen to long streaks. The augen are composed of lenticular 8-cm-wide aggregates of K-feldspar. Some pegmatitic pods in the gneiss are composed of K-feldspar, plagioclase, quartz, and hornblende. In thin section, the rock is chiefly composed of K-feldspar, plagioclase (An_{39}), quartz, hornblende, and biotite. Sphene, zircon, apatite, and hematite occur in accessory amounts. The texture is lepidoblastic, but traces of granulation are singularly lacking.

K-feldspar occurs in xenoblasts up to 4 mm in diameter. Inclusions in the K-feldspar are comparatively uncommon. The K-feldspar is either microscopically nonperthitic or contains small amounts of micropertthite. Grid-twinning is restricted to narrow zones following inhomogeneities and along the edges in some of the xenoblasts (Fig. 1, Plate 3). Most of the K-feldspar grains show an uneven hazy or splotchy extinction. Some K-feldspar grains exhibit orthoclase optics ($Z \wedge b = 0^\circ$). X-ray patterns reveal the K-feldspar to be orthoclase and disordered intermediate microcline (see feldspar chapter). The optic angles of K-feldspar ($2V_x = 56,60$ for antiperthitic patches and $2V_x = 52,54$ for porphyroblasts) indicate low somewhat variable obliquity values which are confirmed by X-ray patterns. Plagioclase is sericitized in widely scattered patches. Patches of hazy extinguishing K-feldspar are common in antiperthitic plagioclase (Fig. 2, Plate 3). Their straight margins show that they were controlled by the plagioclase twinning. The twin lamellae in some plagioclase grains are bent. Quartz shows a weak undulatory extinction. Hornblende ($Z =$ blue green, $Y =$ yellow green, $X =$ pale greenish yellow, $z \wedge c = 17^\circ$) occurs as scattered corroded fragments and encloses grains of plagioclase and quartz. Biotite ($Z =$ dark brown, $Y =$ green brown, $X =$ tan) occurs in fresh idioblastic laths which may be bent. Sphene, which is abundant, is found closely associated with hornblende and biotite. The rock mode appears in Table X.

This augen gneiss (Sp 224 A) comprises part of an augen gneiss zone that parallels the granites so closely (Plate 1) that a genetic relation can hardly be doubted. The augen gneisses exhibit a number of common features, K-feldspar porphyroblasts of variable obliquity (triclinicity), occurrence in hornblende gneisses, antiperthitic plagioclase, and shearing. This augen gneiss (Sp 224 A) is one of the few investigated which is unshered and is undoubtedly postkinematically recrystallized.

The diverse history of these rocks becomes apparent from Fig. 1, Plate 4. Three types of K-feldspar border on each other and are distinguished by their perthite development. One grain has two perpendicular film perthite directions, another grain has one film perthite direction, and the third grain has no visible perthite. Fig. 2, Plate 4 shows a mesoperthitic porphyroblast which is regarded to be an advanced stage of the antiperthite development mentioned previously (Sp 10). Although considerable disagreement over the interpretation of such features may exist, no one would dispute the complicated development of these rocks, which appear to have been arrested in a transitional stage.

The augen gneisses follow the contacts of the granites rather closely. They are found anywhere from right at the granite contact

to two km outside the contact. Augen gneisses are usually present but are less developed around the Ådal granite. The augen gneiss (Sp 420 B) in the shear zone at Bagn is the only one that is not spatially associated with the granite, but no reasons for assigning a different age to this augen gneiss are known, and this rock is petrographically indistinguishable from the other augen gneisses.

Banded Quartz-monzonitic Gneiss.

The banded quartz-monzonite gneisses occur along the east side of the area north of the Ådal granite. These gneisses are characterized by a comparatively high K-feldspar content, a general lack of amphibolites, and the numerous quartz monzonite sills that are interlayered with the gneiss. They may be marked by K-feldspar-rich veins. The dark biotite-plagioclase bands that impart the banded appearance comprise a subordinate amount of the gneiss.

The contact between these rocks and the banded granodioritic rock is gradational. Near Samsjöen (20.5, 0—31.0), layers of tightly folded granitic gneiss interfinger with 10-to 20-m amphibolites which decrease in frequency and thickness as the banded quartz-monzonitic gneiss is approached. The division may be as much tectonic as it is lithologic; these rocks comprise an area of recumbent folding.

Veined Quartz-Monzonitic Gneiss (Sp 590A)

The rock is found 3 km southeast of Nes i Ådal (33.2, 0-42.0) where the flat-lying veined gneiss is the common rock type along Sperillen. The veined gneiss alternates with fine-grained foliated quartz-monzonitic sills that are largely conformable but may be sharply crosscutting in places (Fig. 5). The quartz monzonite permeates the cores of folds (Fig. 5 on right). The gneissic quartz monzonite is strongly foliated parallel to the foliation of the adjacent veined gneiss, even where the contact is crosscutting. Where the quartz monzonite is crosscutting the foliation of the biotite passes from the veined gneiss into the quartz monzonite without being deflected. The veined part of the quartz monzonite is largely composed of bright-red microcline in up-to-1-cm-wide veins and lenses. In thin section, the rock is chiefly composed of microcline perthite, plagioclase (An_{32}), quartz, muscovite, and biotite. Opaque minerals, hematite, and zircon occur in accessory amounts. The texture varies from granoblastic to cataclastic. The rock is strongly sheared and granulated along certain horizons. Grid-twinned microcline occurs in 0.3—1.5-mm xenoblastic grains. Pockets and screens of plagioclase are common along the margins of adjoining microcline crystals. Flame perthite is common in microcline adjacent



Fig. 5. *Veined quartz-monzonitic gneiss interlayered with foliated quartz monzonite. The quartz monzonite is foliated parallel to the veined gneiss and permeates folds in the veined gneiss. Unless otherwise designated all symbols are the same as in Fig. 41.*

Stripet kvarts-monzonitisk gneis skiftevis med foliert kvarts-monzonit. Kvarts-monzoniten er foliert parallelt med den stripedede gneis og trenger gjennom foldene i den. Hvis intet annet er angitt, er alle symboler de samme som i fig. 41.

to plagioclase screens. Plagioclase occurs in 0.6—1.8 mm xenoblastic grains. Plagioclase is polysynthetically twinned and is heavily sericitized. Quartz commonly shows mortar structure and strong undulatory extinction but is finely granulated and sheared into leaves along certain horizons. Some quartz grains extinguish sharply. Scattered granules of quartz are enclosed within large quartz grains. Biotite (Z, Y = brown, X = tan) typically occurs in ragged, bent, and shredded laths but some is fresh and idiomorphic. Finer grained green biotite occurs in the groundmass. Muscovite is mostly ragged and bent, but some undeformed muscovite cuts across a shear plane. Muscovite seems more deformed along the shear planes than biotite is. The shear planes have developed along mica-rich horizons spaced from 0.5 to 2 mm apart. Zircon is euhedral. The rock mode appears in Table X.

Gneissic Quartz Monzonite Sill (Sp 590B)

The occurrence of the gneissic quartz monzonite sill is described in the preceding section. The rock is a medium-grained pink granitic gneiss in which quartz megacrysts and muscovite are conspicuous. In this section the rock is chiefly composed of microcline perthite, plagioclase (An₂₀), quartz, muscovite, and biotite. Opaque minerals, zircon, calcite, and epidote occur in accessory amounts. The texture is granoblastic. Feldspar and quartz tend to occur in separate layers. Microcline perthite occurs in 0.4—1.3-mm xenoblastic grains. Microcline is both Carlsbad twinned and grid twinned, and occurs in untwinned grains with long film perthite and in indistinctly grid-twinned micropertthite. Plagioclase inclusions in the microcline are relatively uncommon; film perthite

occurs commonly. Plagioclase occurs in 0.2—1.8-mm xenoblastic grains. Plagioclase is heavily sericitized in widely scattered patches. Plagioclase screens occur between adjacent microcline crystals. Quartz forms a mosaic texture with strong undulatory extinction and is usually elongated parallel to the foliation. Quartz is highly granulated in pockets and layers between large feldspar grains, but other quartz grains extinguish sharply. Biotite (Z , $Y = \text{brown}$, $X = \text{tan}$) occurs in ragged laths. Biotite is slightly chloritized along its cleavage and contains grains of epidote. Muscovite occurs in fresh xenoblasts up to 3 mm in diameter or as an alteration product with chloritized biotite. Clots of opaque minerals are enclosed within muscovite laths. Zircon has growth rings and is euhedral. The rock mode appears in Table X.

The veined quartz-monzonitic gneiss (Sp 590 A) is characterized by near-horizontal foliation and tight, recumbent folds. The folding is so tight (and also probably sheared out) that these rocks seem to represent a flat-lying "undeformed" succession. The composition in hand specimen ranges from granitic to quartz dioritic. Amphibolites are surprisingly rare in these rocks and form 5-to-10-cm-wide layers when they are found.

Innumerable quartz-monzonitic sills (Sp 590 B) are interlayered with the gneiss (Fig. 5). The sills seem to be more common at a higher elevation than along the shores of Sperillen. The granitic body mapped by Schetelig and Høltedahl (1923) near the top of Tannfjell (750 m a.s.l., 34.5, 0—40.0) probably represents one or more of these sills. The sills can be observed passing laterally into gneisses; however, the distinction is somewhat subjective because they are both strongly foliated rocks.

Because of their similarity in composition and occurrence, some interesting comparisons can be made between the gneiss and the sills. The veined gneiss is typified by sheared horizons, but some postkinematic recrystallization is evident. The quartz monzonite of the sill appears to be considerably recrystallized, but signs of shearing are still observable. Microcline has behaved blastically in both rocks; Carlsbad twins occur only in the gneissic quartz monzonite. The two types of perthite suggest two generations of K-feldspar or two manners of behavior. The postkinematic porphyroblastic character of the muscovite is much more evident in the gneissic quartz monzonite. Plagioclase in the gneissic quartz monzonite is distinctly more sodic than that in the veined gneiss, and the gneissic quartz monzonite has a lower color index.

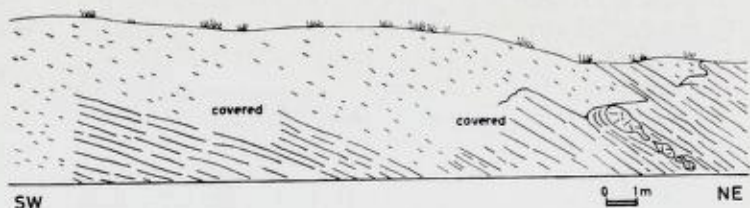


Fig. 6. Foliated quartz monzonite that cuts across the foliation of gently dipping gneisses. The foliation in the quartz monzonite parallels the foliation in the gneiss.

Foliert kvarts-monzonit som skjærer tvers over folieringen i gneis med svakt fall. Folieringen i kvarts-monzoniten er parallell med folieringen i gneisen.

Foliated Quartz Monzonite (Sp 262)

The rock is found by Faasteinodden (32.7, 0-40.4). The rock occurs in a body about 150 m long that cuts sharply across the near horizontal foliation of the surrounding gneiss (Fig. 6). The contact between the two rocks is sharp; however, the foliation of the quartz monzonite parallels that of the surrounding gneiss. Undisturbed pieces of gneiss are found in the quartz monzonite. In hand specimen the rock is a light-gray fine-grained (0.5-1.0 mm) foliated granite that contains scattered larger K-feldspar crystals up to 4 mm long. In thin section, the rock is chiefly composed of microcline perthite, plagioclase, quartz, and chlorite. Biotite, muscovite, calcite, epidote, zircon, apatite, and opaque minerals occurs in accessory amounts. The texture is granoblastic to cataclastic. Microcline occurs in 0.6-to-3-mm xenoblasts that are both Carlsbad twinned and grid twinned. Both coarse and fine film perthite occur in the same microcline grain. Film perthite is variably developed; short fine films and long coarse films are found normal to each other in the same grain. Some microcline grains in the groundmass are micropertthitic. Plagioclase inclusions in the microcline are contiguous with plagioclase films of the perthite and extinguish simultaneously with these films. Plagioclase inclusions in microcline tend to be oriented parallel to (010) of the microcline and extinguish simultaneously. Plagioclase occurs in 0.7-mm idioblastic crystals. Plagioclase pockets commonly indent the borders of microcline grains. Myrmekite is common. Some sodic rims are developed where plagioclase and microcline touch. Plagioclase is heavily sericitized and is polysynthetically twinned. Some plagioclase grains have bent twin lamellae. Quartz is sutured in places; in others it is granulated or sheared into leaves. Quartz is most highly deformed along certain horizons parallel to the foliation. Some quartz grains are fresh appearing and unstrained. Biotite occurs in ragged, deformed crystals and is largely altered to chlorite (pennine). Fresh, undeformed muscovite occurs in and near the chlorite. Calcite occurs along fracture planes. Euhedral zircon shows growth rings. The rock mode appears in Table XI.

This gneissic quartz monzonite (Sp 262) shows considerable effects of being sheared; however, quartz has partially recrystallized. The muscovite has recrystallized postkinematically. In view of the shearing, which must have followed the present foliation, the sharp straight contacts against the gneiss are surprising (Fig. 6). One would expect the contact to be highly irregular and resemble slip folds where the contacts cut directly across the foliation of the gneiss. Although this body is largely emplaced across the foliation of the gneiss and has slightly different mineralogy, this occurrence greatly resembles the quartz-monzonite sill (Sp 590 B) in texture. The foliation of both of these bodies parallels the foliation in the adjacent gneiss. The quartz monzonite must have been formed synkinematically; crystallization has partly outlasted the deformation.

Foliated Fine-grained quartz diorite (Sp 639 B)

The rock is found by Strömmen farm (37.1, 0-48,0). The rock occurs in the core of a tight fold (Fig. 7) and is concordant with the layers of the fold. Biotite flakes, aligned parallel to the axial plane of the fold, impart a distinct foliation to the rock. Megascopically, the rock appears to be a medium-gray, fine-grained (*ca.* 1 mm) granite similar to the fine-grained facies of the Flå granite. In thin section, the rock is chiefly composed of plagioclase (An₂₅), quartz, and biotite; microcline, muscovite, chlorite, opaque minerals, and epidote occur in accessory amounts. The texture is granoblastic. Microcline occurs in xenoblasts that have indistinct grid twinning. Microcline contains small amounts of micropertthitic plagioclase lamellae. Plagioclase occurs in anhedral crystals that exhibit polysynthetic and pericline twinning. Plagioclase is sericitized sporadically. Rectangular patches of microcline occur in a few plagioclase grains and extinguish simultaneously within the same crystal. Quartz forms the largest (up to 4 mm) xenoblasts in the rock. Quartz is slightly granulated and shows undulatory extinction. Quartz is elongated parallel to the foliation. Biotite (Z, Y = green brown, X = tan) occurs in ragged laths. Biotite, chlorite, and muscovite are interlayered in the same grain. Epidote occurs in the chlorite. Muscovite is xenoblastic and commonly interfingers with biotite. A rim of vermicular muscovite surrounds a large opaque-mineral grain. The rock mode appears in Table X.

This foliated quartz diorite (Sp 639 B) forms a body whose shape can best be described as a small phacolith. The foliation of the granodiorite parallels the axial plane of the fold (Fig. 7). A similar parallelism has been described from the Fish Creek phacolith (Dietrich, 1954). This fine-grained quartz diorite is megascopically indistin-

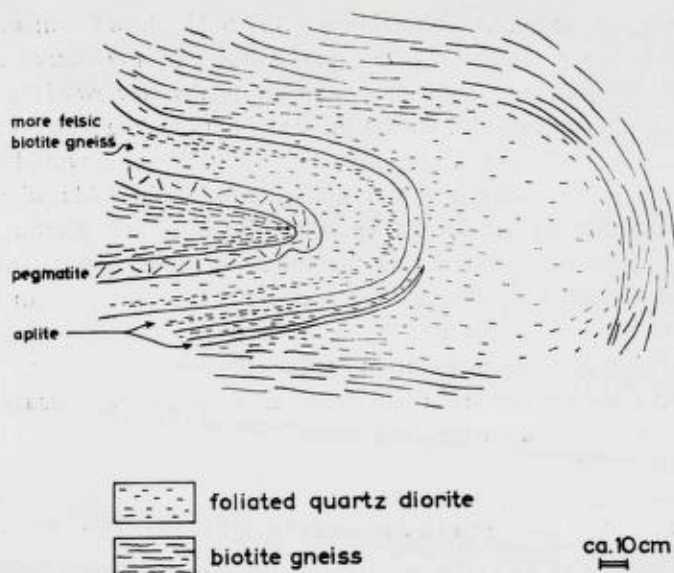


Fig. 7. Foliated fine-grained quartz diorite emplaced in the crest of a recumbent fold. Quartz diorite grades into biotite gneiss on the flanks of the fold.

Foliert finkornet kvarts-diorit, som er trent inn i midten av en liggende fold. Kvarts-diorite går over i biotit-gneiss på siden av folden.

guishable from the fine-grained quartz monzonite in the Flå granite. Antiperthite of presumed replacement origin occurs. No possible feeders or similar rock types have been observed in the adjacent region. Since the foliation of the quartz diorite parallels the axial plane of the fold, this rock must have been formed synkinematically; however, recrystallization must have largely outlasted the deformation.

Banded Quartz-dioritic Gneiss.

Banded quartz-dioritic gneisses are exposed along the valley of the Begna River north of Bagn (Strand, 1954, p. 43). The border of these rocks is marked by the zone of augen gneiss at Bagn, which separates them from the banded granodioritic gneisses to the south. Plagioclase- or zoisite-rich layers alternate with amphibolites. As Strand (1954) has remarked, these gneisses present a sharp contrast with the granodioritic gneisses to the south.

Composition of the Gneisses.

The modal composition of the gneisses (Table X in Appendix and Fig. 8) varies greatly from rocks rich in quartz to rocks rich in mafic minerals. If the extreme compositions represented by orthoquartzite and amphibolites are excluded, however, the remaining gneisses do not vary too greatly in composition. The most striking fact about the modes is the lack of certain minerals. Micas are not present in amounts large enough to form a schist, aluminosilicates are not present at all, and very few rocks are rich enough in quartz to be suggest-

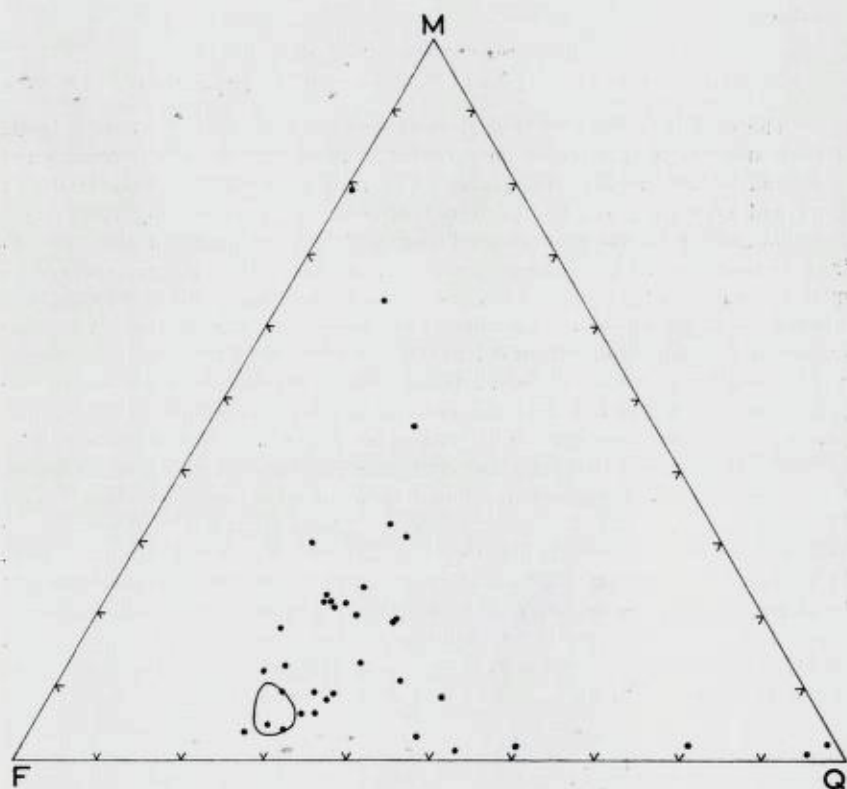


Fig. 8. Modal analyses of the gneisses plotted on a Quartz-Mafics-Feldspar diagram. Contour encloses the maximum concentration of plots from the granite (Fig. 13 a).

Modal-analyser av gneiser som er plottet i et kvarts-mørke mineraler-feltspat diagram. Omrisset inneslutter maksimum konsentrasjon av plottinger fra granitten (Fig. 13 a).

ive of a clastic origin. The typical gneiss contains about twice as much feldspar as it does quartz while biotite is universally present but in smaller amounts.

Granite.

Two principal rock types, fine-grained quartz monzonite and porphyric quartz monzonite, comprise the entire Flå granite. The fine-grained variety composes the center of the Hedal granite (Plate 1) and occurs sporadically in smaller bodies within the Ådal granite (Fig. 9). Dikes and sills of both kinds occur commonly outside the granite.

Fine-grained Quartz Monzonite (Sp 380A)

The rock is found 1.5 km west of Storekrak (29.1, 1-01.5) where it forms a part of a large outcrop of fine-grained granite that is cut by some small amoeboid bodies of porphyric granite. The rock appears fine grained (0.5—1 mm) and medium gray. The preferred orientation of biotite imparts a weak foliation to the quartz monzonite. Fluorite occurs on joints in the rock. In thin section, the rock is chiefly composed of microcline, plagioclase (An₂₈) quartz, and biotite. Opaque minerals, zircon, fluorite, orthite, chlorite, and apatite occur in accessory amounts. The texture is granoblastic. Microcline occurs in anhedral grains from 0.4 to 0.8 mm wide. Grid twinning is common; a few widely scattered Carlsbad twins occur. Perthite is uncommon; fine plagioclase films are found in the centers of some microcline grains. Flame perthite occurs sporadically; most microcline grains are microscopically non-perthitic. Microcline and plagioclase interfinger; myrmekite occurs sporadically. Corroded plagioclase screens are found between adjoining microcline grains. Plagioclase occurs in anhedral to subhedral grains from 0.2 to 0.8 mm wide that are polysynthetically twinned and moderately sericitized. Quartz occurs in anhedral 0.2—0.6-mm grains that show moderate undulatory extinction and local granulation. Biotite (Z, Y = brown, X = tan) occurs in subhedral laths. Zircons surrounded by pleochroic halos are common in biotite. Fluorite occurs in 0.05 mm grains associated with opaque minerals and orthite. The rock mode, chemical analysis, and norm appear in Tables II and III.

Porphyric Quartz Monzonite (413A)

The rock is found 1 km southwest of Sandvatn (26.1, 0-52.5). Pink microcline megacrysts up to 2 cm long occur in the rock and, together with biotite, are aligned to impart a strong foliation to the rock. Biotite-rich shadows and biotite septa are present in the granite. In thin section, the rock is chiefly composed of microcline perthite, plagioclase (An₂₈), quartz, and biotite; chlorite, muscovite, opaque minerals, orthite, zircon, and apatite occur in

accessory amounts. The texture is blastomylonitic. Microcline occurs in porphyroclasts that both enclose numerous plagioclase grains and partially envelop pockets of plagioclase along its margin. The plagioclase inclusions are commonly oriented with their (010) crystal face parallel or perpendicular to (010) of the microcline host (Fig. 1, Plate 5). The aligned inclusions extinguish almost simultaneously. The oriented plagioclase inclusions are usually rectangular, and the unoriented inclusions are subrounded. Carlsbad twins with sharp composition planes are common in the microcline porphyroclasts. Both flame perthite and film perthite are common in the microcline (Fig. 2, Plate 5). Flame perthite interpositions commonly occur contiguous with corroded plagioclase grains or inclusions (Fig. 2, Plate 5) or where microcline inter-fingers with plagioclase. Microcline in the groundmass is micropertitic and inclusion free. Plagioclase occurs in subhedral grains and is sericitized. Plagioclase is polysynthetically twinned. Plagioclase crystals are fractured, and the twin lamellae are bent. Screens of plagioclase occur between adjacent microcline grains; myrmekite is common. Quartz is sheared out into leaves, granulated, and crushed into patchy extinction. Quartz granules are scattered through larger quartz grains; some quartz is unstrained. The quartz leaves wrap around the relatively undamaged feldspar grains. Biotite (Z, Y = dark brown, X = tan) occurs in ragged, bent laths that are pulled out along shear planes. Biotite occurs mixed with both muscovite and chlorite in the same grain. The muscovite is fresh. The rock mode, chemical analysis, and norm appear in Tables II and III.

Fine-grained quartz monzonite forms a large mass of fairly uniform rock in the center of the Heddal granite and is dotted with 10-to-20-m-wide "puddles" of porphyric granite. Foliation is much less common in the fine-grained rocks. Inclusions of gneiss are common, particularly in certain places, within the fine-grained quartz monzonite.

Although the contact relations are not always decisive, the evidence suggests that the fine-grained variety is older than the porphyric quartz monzonite (Fig. 9). The contact between the two types of quartz monzonite may be either sharp (Fig. 9) or gradational. Smaller bodies of fine-grained quartz monzonite occur in the porphyric variety and *vice versa*. The map contact between the fine-grained and the porphyric quartz monzonite in the center of the Heddal granite delineates the general extent of the two rock types which are more variable in detail.

The petrographic features of the fine-grained quartz monzonite are somewhat contradictory. In most thin sections, the rock exhibits a granoblastic texture. In some rocks, however, the texture ranges from granitic to subgranitic (Fig. 1, Plate 6). In fact, both "igneous" and "metamorphic" textural features are found together so that one and

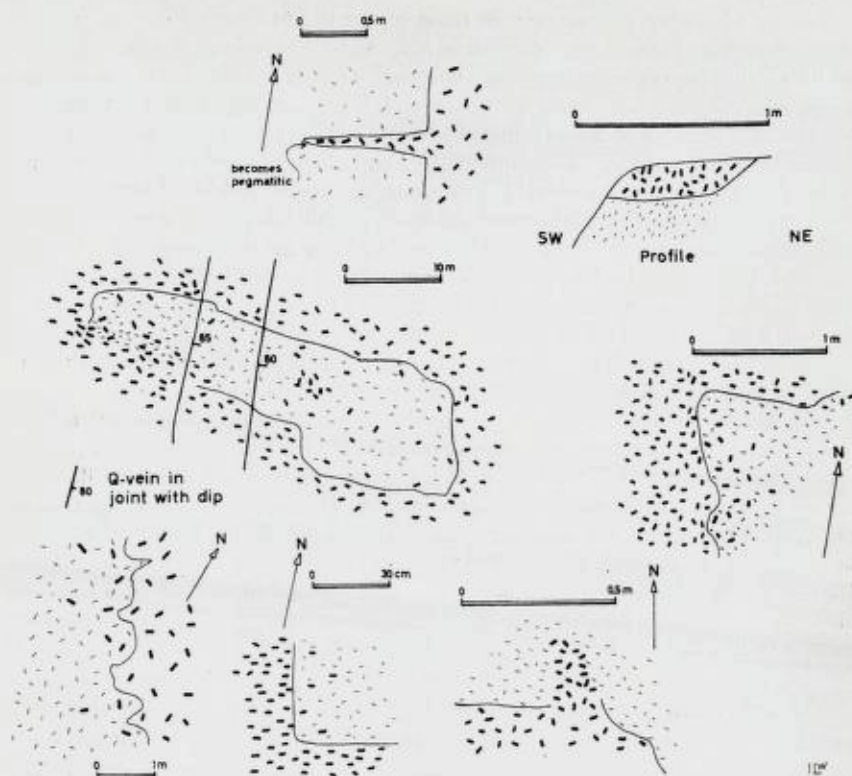


Fig. 9. Contact relations between fine-grained and porphyric granite.

Kontaktforhold mellom finkornet og porfyrisk granitt.

the same rock will appear granitic and granoblastic within a single thin section. As a rule, all specimens show blastic features; *i. e.*, plagioclase corroded by microcline, and plagioclase screens and pockets between coalescing microcline grains.

Progressive zoning is observed in a few plagioclase grains. Myrmekite is universal. Most microcline grains are micropertthitic or non-pertthitic, but some exhibit coarse flame perthite where they appear to be corroding plagioclase. A varied development is implied by the two kinds of perthite.

Signs of shearing are not as evident as in the porphyric variety; however, considerable evidence suggests that the quartz has recrystallized. Deformed plagioclase grains and biotite laths are seen, and quartz can be observed in all states of recrystallization from crushed



Fig. 10. *Porphyric granite in the "tail" of the Adal granite. Microclin megacrysts are egg sized. Gray areas are biotite patches parallel to the foliation which is approximately parallel to the page.*

Porfyrisk granitt i "halen" på Adal-granitten. Mikrolin megakrystaller er av størrelse som et egg. Grå områder er biotit-flekker parallelt med folieringen, som er omtrent parallel med siden.

granules to large slightly strained grains. Some of the rocks with the most granitic appearing textures show the greatest signs of shearing.

Fluorite, which occurs as an accessory mineral in fine-grained quartz monzonite, also coats a healed joint. Some fluorite has been observed in the porphyric quartz monzonite, too, but the occurrence of fluorite in both rock types is extremely rare.

Porphyric quartz monzonite forms an envelope around the entire Heddal granite and comprises almost all of the Adal granite. The porphyric variety contains 1- to 2-cm crystals of microcline and becomes coarser in the "tail" of the Adal granite until the microcline megacrysts attain egg-sized dimensions (Fig. 10). The porphyric quartz monzonite is commonly well foliated (Fig. 11), especially in the Adal granite. Biotite-rich streaks and shadows are almost universally observable in this granite where exposures are favorable (Figs. 10 and 11). This rock is always sheared where it is foliated, and the microcline megacrysts become bright red as the shearing becomes more intense.



Fig. 11. Well foliated porphyric quartz monzonite from the "tail" of the Adal granite. Foliation parallels the hammer handle. A folded inclusion is nearly replaced and partially sheared out.

Godt foliert porfyrisk kvarts-monzonit fra "halen" av Årdal-granitten. Folieringen er parallell med hammerskaftet. En foldet inneslutning er nesten fortrengt og delvis utgnidd.

The texture in the porphyric variety is granoblastic to cataclastic. Microcline dominates the textural features of this rock type. The blastic features (Fig. 12) are the same as in the fine-grained quartz monzonite, but their occurrence is more widespread and their development more extreme.

Microcline corrodes and interfingers with plagioclase. Screens and pockets of corroded plagioclase are enclosed by microcline porphyroblasts. Flame perthite, which comprises up to 40 per cent of a given microcline perthite grain, is closely associated with corroded plagioclase screens and inclusions (Fig. 2, Plate 6). In some cases, corroded slivers of plagioclase are contiguous with coarse perthite films and have the same optical orientation (Fig. 1, Plate 7).

Megacrysts of microcline perthite are shot through with inclusions of plagioclase which are preferentially oriented either normal to (010) or parallel to (010) of the microcline. The well oriented plagioclase

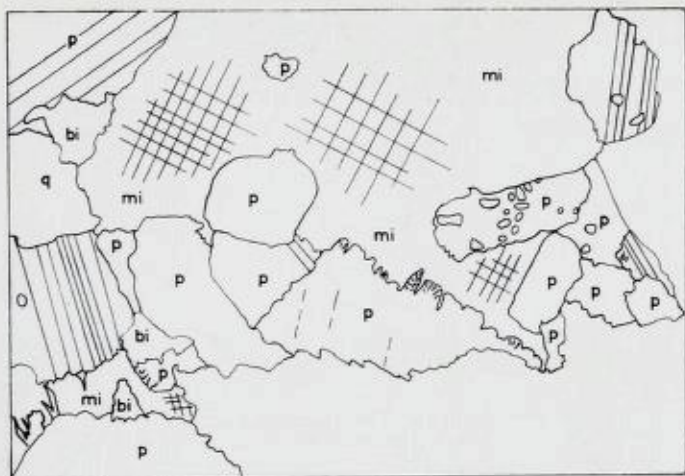


Fig. 12. Tracing of a microphotograph that shows microcline projecting into plagioclase along the latter's cleavage. Fine-lacy myrmekite is developed in the plagioclase along the embayed contact between the two grains. $\times 63$.

Opptrukket tegning av et mikrofotografi som viser mikrolin som trenger inn i plagioklas langs sistnevntes spalteplan. Fin myrmekit er utviklet i plagioklasen langs den innbuktete kontakt mellom de to korn. $\times 63$.

crystals are usually subhedral; the unoriented inclusions tend to be rounded. In some microclines, the inclusions form a box-shaped layer (Figs. 1 and 2, Plate 8). The plagioclase inclusions tend to be in optical continuity with each other and with the perthitic plagioclase films in the microcline.

Coarse film perthite and grid twinning in microcline show an interesting inverse relationship that occurs almost universally — but not without exception. In one and the same microcline individual, grid twinning will occur where there is no coarse film perthite and *vice versa* (Fig. 1, Plate 5). The whole individual is microcline because the untwinned part extinguishes obliquely. The coarse film perthite and the grid twinning would generally seem to be incompatible in these rocks.

Fine-grained microperthitic grid-twinned microcline, resembling the common microcline from the fine-grained quartz monzonite, occurs in the groundmass. Thus two kinds of microcline and three kinds of perthite (fine film, coarse film, and flame perthite) are found in the porphyric granite. These facts indicate a complicated development.

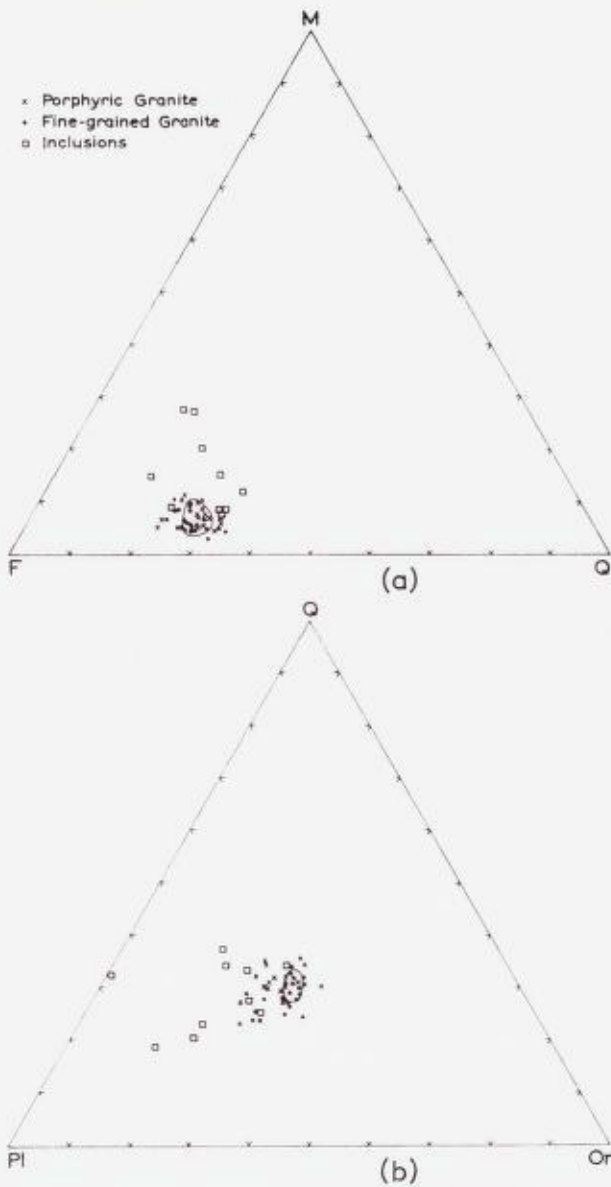


Fig. 13. Thirty-nine modal analyses of fine-grained granite, porphyritic granite, and inclusions plotted on a Quartz-Mafics-Feldspar diagram (a) and a Quartz-Plagioclase-Orthoclase diagram (b). Fine-grained and porphyritic granite occupy the same compositional range. Contour = 15 per cent per 0.2 per cent area.

Niogtredve modal-analyser av finkornet granitt, porfyrisk granitt og inneslutninger plottet i et kvarts-mørke mineraler-feltspat diagram (a) og på et kvarts-plagioklas-ortoklas diagram (b). Finkornet og porfyrisk granitt inntar samme plass i diagrammet. Koter: 15 % pr. 0,2 % areal.

Quartz shows signs of repeated shearing and recrystallization. Quartz occurs in large strained grains, leaves, and granules. Trails of granules running through large grains and sutured grains of unstrained or slightly strained quartz demonstrate recrystallization. A considerable amount of differential movement may have been accommodated by means of translation, granulation, and recrystallization of the quartz.

Biotite has also facilitated the shearing movement. Biotite is shredded and drawn into movement surfaces between quartz and feldspar grains. Biotite is commonly partly chloritized within these sheared rocks.

The strong shearing is mostly confined to the borders of the granites, but it has also been observed in the center of the Ådal granite and the north central portion of the Hedal granite (Fig. 1, Plate 9). A suggestion of shearing is found in some specimens of fine-grained granite from the center of the Hedal granite.

Composition.

The modes of 39 specimens of granite and 8 specimens of inclusions are plotted in QMF and QPIOr diagrams (Figs. 13 a and 13 b). A QMF plot of the gneisses is included for comparison (Fig. 8). These diagrams reveal that the composition of granite is remarkably uniform if the size of the bodies is considered. This granite is similar in composition to the calcalkaline granites of New England (Chayes, 1952) and closely corresponds to the minimum-melting composition in the granite system. The fact that the porphyric granites and fine-grained granites differ little in composition is readily apparent from the diagrams. According to its content of quartz and feldspars, the granite is classified as a quartz monzonite (Grout, 1932).

Chemical analyses (Table II) and normal and modal calculations (Table III) are given for the granites. The fine-grained granite is somewhat more mafic than the porphyric varieties. General agreement between the mesonorms (Barth, 1959, 1962) and modes is good particularly considering the grain size and foliation of the porphyric granites. A rather large discrepancy arises between normal and modal plagioclase. This is due to the sericitization of the plagioclase, which would also consume the corundum that appears in the norm. Refractive indices of only the fresh plagioclases were determined because the

Table II.

Chemical Analyses of Quartz Monzonites.

Weight %	Sp 380 A	Sp 413 A	Sp 312	Cation %	Sp 380 A	Sp 413 A	Sp 312
Si O ₂	65.93	71.36	67.66	Si	62.2	67.4	63.7
Ti O ₂	0.74	0.36	0.47	Ti	0.5	0.4	0.3
Al ₂ O ₃	15.64	14.19	15.65	Al	17.4	15.8	17.3
Fe ₂ O ₃	1.26	0.96	1.57	Fe'''	0.9	0.7	1.1
Fe O	3.21	1.68	1.99	Fe''	2.5	1.3	1.6
Mn O	0.11	0.05	0.06	Mn	0.0	0.0	0.0
Mg O	1.15	0.57	0.95	Mg	1.6	0.8	1.4
Ca O	2.09	1.69	2.04	Ca	2.1	1.7	2.0
Na ₂ O	3.66	3.12	3.27	Na	6.7	5.7	6.0
K ₂ O	4.93	5.04	5.29	K	5.9	6.1	6.3
P ₂ O ₅	0.26	0.14	0.29	P	0.2	0.1	0.2
H ₂ O—	0.08	0.05	0.16				
H ₂ O+	0.89	0.53	0.63				
Total	99.95	99.74	100.03	Total	100.0	100.0	99.9

Sp 380 A. Fine-grained quartz monzonite. Örneflag (29.1, 1—01.5).

Sp 413 A. Porphyric quartz monzonite. Sandvatn (26.1, 0—52.5).

Sp 312. Porphyric quartz monzonite. Huskebudalen (21.7, 0—45.3).

Analysts: K. Haugen and R. Solli, Norges geologiske undersøkelse.

sericitized grains gave inconsistent results. The refractive indices of sericitized plagioclase were consistently lower than those of fresh plagioclase. This fact shows that a sodic andesine has been altered considerably and to a variable degree so that the total plagioclase composition is much more sodic than the original composition determined optically. Sericitized plagioclase is present in every granite specimen; the plagioclase determinations are biased toward an An-content that is too large.

The plots of 11 alkali analyses of the granite appear in Fig. 14, the feldspar system. These chemical analyses can be found in Table XIV in the Appendix. Again, the compositions of the two granite types are similar. The diagram shows that two feldspars would crystallize from a melt of this composition.

Table III.

Norms and Modes of Quartz Monzonites.

Mineral	Catanorm			Mesonorm		
	Sp 380 A	Sp 413 A	Sp 312	Sp 380 A	Sp 413 A	Sp 312
Q	17.6	27.8	21.2	21.3	29.4	23.7
Or	29.5	30.5	31.5	23.3	27.5	27.3
Ab	33.5	28.5	30.0	33.5	28.5	30.0
An	9.0	7.5	8.5	6.5	5.5	7.0
C	1.2	1.0	1.6	2.2	1.8	2.2
Bi	—	—	—	9.9	4.8	6.7
En	3.2	1.6	2.8	—	—	—
Fs	3.2	0.8	1.6	—	—	—
Mt	1.3	1.0	1.6	1.3	1.0	1.6
Ap *	0.5	0.3	0.5	0.5	0.3	0.5
Il	1.0	0.8	0.6	—	—	—
Ti	—	—	—	1.5	1.2	0.9

	Modes		
Quartz	21.8	29.6	22.1
Microcline	29.5	33.4	32.6
ca. % Ab	14	14	14
Plagioclase	38.3	31.5	39.3
% An	28	28	33
Biotite	9.3	5.0	4.2
Accessories	1.1	1.3	0.6
Area Counted cm ²	28	63	62
Number of Counts	1000	1770	1747
IC Number	55	19	21

Granitic Dikes and Sills.

Granitic dikes and sills are found near the granite contact's entire area. Both fine-grained and porphyric dikes and sills are common; aplites occur rarely.

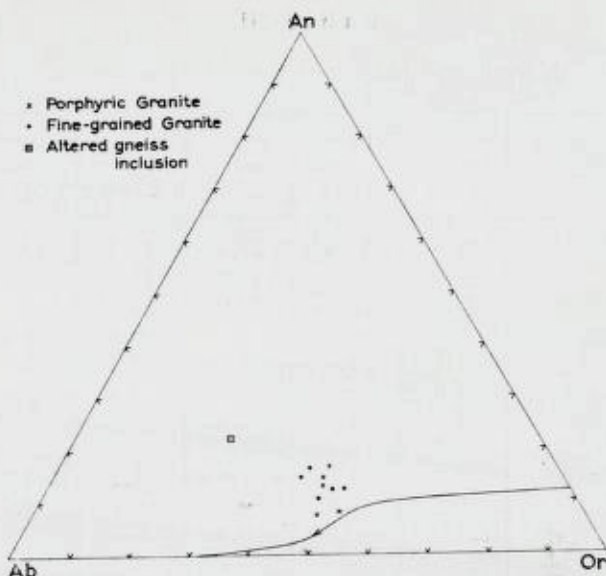


Fig. 14. Eleven partial chemical analyses plotted on the projection of the quaternary system $\text{NaAlSi}_3\text{O}_8(\text{Ab}) - \text{KAlSi}_3\text{O}_8(\text{Or}) - \text{CaAl}_2\text{Si}_2\text{O}_8(\text{An}) - \text{H}_2\text{O}$ at 5000 bars H_2O pressure. Fine-grained and porphyric granite occupy the same composition range. The point nearest the Ab-An sideline is an inclusion (Sp 542).

Elleve partielle kjemiske analyser plottet i et diagram av systemet $\text{NaAlSi}_3\text{O}_8(\text{Ab}) - \text{KAlSi}_3\text{O}_8(\text{Or}) - \text{CaAl}_2\text{Si}_2\text{O}_8(\text{An})$ ved 5000 bar H_2O trykk. Finkornet og porfyrisk granitt finnes i samme område. Punktet nærmest Ab-An linjen er en inneslutning (Sp 542).

Porphyric Quartz Monzonite Dike (Sp 4A)

The rock is found 3 km west of Vikar in Ådal (27.3, 0-43.1). The rock occurs in a conformable 2-m-wide dike which is slightly crosscutting in biotite gneiss. Biotite and red microcline megacrysts that are up to 1 cm long are aligned parallel to the dike contacts and to the foliation of the surrounding gneiss. Clots of biotite and small schlieren of biotite gneiss occur in the dike. In thin section, the rock is composed of microcline perthite, plagioclase (An_{35}), quartz and biotite. Chlorite, muscovite, orthite, sphene, opaque minerals, and zircon occur in accessory amounts. The mineralogy and texture are similar to Sp 413 A described previously. The texture is porphyroclastic and bears the imprint of strong shearing. The quartz is granulated and sheared into leaves, biotite is shredded and bent, and plagioclase exhibits deformed twin lamellae. The shearing has been strongest along certain planes. Plagioclase inclusions, oriented parallel to (010) are common in the microcline porphyroclasts. The rock mode appears in Table XII.



Fig. 15. *Sills of porphyric granite and pegmatites interfingering with the gneiss just outside the granite contact at ø. Kolsjøen (21.0, 0—48.5). Clots and septa of biotite in the sill parallel the foliation in the gneiss.*

Ganger av porfyrisk granitt og pegmatit i gneisen like utenfor granittkontakten ved ø. Kolsjøen (21,0, 0—48,5). Biotit-flekker i gangen parallelt med folieringen i gneisen.

Granite dikes and sills, which are found widely scattered throughout the gneiss adjacent to the granites, occur as far as 5 km from the nearest granite contact. They become extremely profuse just outside the contact where they divide the country rocks into alternating strips of granite and gneiss (Fig. 46). The sills are typically slightly

crosscutting but may branch and join so that they appear concordant at one place and sharply transgressive at another.

The sills present all aspects of development. Some sills of porphyric granite grade into zones in biotite gneiss which are rich in microcline porphyroblasts. The sill, if foliated, is conformable. Other sills, which range from 10 cm to 10 m in width, contain patches and long thin septa of biotite which are parallel to the foliation in the sill and in the adjacent gneiss and interfinger with biotite gneiss along the foliation (Fig. 15). One dike-like body transgressed gradually across the foliation of a tightly folded gneiss. The fold pattern in the gneiss was preserved in the orientation of microcline porphyroblasts in the dike (Fig. 16). The contact between the two rocks is sharp.

A fine-grained granite dike cuts the foliation of the gneiss at right angles, and the foliation in the dike is conformable with its contacts. Some pieces of gneiss enclosed by the dike are rotated, and others appear to be in place. Numerous granitic dikes are foliated parallel to their discordant contacts (Fig. 17); movement parallel to the contacts must certainly have taken place within these dikes. The dikes are welded to the surrounding gneiss which the dikes appear to penetrate along the foliation.

The sills and dikes show signs of shearing just as the granites do, and, as in the granites, shearing and strong foliation accompany each other. The texture in a 30-cm-wide sill is that of a mylonite (Fig. 2, Plate 11). On the other hand, replacement features in a dike (Fig. 16) could not survive such strong shearing. The crosscutting fine-grained dike shows signs of granulation and recrystallization. Apparently the amount of shearing in the sills and dikes varied considerably locally.

Aplite dikes are comparatively rare in the area. They commonly contain red garnet or muscovite. The foliation of the gneiss usually continues into these dikes without deflection; undisplaced pieces of gneiss may be enclosed by the aplite. Such occurrences of aplites indicate a replacement origin.

Textural Features of the Granite.

The textural features of the granite are so characteristic that their explanation represents a major step in the clarification of the evolution of the granite. That this evolution must have been complex can hardly

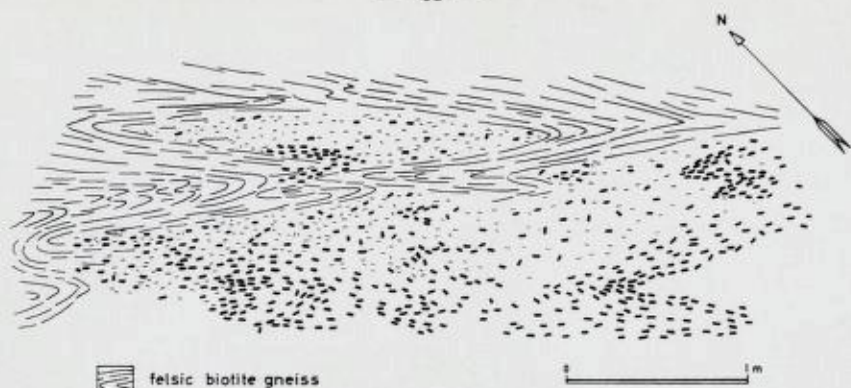


Fig. 16. *Field sketch of a porphyric granite dike transecting tightly folded gneiss at a low angle just outside the granite contact. Megacrysts of K-feldspar in the dike outline tight folds similar to those in the gneiss. The contact between gneiss and granite is sharp. Granite permeates the core of a fold in the gneiss. Between Vestefjell and Vikerfjell (29.2, 0—47.0).*

Feltskisse av en porfyrisk granittgang, som skjærer gjennom en tett foldet gneiss med liten vinkel like utenfor granittkontakten. K-feldspat megakrystaller i gangen tegner opp tette folder, lik dem i gneisen. Kontakten mellom gneiss og granitt er skarp. Granitt trenger frem i kjernen av en fold i gneisen. Mellom Veslefjell og Vikerfjell (29,2, 0—47,0).

by disputed. The history of the granite is certainly coupled to the development of the feldspar, particularly the K-feldspar.

The granites and the surrounding augen gneisses and migmatites contain at least two types of K-feldspar, fine-grained micropertthitic grains in the groundmass and megacrysts composed of both film and flame perthite. The plagioclase in the perthite of the megacrysts may be either coarse and long or very fine similar to the micropertthite in the groundmass. These two occurrences could be called two generations of microcline perthite; however, the two may have formed concurrently but undergone a different development.

The microcline that forms megacrysts has corroded the plagioclase as evidenced by the numerous intergrowths of the two (Fig. 12) and by the screens and pockets of plagioclase between adjacent microclines. These screens, pockets, and inclusions of sericitized plagioclase (Fig. 1, Plate 11) from the groundmass are enclosed by fresh microcline that forms megacrysts. These same features are found in the augen gneisses and inclusions where the growth can safely be assumed to have taken place in a solid medium. The K-feldspar tended

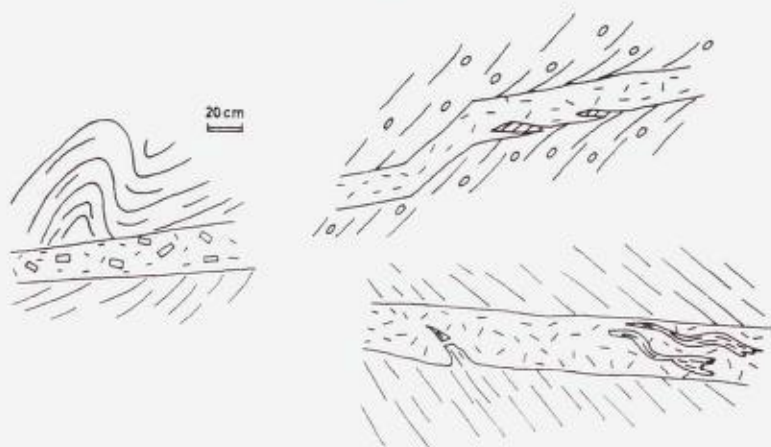


Fig. 17. *Granitic dikes outside the granite contact. Foliation in dike parallels its contacts. Some gneiss fragments in the dike appears to be displaced others do not.*

Granitiske ganger utenfor granittkontakten. Foliasjon i gangen er parallell med dens grenser. Noen gneisbruddstykker i ganger ser ut til å være flyttet; andre ikke.

to form megacrysts largely at the expense of plagioclase, and at least the conclusion of this phenomenon has occurred in a solid medium.

The megacrysts are porphyroblasts. Of particular importance is the fact that the fine-grained granite has the same composition as the porphyritic variety, and this is the minimum-melting composition (Tuttle and Bowen, 1958). The shearing which has imparted the present foliation to the granite outlasted the porphyroblastesis; this shearing conforms to the outlines of the granite.

Inclusions.

Inclusions may be found anywhere within the granite; however, they are most common at the contacts. Inclusions also occur in coalescing dikes and sills within the gneisses. Inclusions within the granites at a distance from the borders appear to be restricted to inclusion-rich areas whose extent may be large.

Veined Inclusion (240B)

The rock is found at the west end of Øvstevann (24.1, 1-01.9). The veined gneiss occurs as an 80-cm-long elliptical inclusion with a rectangular cross section. The numerous inclusions are randomly oriented in porphyritic granite.

The long axis of the inclusion is approximately vertical. The inclusion is composed of alternating biotite-rich and felsic layers. Some felsic layers contain concentrations of pink K-feldspar along their center. In thin section, the rock is chiefly composed of microcline perthite, plagioclase, quartz, and biotite. Muscovite, chlorite, opaque minerals, and zircon occur in accessory amounts. The texture is lepidoblastic. Microcline has two habits, as coarsely perthitic 3—4 mm poikiloblasts in the veins and as interstitial micropertthitic 0.4 mm crystals in the biotite layers. The poikiloblasts may or may not be grid twinned; the interstitial microcline shows a hazy twinning and is micro-to nonperthitic. Many of the larger microcline crystals are untwinned but extinguish obliquely (16°). The poikiloblasts contain variable amounts of long film and flame perthite. Microcline is much more common in the felsic veins. Plagioclase occurs in xenoblastic grains 0.5—1.5 mm in diameter. Plagioclase is polysynthetically twinned with some pericline twinning. Twin lamellae in some crystals are bent. Plagioclase is heavily sericitized in the layers containing microcline and shows clear more sodic rims where it touches microcline. Antiperthitic patches of hazily twinned microcline that have a common optical orientation occur in plagioclase crystals similar to those in Fig. 2, Plate 2. Quartz is xenoblastic and shows undulatory extinction and some granulation. Quartz attains a diameter of 3 mm in the felsic veins and 0.3 mm in the biotite-rich layers. Biotite ($Z, Y =$ reddish brown, $X =$ tan) occurs along layers in ragged laths. Biotite is altered to both chlorite and muscovite. Biotite is almost entirely chloritized in the felsic veins. The rock mode appears in Table XIII.

Spotted-Gneiss Inclusion (Sp 359)

The rock is found by nedre Kolsjöen (20.3, 0-48.4) where it occurs as an inclusion in porphyric granite just inside the granite contact. Numerous inclusions here are in different stages of transformation. Some inclusions are unaltered amphibolite. This rock (spotted gneiss) represents an early stage in the transformation of an amphibolite inclusion. The plagioclase and hornblende form 1-cm clots and impart a spotted appearance to the rock. At a further stage of transformation, hornblende is no longer visible, and scattered clots of biotite are present in a felsic groundmass. In thin section, the rock is chiefly composed of plagioclase, biotite, hornblende, quartz, and microcline. Sphene, opaque minerals, zircon, apatite, chlorite, epidote, and hematite occur in accessory amounts. The texture is granoblastic and very uneven; the grain size of the groundmass is *ca.* 0.5 mm. Plagioclase occurs in both idioblastic crystals and in lathlike subhedral crystals in the groundmass. The idioblasts are always progressively zoned and exhibit an euhedral outline that has small-scale embayments. Plagioclase idioblasts contain oriented hornblende and biotite from the groundmass. Plagioclase is polysynthetically twinned and, in the groundmass, is Carlsbad twinned. Plagioclase is sericitized in patches. A small amount of myrmekite occurs between plagioclase and microcline. Microcline occurs as interstitial fillings and as antiperthitic patches in plagioclase. Microcline is indistinctly twinned and almost nonperthitic. Hornblende ($Z =$ blue green, $Y =$ green, $X =$ pale greenish yellow, $Z \wedge c = 20^\circ$) is highly corroded and is sieved

with quartz inclusions. Hornblende occurs in widely scattered patches. Biotite (Z, Y = olive green, X = tan) occurs in xenoblastic laths. Some biotite is bent. Quartz occurs interstitially and forms some of the smallest grains in the groundmass. The quartz has a moderate undulatory extinction except for the quartz inclusions in hornblende which are unstrained. Sphene is a very common accessory mineral. The rock mode appears in Table XIII.

Transformed Biotite Gneiss (Sp 542A)

The rock is found 2 km west of Övstevann (23.9, 1-02.0) where it appears to be a medium-gray fine-grained granite with widely scattered porphyroblasts of K-feldspar, quartz, and plagioclase. The rock grades laterally into biotite gneiss and is bordered by lighter gray even-textured, fine-grained granite. Fig. 63 of a similar rock shows the effect of shear on the texture. The rock forms a dark smeared-out shadow in the fine-grained granite. Shearing is instrumental in destroying the layering of the gneiss and homogenizing it. In thin section, the rock is chiefly composed of plagioclase, quartz, K-feldspar, and biotite; opaque minerals, apatite, and zircon occur in accessory amounts. The texture is granitic to granoblastic. The groundmass is composed of 0.5- to 1-mm crystals; the porphyroblasts attain a length of 8 mm. K-feldspar occurs sporadically as xenoblasts and in interstitial films and grains in the groundmass. Some K-feldspar xenoblasts are progressively zoned. Progressive zoning in plagioclase is common; some plagioclase porphyroblasts exhibit oscillatory zoning that follows euhedral crystal outlines. K-feldspar patches appear in the larger plagioclase grains. Plagioclase inclusions that are irregularly distributed in microcline porphyroblasts are highly corroded and are oriented so that they extinguish together and with the film perthite. These inclusions are elongated along the perthite direction and are commonly contiguous with a perthite film. Twinning in the K-feldspar is found sporadically and is most common in narrow subparallel strips within a grain. Both coarse film perthite and flame perthite occur in the K-feldspar porphyroblasts; very fine film perthite occurs in K-feldspar of the groundmass. Plagioclase is polysynthetically twinned. The twin lamellae are bent in some grains. Antiperthitic K-feldspar patches occur in the largest plagioclase grains in the groundmass. Both sericitization of the plagioclase and myrmekite occur only sporadically. Biotite (Z, Y = reddish brown, X = tan) forms both ragged and idioblastic laths. The rock mode appears in Table XIII, and a partial chemical analysis appears in Table XIV in the Appendix.

Inclusions exhibit all stages of transformation to granite and are, in places, only recognizable by thin widely separated septa of biotite. The transformation of inclusions follows two general paths: 1) Well foliated gneisses are granitized along foliation planes. 2) More massive amphibolites become filled with feldspar porphyroblasts until they appear granitic (Fig. 18).

Since most of the gneisses are foliated, the transformation of in-

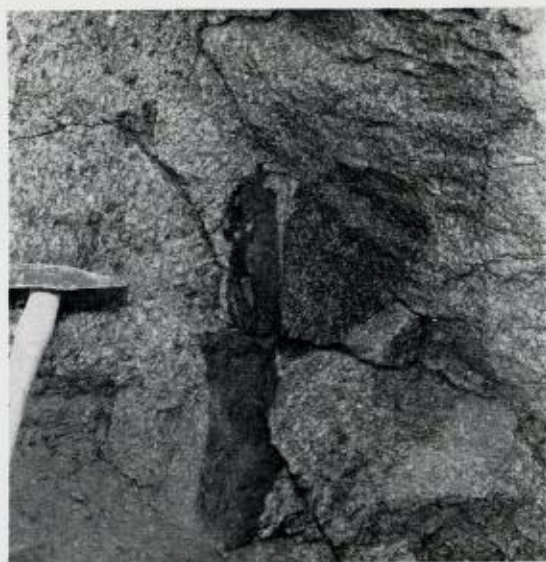


Fig. 18. *Rounded biotite-rich area in porphyric granite marks the position of an almost completely transformed inclusion. The uniform texture suggests that this was originally an amphibolite. Biotite clots near the hammer.*

Avrundet biotitrikt område i porfyrisk granitt markerer beliggenheten av en nesten fullstendig omvandlet inneslutning. Den ensartede tekturen tyder på at dette opprinnelig var en amfibolit. Biotit partier ved siden av hammeren.

clusions generally follows the first path. The gneisses are usually veined and migmatitic before they are incorporated into the main body of granite. Fig. 19 b shows a veined inclusion at the south end of the Hedal granite. This veining presumably continues until the final stage is reached where the presence of foreign matter is only recognizable from thin septa of biotite (Fig. 19 a). Apparently the biotite has concentrated in these septa which are solely composed of biotite. The mode of Sp 240 B demonstrates that these inclusions have attained the composition of the granites even though their origin is immediately apparent from the distinct biotite septa. Fig. 19 a shows that the fold pattern of an inclusion is retained by a biotite septum that is "swimming" in granite.

Until the final stage of transformation, the edges of the inclusions are perfectly sharp and clear. With one exception whose significance is debatable no reaction rims have been found surrounding the inclusions.

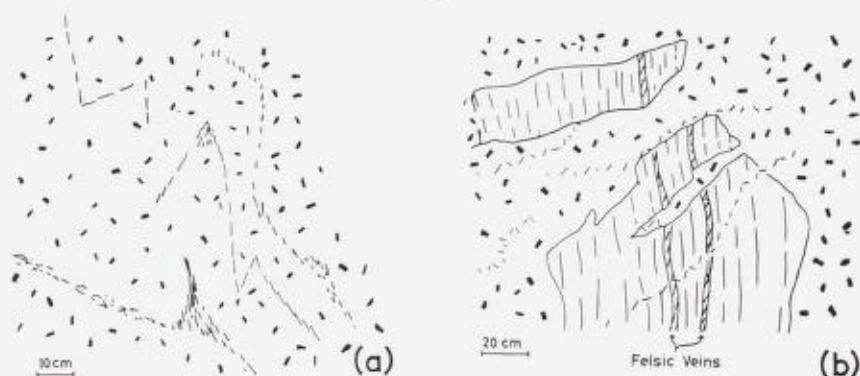


Fig. 19. (a) *Biotite-rich septa in granite. The fold pattern is preserved.* (b) *Veined inclusion of biotite gneiss in the granite. A fragment at the top is undisturbed. Thin irregular pegmatites cut both rocks.*

(a) Tynne biotitrike plater i granitt. Foldemønsteret er bevart. (b) Båndet inneslutning av biotitgneiss i granitten. Et bruddstykke øverst er uforstyrret. Tynne uregelmessige pegmatiter kutter begge bergarter.

Amphibolitic gneisses maintain their uniform appearance during their transformation. The first stage is presumed to be the formation of a spotted gneiss in which the felsic and mafic minerals are clustered in light and dark patches. Then plagioclase porphyroblasts form accompanied by K-feldspar as films in the groundmass and patches in antiperthitic plagioclase. Finally K-feldspar forms porphyroblasts and the mafic constituents are removed until the rock resembles porphyric granite. If the inclusion is still unusually rich in biotite, it will appear as patches and shadows of darker granite (Fig. 18).

Inclusions that pass gradually into granite occur at one place, Muggedalen (41.4, 1—05.0) at the northeast border of the Heddal granite. Here an augen gneiss inclusion (Fig. 20) with a swirly foliation marked by biotite septa passes gradually into foliated granite in which individual biotite flakes are oriented to impart a foliation. The K-feldspar augen lose their oval shape and become more euhedral. The mode of this rock (Sp 482 D) is almost the same as the mode of the typical granite (Table VII). The texture resembles that of a weakly sheared porphyric granite. The one distinct difference between this rock and the porphyric granite is that the K-feldspars in the augen gneiss inclusion are randomly disordered.

Another unusual but somewhat similar occurrence is found in

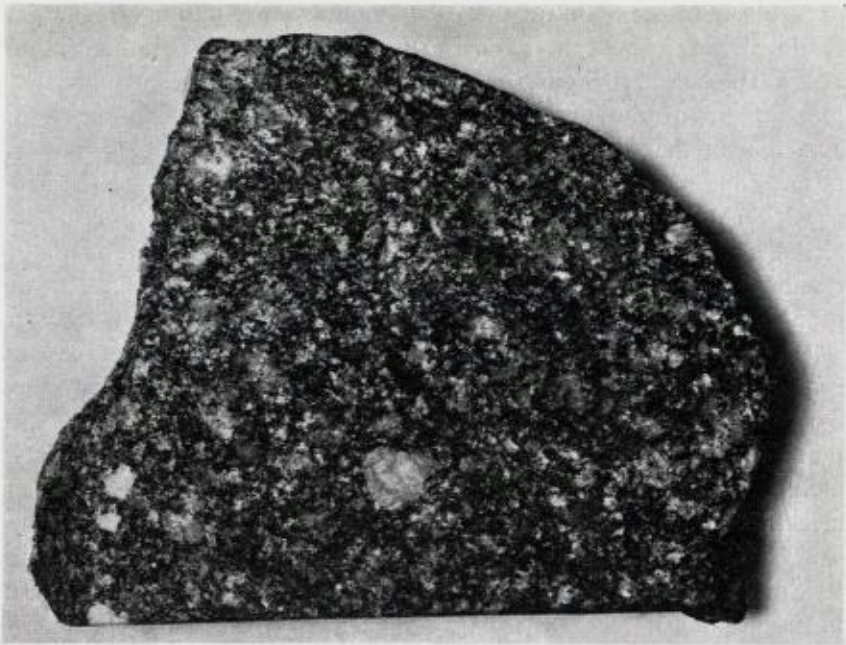


Fig. 20. *Rock that is transitional between augen gneiss and granite. This constitutes one of the few gradational occurrences from gneiss to granite. Some of the microcline porphyroblasts in this rock are randomly disordered (Sp 482, Fig. 61).*

Bergart som danner overgang mellom øyegneiss og granit. Dette representerer en av de få gradvise overganger fra gneiss til granit. Noen av mikroklin porfyroblastene i denne bergart er "randomly disordered".

Muggedalen. Inclusions of veined gneiss pass laterally into banded fine-grained granite. The banding is produced by alternating biotite-rich and biotite-poor zones; the rock is highly sheared. The mode (Sp 486) is that of a typical granite. These inclusions were transformed and sheared to form beautiful "flow layers" or schlieren (Balk, 1937) of granite tectonics.

Shear has influenced the two general kinds of inclusions in two ways. The foliated inclusions are smeared out and homogenized (petrographic description 542 A and Fig. 11). The more massive amphibolitic inclusions appear rounded like fragments in a breccia zone (Fig. 18) and may have been rolled and abraded by shearing.

In fresh exposures dark biotite-rich shadows are common,

particularly in the "tail" of the Ådal granite where biotite streaks and shadows are present in almost every square meter of the granite (Figs. 10 and 11). Signs of foreign material are most common near the borders of the granites; however, so few fresh exposures are available in the centers of the granites that this impression may be false. Signs of transformed gneiss are visible in most of the roadcuts along the road through Hedal that crosses the northern part of the Hedal granite. The evidence suggests that the transformation of inclusions has played an important role in the development of the granite; a quantitative estimate is not possible.

The delicate fold patterns and the biotite septa enveloped by granite (Fig. 19 a) are interpreted to be the remnants of transformed inclusions. The preservation of these features precludes the possibility that the granite immediately surrounding them, which is of minimum melting composition, attained fluidity, or that the inclusions were ever mechanically disintegrated and dispersed (Bowen, 1928).

The quantitative composition of the inclusions attempts to attain that of the granite (Fig. 13). If biotite septa or dark shadows are seen in the granite, its descent from a fragment of gneiss is recognized; if these concentrations of biotite disappear, the patch of rock that was formerly an inclusion is regarded to be "typical granite". The external outlines of an inclusion, which are so commonly retained up to the final stage of transformation, indicate that the process was one of volume for volume replacement. The reaction principle of Bowen (1928) was not followed strictly because it must result in a volume increase (Bowen, *ibid.*).

Inclusions commonly have angular outlines (Figs. 19 b and 45 a). The corners of inclusions are usually sharp even when the only indication of the inclusion is biotite septa spaced 1 to 2 cm apart. Adjacent inclusions that apparently had the same initial composition exhibit considerably different degrees of transformation.

Special features of inclusions are important for an understanding of similar features in the granite and the gneiss. Inclusions that are in the earlier stages of transformation contain monoclinic and/or randomly disordered K-feldspar and antiperthitic plagioclase grains with patches of K-feldspar. The plagioclase in some massive inclusions that are presumed to represent altered amphibolites is commonly zoned. The zoning which may be either progressive or oscillatory occurs most commonly in the plagioclase porphyroblasts. One porphyro-

blast has at least 8 zones that sharply define a euhedral outline (Fig. 2, Plate 9). Zones of the same composition are repeated two or three times. The outer zone of some porphyroblasts is equally calcic as the core. Other grains are progressively zoned toward a more sodic margin.

The same inclusion also shows a Rapakivi texture. A few of the microcline porphyroblasts are mantled or partially mantled by a rim of plagioclase (Fig. 1, Plate 10). This feature is very sporadic.

Microcline porphyroblasts in this inclusion contain oriented inclusions of plagioclase whose (010) faces parallel (010) of the microcline. These do not occur in successive box-shaped rims like those that Maucher (1943) and Frasl (1954) have described. Some microcline porphyroblasts are seen to have enveloped plagioclase inclusions at their margins while the plagioclase grains in the groundmass were crowded away from the porphyroblasts with their long direction parallel to the adjacent crystal face of the microcline (Fig. 2, Plate 10).

As might be expected, the inclusions are generally richer in mafic minerals and plagioclase (Figs. 13 and 14) than the granite is. The compositions of inclusions tend toward the composition of the granite (Figs. 13 and 14), and two inclusions have the same composition as the granite.

Pegmatites.

Pegmatites are widely scattered over the area as small eyes that grade into concordant layers in the gneiss, thin tabular crosscutting bodies, and irregular 5-to-10-m-wide crosscutting bodies. They are mostly of granitic composition; no rare-mineral pegmatites have been observed.

Pegmatite Sp (219C)

The rock is found just north of Gulsvik (23.0, 1-17.1). The pegmatite occurs as an irregular lense-to-podlike body with a vertical dike-like projection that forms an inverted *T* (Fig. 21 a). The pegmatite is composed of microcline, plagioclase (An_{18}), quartz, biotite, muscovite and garnet. The pegmatite contains 10- to 20-cm crystals of microcline perthite in a groundmass of microcline, plagioclase, quartz, and muscovite. Crosshatched microcline perthite occurs in the groundmass; this microcline interfingers along the polysynthetic twinning and intermixes with plagioclase. The plagioclase inclusions in microcline extinguish simultaneously. Where microcline and plagioclase interfinger along twin lamellae, the twin lamellae in the microcline have the same general

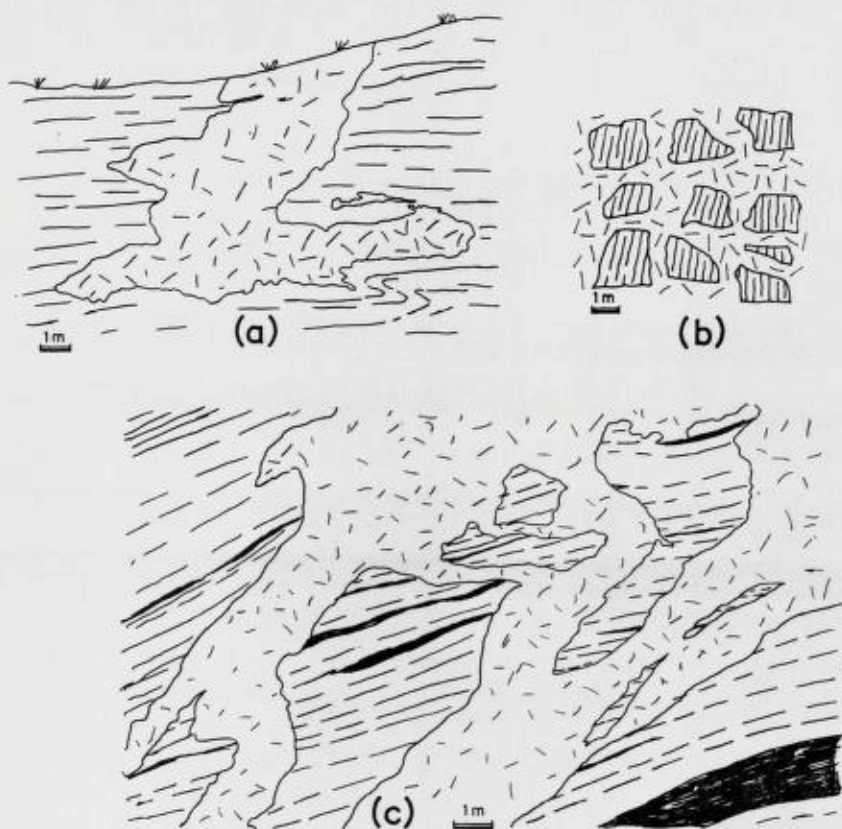


Fig. 21. (a) Granitic garnet-bearing pegmatite that passes from a discordant dike into a partly concordant lens. The country rock is banded granodioritic gneiss. Gulsvik in Hallingdal. (b) Pegmatite that interweaves non-displaced fragments of gneiss. (c) Granitic pegmatites intermixed with fine-grained granite. No displacement of the enclosed fragments of banded granodioritic gneiss is apparent. Four km SE of Flå in Hallingdal.

(a) Granitisk granatførende pegmatit, som går fra en diskordant gang over i en delvis konkordant linse. Den omgivende bergart er båndet granodioritisk gneis. Gulsvik i Hallingdal. (b) Pegmatit mellom uforstyrrete gneisbruddstykker. (c) Granitpegmatiter blandet med finkornet granit. Ingen flytting av de innesluttete bruddstykker av båndet granodioritisk gneis er synlig. 4 kilometer SØ for Flå i Hallingdal.

orientation as those in the plagioclase. The plagioclase of the perthite is developed on three scales: as long thin veins, as thin films normal to the veins, and as very fine films parallel to the veins. Large areas of plagioclase and quartz are completely free of microcline except for a few small patches in the plagioclase. Plagioclase occurs in 1.5 mm grains that are polysynthetically twinned. Plagioclase is sericitized, and sodic rims are found between plagioclase and microcline. Myrmekite occurs in subordinate amounts. Some plagioclase grains are deformed. Quartz occurs in xenoblastic 2-mm grains that show a weak undulatory extinction. Garnet occurs in 1.5–3 mm euhedral grains. Biotite occurs along fractures and some chlorite is developed around the margin of the garnet crystals. Muscovite occurs in xenoblastic crystals within plagioclase. The pegmatitic microcline crystals contain vein (*ca.* An₈) and film perthite; the vein perthite forms at an angle of 63° with (001). Film perthite occupies the areas between the veins and is less abundant immediately adjacent to the veins. Perthite veins abut against plagioclase inclusions and, in some instances, embay the plagioclase inclusions. The perthite veins show the incipient development of polysynthetic twins normal to the vein boundary. Pegmatitic plagioclase is perfectly fresh in contrast to the groundmass plagioclase; 1-mm muscovite crystals occur along the cleavage of the plagioclase.

Tabular Pegmatite (Sp 373B)

The rock is found at the north end of övre Kolsjöen (21.7, 0-48.2). The pegmatite occurs as a 5-cm-wide tabular body that cuts the porphyric granite and dips gently toward the center of the granite. Pink microcline crystals attain a length of 4 cm. Plagioclase, quartz, and biotite are also present in major amounts. Numerous other pegmatites which may be as thin as 1 cm cut the granite and have the same mineralogy and general appearance. The rock is chiefly composed of microcline perthite, plagioclase (An₁₁), quartz, and biotite; muscovite occurs in accessory amounts. Microcline may be both Carlsbad twinned and grid twinned. Both film perthite and vein perthite occur in the same grain. Vein perthite grades into patch perthite. Plagioclase pockets occur at the contact between two microcline grains. A strip of granular plagioclase occurs at the contact between a microcline grain and a plagioclase grain. The distribution of film perthite is uneven. Plagioclase is polysynthetically twinned. Twin lamellae in some plagioclases are bent. Myrmekite is commonly found. The quartz rods of the myrmekite may be very wide (0.4 mm). Some of the myrmekitic quartz is inclosed by the microcline. Plagioclase is sericitized in scattered patches. Xenoblastic muscovite crystals occur in plagioclase.

Pegmatites exhibit a highly varied development in the Flå area. The occurrences range from 15-cm single crystals of microcline to 10-m-wide lenses containing 1-m microcline crystals. Two typical mineral parageneses are recognized. These contain microcline, plagioclase, quartz, and biotite (or chlorite) and microcline, plagioclase,



Fig. 22. Lenticular granite pegmatite emplaced in the Heddal granite. Irregular patches of granite are retained within the center of the pegmatite. Storruste in Hedalen.

Linseformet granittpegmatit i Heddal-granitten. Uregelmessige flekker av granitt er blitt igjen i midten av pegmatiten. Storruste i Hedalen.

quartz muscovite and garnet. The first type is ubiquitous; the second type is generally excluded from the immediate environs of the granites and occurs on the east side of Sperillen and in Hallingdal.

Synkinematic pegmatitic stringers and eyes (Fig. 50) which are restricted to the first paragenesis occur fairly commonly along the foliation. These are usually boudinaged. Most of the pegmatites are crosscutting late-kinematic bodies that, in thin section, show some effects of deformation.

Thin planar or lenticular pegmatites of the first paragenesis are found within the granite (Fig. 22). These seem to have been emplaced along potential tensional fractures and are in turn somewhat crushed. They tail out and begin again along their strike. These planar pegmatites in the granites are very similar to the granites in mineralogy and texture. Some of these envelope irregular patches of the granite and seem to simply represent an advanced stage of megacryst formation

(Fig. 22). The microcline perthite of these pegmatites has a greater plagioclase content than microcline perthites from the granite.

Structural control of pegmatites in the gneisses is indicated where pegmatites are emplaced along fractures and necks of boudins. Although the course of the pegmatite may be somewhat sinuous, definite directions predominate (Fig. 42). These directions are north to north-west and their normals.

The gneisses along the west side of the Hedal granite are interspersed with a net of pegmatites (Fig. 21 b). The blocks of gneiss cut up by the pegmatites show no signs of rotation.

Pegmatites are found in abundance along the main road through Hallingdal. These pegmatites are usually intermixed with fine-grained granite. No displacement of the fragments of banded gneiss enclosed by the pegmatites is evident (Fig. 21 c). These pegmatites must have been emplaced passively.

Eocambrian and Cambro-Ordovician Rocks.

Dark Cambrian slates overlie the Hedal granite at its northernmost exposures. The slates are in turn overlain by Eocambrian sandstones that have been thrust into their present position. The contacts of these rocks are taken from the map of Strand (1954).

The Cambrian slates are deposited on an erosion surface that planes off the crystalline basement rocks of the Precambrian. This surface slopes gently to the north-northeast at a gradient of about 1 : 50 (Strand, *ibid.*).

Permian Dikes.

Permian dikes that are associated with the Oslo igneous province are found commonly in the southern and southeastern parts of the area. These dikes range from 0.5 m to 20 m in width and from felsic to mafic in composition. An occurrence of a syenite porphyry dike on Treknatten (30.9, 0—51.4) is located along the strike of a syenite porphyry dike mapped by Strand (1954) in Muggedalen. Although intervening exposures are scarce (Strand, *ibid.*), this dike must be emplaced along a major fracture.

Tectonics

General Statement.

The tectonics of the area is treated in four sections: (1) The regional tectonics, (2) Granite tectonics, (3) Deformation associated with the granite emplacement, (4) Regional synthesis and conclusions.

The regional tectonic pattern is of prime importance for evaluation of the effects of granite emplacement; therefore, the establishment of the mode of granite emplacement requires a study of the country rocks as much as that of the granite itself. The object of the regional studies is to ascertain the regional geometry in order to demonstrate any changes that accompanied granite emplacement.

Regional tectonics.

Foliation.

The country rocks of the area are almost universally foliated. The foliation is marked by the orientation of platy minerals, by compositional banding, and, in places, by flattened quartz grains. This foliation is designated *S* after the terminology of Sander (1948). The foliation most likely reflects the original compositional layering (stratification) which may or may not have been altered by metamorphic differentiation. Most of the componential movements have probably been accommodated parallel to the layering.

The gneisses on the east side of the granite are often sheared along biotite-rich layers. Amphibolites, which are usually foliated and/or lineated, are the only country rocks which may be nonfoliated. The amphibolites interlayered with quartzites on the west exhibit strongly foliated biotite-rich borders against the quartzites. The greatest movement in these rocks took place at rock contacts and in biotite-rich layers.

Mesoscopic axial-plane foliation has been only rarely observed in scattered localities. The comparatively low content of micaceous minerals has presumably impeded the formation of axial-plane foliation.

*Linear Structures*¹.

The most common linear structures are axes of minor folds, crenulations, dimensional mineral orientation, necks of boudins (the linear narrow-down portion of the boudinaged layer), and striations. The interpretation of type and origin of the lineations will be deferred until the structural geometry has been discussed.

Folding Style.

Axial-plane profiles of folds (Fig. 23) appear to show two individual types, open "V" or chevron folds and strongly appressed, almost isoclinal folds. The two types, however, can be seen grading into each other and are variably appressed. The dip of the axial plane of the folds varies. Many folds have horizontal and vertical axial planes; and, among the folds with inclined axial planes, the majority are overturned to the east. The folds are generally typified by gentle western limbs, steep eastern limbs, and sharp narrow hinges.

Although some of the minor folds illustrated may be drag folds or shear folds, this is clearly not the case with others. Where these folds can be related to larger structures (Fig. 23), they are seen to be just as common at the hinge of the larger fold. These are probably parasitic folds, which de Sitter (1958) ascribes to flattening.

It is evident from the figures that both flexural-slip folds and slip folds exist. Most folds show characteristics of both types of folding; *i. e.*, they have thickened hinges but die out rapidly down the axial plane. Although slip folds are generally ascribed to deeper levels, folds that show undoubted characteristics of flexural slip are so common that flexural slip folding must have been common in the Flå area. The dominant folding process has probably been flexure folding followed by flattening and thickening of the fold hinges so that similar-appearing folds were produced (de Sitter, 1958; Ramsay, 1962).

¹ Linear structure is used for the general term, and lineation is reserved for a linear preferred orientation in a rock (Kvale, 1948, p. 25).

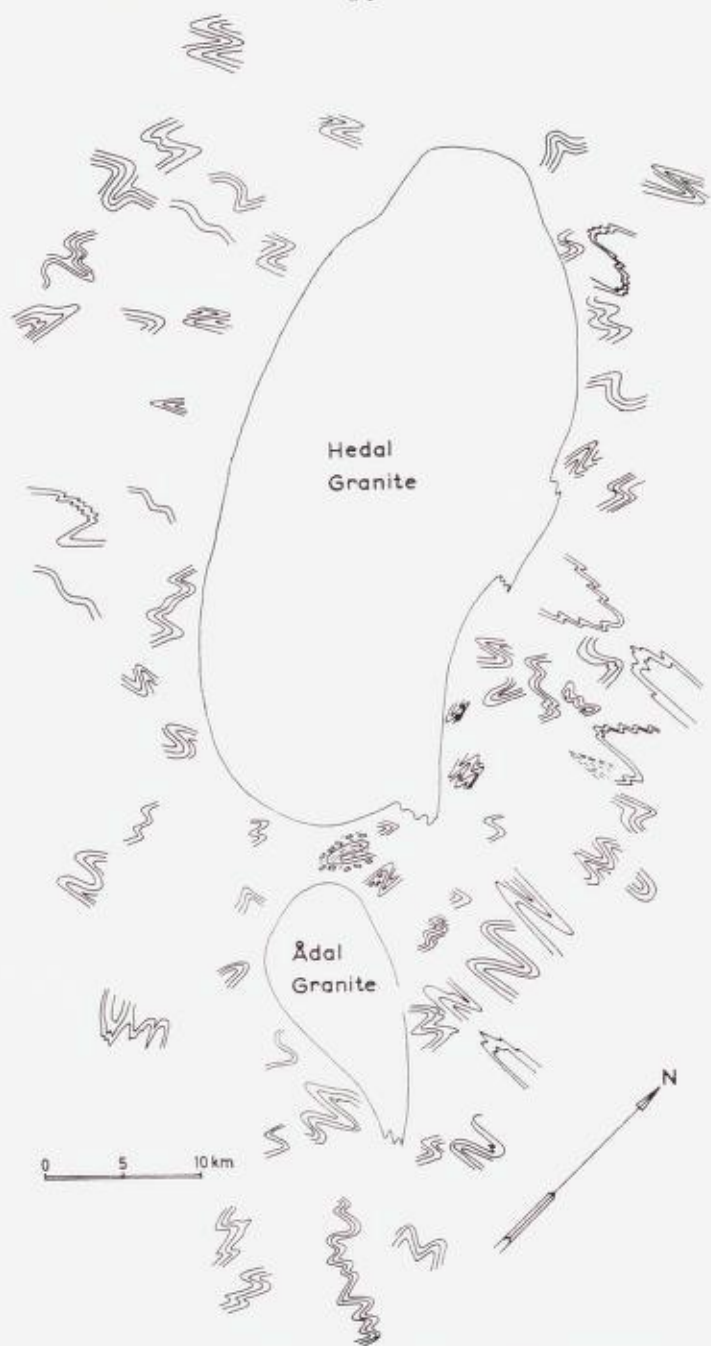


Fig. 23. Axial-plane profiles of folds showing their locations.
Akseplanprofiler av folder som viser deres beliggenhet.

Geometry of S and B.

Stereographic methods for defining the fold geometry have been proposed by Wegmann (1929) and applied more recently by Weiss and McIntyre (1957), Weiss (1959), and Ramsay (1960). The method offers a powerful tool in the study of the geometry of crystalline rocks where the stratigraphy is poorly or incompletely known. If the plotted poles to foliation planes (*S*) fall on a great circle, the folding is cylindroidal (Clark and McIntyre, 1951), and the fold axis is the normal to this great circle. This constructed fold axis is called the β axis (Sander, 1948, p. 132) and may coincide with the B^1 fabric axis.

Normally, the folding is only approximately cylindroidal and then only in a restricted area. The β axis is thus statistically defined by plotted poles that are scattered along a great circle. As the size of the area included in the measurements increases, the scatter increases until ultimately, in areas of complex folding, the poles become randomly distributed. The area around the granite is divided into 55 smaller subareas in which the folding generally approximates cylindroidal geometry (Plate 13). Most of the subareas have areas of 2 to 3 sq km except for subareas 2, 7, 12, 23, 29, and 40 which are about 100 m square.

Minor fold axes are plotted on the same stereographic projection as the *S* from the same subarea (Plate 13). If the folding is cylindroidal and represents a single monoclinic deformation, the plots of minor fold axes and other *B* lineations should cluster around the statistically defined β axis.

β axes, which are plotted together with the general strike of *S* (Plate 14), illustrate the macroscopic fold geometry of the gneiss. The data used to determine β and the geometry of *B* appear in Plate 13. The orientation of β indicates that north-or-south-and northwest-or-southeast-plunging folds characterize the fold geometry of the gneiss. The plunge is generally low to moderate. Near-vertical plunges of β are found along the east side of the Heddal granite and the west end of the Ådal granite. The geometry on the east side of the field area shows the greatest homogeneity; the geometry on the west and particularly the south side varies considerably.

Although most of the subareas exhibit monoclinic geometry for *S* and *B* as was intended, subareas 4, 5, 7, 10, 11, 12, 19, 27, 34, 35,

¹ All tectonic axes referred to in this discussion are the geometric (sym-metrologic) or fabric axes, not the kinematic axes.

37, 38, 39, 42, 44, 50, and 54 suggest a definition of either 2 β 's or girdles in B by the fabric elements. In either case, the fabric is triclinic on the scale of the subarea. For many of these, further subdivision did not eliminate the triclinic symmetry.

A further indication of geometry is provided by a comparison of the πS distribution (Plate 13) and the illustration of folds (Fig. 23). The πS maximum in each stereogram reflects the usual attitude of foliation within that area.

The east side of the area (delimited on Plate 13) shows considerable homogeneity in the synoptic diagram¹ for the geometry of πS (Fig. 24); however, B is distributed along a subhorizontal partial girdle. This girdle development of B requires overall triclinic geometry even though the regional πS appears to be tautozonal. As Weiss and McIntyre (1957) note, the proof of the overall fabric symmetry is in the orientation of β among the subareas; they demonstrate that a synoptic diagram from an area of superposed folding and triclinic geometry may yield a πS girdle (*ibid.* p. 588—89). The orientation of β over most of the eastern area diverges by about 44°² in trend and plunge. Although the structural geometry is triclinic, the variation is surprisingly moderate for so large an area of Precambrian gneisses.

The west-plunging β in subarea 1 is related to movements along the shear zone at Bagn. The significance of the near vertical β 's on the eastern side will be discussed in connection with the granite emplacement.

The attitude of S is generally subhorizontal from 4 to 10 km east of the Heddal granite. These predominant attitudes are reflected in the two S concentrations from the synoptic diagram (Fig. 24).

Gneiss, whose foliation is subhorizontal, is found east and northeast of Lake Sperillen. The mesoscopic recumbent folds found here are usually strongly appressed, and the fold hinges or limbs may be sheared out (Fig. 25) so that recognition of folds is difficult. Thin sections of these rocks (petrographic description 590 A) reveal considerable shearing localized along biotite layers parallel to the foliation. The fold limbs are compressed to near parallelism and the hinges are erased so that the gneiss appears to be unfolded over a wide area.

¹ Subareas with deformation attributed to the granite emplacement are excluded from the synoptic diagrams.

² A circle = 400g.

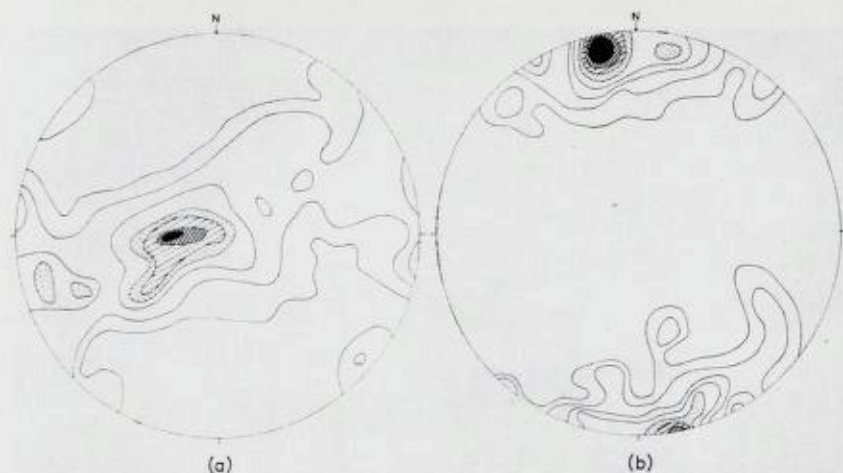


Fig. 24. Synoptic diagrams of the geometry from the eastern district (A) 257 π S; contours 7-6-4.5-3.5-1-0 per cent per 1 per cent area. (b) Axes of 100 minor folds, B; contours 14-12-10-8-6-4-2-0 per cent per 1 per cent area. Schmidt net. All stereo diagrams employ the lower hemisphere.

Samlediagram over geometrien fra det østre området (A) 257 π S: koter 7-6-4,5-3,5-2-1-0 prosent pr. 1 prosent areal. (b) Akser av 100 mindre folder 14-12-10-8-6-4-2-0 prosent pr. 1 prosent areal. Til alle stereo-diagrammer er brukt nedre halvkule. Schmidt nett.

Broad, low-amplitude undulations on axes plunging gently east to east-southeast were observed in subareas 13 and 15 and east of subarea 7. These undulations are the only crossfolds that have been found; however, greatly divergent minor fold axes were noted 3 km east of subarea 13 (32.1, 0—34.5). Although the orientation of β varies in the eastern area, a strong superposed regional folding seems unlikely since it is not manifested in the considerable area of flat-lying gneiss where it should be easily detected.

The south side of the area (delimited on Plate 13) shows a π S concentration at the intersection of several weakly defined girdles in the synoptic diagram (Fig. 26 a). B is distributed along an incompletely defined girdle. Both of these facts strongly suggest triclinic geometry which is confirmed by the orientation of β within the subareas where β varies considerably in trend and especially plunge. The structural geometry on the southern side seems to be the most complicated of the Flå area.

The π S concentrations in Fig. 26 a correspond to foliation striking

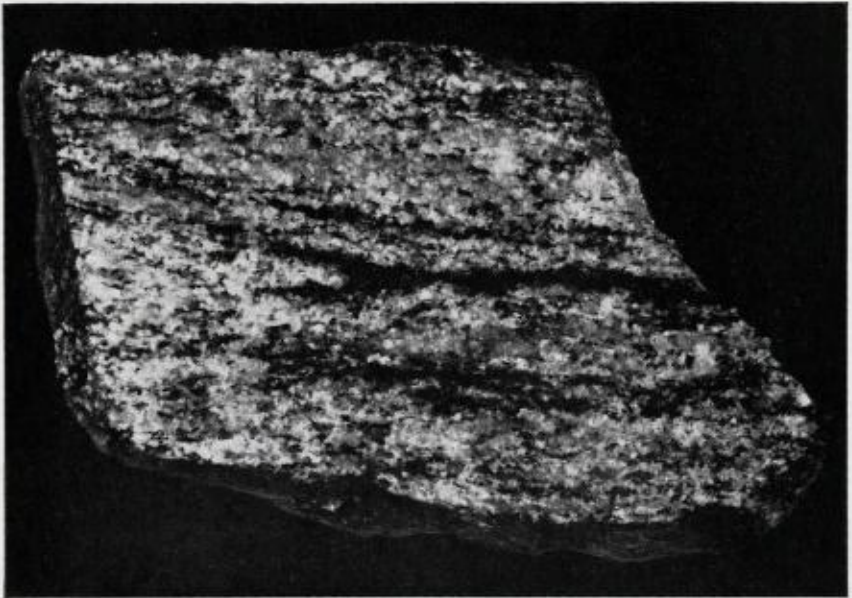


Fig. 25. Hand specimen of banded quartz-monzonite gneiss showing a fold hinge with sheared off limbs in a biotite layer.

Håndstykke av båndet kvarts-monzonitisk gneiss som viser ombøyningen av en fold med avskårne sider i et biotittlag.

northwest and dipping *ca.* 70° southwest. Chevron type folds are probably developed (Fig. 23) and have a dominant steep limb and an attenuated subhorizontal limb. The observed flat limb is expressed by the small closure in the center of the π S synoptic diagram.

Amphibolites are common in the banded gneiss on the southern side. Their relative competency and the development of amphibolite boudins may have influenced the geometry of the folds. In addition, several prominent fault zones run through this area. The necks of some boudins are parallel to *B*, others are parallel to *a*, and still others do not parallel any of the geometric axes. Necks of boudins that develop in *a* would cause a weak rotation normal to *B* and form an apparent β' axis.

The uniform attitude of the foliation demonstrates the susceptibility of these gneisses to yield secondary π S girdles. Either boudinage non-parallel to *B* or fault drag will rotate the foliation of the gneisses around secondary axes unrelated to the regional folding. Drag

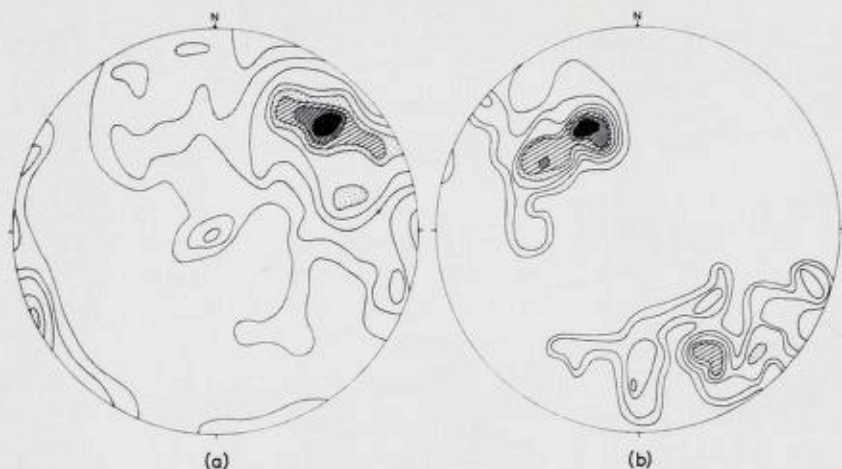


Fig. 26. Synoptic diagrams of the geometry from the southern district. (a) 250 πS from the south side of the area; contours 8-7-6-5-4-2.5-1 per cent per 1 per cent area. (b) Axes of 57 minor folds, B; contours 11-9-7-5-3.5-1-0 per cent per 1 per cent area. Schmidt net.

Samlediagram over geometrien i det sørlige område. (a) 250 πS fra sørsiden av området. Koter 8-7-6-5-4-2,5-1 prosent pr. 1 prosent areal. (b) Akser fra 57 mindre folder, B; koter 11-9-7-5-3,5-1-0 prosent pr. 1 prosent areal.

along a breccia zone is suggested to be the cause for the greatly divergent geometry of subarea 28, and either boudinage or fault drag may have caused the spreading of πS in subarea 26 and 27.

Some boudinage is developed parallel to neither *a* nor *B* of a subarea. This in itself renders the fabric triclinic so that superposed deformation is a possibility, especially because the overall geometry is triclinic.

The west side of the area (delimited on Plate 13) shows a πS concentration at the intersection of a moderately well defined girdle and a poorly defined girdle in the synoptic diagram (Fig. 27). *B* defines an almost complete subhorizontal girdle. The overall triclinic fabric is demonstrated by the synoptic diagrams and by the variability of β within the subareas.

The symmetry of the πS diagrams can be related to the mesoscopic folding style. Most of the observed folds are appressed chevron folds in which both limbs dip southwest. This general attitude is expressed by the corresponding position of πS concentrations in the subareal stereograms and in the synoptic πS diagram.

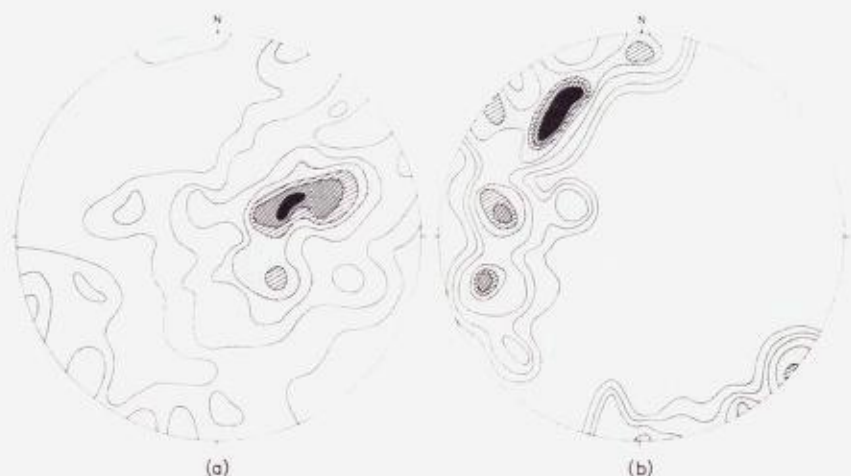


Fig. 27. Synoptic diagrams of the geometry from the western district. (a) 273 πS , contours 7-5.5-4.5-3-2-1-0 per cent per 1 per cent area. (b) Axes of 65 minor folds, B; contours 10-8-6-3.5-1.5-0 per cent 1 per cent area. Schmidt net.

Samlediagram over geometrien fra det vestlige område. (a) 273 πS , koter 7-5,5-4,5-3-2-1-0 prosent pr. 1 prosent areal. (b) Akser fra 65 mindre folder, B', koter 10-8-6-5-3-1,5-0 prosent pr. 1 prosent areal. Schmidt nett.

A second girdle about a southwest-plunging axis is evident in subarea 44. Boudinage with approximately the same axis was observed in amphibolite layers from 10 to 20 m thick. The second girdle in subarea 44 and the scatter of πS in subarea 46 are ascribed to boudinage; however, they may also be examples of folds forming in α (Strand, 1944; Balk, 1953).

All β axes from the entire Flå area including those probably disturbed by the granite emplacement appear in Fig. 28. Their orientations exhibit a tendency toward girdle development; this fact is additional confirmation of the overall triclinic symmetry for the structural geometry. The distribution of β is surprisingly similar among the three districts.

Faults and Fractures.

A medium-angle reverse fault strikes north-south 3 km east of Nesbyen in Hallingdal (34.5, 1—32.5). The fault plane is poorly exposed, but the topography and prominent fractures suggest that the fault plane dips to the west at about 35°. Along highway 20 in Hallingdal (29.3, 1—30.2), small thrust faults are exposed in a roadcut

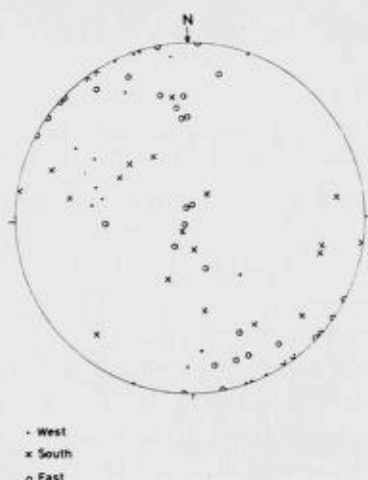


Fig. 28. Synoptic diagram showing the geometry of all β axes. Wulff net.
Oversiktsdiagram over alle β akser. Wulff nett.

(Fig. 29) near the trace of the major fault. The fault surface and other fractures are filled with epidote and K-feldspar. Folding here is isoclinal; drag in the quartzites and amphibolites shows that the relative movement has been an overthrusting to the east.

A zone of mylonite and augen gneiss crops out at Bagn in Begndal (Plate 1) and again at Bruflåt in Etnedal (Strand, 1943, 1954). This zone is developed between the plagioclase gneisses to the north of

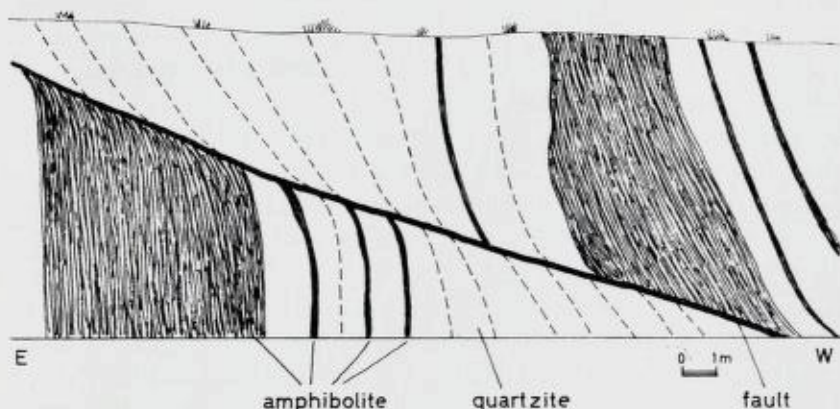


Fig. 29. Thrust fault in Telemark orthoquartzites and amphibolites.
Foldeforkastning i Telemark ortokvartsit og amfibolit.

Bagn and the granodiorite gneiss to the south and separates the two gneiss areas. The mylonite zone dips *ca.* 35° to the north under the plagioclase gneisses. In the south part of the zone the rock is an augen gneiss in which the quartz is highly granulated and the other minerals are less granulated (petrographic description 420 B). On the north side, the rock becomes a true mylonite in which K-feldspar augen rest in a flinty, fine-grained matrix.

The field evidence indicates that this zone separates gneisses of markedly different composition. Strand (1949) named this zone a front for the formation of K-feldspar. There is little doubt that K-feldspar has formed in the gneiss along this shear zone and, in turn, been sheared. Strand (1943, 1954) has found evidence for a supra-crustal origin of the plagioclase gneisses north of the shear zone and has called this zone a migmatite front (1949). This shear zone might, therefore, be regarded as the *Abscherungszone* of Wegmann (1935) that separates the migmatitic infrastructure from the nonmigmatitic superstructure.

Numerous faults and breccia zones are found in the area (Fig. 30). The most prominent of these is the northern extension of the great friction breccia (A. Bugge, 1928; Selmer-Olsen, 1950) which runs all the way from Kristiansand. Like the southern breccia, the northern one branches out. This fault is marked by fractures, which are filled with either quartz and plagioclase or epidote and by mylonites. These veins are again sheared; the upthrown side is on the northwest. The displacement along the breccia zone is unknown but the rocks are similar on both sides of the fault.

The fractures of the area are most commonly developed in two major directions, northeast and northwest (Fig. 30) and have near vertical dips. Most of these are joints but some of them are minor breccia zones marked by thin mylonites and rock breccias. The fractures have approximately the same attitude inside and outside the granite contacts but are more prominent inside the granite.

A series of north-south striking fractures which are presumed to date from the Permian is also found, particularly in the southern part of the area. The great rhomb porphyry dike (Brögger, 1933 b) follows one of these fractures. It has in turn been fractured and cut by quartz veins; therefore, movement has been recurrent. Other smaller Permian dikes follow north-south lines of weakness, and a syenite dike strikes 170° for a long distance. The displacements along these faults and fractures are not known because good markers are lacking.

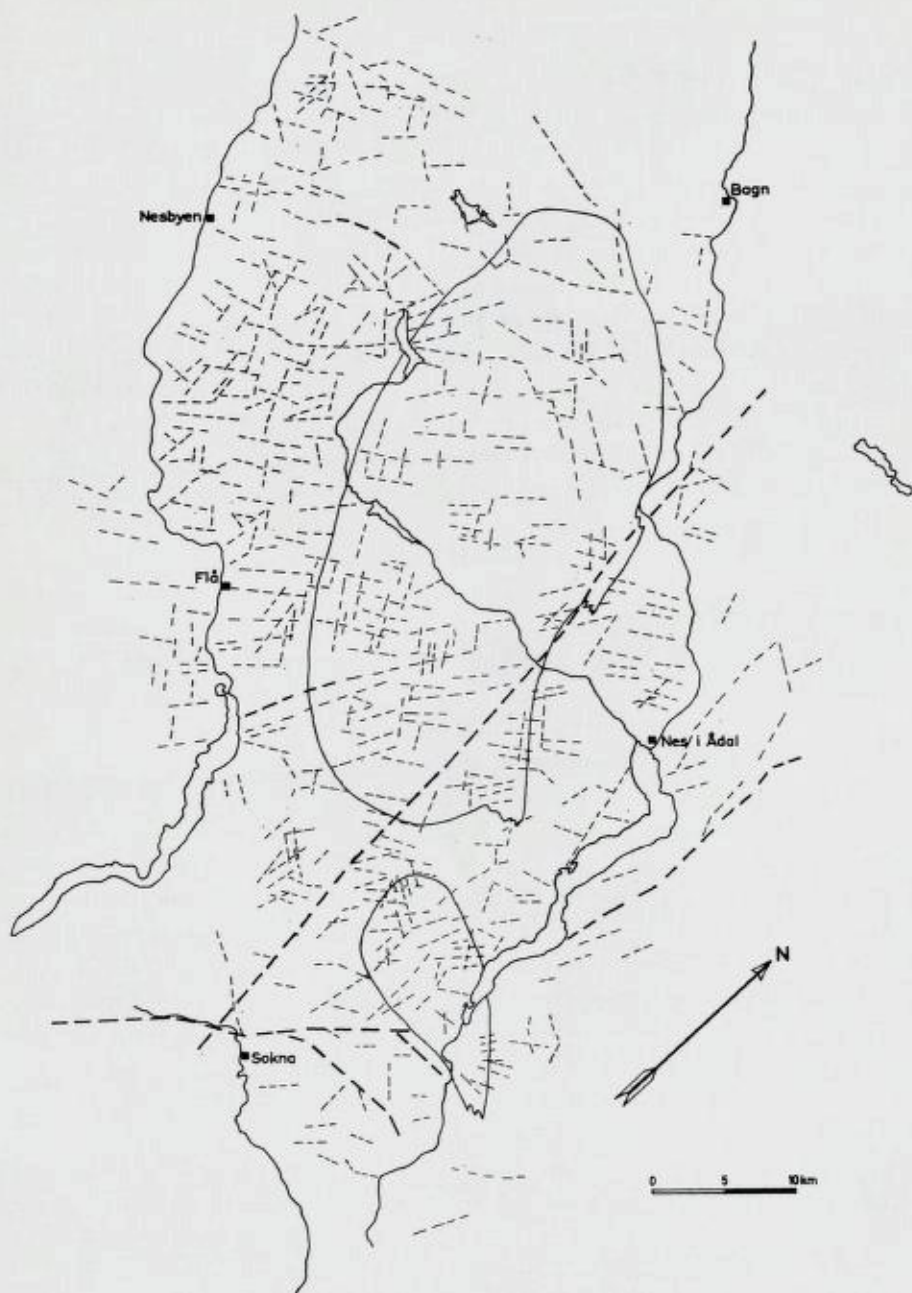


Fig. 30. Map of faults and fractures. The heavier line designates major fractures.
Kart over forkastninger og brudd. Den tykkere linje betegner større sprekker.

Geometry of Linear Structures.

Sander (1948) attaches great importance to lineations for determining the movement picture. Probably lineations have most commonly formed in a B direction, but the difficulties in relating movement directions to lineation alone have been pointed out by Strand (1944), E. Cloos (1946), and Kvale (1948, 1953).

Cloos (*op. cit.*) states that lineation may form in either a or b . Kvale (1948) notes that lineation which represents the direction of least resistance may develop at any angle to the principal movement direction in metamorphic rocks, and H. Cloos (1936) has mentioned the same principle in granite tectonics. Turner (1957) points out that many lineations that appear to coincide with the regional a direction may actually represent local B lineations.

Minor-fold axes. Minor-fold axes are shown in the πS diagrams (Plate 13) to generally coincide with the β axis. They may, therefore, be regarded as fairly reliable B lineations.¹

Boudinage. Boudinage is a phenomenon that reveals an extension direction (E. Cloos, 1946; Ramberg, 1955) and is, therefore, of great importance for interpreting the movement picture. Unfortunately it is often difficult to observe. Boudinage (Fig. 31) has been observed in amphibolite layers up to 15 m thick and may be assumed to exist on a still larger scale. The orientations of the "necks" of boudins are measured as a linear structure.

The orientation of boudins appears in Fig. 32; it is expedient to compare this diagram with Fig. 28, the synoptic diagram of β axes. The orientation of boudins forms a broad girdle that coincides with the girdle defined by the β axes. If the orientation of boudinage is plotted in the stereograms for the individual β axes, some fall in B , some fall in a , and others appear to be unrelated to the local geometric fold axes. The orientation of boudinage can, therefore, be related to the geometric fold axes of the subareas, but on a regional scale, their orientation defines a girdle indicative of the regional triclinic symmetry.

As has been mentioned previously, boudinage like Fig. 31 may exert a strong influence on the folding. Boudinage in B would not

¹ Coordinates referred to are the geometric coordinates. Weiss (1959, p. 92) points out that only as a special case will lineations be parallel to the kinematic B axis in slip folding.



Fig. 31. *Boudinage in an amphibolite layer of banded granodioritic gneiss. Flå in Hallingdal.*

Boudinage i et amfibolittlag i båndet granodioritisk gneis. Flå i Hallingdal.

exert any noticeable influence on the folding, but boudinage in a , especially in thicker layers, could have the same effect as open cross-folding on the fold geometry.

Weiss (1954, p. 16) has proposed a similar mechanism for the formation of a β' axis in deformed marbles and quartzites. The apparent β' axes on the southern and western sides may be caused by flow into the necks of boudins and would not be related to a kinematic B axis.

Although it has not been observed directly in the field, the geometry of the boudinage (Fig. 32, Plate 13) makes it likely that the boudinaged layers are divided into rectangular pieces. Ramberg (1955) states that most boudins are probably rectangular and have undergone two-dimensional extension. Extension in a is easily explained; however, extension in B seems to be a fairly common phenomenon that is unexplained by present theories of deformation. Extension in B has been particularly common in the gneisses on the west side of the granite.

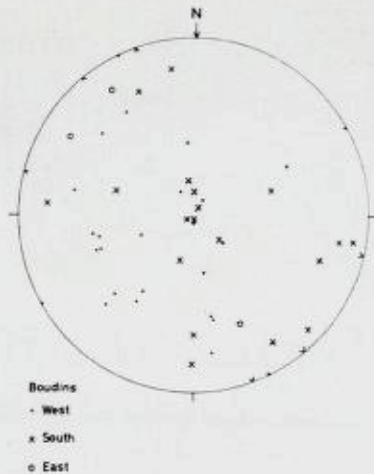


Fig. 32 Geometry of the "necks" of 49 boudins from the entire area. Wulff net.
 Diagram av "halsene" på 49 boudins fra hele området. Wulff nett.

Mineral Orientation and Striations. Mineral orientation on foliation surfaces is fairly common throughout the area. Hornblende, which also forms a lineation in unfoliated amphibolite, biotite, muscovite, and, in some places, chlorite are the minerals that impart the lineation. Striations, resembling slickensides which occur on foliation surfaces, are considered together with mineral parallelism because they are seen to grade into each other and have the same orientation.

Fig. 33 a shows the geometry of mineral orientation and striations from the east side. The oriented minerals that trend north-northeast and south-southeast certainly form *B* lineations; however, the remaining northwest-southeast-striking girdle cannot be related to either a *B* or an *a* direction in the fold geometry. This girdle is formed both of mineral orientations and striations on the foliation surface. On some surfaces, the striations can be seen to erase a *B* lineation in biotite; on others, the preferred orientation of biotite parallels the striations. Evidently movement that formed this girdle was postcrystalline in places and paracrystalline in others.

Only four lineations are measured in the mylonite zone at Bagn, but these four fall on the girdle (circles in Fig. 33 a) so they may be related. The movements producing these lineations appear to have been effective over a wide area.

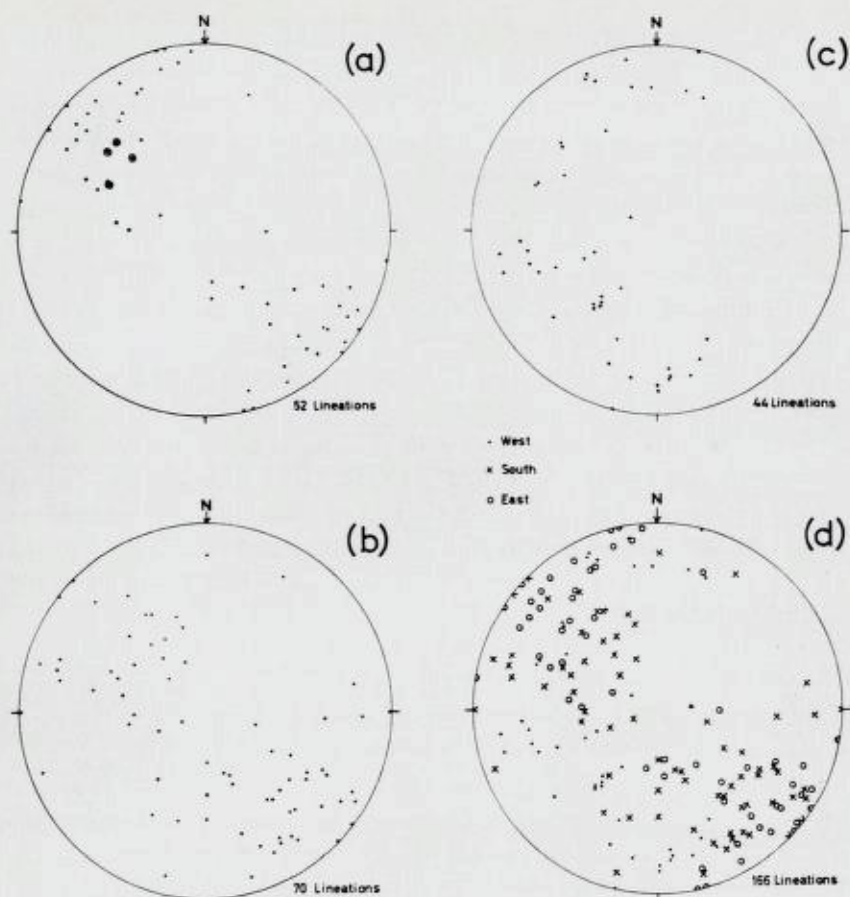


Fig. 33. *Geometry of preferred mineral orientations and striations.*
(a) 52 lineations from the eastern district.
(b) 70 lineations from the southern district.
(c) 44 lineations from the western district.
(d) Synoptic diagram of 166 lineations from the entire area. Wulff net.

Plotting of mineral-orienteringer.

- (a) 52 lineasjoner fra det østlige område.
- (b) 70 lineasjoner fra det sørlige område.
- (c) 44 lineasjoner fra det vestlige område.
- (d) Samlediagram av 166 lineasjoner fra hele området. Wulff nett.

The mineral orientations from the south side are also grouped roughly on a girdle (Fig. 33 b). Some of the mineral orientations are *a* or *B* lineations, others are not (Plate 13). The writer has observed in the field that the orientation of hornblende needles is often related to local flow directions connected with boudinage. This fact probably accounts for some of the scatter around the girdle. A striking similarity, however, is that this girdle coincides with the one from the east side.

The geometry of mineral orientation (no striations were recorded here) on the west side (Fig. 33 c) can be largely related to the *a* and *B* directions in the subarea. The *a* lineations are found widely distributed east of the reverse fault, and *B* lineations are common immediately west of this fault.

The occurrence of strong *a* lineations under thrust planes has been observed by Strand (1944), Kvale (1948), and Balk (1953). The lineations in this area occur far (up to 5 km) away from the fault trace but could be related to strong tectonic transport in the direction of the thrusting. The lineations form a girdle indicative of an overall triclinic fabric.

The synoptic diagram of all mineral orientations and striations (Fig. 33 d) shows a surprising degree of homogeneity caused by the similar attitude of the girdles from the three districts. These lineations define a broad girdle that coincides with the girdles formed by β and by the boudinage. These girdles reflect the overall triclinic symmetry of the structural geometry; however, the orientation of many of these linear structures can be linked to the *a* and *B* geometric axes of folding in the subareas. The origin of the northwest-southeast-striking girdle in the eastern area is unexplained, but the near coincidence in the girdles formed by the different mesoscopic and macroscopic fabric elements constitutes a striking feature.

Granite Tectonics.

General.

Granite tectonics is defined as the structural features of plutons and the relationship among these features (Billings, 1942). The purpose of granite tectonics is to demonstrate the movements that have taken place in a granite body during its emplacement.

Lineation.

A lineation in this granite is formed by the orientation of microcline crystals (Fig. 34 b, c) and of elongate inclusions. Lineation, which may occur together with foliation, is elusive at best; however, the fact that lineation in foliation planes has been found in only the most favorable exposures suggests that it occurs more commonly than it has been observed. Lineation usually reflects the local direction of extension (flow), and may develop normal to the general extension direction (H. Cloos, 1936, p. 87).

Foliation.

The term, "foliation", is used in place of the term, "platy flow structure", of Balk (1937, p. 14) for a planar orientation of minerals within the granite. Schlieren is used in the sense of Balk (*ibid.*) for mineralogical banding that Balk has also called flow layers.

Foliation is formed by the preferred orientation of K-feldspar megacrysts and, to a lesser extent, biotite and quartz in the porphyric granite (Fig. 34 a). Foliation is most strongly expressed by the preferred orientation of biotite in the fine-grained granite. An alternation of biotite-rich and biotite-poor layers form schlieren in fine-grained granite (Fig. 34 d).

Foliation varies from being perfectly distinct such as in the "tail" of the Ådal granite to being extremely faint; schlieren rarely occur.

A preferred orientation may have arisen in four ways: 1) Inherited from an older foliated rock 2) Formed during the regional metamorphism 3) Formed by fluid flow in a partially crystalline magma 4) Formed by solid flow as part of an intrusive episode after the main deformation.

1) The first possibility, has been advocated as an important process by Sederholm (1923). In the Flå granite there can be no doubt that an apparent foliation is formed sporadically by partially transformed inclusions. This apparent foliation is easily recognizable in good exposures and has not been included as a structure of the granite. This has, however, been an active process in the formation of schlieren. Swirly, migmatic inclusions occur together with schlieren in Muggedalén (40.2, 0—59.0). Here the inclusions have been sheared out into alternating biotite-rich and biotite-poor layers. In thin section, the rock

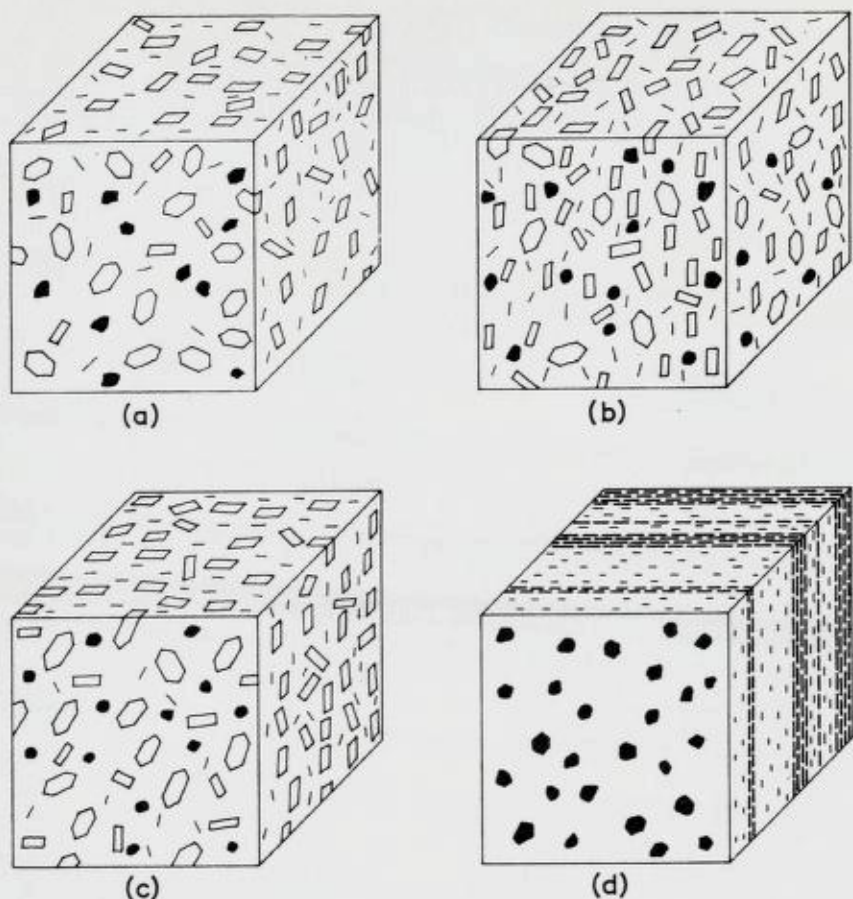


Fig. 34. Structure in the granite. (a) Foliation. (b) Lineation. (c) Foliation and lineation. (d) Banding (schlieren).

Strukturer i granitten. (a) Foliasjon. (b) Lineasjon. (c) Foliasjon og lineasjon. (d) Bånding.

is highly sheared; quartz is leafed and granulated. The movement has taken place by solid flow.

2) An origin during the regional metamorphism hardly agrees with the field relations of most of the foliation in the granite. The foliation generally conforms to the attitude of the contacts and, in places, wraps around inclusions. Also the foliation of the inclusions may have a different attitude from that of the adjacent granite and no second foliation is impressed on either. The foliations of the granite

and inclusions are usually parallel when the longer dimensions of an inclusion parallel its foliation. All these features suggest postmetamorphic flow within the granite.

The possibility does exist that the approximately vertical foliation in the fine-grained granite in the center of the Hedal granite represents an axial-plane foliation that is retained from the regional metamorphism. Dietrich (1954) has described a granite phacolith in which both an axial-plane foliation and a lineation are inherited from the regional metamorphism and deformation. A similar phenomenon was found in a fine-grained quartz diorite emplaced in the crest of a small fold (Fig. 7). Attitudes of foliation in the center of the Hedal granite do not describe the typical domal structure of intrusive granites (H. Cloos, 1936; Balk, 1937). An origin by a regional stress cannot be excluded for this foliation but it seems unlikely.

3) and 4). An origin by magmatic flow cannot be excluded for the foliation of the fine-grained granite in the center of the Hedal granite; however, signs of shearing are found in some specimens. The porphyric granite is both the most commonly foliated and the most distinctly foliated granite. *In most cases that have been investigated (40 thin sections), the foliated granite is highly sheared.* Quartz is leafed, granulated, and usually partially recrystallized. The shearing has outlasted the crystallization of the microcline megacrysts, which have resisted granulation better than the other minerals. These sheared, foliated rocks are characterized by bright-red microcline megacrysts. The fairly common occurrence of chlorite in sheared granite suggests the presence of a certain amount of water, possibly as an adsorbed film. The unsheared porphyric granite is unfoliated. Although magmatic flow followed by late shearing of the crystallized rock cannot be excluded, a magmatic stage has not left behind a distinguishable flow pattern. The foliation and lineation in the porphyric granite have originated by solid flow.

Jointing.

Joints in the granites are mostly developed in the two northeast- and northwest-striking directions that are found throughout the area (Fig. 30). These joints, which dip steeply, are well developed in the granite. In the gneiss, the same joint pattern persists; however, the joint that most closely parallels the foliation is poorly developed or missing in many places.

The Foliation and Lineation Pattern.

The geologic map (Plate 1) shows that the foliation in the granites generally follows their borders. The foliation may, however, be highly variable in attitude and distinctness within a few ten's of meters.

Ådal granite is more distinctly foliated than the Hedal granite; foliation or lineation can be found almost anywhere in the Ådal granite. The foliation generally parallels the nearest contact of the granite. The foliation of the Ådal granite becomes both more consistent and more distinct in the "tail" of the granite. In the comparatively wide western end, the foliation, which dips vertically, is weaker and changes in strike but generally tends to follow the western contact. This behavior can be compared with the salt-dome model experiments of Escher and Kuenen (1929), who found that a plug of plastic material extruded through a hole in rigid material developed parallel foliation adjacent to the walls of the hole and developed folds on vertical axes in the center. Possibly, this variable foliation in the western end of the Ådal granite can be compared with the center of the plug where the frictional effect of the walls is reduced.

The dips of most foliations approach the vertical so that a central dome structure is not delineated (Plate 1 and 18). There is a suggestion of this in the center of the "tail"; however, local variations in attitude seem more likely in view of the statistical predominance of steep dips.

Lineations plunge steeply in the western part of the granite but a second weak lineation is subhorizontal. Strong subhorizontal lineations are found in the "tail" of the Ådal granite. These strong subhorizontal lineations are formed in almost completely transformed sheared inclusions and in subrounded elongate amphibolitic inclusions that may have been rolled.

Movement in the Ådal granite has taken place in the foliation planes parallel to the contacts of the granite. The movement that is reflected in the foliation of the granite has occurred in solid rock. The available lineations indicate that movement was approximately vertical in the western part but there may have been a horizontal component caused by an expansion of the mass. The subhorizontal lineation in the "tail" of the granite has probably formed normal to the movement direction, which is further indicated by drag folds in the gneiss at the contact (Fig. 52 a).

Hedal granite lacks the widespread foliation of the Ådal granite,

and, when foliation does occur, it is usually weaker. The lack of foliation symbols in the northern part of the Hedal granite is partly attributable to the poor exposures as well as to a true lack of foliation because foliation was found in a sheared granite near the middle of the northern end (42.7, 1—14.3). Foliation is stronger and more common near the eastern border which it roughly parallels. Foliation in the fine-grained center of the granite is found sparingly; however, some hand specimens were found to be foliated after being stained for modal analysis when a careful search in the field had failed to detect a foliation. Nevertheless, the Hedal granite is certainly not only more weakly foliated but also much less commonly foliated than the Ådal granite. Foliation is strong and almost universally present in the southeastern offshoot of the granite which resembles the "tail" of the Ådal granite. Foliation is also distinct around the southern curve of the Hedal granite. Lineations here plunge vertically or steeply to the southeast.

Movement at the borders of the Hedal granite has been within the foliation of the granite approximately parallel to the granite contacts. The few lineations indicate an almost vertical direction of movement. The movement which has occurred by solid flow has been stronger along the eastern and southern contact of the Hedal granite than along the western contact.

The significance of the foliation in the fine-grained granite in the center remains problematical. These rocks are somewhat granulated in places. This foliation could descend from fluid flow and subsequent slight shearing or shearing of solid rock and subsequent recrystallization. A regionally induced axial-plane foliation remains an outside possibility.

Relation of the Granite to the Gneiss.

The foliation in the gneiss generally parallels the adjacent granite contact (Plate 1). The only exception occurs on the southwest side of the Hedal granite where the foliation of the gneiss has turned to an east-west strike and is cut sharply by the granite. According to the Cloosian terminology (H. Cloos, 1928), the Ådal and Hedal granites represent concordant, conformable plutons.

Dikes and sills, which occur in great abundance around the granites, are commonly foliated. Parallel to subparallel tabular bodies of granite are the more common. These again are sheared when foliated. In some the recrystallization of quartz is considerably ad-

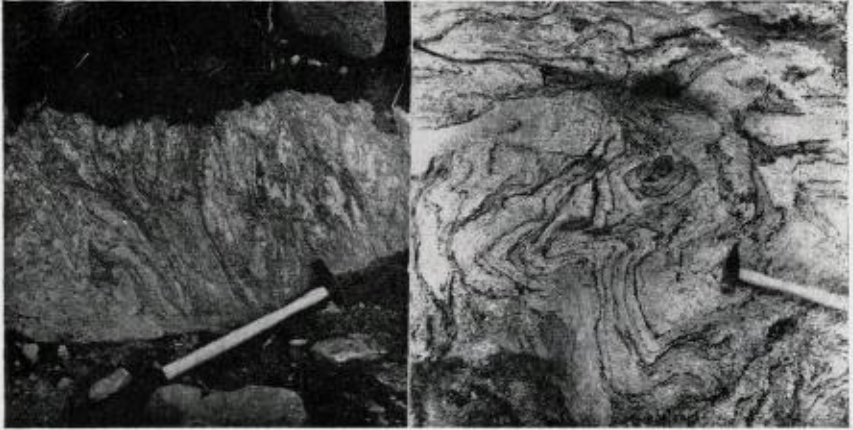


Fig. 35. *Flow folds adjacent to the granite. (a) South side of the Adal granite. (b) West side of the Hedal granite. Highly granitized.*

Flytefolder, som støter opp til granitten. (a) Sørsiden av Adal-granitten. (b) Vestsiden av Hedal-granitten. Sterkt granitisert.

vanced. Some sills on the east side of the Hedal granite are highly sheared, and inclusions of gneiss in the sills are rolled out. The foliation of granite dikes usually parallels the contacts of the dike and transects the foliation of the surrounding gneiss (Fig. 17). The occurrence of a porphyric granite sill (Fig. 16) is a paradox. This sill retains the imprint of folding in the gneiss; however, similar dikes are usually sheared. Any shearing of this sill must have been too small to destroy the pattern of the folding.

Pegmatite dikes may have tabular shapes suggestive of fracture fillings. These pegmatites must have formed in potential fractures late in the movement history of the granite because some of the pegmatites may in turn be sheared. The attitudes of these pegmatites are highly variable, and insufficient observations were available to determine a pattern.

Flow Folds.

Flow folds occur within the area studied in the immediate vicinity of the granite (Fig. 35). They must be ascribed to the same cause as the granite because of their close spatial and probable temporal connection. The effect of these folds on the structural geometry will be discussed in a later paragraph. Granitization that accompanied flow folding has, in many instances, outlasted the folding and tends to erase it.

Deformation Associated with the Granite Emplacement.

General.

The regional geometry was determined in order to reveal any possible deformation associated with the granite. Deformation caused by the granite emplacement may not always be distinctive enough to be observed; nevertheless, if the granite emplacement caused a second deformation within the gneisses, this should be detectable.

Geometry of S and B Adjacent to the Granites.

Since the β axis in subarea 4 (Plate 14) trends more to the westward in concordance with the adjacent granite contact, this axis may have been deflected into this position by the granite emplacement. In addition, the girdle of linear structures (Plate 13) indicates superposed deformation.

Subareas 5, 7, 10, and 12 exhibit similar geometry because two β axes are defined in each subarea where the geometry is triclinic on an outcrop scale. One β axis follows the regional trend and the other one plunges steeply. The orientation of linear structures in these areas diverges greatly and forms a girdle in three of these subareas. Three of these subareas contain swirly migmatites, augen gneisses, and granitized folds that occur together with granitic dikes.

In subareas 15, 16, and 17, the β axes are horizontal and trend northwest-southwest so that they parallel the contact of the Ådal granite. Although these β axes differ in attitude from those a few kilometers to the north, it is impossible to state they were deformed into this northwest trend by the granite. All the fold axes in the southern part of the area have the same general trend, and the direction of folding has more likely determined the general direction of the Ådal granite's contacts. The geometry of linear structures in subarea 17 demonstrates superposed folding; this may have been caused by the granite emplacement.

The β axes swing around into concordancy with the granite contact when they pass from subareas 26, 27, and 31 into subareas 29, 30, and 32. A late diabase dike in subarea 32 provides a useful datum plane to decipher the movements. This dike, which is weakly foliated and metamorphosed to an amphibolite, cuts the gneisses at a low

angle. The associated amphibolites are strongly boudinaged, and the boudins are rotated 90° in a sense that indicates the east side of the layer was moving northward relatively. The diabase dike, however, was only slightly boudinaged, but it was bent in a broad concentric fold. This fold is plotted on the πS diagram for subarea 32 (Plate 13). The axis of this folded dike coincides fairly closely with the β axis. The dike must have been intruded late in the regional deformation so that its folding is most reasonably attributed to the granite uprise. The geometry of the β axis must have been developed at the same time.

The complicated geometry around the west end of the Ådal granite is repeated in subareas 34, 35, 37, 38, and 39, and β' axes are defined in subareas 34 and 35: B forms girdles that indicate superposed folding in all these subareas. The most interesting feature is that near vertical β or β' axes adjoin the granite contacts.

Weiss (1959) demonstrates that, in areas of superposed deformation, the first πS girdle will tend to be erased by the second deformation. Lindström (1961) maintains, however, that πS diagrams may yield both β and β' in regions where the foliation is subhorizontal after the first folding. In subarea 34, β is largely defined by subhorizontal foliations; near-vertical foliations are rotated into a partial girdle defining β' .

Boudins are nearly vertical in subarea 34 and 37. This could indicate horizontal stretching during the granite emplacement, but boudinage formed in α during the regional deformation would have about the same attitude.

In a synoptic diagram for subareas 36 and 37 (Fig. 36), S defines a steeply plunging β axis, but the geometry of B which delineates an incomplete girdle that is a small circle is particularly significant. This is the geometry of a B lineation refolded by concentric folding (Weiss, 1959; Ramsay, 1960). The first B lineation is rotated around a second B' axis and the angle between them is one-half the apical angle of the cone defined by the small circle of the net. The axis so determined plunges *ca.* due north at 88° and forms an angle of 37° with B' . This angle is incompatible with the near-vertical β' axes imposed by the granite emplacement and the typical gently plunging B unless the foliations containing B were tilted before they were buckled during the granite emplacement. In this subarea, a minor fold surrounded by granite was refolded around a steeply plunging axis (Fig. 23).

The direction of tectonic transport during the second deformation

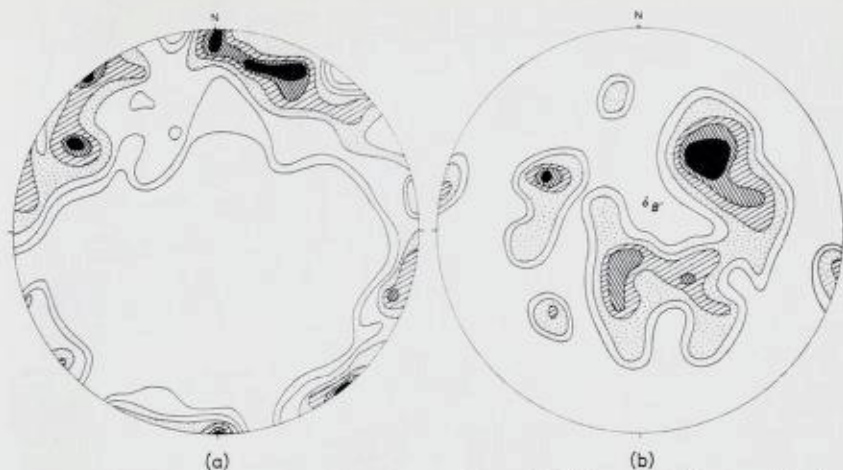


Fig. 36. Synoptic diagrams for subareas 36 and 37 located between the two granites. (a) $76 \pi S$; contours 8-6.5-5-4-2.5-1-0 per cent per 1 per area. (b) Axes of 51 minor folds, B; contours 8-6-4-2-0 per cent per 1 per area. B' is the axis about which B linear structures are rotated. Geometry of B is that of a linear structure refolded by concentric folding.

Oversiktsdiagram for områdene 36 og 37 mellom de to granitter. (a) $76 \pi S$; koter 8-6,5-5-4-2,5-1-0 prosent pr. 1 prosent areal. (b) Akser for 51 mindre folder, B; koter 8-6-4-2-0 prosent pr. 1 prosent areal. B' er den akse som de lineære strukturer B er rotert om. B's geometri er som for en lineær struktur, som er foldet igjen ved konsentrisk folding.

may be constructed from the stereogram for subarea 34. For a second deformation by shear folding, the kinematic α' axis is contained in the intersection between the axial plane of the β' axis and the plane containing the B lineations (Ramsay, 1960). Although the choice of the axial plane for the β' axis is somewhat arbitrary, any selection will yield an α' axis that almost coincides with β' . If α' coincides with β' , then the second deformation has formed folds around axes in the direction of transport. A similar construction yields $\alpha' = \beta'$ for the other subareas with near vertical β' where the data are sufficient. E. Cloos (1947) has ascribed a somewhat similar occurrence of vertical folding around the direction of tectonic transport in a synkinematic granite to differential vertical movements between domes and basins. The most likely cause for vertical movements around the Heddal and Ådal granites during the second deformation is the uprise of the granites.

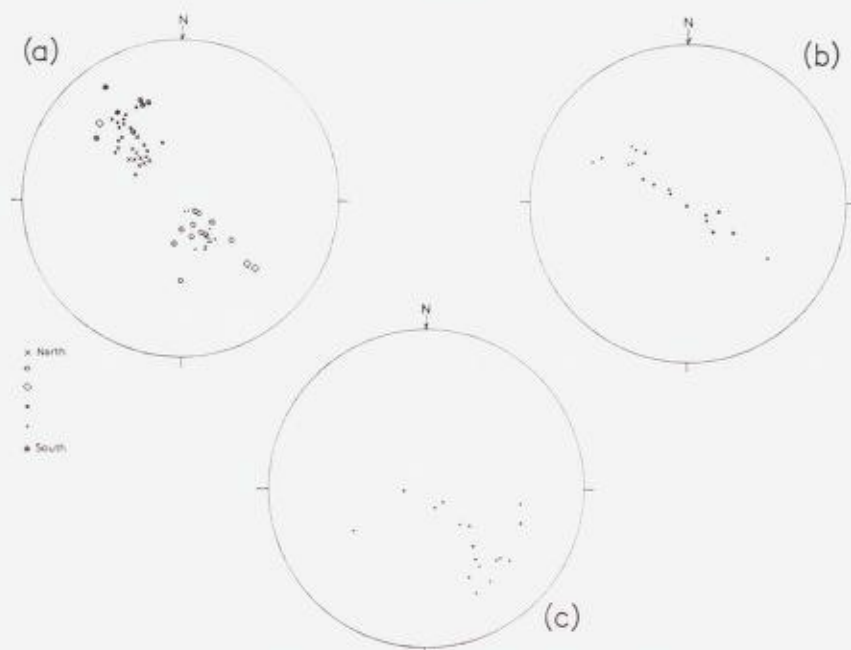


Fig. 37. Geometry of minor-fold axes at the granite contacts. (a) Symbols represent different outcrops up to 500 m apart going from south to north in subarea 56. (b) One outcrop in subarea 57. (c) One outcrop in subarea 58. Wulff nett.

Diagram av akser for mindre folder ved granittkontaktene. (a) Symbolene representerer forskjellige blotninger op til 500 m fra hverandre fra sør mot nord i område 56. (b) En blotning i område 57. (c) En blotning i område 58. Wulff nett.

Vertically plunging folds have not been observed on the west side of the Hedal granite except in subarea 42 on the southwest end of the granite. Open crossfolds were found in the foliation; the πS diagram suggests several trends.

Minor folds. The geometry of minor folds in subareas 56, 57, and 58 adjacent to the granite provides some interesting patterns (Fig. 37) that recall the *B* girdles in other subareas adjacent to the granite. They are highly variable but define partial girdles. Minor folds in subarea 56 show a regular spatial variation in attitude. These folds alternate between a northerly plunge and southerly plunge in going from south to north in a 4-km-long stretch just outside the granite contact. Minor folds in subarea 57, however, are all within 100 m of each other.



Fig. 38. "Arrowhead" hinge remnant of a folded amphibolite layer in subarea 58. The fold hinge is surrounded by migmatite. The amphibolitic limbs of the fold have been sheared out and have disappeared. The axial plane of this fold is folded; the deformation is triclinic. Nevlingen (31.7, 1—14.0).

Rest av pilespissformet ombøyning av et foldet amfibolittlag i området 58. Foldens ombøyning er omgitt av migmatit. Foldens amfibolittiske sider er gnidd ut og er forsvunnet. Deformasjonen er triklin. Nevlingen (31,7, 1—14,0.)

These define a partial girdle. The outcrops at subarea 58 exhibit folded axial planes (Fig. 38) and the minor-fold axes lie on a poorly defined partial girdle. Some of this geometry may be explained by flow folding.

Flow folds have been noticed at all these locations except subarea 56 but they are by no means universally present. Flow folds are known with highly variable orientation of the axes, but axes with highly variable plunge and a common trend are characteristic (Gustafson and others, 1950; Carey, 1953). An origin by flow folding in a milieu mobilized during formation of the granite seems likely for these folds.

The folds of alternating plunge in subarea 56 must have another explanation. Possibly they originated by variable flattening (Ramsay, 1962) but variable extension in a caused by shear instituted during the granite emplacement seems more likely. Whatever the origin of all

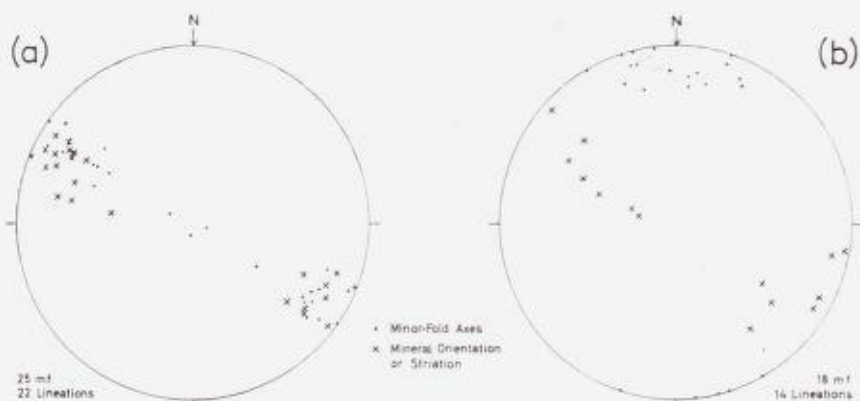


Fig. 39. (a) Geometry of minor-fold axes, preferred mineral orientations, and slickensides from one outcrop at the northern contact of the Adal-granite. (Subarea 18.) (b) Geometry of minor-folded axes, mineral orientations, and slickensides from subarea 11 about 17 km north of the contact. Note the similar attitude of the girdles. Wulff net.

Diagram for småfolde akser, mineral orientering og glidestriper fra en blotning ved Adalsgranittens nordgrense. Geometri for småfoldeakser, mineralorientering og glidestriper fra område 11 omtrent 17 km nord for kontakten. Legg merke til likheten i beltene. Wulff nett.

these minor folds, that they are closely related to the granite is an important empirical fact, whose elucidation requires a more detailed study.

Linear structures from the north contact of the Ådal granite at Sperillen community are plotted in a stereogram for comparison with the linear structures from an outcrop 17 km north of the granite (Fig. 39). Striations on foliation surfaces at the granite contact parallel mineral orientations and minor fold axes, and, where striations occur, they conceal the mineral orientations. All three of these elements are parallel except for three steeply plunging minor folds and are *B* lineations that exhibit a small amount of scatter. If the strike of these *B* lineations is compared with the lineations of undetermined origin that obliquely transect the *B* lineation in subarea 11, the strike of the former is 134° and that of the latter is 143° . They nearly coincide with each other and also with the northwest-southeast-trending girdles of lineations in Figs. 28 and 33. A close causal relation is suggested; this direction is also found in the lineations from the shear zone at Bagn.

Sequence of Events in the Area.

The following succession of events is proposed for the area studied. Many of them necessarily overlap in time but are initiated at different intervals.

1. Deposition of a supracrustal succession of rocks.
2. Intrusion of basic dikes.
3. Folding and regional metamorphism accompanied by synkinematic granitization in some areas; formation of migmatites, augen gneisses, and concordant pegmatites.
4. Intrusion of basic dikes.
5. Uprise of granite as final act of regional folding passing into diapirism; older structures adjacent to the granite are deformed; recrystallization of quartz in the granite and local chloritization; granite slightly preceded in time and space by granite dikes and augen gneiss.
6. Thrusting. This position is somewhat arbitrary because it represents brittle movements that cut across the folds but this may be caused by a higher tectonic level.
7. Pegmatites form in fractures and are in turn deformed slightly.

In addition to the above events, the area has been affected by late Precambrian peneplanation, deposition of Cambro-Silurian sediments, Caledonian deformation, and Permian north-south faulting and dike intrusion.

Regional Synthesis and Conclusions.

The regional folding is about axes that trend between north-south and northwest-southeast. The one reverse fault observed is overthrust to the east, and folds throughout the entire area are most commonly overturned to the east or northeast although axial planes are inclined in other directions. With the exception of movement along the shear zone at Bagn, the main tectonic transport has been to the east or northeast.

A main problem of the regional tectonics is the origin of the west-northwest-trending folds on the west side of the area. Folds in the two trends are found in the same foliation surface, the only megascopic foliation visible in the area. Foliation surfaces with the regional north-

northwest strike wrap around to the east-west strike on a fold axis plunging northwest at 35°; moreover, northwest-trending folds are fairly common throughout the areas so that this fold does not deviate so greatly. Strand (1944) has suggested that folds in the regional *a* direction under a thrust sheet formed simultaneously with *B* folds. The formation of strong *a* lineations and folds in rocks underneath thrusts has been confirmed from several areas (Strand, *ibid.*; Balk, 1953; Kvale 1948, 1953). Some mesoscopic crossfolds on the west side of the granite have probably been formed in connection with a strong tectonic transport in *a* in front of the thrusting, but the major west-plunging fold is far from the nearest thrust. The west-to northwest-trending folds were probably formed simultaneously with the other folds of the area as a result of triclinic deformation (Strand, 1944) caused by heterogeneity of material or varying intensity of movement (Kvale, 1953).

The geometry of the mesoscopic fabric elements is characterized by two important features:

- (1) *The girdle development of each fabric element that indicates triclinic symmetry.*
- (2) *The similar attitude of the girdles developed by each fabric element.*

There is a marked tendency for the fabric elements over wide areas to be coplanar.

The overall triclinic geometry that appears in all the structural elements of the area does not necessitate two periods of deformation. Variable extension in *a* could account for the variable trends and plunges of most folds and would distribute the fabric elements around different orientations within a single plane (*ab* plane). This is likened to the variable flattening of a fold which produces a bowed fold axis (Ramsay, 1962). Weiss (1955) has demonstrated that a triclinic fabric may originate from one deformation if the kinematic *B* axis does not lie in the plane of layering. Although local movements may have been more complicated, the writer prefers to interpret the regional structures as the results of one major period of deformation.

The granite contacts are concordant with the foliation of the country rocks, and the foliation of the granite is conformable with the contacts. All foliation of the granite is apparently produced by solid flow. If an earlier magmatic stage cannot be excluded, neither is it required. Granites with sheared border facies are not rare (H. Cloos,

1925, 1936; Balk, 1937; Waters and Krauskopf, 1941; Martin 1952; Akaad, 1956). These protoclastic borders are generally attributed to a final push in nearly solidified magma (numerous authors) or to intrusion of a largely solid mush of anatectic magma (Waters and Krauskopf). In the Flå granite traces of cataclasis are found in the centers of the granites; therefore movement by solid flow has taken place throughout the entire granite.

The possible effect of shear over a breadth of 8 to 18 km in the granite can account for an important amount of differential movement. If, for instance, a vertical differential movement of 1 mm occurs along vertical shear planes spaced 1 mm apart, the total differential movement between the center of the granite and its borders can attain a value of 2 km in the Ådal granite and 5 km in the Hedal granite. The sheared sills indicate that considerable differential movement has been accommodated in the country rocks. The effect is that of affine deformation if movements are equal on each slip surface and nonaffine (shear folding) if movements are unequal.

A problem of primary importance is whether the vertical β and β' axes and the girdle distribution of B have arisen from movement caused by the granites' emplacement or whether they are part of the regional deformation pattern. Girdles of B lineations are undoubtedly found outside the area that could have been influenced by the granite emplacement, and the regional deformation fabric is triclinic. On the other hand, the structural geometry indicating superposed deformation is so overwhelmingly spatially concentrated around the margins of the granites that a close causal connection must be supposed. In addition, the only refolded fold, which was surrounded by granite, was observed between the two granites where the B girdle suggested superposed concentric folding, a second-folding mechanism which occurs rarely in superposed regional deformation (Weiss, 1959; Ramsay, 1960). The emplacement of the granite has probably caused a second deformation in the gneisses; the structural geometry indicates that transport in a vertical direction occurred during the granite emplacement.

The vertical rise of the granites by nonaffine slip could produce the girdle distribution of linear structures found in many subareas around the granite. This could not, however, account for the folding around vertical β' axes (Ramsay, 1960). These vertical β' axes suggest a buckling mechanism and buckling is also required to form the small-circle girdle of B linear structures which is caused by a deformation

of a *B* lineation by concentric folding. Buckling of the gneisses, which may have produced some of the vertical boudinage around the granite, around vertical axes requires an expansion of the granite.

The movement picture proposed during the granite emplacement becomes complicated. The great-circle *B* girdles and the construction of the vertical *a'* axis indicate and presuppose slip folding during the second deformation. The small-circle *B* girdle and buckling require concentric folding. Movements were probably a combination of these two mechanisms.

The mechanism of concentric folding at the west end of the Ådal granite is extremely significant for the emplacement of the granite. This means that the Ådal granite must have expanded and pushed out on its walls; therefore, material must have flowed into the granite at this end. This is the strongest and, in fact, the only real suggestion of the participation of magma in the tectonics of the granite. On the other hand, many geologists, particularly tectonicians, maintain that rising domes and diapiric structures in migmatite and granite can form by tectonic and metasomatic mobilization of gneisses without the intervention of magma (Wegmann, 1935; Haller, 1956, Kranck, 1957).

The available information indicates that the major movements in the granites were near vertical; doming is not evident. Vertical lineations in the Ådal granite are accompanied by a weaker horizontal lineation except in the "tail" where strong subhorizontal lineations that parallel the lineation in the adjacent gneiss are found. The Ådal granite has probably expanded somewhat in the west end while it rose.

Steeply dipping lineations are commonly found around granite gneiss domes (Härme, 1954) and granite plutons (E. Cloos, 1947; Compton, 1955; Elders, 1961). They are singularly lacking around the Flå granite. Even at the contacts of the Ådal granite where the foliation in the granite is strong, the adjacent gneiss carries a subhorizontal lineation. The granite, however, may exhibit a vertical lineation and a weaker horizontal lineation occurs. Drag features at the contact of the granite indicate that the granite has moved upward with respect to its wall rock, but horizontal lineations prevail in the gneiss. Vertical structural elements in the gneiss are singularly lacking except for β' axes and the comparatively rare steeply plunging minor folds. The uprise of the granite must have produced a rolling around *B* which resembled the movements during the regional folding in the gneisses. The vertical movements during the rise of the granite were a continuation of the extension that occurred in *a* during the regional deformation.

The Flå granite provides an interesting case history in the tectonic classification of granites. At first glance the granite appears to be a typical postkinematic batholith bordered by an intrusive breccia. A closer examination suggests that the granite is at least late-kinematic and has some characteristics of a synkinematic granite.

The Ådal granite spans the gap between a synkinematic and a late-kinematic granite. The granite in the "tail" is highly crushed and uniformly foliated, is lineated parallel to the lineation in the gneiss, has not buckled the country rocks, and passes into the country rocks through a zone of migmatic and augen gneiss. The granite in the west end has expanded and deformed the country rocks, is vertically lineated, and has a variable foliation pattern. The Ådal granite is, therefore, synkinematic at one end and late-kinematic at the other.

The Hedal and Ådal granites present an interesting combined picture because the Hedal granite parallels the regional trend, and the Ådal granite lies athwart the regional trend. Both granites are generally concordant, but again the Ådal granite seems to be the "more intrusive" of the two. In light of the structural details, however, this apparent discordancy of the Ådal granite loses its validity.

The Ådal granite generally parallels the trends of folds in the southern part of the area; furthermore the same fold trends are found a considerable distance away on the west side of the Hedal granite. The trend of the Ådal granite can be followed past the south end of the Hedal granite into the gneisses west of it. In other words, the northwest fold trend constitutes a prominent, if secondary, structural feature that is likely to have determined the position of the Ådal granite.

If the two fold trends crossed, a granite body might be pre-disposed to rise at the junction point (Stille, 1925; Wegmann, 1930). This may be what occurred at the western end of the Ådal granite where the granite seems to be the "most intrusive" of the entire area. The regional structure has determined the location and behavior of the granites; the granites have determined the orientation for some of the local structures.

The data and ideas presented represent a survey and an interpretation of the tectonics of the area. A number of facts have been established, but more information is obviously desirable in such a complicated area. The writer is certain that further structural studies in the area will reveal the most useful and unequivocal information about the granites. Their history is closely connected to the structural geometry and kinematics of the region.

The Contact Relations.

General Statement.

Olaf Andersen (1921) first described the contact relations of the Flå granite as "an eruptive breccia on a hugh scale" in referring to the numerous large inclusions of gneiss that are found in many places. For a short summary of the contact relations, the writer can do little to improve upon the following description given by Strand (1954, p. 18, writer's translation): "As mentioned above, the Flå granite has sharp borders against the gneisses so that at every single place the contact appears as a sharp line. On the other hand, there is a transition zone so that, in going from the gneiss to the granite, we come to an area where the gneiss is crisscrossed by numerous granite dikes. This area is followed by a zone where granite predominates in amount but contains numerous larger and smaller angular and sharply bordered fragments of gneiss." In general, the contact between granite and gneiss (whether between dikes, inclusions, or in favorable exposures of the actual contact) appears knife sharp; however, the above mentioned transition zone renders the position of the contact arbitrary in some cases and highly debatable in others.

Hedal Granite.

The northwest contact of the Heddal granite is extremely difficult to place on a map. The area is largely covered by glacial drift, and the outcrops present a varying pattern of granite, gneiss, and pegmatite. Near Hövren, the gneiss dips gently west and contains numerous dikes and sills of fine-grained granite which range in width from 30 cm to 5 m. Some of the dikes are foliated parallel to their contacts. To the west of here, biotite gneisses with feldspathic streaks and augen intermixed with large amounts of granite crop out.

South of Hövren, the outcrops consist of gneiss and granite in equal amounts. The gneiss dips *ca.* 30° northwest and appears as blocks "floating" in fine-grained granite. The granite is largely cross-cutting and appears unfoliated. Since the attitudes of numerous fragments of gneiss are nearly the same over hundreds of meters, the gneiss blocks are presumed to be in place, and the granite contact is placed east of here. A β axis is defined by the attitudes of these patches of gneiss. Farther west by Valdreslii (41.0, 1—27.0) granite crops out

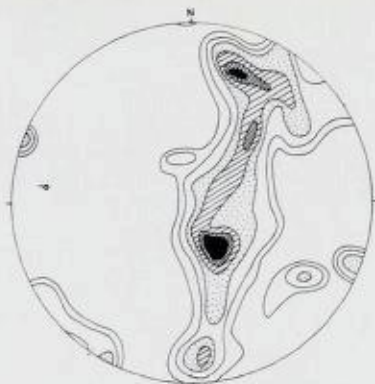


Fig. 40. *S* diagram for inclusions in subarea 48 inside the Hedal granite. This β axis closely corresponds to the β axis just outside the granite in subarea 49 60 π S.

π S diagram for inneslutninger i område 48 innenfor Hedalsgranitten. Denne β akse svarer til β akse like utenfor granitten i område 49 60 π S.

over a wide area. To the east between Alketjern and Vangen (40.5, 1—20.0) gneiss with subhorizontal attitude predominants. This gneiss is crosscut by small amounts of granite and by numerous planar pegmatites. In this area, Strand (1954, p. 19) found an exposure of gneiss large enough to appear on his map at 1 : 100,000. As the center of the granite is approached, the amount of granite increases greatly and the widely scattered inclusions assume different attitudes.

The northwest contact area is characterized by erratically located occurrences of granite and gneiss cut by granite and abundant pegmatite. The gneiss usually dips gently. This area may constitute part of the roof, under which the Hedal granite plunges gently to the northwest.

In the area immediately north of Ströen (48.5, 1—19.0) gneiss inclusions, which may be up to 20 m long and are widely scattered, increase in amount as the contact is approached. At the contact, the gneiss is interwoven with granite dikes and sills. Granite sills and particularly lenticular pegmatites are found in a 4 km wide band west of the contact. The gneisses dip *ca.* 40° west at the contact and steepen to 75° 2 km to the west.

The numerous fragments enclosed by the granite in this area seem to have widely diverse attitudes. The attitudes (*S*) of these inclusions

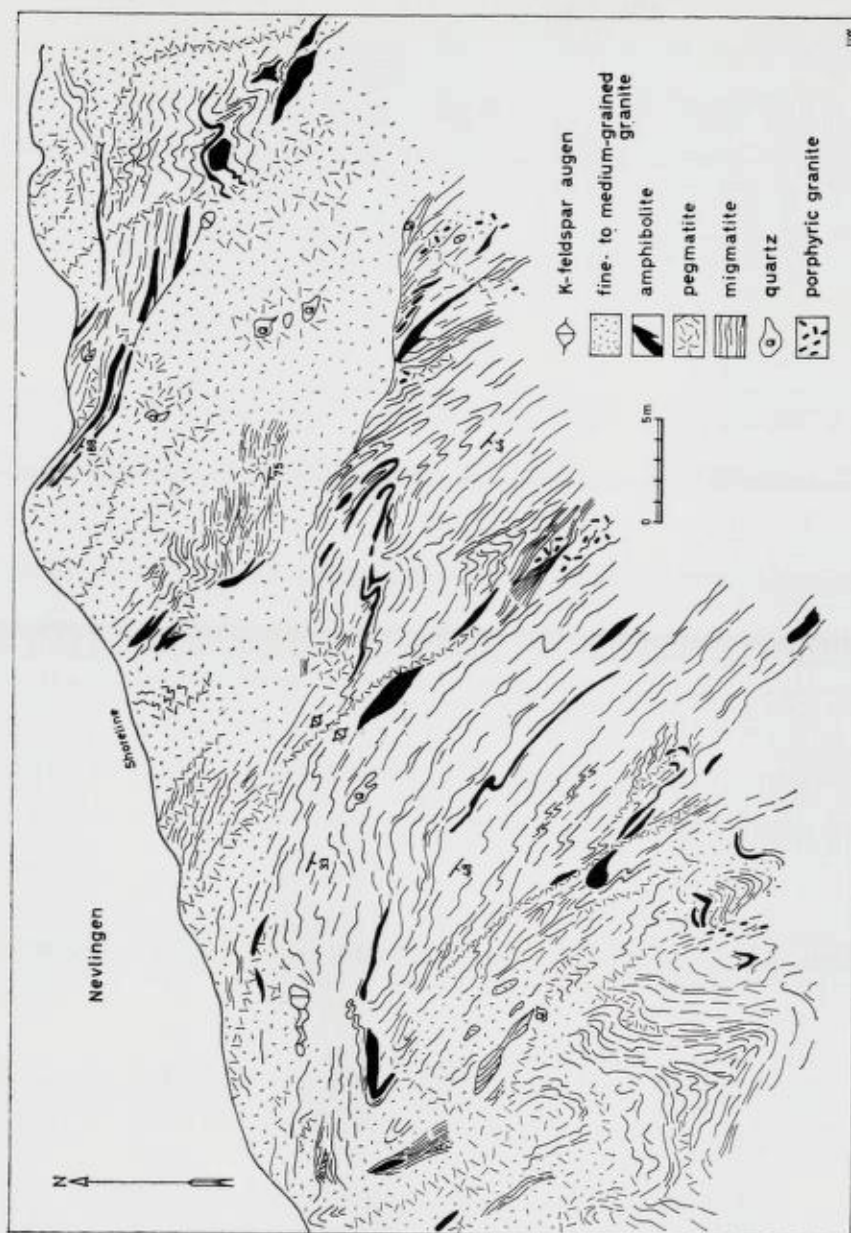


Fig. 41.

are plotted on a Schmidt net (Fig. 40) and define a β axis plunging west-northwest. This axis coincides fairly closely with the β axes found outside the granite here (Plate 14); therefore, the inclusions have not been displaced. Some of the inclusions may have been roof pendants, but the size of the inclusions compared to the amounts of surrounding granite precludes this possibility in most cases. In this area, the term breccia is applicable in a descriptive sense but certainly not in a genetic sense. The emplacement of the granite that encloses these fragments can hardly have caused a greatly increased plasticity (or fluidity).

The western contact is marked by the rather abrupt appearance of numerous gneiss inclusions that grade into gneiss cut by abundant granite dikes and sills. Some of the inclusions seem to have been rotated. The gneiss dips southwest at 30° to 40° outside the granite contact. Flat-lying granitic pegmatites become very common 1 to 2 km outside the contact. In some places (Raufjell) they dominate the exposures.

Contact relations at Nevlingen appear in Fig. 41. The dip here is only moderate but the disruption of the amphibolite layers illustrates the extent to which these rocks have been tectonized. The "arrowhead" in Fig. 38 is a remnant of a fold in an amphibolite layer whose flanks have been completely sheared out. Several dikes which are visible in Fig. 41 cut the gneiss at low angles. Granite permeates the gneiss everywhere and "flow structure" has been produced where highly granitic folds were sheared.

Seven kilometers southeast of Nevlingen the contact relations are unique because the granite cuts the foliation of the gneiss at a high angle (Fig. 42). The foliation of the gneiss strikes east-west. A train of inclusions extends 6 km eastward into the granite but their strikes

Fig. 41. Sketch map of migmatitic gneiss permeated and cut by granite just outside the west contact of the Heddal granite at Nevlingen (31.7, 1—14.0). Tectonization is extreme. Gneiss fragments in dikes do not appear to be displaced. "Flow structure" is produced where limbs of folds have been sheared out in granitic rock (southwest corner).

Skisse av migmatitisk gneis, gjennomtrennt og overskåret av granitt like utenfor Heddal-granittens vestgrense ved Nevlingen (31,7, 1—14,0). Tektoniseringen er meget sterk. Gneis bruddstykker i ganger ser ikke ut til å være flyttet. "Flyttestrukturer" er fremkommet der hvor foldenes sider er blitt gnidd ut i granitisk bergart (sørvestre hjørne).

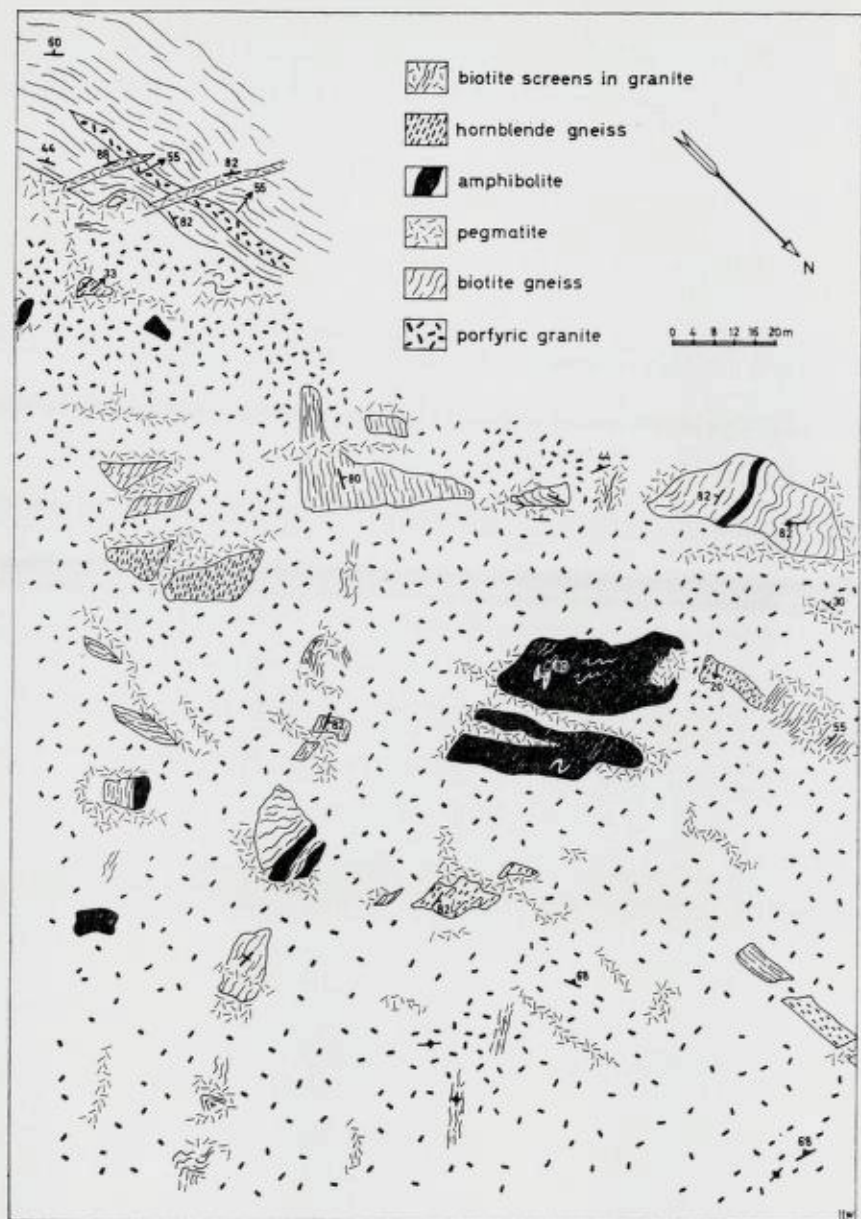


Fig. 42.

vary considerably around northwest. Fig. 42 discloses the agmatitic nature of the breccia. The gneiss is interwoven with dikes and sills of granite and pegmatite. If there has been a general rotation or displacement of the enclosed blocks it is not apparent. Pegmatite becomes very common 500 m west of the contact. The pegmatite interweaves the fragments of gneiss which are not displaced (Fig. 21 b). A zone of augen gneisses parallels the Heddal granite on its southwest side.

The passive character of the numerous dikes and sills that are interspersed throughout the country rock is evident in Fig. 43. The granite intermingles with the gneiss in every direction but exhibits a subparallelism with the foliation of the gneiss. The appearance at this outcrop again suggests a permissive mode of emplacement.

The southern contact is marked by a broad, 2-km-wide transition zone in which granite predominates. Augen gneisses are located just outside the contact. Rotated inclusions are locally common in this zone; some inclusions appear to be in place. Smearied out shadows of biotite-rich fine-grained granite similar to Sp 542 A (rock description) grade into biotite-gneiss inclusions. At the inner border of the transition zone, the orientation of bright-red microcline megacrysts imparts a distinct steeply dipping foliation to the granite.

The southern contact is again characterized by alternating layers of granite and gneiss. The granite forms slightly crosscutting dikes which cut sharply across the gneiss layers in places and coalesce. Smaller inclusions in the dikes are rotated and displaced relative to each other. Foliation is elusive but, when observed, is parallel to the contacts of the dike. The succession of alternating granite and gneiss layers, which range from 10 to 20 m in width, is approximately flat-lying outside the granite contact and whips around to dip steeply southward at the contact. Just inside the granite, a number of steeply dipping gneiss inclusions probably represent the ends of inclined gneiss layers.

Foliation around the south end of the granite is distinct and dips

Fig. 42. Sketch map of contact relations at Damtjern (29,0, 1—10,0) on the west side of the Heddal granite. Most fragments of gneiss seem to be in place.

Unless designated otherwise, all symbols are the same as those in Fig. 41.

Skisse av kontaktforholdene ved Damtjern (29,0, 1—10,0) på vestsiden av Heddal-granitten. De fleste gneisbruddstykker ser ut til å være på plass. Hvis intet annet er sagt, er alle symboler de samme som i fig. 41.

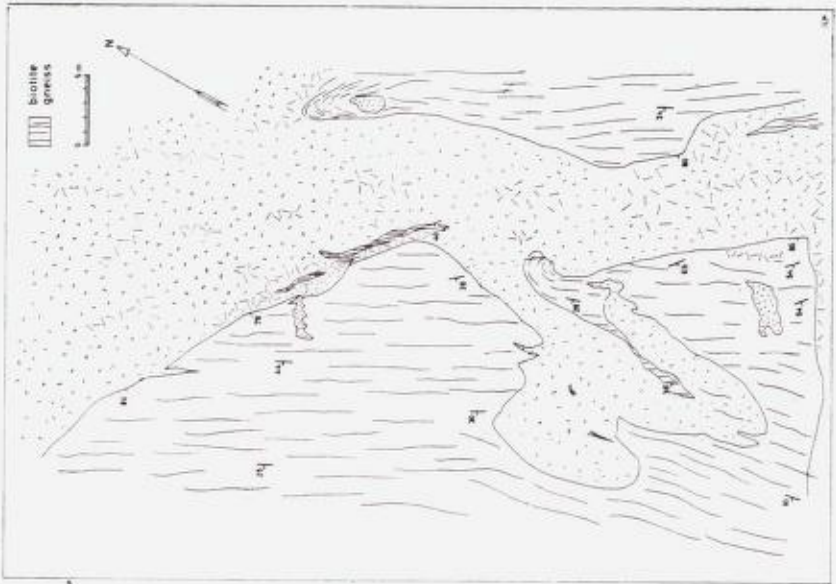


Fig. 43. Sketch map of gneiss cut by granitic dikes at western contact of the Hedal granite by Skarsæter (27.3, 1—08.5).

Skisse av gneiss overskåret av granitiske ganger ved Hedal-granittens vestgrense ved Skarsæter (27,3, 1—08.5).

steeply southward; elongate inclusions plunge steeply parallel to the foliation. At Buvatn (27.5, 0—56.5), 1 km inside the contact, inclusions are definitely rotated and displaced (Fig. 44 a) because they transect each other at right angles.

South of Sandvatn (25.5, 0—51.5), the succession of alternating granite sills and gneiss layers, dipping 50° southeast, is exposed along a stream valley (Fig. 44 b). The sills are from 5 to 20 m thick. The foliation when present usually parallels the adjacent contact so that where the sill continues into a crosscutting dike, which connects with another sill, the foliation in the granite is transgressive. Subparallel inclusions of gneiss form an extensive eruptive breccia at the contact here.

The southeast prolongation of the granite at Vikerfjell (28.0, 0—46.0) provides a somewhat different aspect of the transition from granite to gneiss. The highly sheared, perfectly foliated granite in this prolongation interdigitates with the gneiss at its south end. Inclusions are found almost everywhere; many appear to be rotated. The inclusions

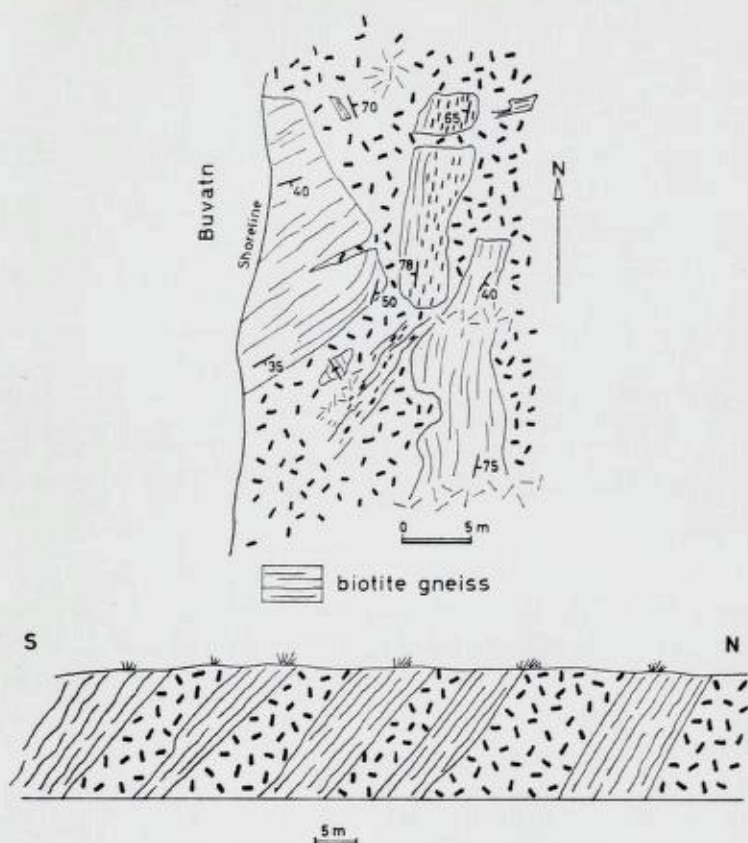


Fig. 44. (a) Field sketch of rotated inclusions at the south end of the Heddal granite by Buvatn (27.5, 0—56.5). (b) Alternating sills of porphyric granite and layers of biotite gneiss. Profile along Sandvasselva (25.5, 0—51.5) at the south contact of the Heddal granite.

(a) Feltskisse av roterte inneslutninger ved sørenden av Heddal-granitten ved Buvatn (27,5, 0—56,5). (b) Alternierende ganger av porfyrisk granitt og biotitgneislag. Profil langs Sandvasselva (25,5, 0—51,5) ved Heddal-granittens sørgrense.

are angular in plan and also in cross section (Fig. 45 a). Inclusions that appear to have had the same initial composition and occur close together exhibit all stages of transformation from veined biotite gneiss to widely separated (3—4 cm) biotite septa in granite. Some inclusions almost touch each other at right angles (Fig. 45 b). A succession of porphyric-granite sills parallels the prolongation on its east side.

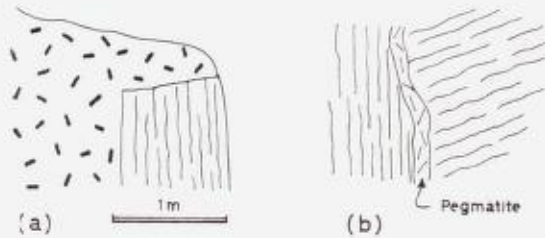


Fig. 45. Gneiss inclusions in the southeast prolongation of the Hedål granite at Vikerfjell (28.0, 0—46.0). (a) Profile of a rectangular inclusion transected by porphyric granite. (b) Two inclusions of gneiss separated by a pegmatite abut against each other.

Gneissinneslutninger i den sørvestre forlengelse av Hedål-granitten ved Vikerfjell (28,0, 0—46,0). (a) Profil av en rektangulær inneslutning gjennomskåret av porfyrisk granitt. (b) To gneissinneslutninger atskilt av pegmatit er dreid i forhold til hverandre.

The extension of gneiss into the granite at Svarttjernkollen (27.1, 0—47.0) on the west side of the granite prolongation is composed of flat-lying gneiss interlayered with granite sills and lenses. Since the granite to the east is steeply dipping, the development of the granite as well as the outcrop pattern may have been controlled by the structural geometry.

Large amounts of porphyric granite are found in the gneiss south and east of Vikerkøia (27.0, 0—45.8). The granite is strongly foliated and contains sheared inclusions of gneiss.

The entire eastern contact is characterized by steep foliation in the gneiss and granite. Sills of porphyric granite alternate with gneiss layers in the contact zone (Fig. 46), which is also marked by zones of augen gneiss (Fig. 46). The microcline megacrysts in the granite just inside the contact are augen shaped in some places. The gneiss is tightly small-folded adjacent to the granite. Many of the dikes and sills are highly sheared (Fig. 2, Plate 11) and contain bright red K-feldspar; however, palimpsest structures from the gneiss are retained in other dikes (Fig. 16). Inclusions occur commonly; their spatial relations indicate possible displacement for some and nondisplacement for others. The gneiss and granite interfinger along Begnadal to form a large scale migmatite.

The northeast contact parallels a broad zone of alternating granite dikes and gneiss layers. The foliation of the granite and the gneiss

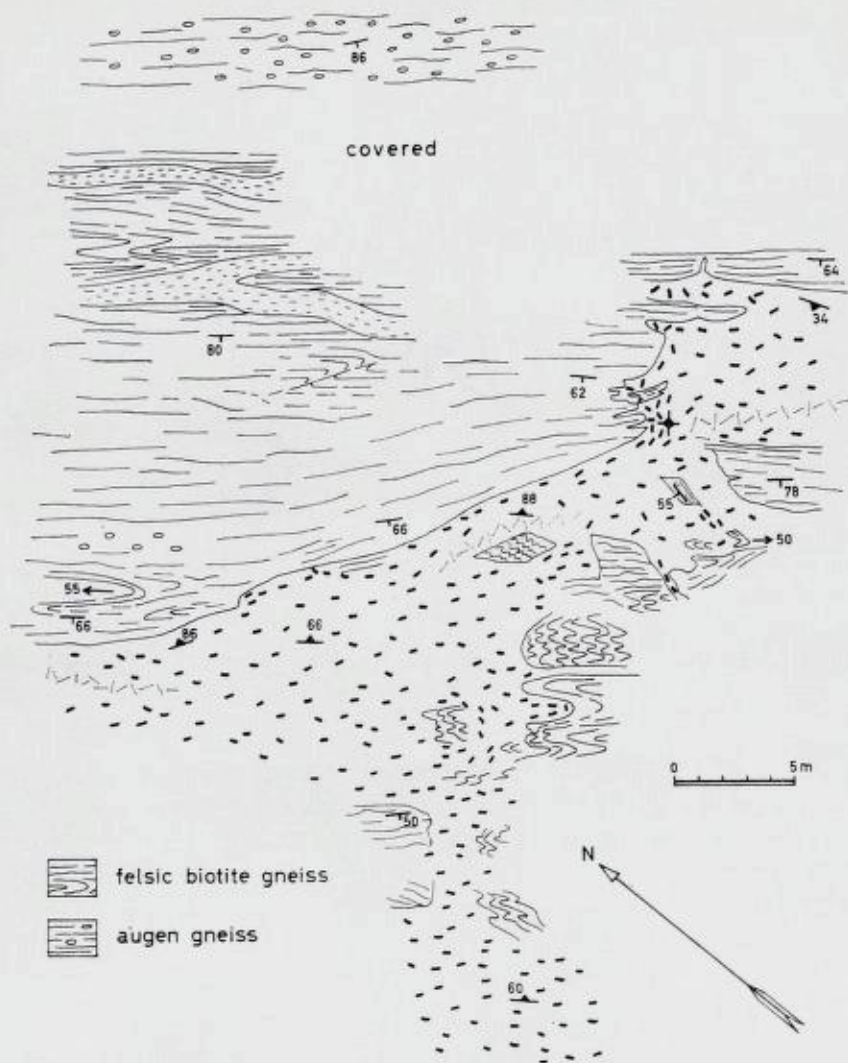


Fig. 46. Sketch map of the east contact of the Heddal granite between Veslefjell and Vikerfjell (29.2, 0—47.0). Granitic dikes and sills and zones of augen gneiss are found outside the contact. Some inclusions appear to be rotated; others appear to be in place.

Skisse av Heddal-granittens østgrense mellom Veslefjell og Vikerfjell (29,2, 0—47,0). Granittiske ganger og soner med øyegneis finnes utenfor kontakten.

Noen inneslutninger ser ut til å være rotert; andre synes å være på plass.



Fig. 47. Profile of fine-grained granite sill that permeates the gneiss at the northeast contact of the Hedal granite. Biotite clots appear to be drawn out, but the fold pattern is retained in the thin biotite layers surrounded by granite. Bårdli (45.7, 1—07.0).

Profil av finkornet granittgang, som trenger gjennom gneisen ved Hedalgranittens nordøstlige grense. Biotitflekker synes å være dradd ut, men foldemønsteret er beholdt i de tynne biotitlag omgitt av granitt. Bårdli (45,7, 1—07,0).

strikes northwest and dips nearly vertical. Some inclusions appear to be rotated, but most parallel the granite contact.

Delicate folds in biotite septa within the dikes retain the style of the regional folding (Fig. 47), but the same dikes show movement in places. Other sills and dikes of the same type of granite have certainly flowed and displaced their inclusions. Shearing and plastic flow may account for much of these movements; however, fluid flow may also have occurred.

Ådal Granite.

The southern contact is marked by alternating layers of porphyritic granite and migmatitic gneiss (Fig. 48); the layers are up to 20 m wide. "Flow structures" are common; however, the imprint of shearing is so marked in both granite and gneiss that this is the probable cause of the "flow structures" (Figs. 48 and 49). The foliation of the granite and gneiss is nearly vertical. The contact between the gneiss and the granite sills or the main body of granite are knife sharp (Figs. 48 and 49). The granite is conformable on a large scale and transgressive in



Fig. 48. (a) Migmatitic gneiss interlayered and interfingering with strongly foliated porphyric granite sills. (b) Close-up of gneiss interlayered with granite sills. The contact with the sills is sharp on the right side and somewhat gradational on the left. Foliation is very distinct in the granite. Streaks of biotite are visible in the granite. Macfic layers in the gneiss are highly drawn out; a pegmatitic layer is folded. Near Tjuvenborg (19.6, 0—43.6).

(a) Migmatitisk gneis lagvis og innfiltret med sterkt folierte porfyriske granittganger. (b) Nærbilde av gneislag vekslende med granittganger. Kontakten med gangene er skarp på høyre side og noe gradvis på venstre. Foliasjon er meget tydelig i granitten. Streker av biotit er synlig i granitten. Mørke lag i gneisen er sterkt uttrukket; et pegmatitisk lag er foldet. Nær Tjuvenborg (19,6, 0—43,6).

detail (Fig. 49). In some places, inclusions of gneiss are abundant inside the granite; many are certainly displaced. Screens of biotite are found in the granite sills (Fig. 48). The tight folds, boudinaged pegmatites and amphibolite layers, and shearing suggest that the tectonic effects which accompanied the granite emplacement were extreme.

The western contact remains concordant because the gneisses swing around and strike north-south parallel to the granite contact. Dips of the foliation in both the granite and gneiss are near vertical. A 400-m-wide zone of sills, which are transgressive on a small scale (Fig. 50), is developed by Kolsjöen (21.0, 0—48.5) at the southwest corner of the granite. Some of the sills intertongue with gneiss layers and clots and septa of biotite that are parallel to the foliation (Fig. 15). These sills exhibit textures intermediate between porphyric granite and biotite gneiss. The zone of alternating layers of granite and gneiss passes into a zone in which granite surrounding disoriented gneiss inclusions predominates.

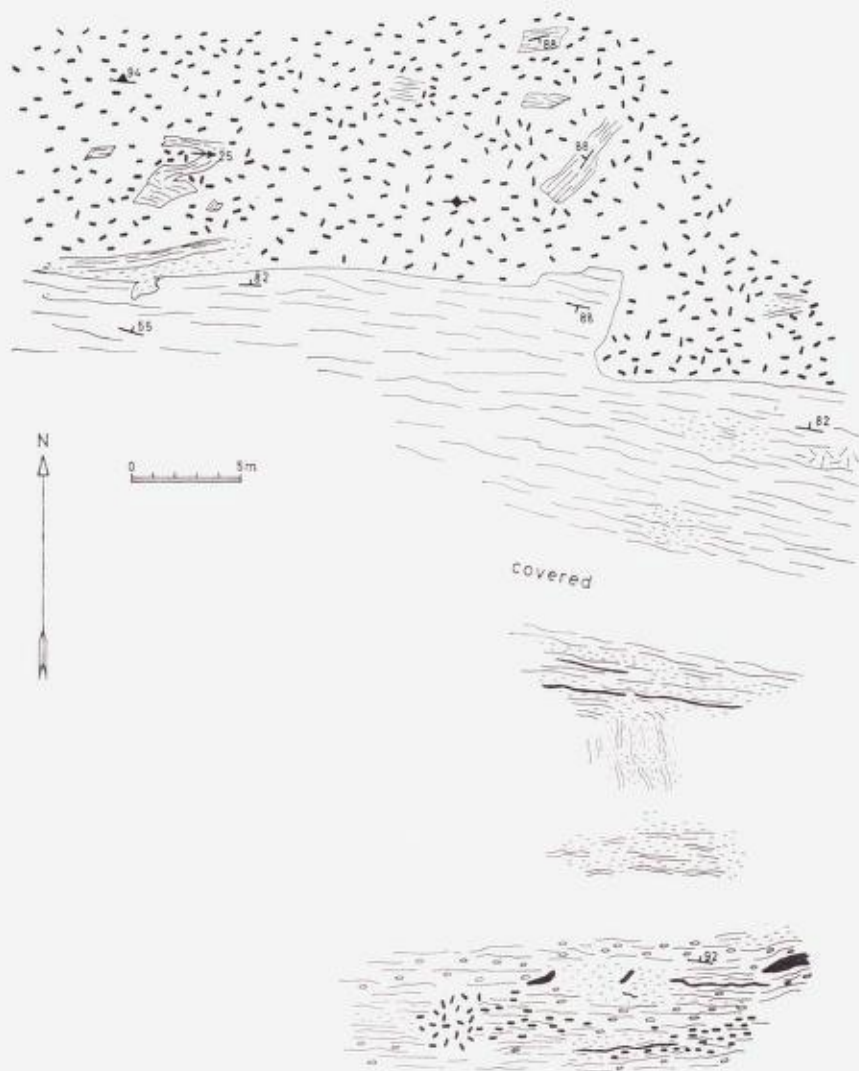


Fig. 49. Sketch map of the south contact of the Ådal granite near Tjuvenborg (19.6, 0—43.6). The contact is sharp. Granitic patches and sills are found in the gneiss. The rocks are highly sheared. Some inclusions are probably rotated.

Skisse av Ådal-granittens sørgrense nær Tjuvenborg (19,6, 0—43,6). Kontakten er skarp. Granitiske flekker og ganger finnes i gneisen. Bergarten er sterkt tektonisert. Noen inneslutninger er antagelig rotet.

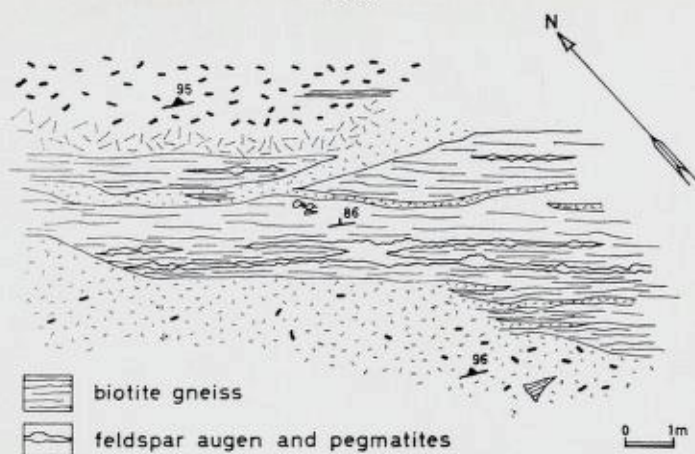


Fig. 50. Sketch map of granite sills at the southwest corner of the Ådal granite by ø. Kolsjøen (21.0, 0—48.5). Sills and gneiss layers alternate over a 400-m-wide zone.

Skisse av granittganger ved det sørvestre hjørne av Ådal-granitten ved ø. Kolsjøen (21,0, 0—48,5). Ganger og gneislag veksler i en 400 meter bred sone.

Along Eivaskollen on the west side of the granite (22.8, 0—40.6), a broad strip of fine-grained granite crops out about 2 km outside the actual granite contact. This strip contains numerous inclusions of biotite gneiss in various stages of assimilation. Most of the inclusions appear to have been rotated; however, the migmatitic gneiss here is commonly swirled so that determination of displacement is difficult.

The northern contact is concordant, and the foliation of the gneiss and granite dips vertically. A 2- to 3-km-wide zone of gneiss layers and granite sills parallels the contact at the northwest corner. Inclusions of gneiss in a small granite body that occurs in the gneiss by Kjölfjell (25.5, 0—48.0) were certainly rotated and displaced (Fig. 51). The numerous inclusions in the granite here appear to be unoriented.

Further east between Holmetjern and Ringerudsæter (24.5, 0—45.0), the gneiss runs perpendicular to a granite sill but swings around abruptly into concordance with the sill at its contact. At Høgfjell near the center of this granite, inclusions of amphibolite and biotite gneiss parallel the granite contacts and the foliation in the granite.

The northeast contact is beautifully exposed in a roadcut 1 km south of Sperillen community (22.6, 0—38.1). The contact is knife

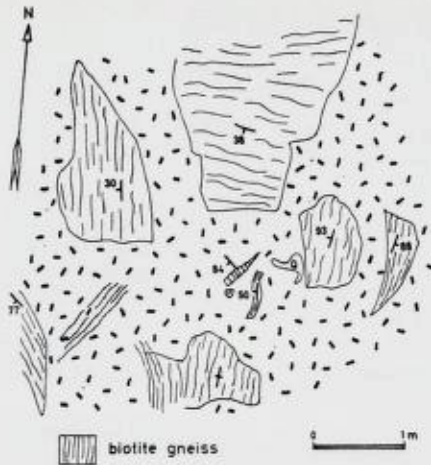


Fig. 51. Field sketch of rotated inclusions in a small body of porphyric granite that occurs in the gneiss that separate the two granites. Kjølffjell (25.5, 0—48.0).
 Feltskisse av roterte innslutninger i et lite område med porfyrisk granitt i den gneisen som skiller de to granitter. Kjølffjell (25,5, 0—48,0).

sharp (Fig. 52). The foliation of the granite and gneiss is conformable with attitude of the contact which dips under the granite at 78° . The gneisses at the contact are highly deformed. Folding and faulting indicate that the granite moved upward in relation to the gneisses. A drawn-apart gneiss layer that is parallel to the contacts is separated from the country rocks by a sill developed at the contact and has been more or less incorporated as part of the granite. Similar gneiss inclusions that are subparallel to the contacts and foliation of the granite are found near the center of the granite's "tail". Numerous streaks and shadows are pulled out parallel to the foliation of the granite, but the foliation is not particularly strongly developed at this contact. Bands of augen gneiss parallel the granite up to 500 m outside the contact but granite sills are conspicuously rare.

The southeast end of the granite grades into the gneiss by passing through alternating zones of migmatite, augen gneiss, and foliated granite which contains inclusions of gneiss. Layers of gneiss project into the granite parallel to the foliation and *vice versa*. All the rocks are highly sheared. Gradual transitions from augen gneiss to sheared porphyric granite can be followed across the strike.

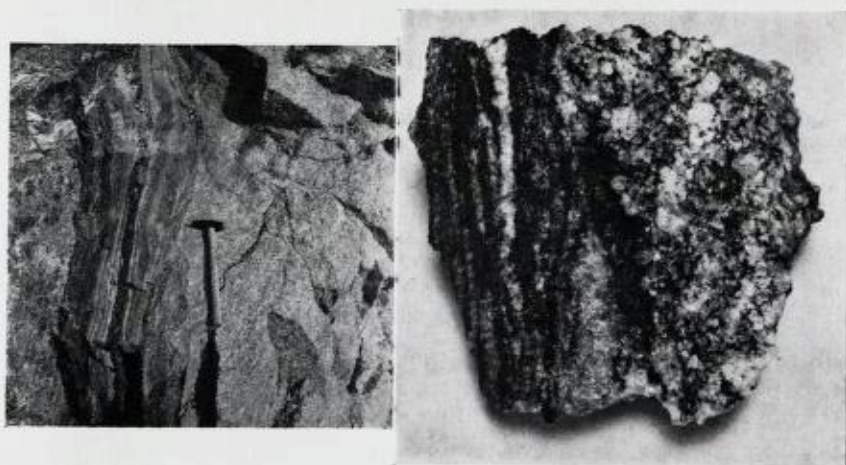


Fig. 52. (a) The northeast contact of the Adal granite south of Sperillen community (22.6, 0—38.1). Porphyric granite on the right against banded gneiss. The contact is sharp. (b) Hand specimen containing the granite contact from the same locality as (a). Some K-feldspars in both the granite and the gneiss from this specimen (Sp 509 G in Table VII and Fig. 61) exhibit low and/or variable obliquity.

(a) Adal-granittens nordøstre kontakt sør for Sperillen kommune (22,6,0—38,1). Porfyrisk granitt til høyre mot båndgneis. Kontakten er skarp. (b) Håndstykke med granittkontakten fra samme lokalitet som (a). Noen kalifeltspater både i granitten og i gneisen fra denne prøve (pr. 509 G i tabell VII og figur 61) viser lav og/eller varierende triklinitet.

The Origin of the Contact Features.

The descriptions of contact relations and the illustrations provide a reasonably clear picture of how the inclusion-rich border zone, the "eruptive breccia", developed. The first stage is certainly the formation of granite sills parallel to the main structure (the granite contacts) in the gneiss, possibly through an intermediate stage as an augen gneiss. These sills pass into short dikes that transect the gneiss layers in both vertical and horizontal sections. The sills then coalesce and grow until the amount of granite predominates over gneiss. It is here that the granite contact is drawn. Thus inclusions showing various states of transformation and displacement have been incorporated into the granite along its borders. In the process, some inclusions become

rotated either by shear in the solid rock or by flow in a rock that has become fluid. Finally, only scattered inclusions remain. In some areas, (subarea 48, Plate 13), the end product that we see today has most likely never gone through a liquid stage.

Although the fragments of gneiss are most common along the borders of the granites, they may be found anywhere in the granites. When they do occur, they are likely to be found in large numbers.

The "eruptive breccia" can be aptly described as a large-scale migmatite or agmatite (Sederholm, 1923) depending on the relations observed. What appear to be randomly oriented fragments of gneiss in granite may actually define a fold axis (Berthelsen, 1960, p. 117). The term agmatite is much more suitable to describe the contact phenomena of the Flå granite. In the light of the evidence, this agmatite ("eruptive breccia") cannot be directly ascribed to the upthrust of magma which has disrupted and disoriented the gneiss.

Gravimetry

General Statement.

Negative gravity anomalies caused by relatively low-density material are properties of granites that are nearly as characteristic as their petrography (Bott, 1956; Smithson, 1963). For this reason, a gravity survey offers a most useful method to arrive at the 3-dimensional shape and mass deficiency of a granitic body. This gravity survey was undertaken in order to determine the "thickness" and the shape of the Flå granite.

The field methods and computations employed in the gravimetry have been discussed previously by the writer (Smithson, 1963). Only those methods that are different or would cause a different error in the results will be mentioned here. The description of the field procedure and of the computations appears in the Appendix.

Density Determinations.

Hand-specimen-sized rock samples were weighed using a Mettler balance. The precision of the method is 0.002 gm/cm³. The rock densities appear in Table IV. The eastern gneisses have a smaller mean density than the western and southern gneisses. The mean densities

Table IV.
Rock Densities.

Rock type	No. of Samples	Mean Density	Standard Deviation	Range of Values
Hedal Granite	33	2.65	0.023	2.59—2.68
Ådal Granite	14	2.65	0.020 ¹	2.61—2.66
Eastern Gneisses	36	2.74	0.121	2.62—3.14
Western and Southern Gneisses	56	2.78	0.152	2.61—3.16
Porphyric Granite	24	2.65	0.020 ¹	2.59—2.68
Fine-grained Granite	25	2.64 ₅	0.028 ¹	2.60—2.69

¹ Corrected.

of Hedal and Ådal granites are equal; the mean densities of the porphyric and fine-grained granites are almost equal. Like the modal analyses, the density determinations indicate that the differences within each type of granite are greater than the differences between them.

The Bouguer Anomaly Map.

The Bouguer anomaly map (Plate 15 in pocket) shows one distinct feature, the strong gravity gradient that is directed downward to the northwest. The gradient is found on one flank of a gravity trough that parallels the Caledonian thrust front. Troughs of negative anomalies commonly follow the strike of mountain ranges (Heiskanen and Vening Meinesz, 1958). This gradient, which attains a maximum value of *ca.* 2 mgal/km, is attributed to the combined positive effect of the Oslo region (Grønhaug, 1963) and the negative effect of the Caledonian mountain range. The map area occupies the region between these two features of opposite sign so that the gradient could be expected to be large. This gradient is a large regional feature that cuts across the local geology and is, therefore, attributed to deep crustal features.

Superposed on this gradient are small bends and closures of the isoanomaly lines caused by local geologic features. A closure in the —87.5-mgal line suggests a negative anomaly over the northwest

corner of the Hedal granite. A small embayment is found in the iso-anomaly lines over the Ådal granite, and a stronger embayment is visible southeast of this granite. Positive features are suggested north-east and west of the Hedal granite.

Indications of small anomalies are evident on the Bouguer anomaly map; however, the true shape and amount of the anomalies are concealed by the strong gravity gradient. In order to obtain a clearer picture of the local anomalies, the effect of the gravity gradient must be removed.

The Regional and Residual Anomaly Maps.

The Bouguer anomalies are to be separated into two components, the regional anomalies caused by deep large-scale features, and the residual anomalies caused by shallower, local geologic features. In order to accomplish this, a series of profiles were drawn across the Bouguer anomaly map, and smoothed gravity curves were drawn along these profiles (Dobrin, 1960, p. 244). The smoothed curve represents the regional anomalies and the difference between the smoothed curve and the measured profile at a particular point is the residual anomaly at that point.

Plates 16 and 17 (in pocket) are the regional anomaly map and residual anomaly map so obtained. The regional anomaly map shows a smooth decrease in gravity that reaches its minimum value near Gol in Hallingdal.

The residual anomaly map, Plate 17, reveals numerous small closures in the gravity field. Gravity minimums are found over the Hedal and Ådal granites. In addition these gravity lows are seen to coincide better with the contacts of the granites. The "low" over the Hedal granite reaches a maximum value of -6 mgal over the north-west corner of the granite; the "low" over the Ådal granite amounts to -3 mgal over the center of the granite. A "low" of -6 mgal is found southeast of the "tail" of the Ådal granite.

The largest feature on the map is the partially revealed gravity "high" north of Bagn. This is the southern flank of a large positive gravity feature in Slidre. This positive gravity anomaly begins at Bagn right by the shear zone that separates the banded quartz-dioritic gneisses on the north from the banded granodioritic gneisses to the

south. Strand (1954) has remarked about the distinct petrographic difference between the two rock types, and this difference seems to be further reflected in the gravity anomalies. The writer is at present investigating this "high" which will be the subject of a future gravity publication.

Small gravity highs are indicated north of the Ådal granite and west of the Hedal granite. A gravity high that may be fairly large is suggested south of Sokna.

Interpretation.

The positive anomalies are poorly defined and difficult to interpret in terms of the surface geology without more information. One such occurrence is the elongate north-south-striking high of 5 mgal west of the Hedal granite. Although only two profiles across this feature are measured, its position coincides closely with the area of Telemark supracrustal rocks, the interlayered quartzites and amphibolites. Amphibolite and quartzite are estimated to occur in approximately equal amounts so that the mean density of these rocks is probably greater than that of the underlying gneiss and causes the anomaly.

The Hedal granite is characterized by the gravity low that straddles the northwest border of the granite. Granites are commonly less dense than their surrounding rocks (Bean, 1953; Bott, 1956; Smithson, 1963), and the density determinations demonstrate that this is also the case for the Hedal and Ådal granites. The negative anomaly that is found over the Hedal granite must be caused by the mass deficiency of the granite.

The attitudes of granite contacts can often be determined from gravity calculations (Romberg and Barnes, 1944; Bean, 1953; Smithson, 1963) so that a rather exact determination of a granite's form constitutes one of the most important results of the interpretation. Although the attitudes of contacts will be illustrated in the following models, these attitudes are not considered to be at all definitive. The size of the errors encountered in the gravity anomalies coupled with the small size of the anomalies over the granites precludes the possibility of calculating an accurate model at the borders of the granites. Realistic calculations are further impeded by the transitional nature of the granite contacts. The most useful aspect of the gravity inter-

pretation will be to compute the "thickness" of the granites; "*thickness*" is understood to mean the vertical extent of the density contrast.

A density contrast of -0.11 gm/cm^3 (the mean of the gneiss densities, 2.76, minus the granite density, 2.65) is used for the calculations. Dips are vertical along the east border, 60° to 80° along the south border and west border, and 20° to 30° along the northwest border of the granite. Models are calculated for three profiles through the Heddal granite (Fig. 53)¹. All three models portray the Heddal granite to be a thin plate that has a gently undulating lower surface. The thickness of the models in Fig. 53 b and 53 c is just over 1 km; the model in Fig. 53 a attains a thickness of 1.5 km.

The gravitative effect of the material between sea level and the station elevation was removed in computing the Bouguer anomaly. Since the granite crops out at elevations between 900 m in the north and 1285 m in the south, these thicknesses can be added to those of the calculated models. A thickness of 2.5 km in the north and 2.3 km in the south is thus obtained.

Although part of the granite is obviously eroded, both the anomalies and the geology at the northwest border of the granite suggest that this may be very near the original thickness. The writer has drawn his northwestern granite contact several kilometers east of the contact drawn by Strand (1954). The area in between is marked by numerous blocks of gneiss surrounded and cut by granite. The blocks of gneiss appear to be in place, and, in fact, foliation in them has yielded a β fold axis (subarea 51). This fact together with the gravity "low" right over the writer's contact suggests that this is the roof zone so that the granite plunges gently under the gneiss here. This hypothesis is further confirmed by the thinning of the granite models toward the south (Fig. 53). The calculated thickness in the northwest corner should, therefore, be very near to the maximum thickness of the granite before erosion.

All three models show a thinning of the granite toward the east contact. Since this thinning is found in every model and since it has the same order of magnitude in each model (one-half the maximum thickness), the thinning is very likely real and must be explained in the development of the granite. The reader should remember that foliation along the eastern contact is much more common than along the western contact.

¹ Computed by the line-integral method of Hubbert (1948 b).

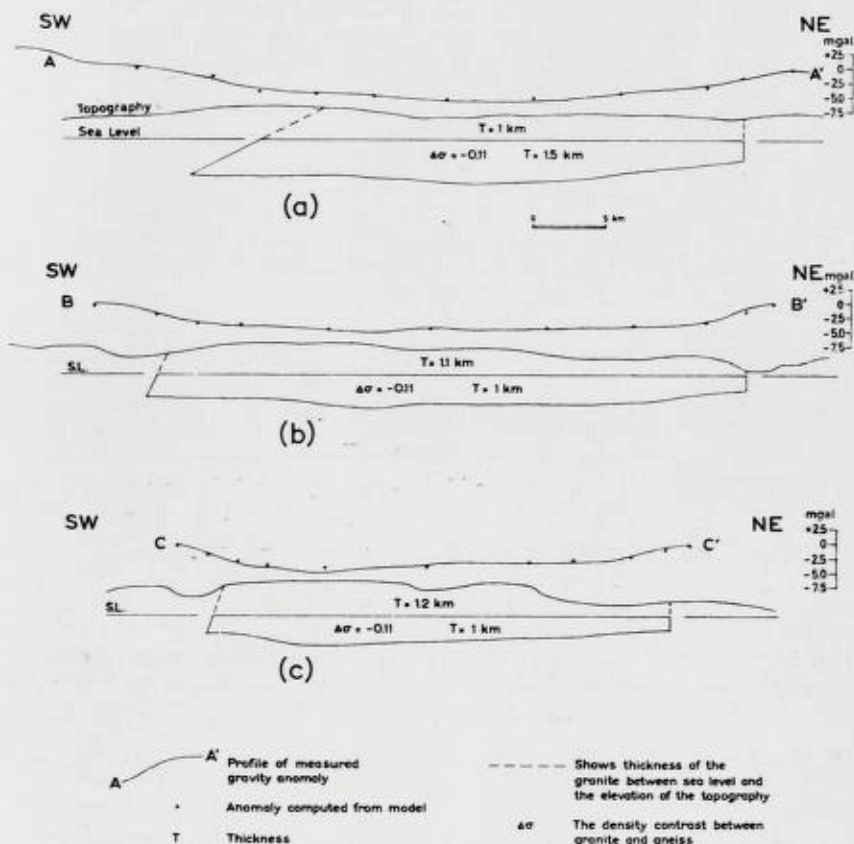


Fig. 53. Profiles through the residual anomalies over the Heddal granite and the models computed to satisfy these anomalies. Since the gravity anomalies are reduced to sea level, the computed model represents the thickness below sea level. One kilometer of granite is found above sea level; therefore, the maximum thickness is 2.5 kilometers.

Profiler gjennom anomalier i Heddal-granitten og de modeller som er konstruert for å forklare disse anomalier. Siden tyngdeanomalierne er redusert til havets overflate representerer den beregnede modell tykkelsen under havets overflate; den maksimale tykkelse er derfor 2,5 kilometer.

The gentle dip of the western contact in Fig. 53 a is necessary to satisfy the measured profile. Since errors in the Bouguer anomalies are probably small in this part of the area and the anomaly is fairly large, the contact attitude may approximate the true conditions. Small undulations along the lower surface of the gravity models may not be significant.

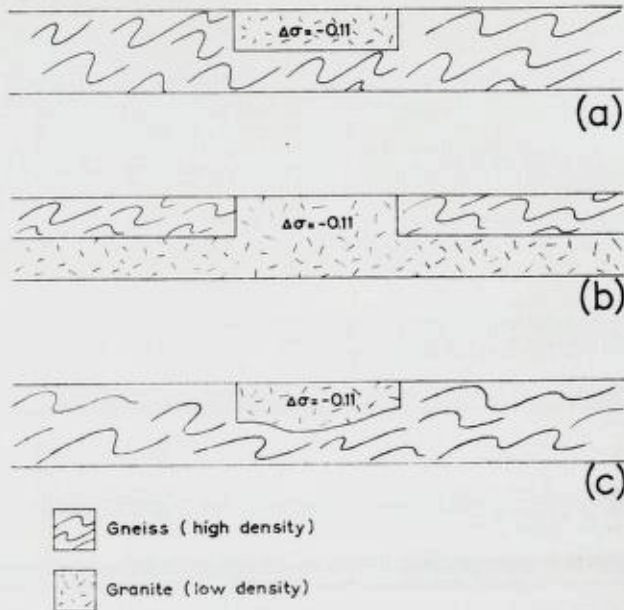


Fig. 54. A gravity model with a flat lower surface can be interpreted in the form of either (a) or (b). A gravity model with an irregular lower surface can only be interpreted as (c).

En tyngdemodell med en flat underside kan tolkes enten som (a) eller (b).
En tyngdemodell med en uregelmessig underside kan bare tolkes som (c).

Generally for a flat bottomed gravity model (Fig. 54), two interpretations exist. One is a slab of rock (granite in this case) "floating" in gneiss; the other is a layer of rock that projects through the overlying gneiss layer. In each case the vertical density contrast is the same and the anomaly produced is the same. Obviously the example in Fig. 54 a has a higher background anomaly. In the case of a model with an irregular lower surface, however, only one possibility exists; a slab must be floating in gneiss (Fig. 54 c).

This interpretation suggests that the Heddal granite is a slab-like body, but other possibilities cannot be excluded. The distribution of inclusions, a gradational contact, or a variable density distribution within the granitic rock (Bott, 1960; Smithson, 1963, p. 83) could produce the same gravity effect for the granite-layer hypothesis (Fig. 54 b). In view of the low resolution power of this gravity survey and the complications that may exist in nature, the other hypotheses cannot be excluded.

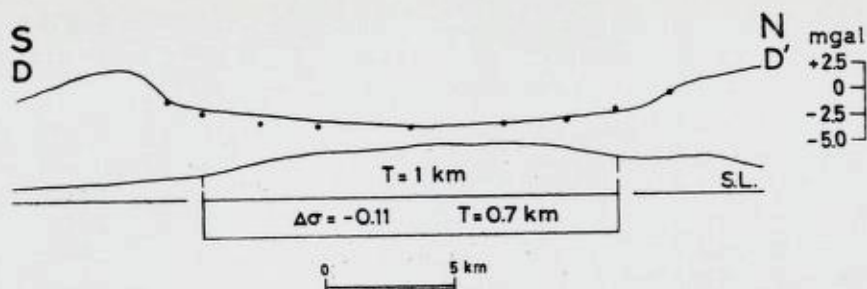


Fig. 55. Profile through the residual anomaly over the Adal granite and the model computed to satisfy the anomaly. The maximum thickness is 1.7 kilometers.

Profil gjennom residual anomalien over Adal-granitten og en beregnet modell som forklarer anomalien. Den maksimale tykkelse er 1,7 kilometer.

The Adal granite is associated with a -3 -mgal low that is centered over the granite. As in the case of the Hedal granite, the negative anomaly is attributed to the mass deficiency of the granite; a density contrast of -0.11 gm/cm³ is used. Dips are almost vertical all the way around the Adal granite. The gravity model that satisfies this profile is a 0.7-km-thick plate (Fig. 55). As before, the effect of 1 km of granite was removed in computing the Bouguer anomalies; therefore, the thickness of the granite is 1.7 km.

The "low" of -6 -mgal southeast of the Adal granite occurs along the strike direction of the "tail" of the granite. Furthermore, the anomaly occurs over a strip of felsic gneiss in which granite dikes and sills are emplaced. In places, biotite gneiss grades into fine-grained granite. This strip extends from the southeastern tip of the granite southeastward to the gravity traverse along Vælsvatn. This gravity low appears to be caused by the effect of a buried extension from the granite, of a granitized zone in the gneiss, or of both.

The first model presupposed that the negative anomaly is solely produced by a buried granite (Fig. 56 a). The density contrast is assumed to be -0.11 gm/cm³. The width of the buried granite is assumed to equal the width of the felsic zone. The distance to the top of the mass is 1 km, and the thickness of the mass is 4 km.

The second model assumes that the felsic gneiss cut by granite overlies a granitic body at depth. A density contrast of -0.11 gm/cm³ is used for the granite, and a density contrast of 0.05 gm/cm³ is arbitrarily chosen for the overlying felsic zone. The thickness of the

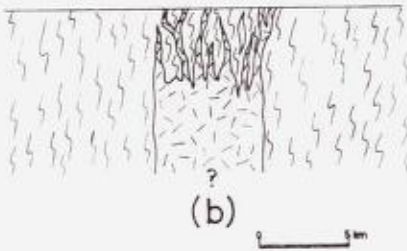
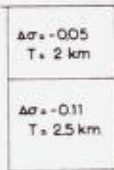


Fig. 56. Profiles through the residual anomalies southeast of the Adal granite and the calculated models. The gravity low is presumed to be caused by a concealed extension of the granite. (b) Presumes that the granitized gneiss which overlies the granite contributes to the gravity "low".

Profilen gjennom residual-anomalier sørøst for Adal-granitten og de beregnede modeller. Tyngde minimum antas å skyldes en skjult utløper av granitten. (b) Antar at den granittiserte gneiss som ligger over granitten bidrar til tyngdeminiimum.

granitized zone is 2 km and the thickness of the granite is 2.5 km (Fig. 56 b). This model is seen to agree slightly better with the measured anomaly.

The second model is preferred because it provides better agreement with the geological information and with the measured gravity profile. This model is interpreted as a buried extension of the Ådal granite overlain by a zone of granitized gneiss. This model implies that the maximum thickness of the granite before erosion is *ca.* 2.5 km.

If this is a buried granite, and it probably is either a buried granite or granitized zone, then some important petrologic conclusions can be drawn. If a basic front surrounds the granite, it should be detectable in the gravity anomalies (Bott, 1956). None, however, is reflected in the gravity profile (Fig. 56). Since the granite has not yet been bared by erosion, any material composing a basic front is unlikely to have been removed. Bott (1953, 1956) has also failed to detect a basic front surrounding a buried granite.

If metasomatic granite exists in the Flå area, it is certainly the "tail" of the Ådal granite. Hardly a square meter of the granite exposed along highway 60 is without an inclusion or a biotite-rich shadow. If the postulated extension has the same appearance as the exposed "tail" of the Ådal granite, a tremendous amount of dense material must have left the granite. This material is not reflected in the shape of the anomaly as it would be if it were concentrated above or around the granite.

It is important to note that the survey over and around this "tail" is not detailed enough to draw definite conclusions regarding the disposition of the missing mass. On the other hand, no evidence of a concentrated basic front or a basic behind can be inferred from the available gravity measurements.

If the thicknesses of the models for the granites are compared with the occurrence of foliation, the following facts are revealed:

- (1) The Ådal granite is the thinnest and has the strongest most widespread foliation.
- (2) The Heddal granite is thinnest along the eastern margin where it is most strongly foliated.

The movements that caused the foliation could have caused a greater upwards extension of the foliated part of the granite so that the granite is effectively thinned by subsequent erosion in these places.

Four important conclusions can be drawn from the gravity interpretation:

- (1) The usual thickness of the granite is *ca.* 2 km, a value that is considered to be reliable and can hardly be altered by a detailed survey.
- (2) Maximum thicknesses of 2.5 km are determined at the ends of both the Ådal and the Hedal granites. That they agree so closely may be fortuitous, but even a somewhat poorer agreement would have significance.
- (3) Gravity measurements support the geologic interpretation of a roof zone at the northwest contact of the Hedal granite and of a buried continuation southeast of the Ådal granite.
- (4) *The granites which appear to be batholiths that "continue" to the "eternal depths" from the field mapping are revealed by the gravity interpretation to be thin plates, lenses, or thin projections from a granitic substratum.*

The reader should note that gravity interpretation is inherently ambiguous (Nettleton, 1940, p. 120); the fact that the attraction of a calculated model closely satisfies the measured gravity field does not guarantee the correctness of the model. On the other hand, when geologic contacts and densities are known or approximated, much of the ambiguity is removed. The only possibility for the computed model to be greatly in error would be if the density contrast between granite and country rocks varied considerably not far below the present surface.

A block diagram (Plate 18) that combines the information gained from structural studies, contact relations, and gravity interpretation has been constructed for the Flå area. The block, which is somewhat thinner than the granite thickness determined gravimetrically, shows the general geometric relations of the rocks.

The Feldspars.

General Statement.

The history of the granite is reflected in the history of the feldspars. If their evolution could be deciphered, the petrogenesis would become much clearer. Three aspects of the feldspars are treated:

- (1) Interpretation of textural features from the feldspars.
- (2) The composition of the feldspars.
- (3) The symmetry relations of the K-feldspar.

The data from the latter two sections could be applied to geologic thermometry as well as the development of the granite.

Interpretation of Textural Features.

Origin of the Antiperthite.

The interpretation of petrographic textures encounters numerous ambiguities; nevertheless, a number of facts concerning antiperthite is highly suggestive:

1. Its occurrence in the Flå area is restricted to inclusions, augen gneisses, and migmatites, rocks showing K-feldspar porphyroblastesis which many petrologists ascribe to metasomatism and most petrologists ascribe to a complicated history.
2. The occurrence of the K-feldspar patches in the plagioclase is erratic both among grains and within a single grain (Fig. 2, Plate 2).
3. Some grains are mesoperthitic (Fig. 2, Plate 4).
4. The K-feldspar patches tend to follow the plagioclase twin lamellae.
5. Some of the antiperthitic interpositions are randomly disordered K-feldspar; some are grid-twinned microcline.
6. The rocks in which the antiperthite usually occurs contain both randomly disordered and low-obliquity K-feldspar porphyroblasts. The composition of the plagioclase involved is *ca.* An₄₀.
7. The gneisses in which this antiperthite occurs belong to the amphibolite facies.

Exsolution and replacement are the two commonly proposed modes of formation for perthite and antiperthite. The amount of K-feldspar in the plagioclase (An_{40}) far exceeds the amount that can be held in solid solution (Sen, 1959); moreover, the only known occurrence of exsolution antiperthite in metamorphic rocks is from the granulite facies (Sen, *ibid.*). The erratic occurrence is not typical of exsolution phenomena. An origin by exsolution must, therefore, be excluded. The erratic distribution, the preference for plagioclase twin lamellae, and the general geological milieu all indicate a replacement origin, which has been suggested previously by several authors (Drescher-Kaden, 1948; Sen, 1959).

On Flame Perthite.

The flame perthite shows such a characteristic occurrence that it must be closely related to the formation, or a phase in the formation, of the granite. The flame perthite is most common in rocks in which the K-feldspar appears to have grown and corroded the surrounding plagioclases. The flame perthite is commonly found in augen gneisses and in some fine-grained granite as well as in the porphyric variety.

Flame perthite exhibits the following features:

- (1) Common occurrence in rocks in which fresh microcline grains show indented borders against sericitized plagioclase and in which pockets and septa of sericitized plagioclase occur between K-feldspar grains (Fig. 1, Plate 11).
- (2) The distribution is uneven between grains and in single grains (Fig. 2, Plate 6); some grains contain up to 40 per cent plagioclase.
- (3) A preference for indented and interfingering grain boundaries against plagioclase (Fig. 2, Plate 5; Fig. 2, Plate 7) or for plagioclase inclusions and trains of inclusions in K-feldspar (Fig. 2, Plate 6).
- (4) In K-feldspar, plagioclase lamellae are in optical continuity with and are contiguous with inclusions of plagioclase, which are the same as the groundmass plagioclase (Fig. 2, Plate 6; Fig. 1, Plate 7).

Andersen (1928) suggested that perthites may form in three main ways: (1) By exsolution (2) By simultaneous (eutectic) crystal-

lization (3) By replacement, Andersen related the position of the plagioclase lamellae in the perthite to thermal contraction in a K-feldspar crystal. He ascribed the mesoperthites to simultaneous crystallization, the string and film perthites to exsolution, and the vein and patch perthites to replacement along fractures. Alling (1932) proposes exsolution and replacement as the two important processes in perthite formation. Alling emphasizes the importance of deuteric solutions in the development of replacement perthite. Bowen and Tuttle (1950) demonstrated that a homogeneous high temperature alkali feldspar will exsolve into a sodic and potassic phase at lower temperature. Rosenqvist (1950) related the position of the plagioclase lamellae to the rate of diffusion in a K-feldspar during unmixing. Gates (1953) has summarized the literature and concluded that the albitic phase of exsolution perthites is highly mobile and may migrate to form concentrations of albite.

In light of modern experimental results (Tuttle and Bowen, 1958), an exsolution origin for perthite must be considered first. An exsolution origin, however, is incompatible with the erratic distribution of flame perthite, particularly when some grains contain no flame perthite and others contain up to 40 per cent plagioclase in the perthite. Tuttle and Bowen (*ibid.*) have suggested that exsolved plagioclase may be thrown completely out of an original alkali feldspar and form discrete grains. If this were the case with the flame perthite, the plagioclase component would have to be completely expelled from some grains and incorporated into others. The erratic distribution of flame perthite renders an exsolution origin extremely unlikely.

The petrographic observations indicate that porphyroblastesis has been an operative process in these rocks. Since the K-feldspar appears to be fresh and porphyroblastic throughout the entire Flå area, while the plagioclase shows a strong sericitization, the K-feldspar is probably replacing plagioclase to a certain extent. This conclusion is further confirmed by the numerous corroded inclusions of plagioclase in K-feldspar, by embayed plagioclase grains (Fig. 12), and by pockets of plagioclase between microcline grains. The development of flame perthite is intimately associated with this porphyroblastesis.

The plagioclase component of the flame perthite is commonly contiguous with corroded plagioclase grains, septa, and inclusions (Fig. 2, Plate 5; Fig. 2, Plate 6; Figs. 1 and 2, Plate 7). The rectilinear border of some plagioclase "flames" within a K-feldspar grain

suggests that two K-feldspar grains may have coalesced and completely replaced an intervening plagioclase grain (Fig. 2, Plate 5). The plagioclase inclusions are oriented so that they extinguish simultaneously with the plagioclase lamellae of the perthite, and the inclusions seem to grade into the plagioclase lamellae (Fig. 2, Plate 6; Fig. 1, Plate 7).

The writer suggests that the flame perthite is a replacement perthite; however, the plagioclase lamellae are considered to be a residual (remnant) left behind by a replaced plagioclase grain rather than introduced from the outside. As the plagioclase grain is replaced by K-feldspar, some of the albitic component of the plagioclase is enveloped by the K-feldspar, and the intergrowth appears as flame perthite.

Although the above hypothesis agrees with the occurrence and distribution of flame perthite, the proposals of other petrographers (Alling, 1932; Goldich and Kinser, 1939) demonstrate the disagreement that can arise over the interpretation of textural features. Alling (*op. cit.*) attributed flame perthite to deuteric reactions in the final stage of magmatic crystallization. He suggested that the plagioclase was introduced from outside the perthitic grain but from within the system. Goldich and Kinser (*op. cit.*) proposed that the plagioclase component of flame and braid perthite was introduced during an albite metasomatism.

As the writer has already noted, no evidence for sodium metasomatism exists; however, strong evidence of potassium metasomatism is found in the area. Furthermore, the albitic portion of the flame perthite can be derived right in place from the replaced plagioclase.

There also seems to be a transition from oriented sericitized plagioclase inclusions to sericitized plagioclase slivers grading into plagioclase "flames" and films. On the other hand, Alling (1932) states that plagioclase inclusions in K-feldspar may influence the location of plagioclase lamellae by differential contraction so that exsolved plagioclase films may accumulate around inclusions. This does not, however, explain the common occurrence of flame perthite along highly corroded borders between plagioclase and K-feldspar. Although the origin for flame perthite proposed by the writer cannot be demonstrated unequivocally, no other explanation fits the facts; therefore the writer believes it to be probable enough to be considered when the development of the granite is discussed.

On Aligned Inclusions in K-feldspar.

The striking alignment of plagioclase inclusions within K-feldspar megacrysts has attracted considerable attention among petrographers (Maucher, 1943; Drescher-Kaden, 1948; Frasl, 1954; Schermerhorn, 1956). Drescher-Kaden has ascribed these oriented plagioclase inclusions to metasomatic processes, but Maucher, Frasl, and Schermerhorn have postulated a magmatic environment to be necessary. Frasl and Schermerhorn, in fact, state that oriented plagioclase inclusions in K-feldspar constitute strong evidence in favor of a magmatic origin for the rock.

The plagioclase inclusions in K-feldspar from rocks of the Flå area are commonly orientated (Fig. 1, Plate 5; Figs. 1 and 2, Plate 8) but do not show the striking layering that Maucher and Frasl (*ibid.*) have described. The plagioclase inclusions, which range in length from 0.1 to 0.5 mm usually exhibit a preferred orientation so that their (010) face is either parallel or perpendicular to the (010) face of the K-feldspar host. In some cases, plagioclase inclusions parallel the (110) face of the host. Most of the plagioclase inclusions in a single megacryst extinguish simultaneously with each other and with the plagioclase lamellae of the perthite.

The inclusions are generally rectangular but may be rounded, corroded, and irregular. The rectangular inclusions generally exhibit the best preferred orientation; however, many sliver-like or corroded inclusions that grade into perthite display a preferred orientation and simultaneous extinction (Fig. 2, Plate 6; Fig. 1, Plate 7). The inclusions are usually scattered throughout the host grain instead of being arranged in concentric layers.

The composition of the plagioclase inclusions is of utmost importance for determining the processes by which such a textural feature developed. The composition of the plagioclase inclusions is about the same as the composition of plagioclase grains in the ground-mass (*ca.* An₃₀).

The key to the process of formation for this texture can be found in inclusions of gneiss within the granite, particularly massive inclusions that are presumed to have been amphibolite. *The K-feldspar porphyroblasts from the inclusions contain the same oriented plagioclase inclusions as the megacrysts from the granite.* The plagioclase grains within inclusions of gneiss can be seen in various stages of incorpora-

tion within K-feldspar porphyroblasts (Fig. 2, Plate 10). The plagioclase grains are pushed out by the growing K-feldspar porphyroblast and rotated into parallelism with the adjacent crystal face of the porphyroblasts. Then the plagioclase grain is enveloped by the K-feldspar porphyroblast. Layers of well oriented plagioclase inclusions are found in microcline porphyroblasts within amphibolite inclusions from the Vrårdal granite as well (A. Sylvester, oral communication). *The conclusion is unavoidable that oriented plagioclase inclusions in K-feldspar megacrysts can arise in a solid medium.*

That a perfect parallelism is not always achieved is manifested by the randomly oriented plagioclase inclusions that are usually present. *The growing K-feldspar porphyroblast must, however, be able to rotate most of the plagioclase grains into optical continuity with each other and with the plagioclase lamellae of the perthite, and does this within a solid medium.*

Maucher (1943), Frasl (1954), and Schermerhorn (1956) have all visualized a fluid medium (magma) to be necessary for the occurrence of oriented plagioclase inclusions in K-feldspar megacrysts. Their occurrences showed a concentric layering of the plagioclase inclusions which was not found in the writer's rocks. They have suggested that plagioclase grains freely swimming in a fluid adhered to the faces of growing K-feldspar grains and were rotated into optical continuity by the lattice forces of the K-feldspar. It is difficult to conceive how such a layering and zoning could develop in a solid medium unless the K-feldspar porphyroblast grew in pulses; *i. e.*, each layer corresponds to a growth pulse.

It is not the intention of the writer to interpret the origin of the above writers' rocks; however, there are some inconsistencies in the fluid-medium hypothesis. When all the plagioclase inclusions have the same composition as each other and as the groundmass plagioclase, magmatic crystallization would have to follow a path different from that indicated by present-day information. There is no sign of fractional crystallization; all the plagioclase must have crystallized before the K-feldspar megacryst started to form. This seems unlikely in a conventional-type magma.

The other contradiction is in the grain outline of the plagioclase inclusions. Many plagioclase inclusions have irregular non-flat inner surfaces toward the K-feldspar megacryst but exhibit the same perfect orientation as the rectangular plagioclase inclusions. Such irregular

inclusions would never adhere stably to a flat surface in their present position. The conclusion is inescapable that these inclusions have either been corroded (replaced) in a solid medium or that they have been rotated to their present parallelism in a solid medium even if they were swimming in a fluid medium at the time of incorporation. In either case, the necessity for a magma becomes weakened.

Some megacrysts in the Flå granite have a single incompletely developed layer of plagioclase inclusions (Figs. 1 and 2, Plate 8). The L-shaped plagioclase inclusions at the corner of both K-feldspar megacrysts can hardly have been adsorbed in a magma. These layers probably represent plagioclase rims that formed on a K-feldspar megacryst (Rapakivi texture) and were later enveloped by the megacryst.

Plagioclase rims on microcline are found in some inclusions (Fig. 1, Plate 10). They seem to be characteristic of the inclusions.

The geometry of both rims (Figs. 1 and 2, Plate 8) suggests that the final state, at least, was attained in a solid medium. The appendage on the large L-shape plagioclase inclusion (Fig. 1, Plate 8) is in physical and optical continuity with the appendage of plagioclase to the right of it. This configuration could most easily arise by partial replacement of a plagioclase rim by K-feldspar. In Fig. 2, Plate 8, a large plagioclase grain extends from outside the microcline megacryst through the plagioclase layer that the megacryst encloses. This is not a stable position for the plagioclase grain to assume in a fluid medium. It would rather seem to have been a plagioclase grain from the groundmass that was caught and retained in this position by a growing porphyroblast.

Shand (1950 b) studied the Cortlandt igneous complex and concluded that poikilitic hornblende was formed deuterically after the magmatic crystallization. He generalizes that a poikilitic texture in any rock is good evidence of recrystallization of a solid rock (Shand, *ibid.*, p. 169).

Some of the most suggestive evidence comes from the K-feldspar phenocrysts of extrusive rocks and of undoubtedly magmatic intrusive rocks. Such oriented plagioclase inclusions are uncommon in the phenocrysts of these rocks. Where they are common is in the megacrysts from gneisses and deep-level granites, the very rocks from which porphyroblastesis is so commonly described.

In conclusion, although K-feldspar megacrysts that contain ori-

ented plagioclase inclusions *may* have formed in a magma, a fluid medium is not required. Apparently a K-feldspar porphyroblast is capable of rotating a plagioclase grain into physical and optical conformity. The plagioclase inclusions in K-feldspar bear the imprint of processes taking place in a solid medium at the last stage, at least. The plagioclase layers in some cases may be related to Rapakivi rims of plagioclase that have subsequently been engulfed. In this area, the true Rapakivi feldspars are confined to inclusions within the granite. Although the evidence is, as usual, not unequivocal, we might just as well turn the argument around and state that oriented plagioclase inclusions in K-feldspar are evidence for growth in a solid medium.

Composition of the Feldspars.

Plagioclase.

The composition of most plagioclase was determined from two refractive indices measured with index liquids in cleavage flakes lying on (001). The refractive indices are determined to ± 0.002 or better; curves of Crump and Ketner (1953) were employed for the compositions. Some plagioclase were determined on a U-stage by measuring the maximum extinction angles of albite twins from the trace of (010) in sections normal to (010).

The plagioclase from the amphibolites contains the highest mean proportion of An-molecule (An_{49}); plagioclase from the quartz-bearing gneisses contains less ($An_{33.6}$); and plagioclase from the granites contains the least mean An-molecule. The porphyric granites contain plagioclase (An_{28}) whose mean value is identical to that from the fine-grained granites (An_{28}). Plagioclase from the augen gneisses ($An_{96.6}$) has a higher mean proportion of An than equally felsic rocks.

Plagioclase from the granites exhibits a variable composition within a single hand specimen. The composition of fresh modal plagioclase is much more calcic than that of the normative plagioclase (Table III in petrography). Sericitized plagioclase grains were observed to have consistently lower indices of refraction than the associated fresh plagioclase. In some cases, different indices of refraction were observed within the sericitized and the fresh parts of the same cleavage flake; different indices are also found within a single highly sericitized plagioclase grain. Sericitization of the gneisses is much less common

but is directly proportional to the amount of K-feldspar in the rock. The sericitization has resulted in the formation of a more sodic plagioclase so that the plagioclase composition covers a range of 10 to 20 parts An.

Oscillatory-zoned plagioclases are common in porphyroblasts in partially transformed inclusions (Fig. 2, Plate 9). Concentric zones of the same composition are usually repeated, possibly several times. The core in some grains is more sodic, in others more calcic. The outermost zone is usually more sodic than the adjacent zone but may be equally sodic as the core. The zoning sequence in no two porphyroblasts is the same. A few progressively zoned grains are found in the same rock; they become more sodic toward the border. Not one oscillatory zoned plagioclase has been found in the granite itself. Some weakly zoned plagioclases that become progressively more sodic toward the border are widely scattered throughout the granite.

K-feldspar.

The composition of K-feldspar from the rocks of the Flå area was determined by means of an X-ray method developed by Orville (1960). The method is ideally suited for the K-feldspars of Norwegian Precambrian granites which commonly contain microcline megacrysts that enclose numerous small plagioclase grains.

The $(\bar{2}01)$ spacing of alkali feldspar varies according to its solid-solution plagioclase content; therefore, the position of this reflection with respect to a standard (in this case $(10\bar{1})$ of KBrO_3) is a measure of the composition for alkali feldspar (Orville, *ibid.*). All X-ray films were exposed using the powder method on a Guinier-Nonius quadruple focusing camera. For measuring, the films were enlarged by means of a 35-mm slide projector.

Laves (1950) and Goldsmith and Laves (1961) have stated that the $(\bar{2}01)$ spacing can give erratic results when used on perthites. Since the bulk composition of the alkali feldspar was of primary interest, the samples of perthite were heated and homogenized first so that this problem is not a consideration. The K-feldspar samples were heated 48 hours at 1025°C . Heating for periods of 96 hours gave identical results; both results agreed with the chemically analyzed composition. Heating for 12 days, however, caused the plagioclase content that was determined to be too high.

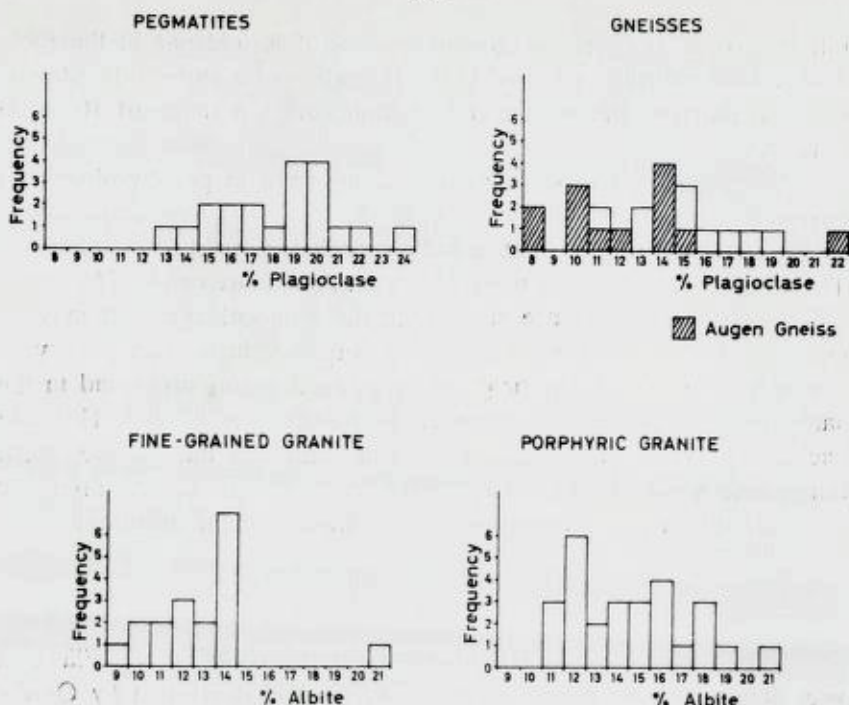


Fig. 57. Graphs showing the distribution of the amount of plagioclase in perthite from the different rock types.

Diagrammer som viser fordelingen av plagioklasmengden i perthit fra de forskjellige bergartstyper.

Orville has published data for two curves, one corresponding to synthetic sanidine and the other to synthetic microcline. The two curves are displaced about 3 parts plagioclase apart; therefore, the obliquity of the alkali feldspar must be known approximately.

The samples were all picked by hand. The results are therefore biased toward grain sizes of 1 mm and larger.

The method was checked by determining the composition of 20 microcline perthites that had been separated with heavy liquids and analyzed chemically. These perthites ranged from Ab_{10} to Ab_{90} in composition. The mean difference between the X-ray determination and the chemical analysis was +1.0 part plagioclase and the standard deviation of the differences was 1.14. This positive bias is to be expected because the X-ray method yields total plagioclase content of the perthite but the chemical analyses were only for K_2O and Na_2O .

An analysis of one alkali feldspar was repeated 10 times using the X-ray method. The precision of the method (standard deviation) is 1.7 parts plagioclase.

The alkali-feldspar compositions from fine-grained granites, porphyric granites, pegmatites, inclusions and gneisses appear in Tables XVI to XX in the Appendix and are graphically illustrated in Fig. 57. Alkali feldspars from all the rock types cover the same range of values except those from pegmatites which are distinctly richer in plagioclase (Fig. 57). The alkali feldspars from fine-grained granite are the most uniform; the others are characterized by their great dispersion. The alkali feldspars from augen gneisses are displaced toward lower plagioclase contents. The compositions of alkali feldspars from pegmatites lie fairly close to the common value of $Or_{78} Ab_{22}$ mentioned by Barth (1956, p. 25) for pegmatite feldspars.

The above results might have been anticipated from petrographic observations (see photomicrographs). The amount of plagioclase lamellae varies greatly from grain to grain, particularly in the porphyric granite. Of all the rocks, the fine-grained granite has the most uniform appearing microcline perthites in which flame perthites are developed in subordinate amounts.

This visibly uneven distribution suggests that it should be possible to find alkali feldspars of different composition within the same rock. Dietrich (1960) has suggested that one of the difficulties in applying the feldspar thermometer (Barth, 1956) may be that the composition of alkali feldspars varies with grain size. Accordingly, a number of samples were selected from the same hand specimen. The results (Table V) show that the composition varies from one grain to another.

The composition is given in parts plagioclase (P, Table V). The An content of the perthite lamellae is presumed to be insignificant (*ca.* An_{10}). The most significant values are starred because they represent K-feldspars that have been X-rayed twice and measured four times, and they represent the maximum differences for the last two specimens. Note that *k*, the distribution constant (Barth, 1956) for the feldspar thermometer, varies considerably within the same hand specimen.

The variation in composition of microcline perthites within these rocks cannot be directly correlated with grain size according to petrographic observations. As a rule, the smallest grains of microcline perthite in the groundmass contain small amounts of plagioclase films;

Table V.

Variation in Composition of Microcline Perthites from the Same Rock.

Hand Specimen	Composition		
	Plagioclase in Alkali Feldspar	Albite in Plagioclase	k
95 1 mm grain	P ₁₆ *	75	0.21
95 1 cm grain	P ₁₇ *	75	0.23
95 3 cm grain	P ₂₂ *	75	0.29
413 #1	P ₁₄	72	0.19
413 #2	P ₁₂ *	72	0.17
413 #3	P ₁₉ *	72	0.26
413 #4	P ₁₆	72	0.22
262 #1	P ₁₆	61	0.26
262 #2	P ₁₃	61	0.21
262 #3	P ₁₃ *	61	0.21
262 #4	P ₁₈ *	61	0.29

* Mean of two determinations.

however, some of the smaller grains exhibit *ca.* 30 to 40 per cent plagioclase that forms flame perthite. The K-feldspar megacrysts are seen to contain highly variable amounts of plagioclase lamellae in the same crystal and between different crystals. This feature characterizes the microcline perthites from these rocks irregardless of grain size.

The feldspar thermometer (Barth, 1956) is readily applied to rocks in which the compositions of the two feldspar phases are known and lie within a certain compositional range. The feldspar thermometer presupposes that albite will be distributed between an alkali feldspar and a plagioclase crystallizing together under equilibrium conditions according to the temperature at which the crystallization takes place. This distribution constant, *k*, is then

$$k(T,P) = \frac{\text{Mol fraction of Ab in alkali feldspar}}{\text{Mol fraction of Ab in plagioclase.}}$$

The *k*-value is correlated with empirically determined temperatures to arrive at a temperature-*k*-value graph (Barth, *ibid.*, p. 15). In order for the feldspar thermometer to be applied, equilibrium must have been

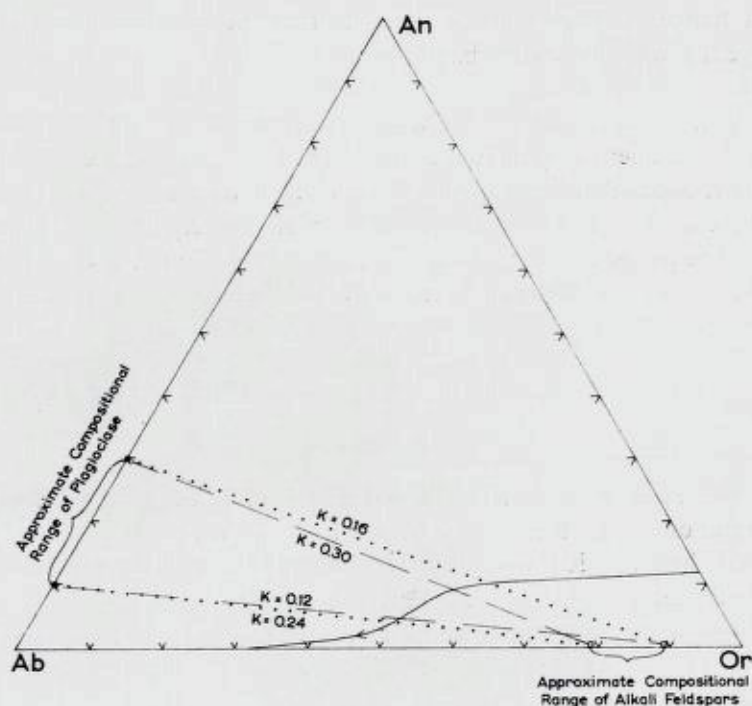


Fig. 58. Diagram showing the approximate compositional ranges for alkali feldspar and plagioclase from the same rock. Tie-lines represent some of the possible k -values that could result. Plotted on the projection of the system $KAlSi_3O_8-NaAlSi_3O_8-CaAl_2Si_2O_8-H_2O$ at 5000 bars pressure.

Diagram som viser de omtrentlige sammensetningsområder for alkalifeldspat og plagioklas fra samme bergart. Linjene viser noen mulige k -verdier som kunne eksistere. Plottet på projeksjonen av systemet $KAlSi_3O_8-NaAlSi_3O_8-CaAl_2Si_2O_8-H_2O$ ved 5000 bar trykk.

attained between the two feldspar phases at constant temperatures, pressure, and chemical composition.

The impossibility of applying the feldspar thermometer to the rocks from the Flå area is illustrated in Fig. 58. The compositional variability of both plagioclase and alkali feldspar from the same hand specimen has been demonstrated. The choice of which alkali feldspar to equate with which plagioclase is purely arbitrary; therefore, k can assume a wide range of values (Fig. 58). The k -values from Table XVIII in the Appendix, in which the k -values for one rock type vary over a range corresponding to 150 C., show that this is in fact

what happens. The evidence suggests that the k -values could differ as greatly within a single hand specimen as they differ between rock types.

In a previous section, the writer suggested that the flame perthite is of replacement origin. Replacement perthites exclude the utilization of the feldspar thermometer. The compositions of the feldspars indicate that the rocks have been subjected to a sliding equilibrium during a change in temperature, pressure, or bulk composition or a combination of the three. The feldspar thermometer is, therefore, not applicable to these rocks.

The Symmetry Relations of K-feldspar.

General.

The symmetry relations of the alkali feldspars may yield useful information about the history of the rocks in which they occur. Rao (1960) has applied obliquity (triclinicity) values to the study of thermal metamorphic effects, Emerson (1960) investigated obliquity relations within a granite, and Heier (1957, 1960) and Guitard and others (1960) have studied the distribution of alkali-feldspar obliquities within regional metamorphic terrains. When the obliquity values of the K-feldspars in rocks from the Flå area were determined, almost all the obliquity values in the granite were similar; however, unusual values which did occur in some gneisses, particularly augen gneisses, were surprising and led to a further investigation of these rocks and to a comparison of the augen gneisses with the granite.

A total of 337 specimens of alkali feldspar was X-rayed. Once the pattern of peculiar obliquities in augen gneisses became apparent, specimens from the Telemark and Bamble rocks along the southeast coast (Sörlandet) of Norway were also included in order to determine whether the same peculiarities occurred there.

The rocks sampled along the southeast coast of Norway were augen gneisses and migmatites. These rocks occur interlayered with the supracrustal rocks of the Bamble area southeast of the "great friction breccia" and in the granitized gneisses of the Telemark rocks northwest of the breccia, a major fault separating the two areas. The Herefoss, Grimstad, and Levang granites are several of the syn- and postkinematic granites which are emplaced within the Telemark and Bamble rocks.

The rocks of the Flå area are placed in the middle amphibolite facies. The rocks sampled in the Bamble-Telemark area are also in the amphibolite facies; both areas are classed as upper catazonal.

Method.

X-ray technique: All X-ray films were taken using the powder method on a Guinier-Nonius quadruple camera. The films were measured after enlarging them on a screen by means of a 35-mm-slide projector. The precision of the method is 0.03 Δ units.

Sampling: The large number of rock samples which were collected during the geologic mapping of the area supplied the alkali feldspars that were X-rayed. Twenty-five specimens were pulverized and separated by means of heavy liquids. These, of course, represent an estimation of the obliquity of the K-feldspar from the entire rock. The remaining feldspars were hand picked. The sampling is therefore limited to crystals greater than *ca.* 1 mm; most of the hand-picked specimens were of megacrysts and porphyroblasts.

Definitions: Goldsmith and Laves (1954 a) have defined the separation of the 131 and the $\bar{1}\bar{3}1$ reflections in X-ray powder patterns as a measure of obliquity. The spacing of these two reflections is called Δ , and Δ is defined so that $\Delta = 0.0$ is monoclinic feldspar and $\Delta = 1.0$ is microcline of maximum obliquity. Δ , which is a measure of Al-Si order-disorder may assume any value between 0.0 and 1.0. Examples of the 131 and $\bar{1}\bar{3}1$ reflections from maximum microcline ($\Delta = 1.0$) intermediate microcline ($\Delta = 0.5$), and monoclinic K-feldspar ($\Delta = 0.0$) appear in Fig. 59 a, b, and c. In addition to Δ with a definite value, diffuse reflections which represent variable Δ -values within a single crystal are encountered (Goldsmith and Laves, 1954 b; Christie, 1962). These may vary from reflections which are diffuse about a definite Δ -value (Fig. 59 i) to reflections that are evenly diffuse up to a certain Δ -value (Fig. 59 e). The latter have been called randomly disordered (*RD*) by Christie (1962). The *RD* K-feldspar crystals are composed of small domains that have every possible Δ value between 0 and a fixed maximum value. If the frequency of a certain Δ value predominates, the corresponding reflections will be more intense and appear as darker lines superposed on a diffuse background (Fig. 59 d, f, g). Because these K-feldspars of variable obliquity obviously repre-

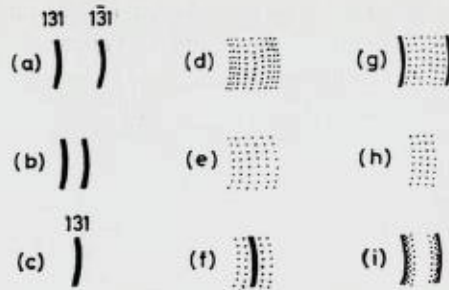


Fig. 59. Appearance of 131 and $\bar{1}\bar{3}1$ reflections used to measure obliquity in X-ray powder patterns. (a) Maximum microcline, $\Delta = 1.0$. (b) Intermediate microcline, $\Delta = 0.5$. (c) Sanidine and orthoclase, $\Delta = 0.0$. (d) Microcline with Δ varying from 0.0 to 1.0, $\Delta = 1.0$ commonest. (e) RD microcline, maximum $\Delta = 1.0$. (f) Monoclinic K-feldspar with some variable obliquity. (g) Maximum microcline on a RD background. (h) RD intermediate microcline, $\Delta = 0.5$. (i) Somewhat disordered microcline, maximum $\Delta = 1.0$.

131 og $\bar{1}\bar{3}1$ refleksjoner anvendt til måling av triklinitet i røntgen pulverdiagrammer. (a) Maksimum mikroklin, $\Delta = 1,0$. (b) Intermediær mikroklin, $\Delta = 0,5$. (c) Sanidin og ortoklas, $\Delta = 0,0$. (d) Mikroklin med Δ varierende fra 0,0 til 1,0, $\Delta = 1,0$ sterkest. (e) RD mikroklin, maksimum $\Delta = 1,0$. (f) Monoklin kalifeldspat på RD bakgrunn. (g) Maksimum mikroklin på RD bakgrunn. (h) RD intermediær mikroklin, $\Delta = 0,5$. (i) Noe uordnet mikroklin, maksimum $\Delta = 1,0$.

sent departures from equilibrium, they have received as much attention in this investigation as the K-feldspars of low to intermediate obliquity values.

Distribution of Obliquity among the Rock Types.

Table VI shows the numerical distribution of Δ -values of K-feldspars, which are usually perthitic, for the different rock types. The range of Δ from 0.0 to 1.0 has been arbitrarily divided into four intervals, and each interval has been subdivided into groups of uniform (sharp reflections) obliquity and variable obliquity (diffuse reflections). The areal distribution of the Δ -values appears in Fig. 60.

That the K-feldspars from granites and pegmatites fall into a grouping characterized by maximum obliquity is immediately apparent. The Herefoss granite (Nilssen, 1961) and the Levang granite (T. Elder, oral communication) also contain alkali feldspars that are mostly near maximum microcline. K-feldspars of variable obliquity are almost completely lacking within the granites and pegmatites.

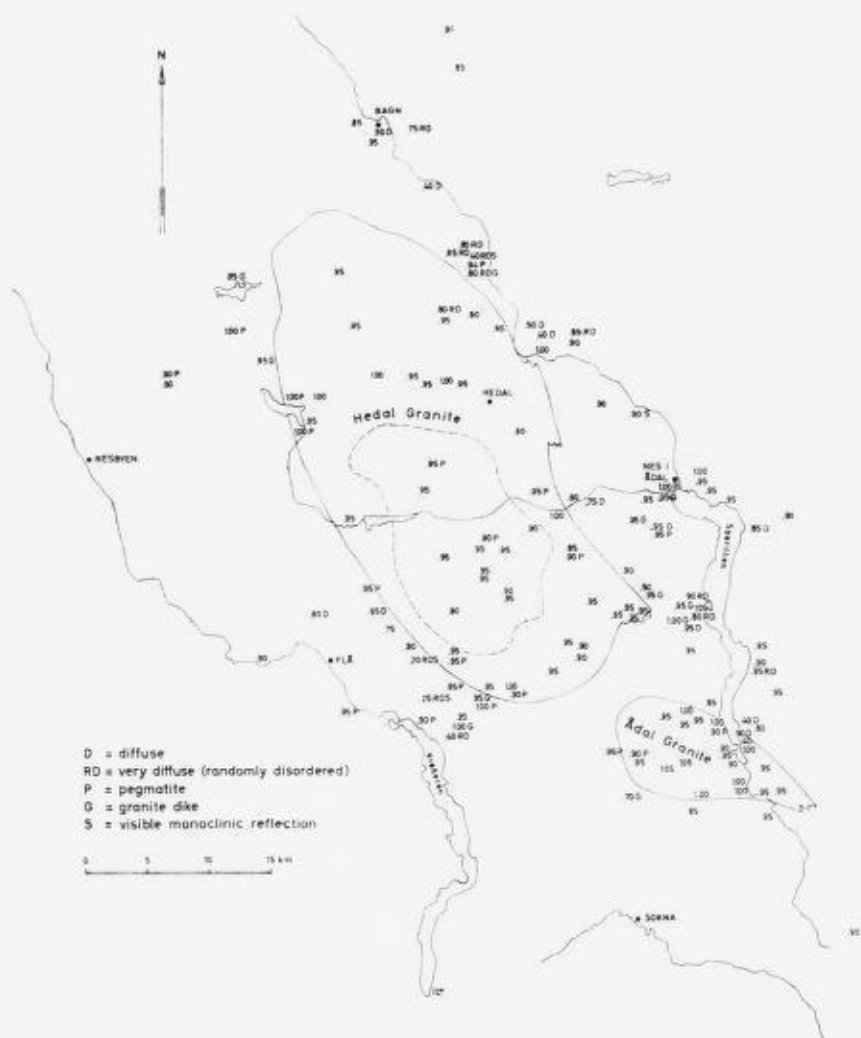


Fig. 60. Map of the Flå granite area showing the areal distribution of K-feldspar obliquities in granite and the surrounding gneisses. The lower Δ -values follow zones of augen gneiss and migmatite.

Kart over Flå-granittområdet, som viser fordeling av K-feldspat trikliniteter i granitten og de omgivende gneiser. De lavere Δ -verdier følger soner med øyegneis og migmatitt.

Table VI.

Distribution of Obliquity Values among the Different Rock Types.

Δ	Pegmatite	Inclusions	Granite	Gneiss	Augen Gneiss
>0.87 Diffuse	28	4 1	65	15—5* 2—2*	9—1* 1—4*
0.70-0.87 Diffuse	1	1	1 2	5 6—2*	9—2* 8—2*
0.35-0.70 Diffuse		1	1 1	2	5—2*
<0.35 Diffuse				1	1—1* 2—3*

* Indicates samples from the south coast of Norway.

Most of the gneisses, which include migmatites in Table VI, contain maximum microcline. K-feldspars of low and intermediate obliquity occur, however, and alkali feldspars of variable obliquity are fairly common. These latter two types including an occurrence of orthoclase are found in migmatites in which the alkali feldspar becomes distinctly porphyroblastic.

The augen gneisses include most of the samples which have low to intermediate obliquity and which had variable obliquity. Orthoclase is found within the augen gneiss although it occurs rather sporadically. The maximum of these rocks falls in the Δ range from 0.70—0.85 even though this is the smallest interval. Variable obliquity within one crystal is common. Obliquity measurements on some K-feldspars from the Telemark-Bamble area were undertaken in order to determine whether this peculiarity was confined to the Flå area. The Herefoss granite in the Telemark-Bamble area contains K-feldspar that is predominantly near maximum microcline (Nilssen, 1961), but the augen gneisses again exhibit K-feldspar of variable obliquity. The measurements indicate that low-to intermediate and variable K-feldspar obliquities are common in augen gneisses in the upper catazone rather than being confined to a specific area. These results are very similar to those reported by Guitard and others (1960) for the augen gneisses from

the mesozone. The augen gneisses can then be regarded as a group of rocks possessing unusual K-feldspar obliquity.

These augen gneisses are characterized by the mineral assemblage, hornblende, alkali feldspar, quartz, plagioclase, and biotite. The alkali feldspar is porphyroblastic; the plagioclase commonly contains small patches of hazy-appearing K-feldspar along the twin lamellae (Fig. 2, Plate 2). This mineral paragenesis is uncommon in the area except for these restricted zones. Associated rocks contains very little K-feldspar and more hornblende than the augen gneisses. K-feldspar in rocks containing major amounts of hornblende and K-feldspar usually shows variable obliquity. The variable obliquity as well as the occurrence reflect replacement and/or growth conditions within the augen gneisses.

Obliquities of K-feldspars from inclusions in the granite are usually near maximum, but some have variable obliquity. One of these was a rather large (10—20 m) inclusion of augen gneiss that graded imperceptibly into porphyric granite. K-feldspars from this inclusion (Sp. 482 in Fig. 61 and Table VII) exhibit variable obliquity within some individuals, but typically attain a maximum value of about 0.90 which probably represents equilibrium. The obliquities of K-feldspar from this rock are more typical of augen gneisses than the enclosing granite.

Some inclusions exhibit the K-feldspar patches in plagioclase. These K-feldspar patches and some of the K-feldspar porphyroblasts in the inclusion are of variable intermediate obliquity.

An alkali feldspar from the Hedal granite at the contact of the Permian rhomb porphyry dike was X-rayed. The 131 and $\bar{1}\bar{3}1$ reflections were evenly diffuse, and a monoclinic reflection appeared (similar to Fig. 59 f). These K-feldspars are microscopically non-perthitic. Because K-feldspars from granite several hundred meters away from the dike showed maximum obliquity, this phenomenon must be ascribed to thermal metamorphism by the dike.

The K-feldspar from a pegmatitic 15-cm alkali feldspar crystal (Fig. 62) that falls in the upper intermediate obliquity class constitutes an unusual occurrence. The pegmatitic crystal is found in a fine-grained granite dike which also contains *RD* K-feldspar.

The north contact of the Ådal granite is characterized by K-feldspar that has variable and intermediate obliquity (Sp. 509 G, Fig. 61; Sp 509 C, Fig. 61 and Table VII). These two specimens are of the contact (Sp 509 G) and from 10 m inside the contact (Sp 509 C).

Table VII.

2V_x of K-feldspars.

Sp. No.	Rock Type	2V _x ± 2°
413 A	Porphyric Granite	82, 84, 85, 86
312	Porphyric Granite	75, 82, 86
509 C	Porphyric Granite near Contact	64u—74u, 83, 84
509 G	Porphyric Granite and Gneiss of Contact	48—78, 63u—74u, 81u, 82u
514 D	Biotite-rich Inclusion	64u—82, 70u, 80, 80, 82, 82, 85
542 A	Transformed Gneiss Inclusion	68u—80u ¹ , 71u—74u, 78u—84u, 86
482 D	Augen Gneiss Inclusion	77u—82u—85u, 80u, 80, 81u—84u, 85
248	Porphyric Granite that surrounds an inclusion	78—83, 84, 86
10	Quartz-dioritic Gneiss	62 ¹ , 66u, 74u, 84 ¹
219	Quartz-dioritic Gneiss	62, 66 ¹ , 68u, 70u ¹ , 82
102 A	Augen Gneiss	74 ¹ , 74u, 76u—82u, 78u, 78u ¹ , 80u, 84
224 A	Augen Gneiss	54, 56u, 58 ¹ , 60u ¹

"64u—74u" means 64° and 74° with undulatory extinction in the same grain.

¹ signifies 2V_x measured in K-feldspar patches in antiperthite.

Some of the K-feldspar microscopically resembles the K-feldspar from augen gneisses (Fig. 1, Plate 3) in 2V, undulatory extinction, beginning twinning, and overall appearance. These feldspars contain slivers of probable groundmass plagioclase along which beginning twinning is concentrated. They also partially enclose septa of plagioclase where they are molded against adjacent megacrysts (Fig. 1, Plate 12). The specimen of the contact contains more disordered K-feldspar than the one 10 m inside the contact.

In a quartz-dioritic gneiss (Sp 10, petrographic description), shadowy-appearing alkali feldspar is found as interstitial fillings and films between grains and as replacement patches in plagioclase (An₃₅). The K-feldspar is randomly disordered but has a maximum Δ of ca. 0.8. The 2V of these antiperthitic K-feldspar patches (Table VII) indicates that they commonly have variable, intermediate obliquity. When grid twinning is visible in the patches, they have optic angles greater than 80°. This antiperthitic K-feldspar, which has previously

been interpreted as a replacement feature, exhibits variable intermediate obliquity.

The 2V is an indication of the order in a K-feldspar (Goldsmith and Laves, 1954 b), and ranges from 54° in orthoclase from the augen gneiss to 86° in microcline from a porphyric granite (Table VII). Undulatory extinction is common in the intermediate K-feldspars. Many K-feldspars grains have different values for the optic angle and must have variable obliquity in microscopically visible domains.

Distribution of Obliquity in Single Hand Specimens.

An estimate of the distribution of obliquity within a single hand specimen was desired in order to obtain a better insight into the variation of K-feldspar obliquity within a small volume of rock. Accordingly, approximately 10 alkali feldspar crystals were picked from each one of selected specimens. The results of this study, which show surprising variability in some rocks, appear in Fig. 61.

The granite (Sp 413 A) from the Heddal granite contains near maximum microcline (Fig. 61). More unusual is Sp 4 A of a porphyric granite sill. Two of the 10 alkali feldspars showed obliquities that vary from 0 to 0.85. Sp 509 G of the contact (within 0—5 cm of the contact) of the Ådal granite contains some K-feldspars of low or variable obliquity (Fig. 61), and Sp 509 C from 10 m inside the contact contains traces of orthoclase within one grain (Fig. 61).

The K-feldspars from augen gneisses and certain migmatites are highly variable, both among and within hand specimens. Some K-feldspars from augen gneisses (Sp 621 and Sp 664) exhibit a common value which has an obliquity equal to granite K-feldspars, but they both contain alkali feldspars with variable obliquity. Alkali feldspars from the other augen gneisses and migmatites range from monoclinic to almost maximum triclinic within the same hand specimen. They also commonly contain crystals with variable obliquity in which Δ ranges from 0.0 to 0.9. Although both orthoclase and maximum microcline are not rare in these specimens, K-feldspars of variable obliquity are most common. Both monoclinic domains and domains of unequal obliquity may be found in the same crystal (Fig. 61, Sp 466 B), or domains of unequal obliquity and domains of uniform maximum obliquity may occur in the same (Fig. 61, Sp 665).

Three specimens from one large (5 cm) alkali feldspar eye in



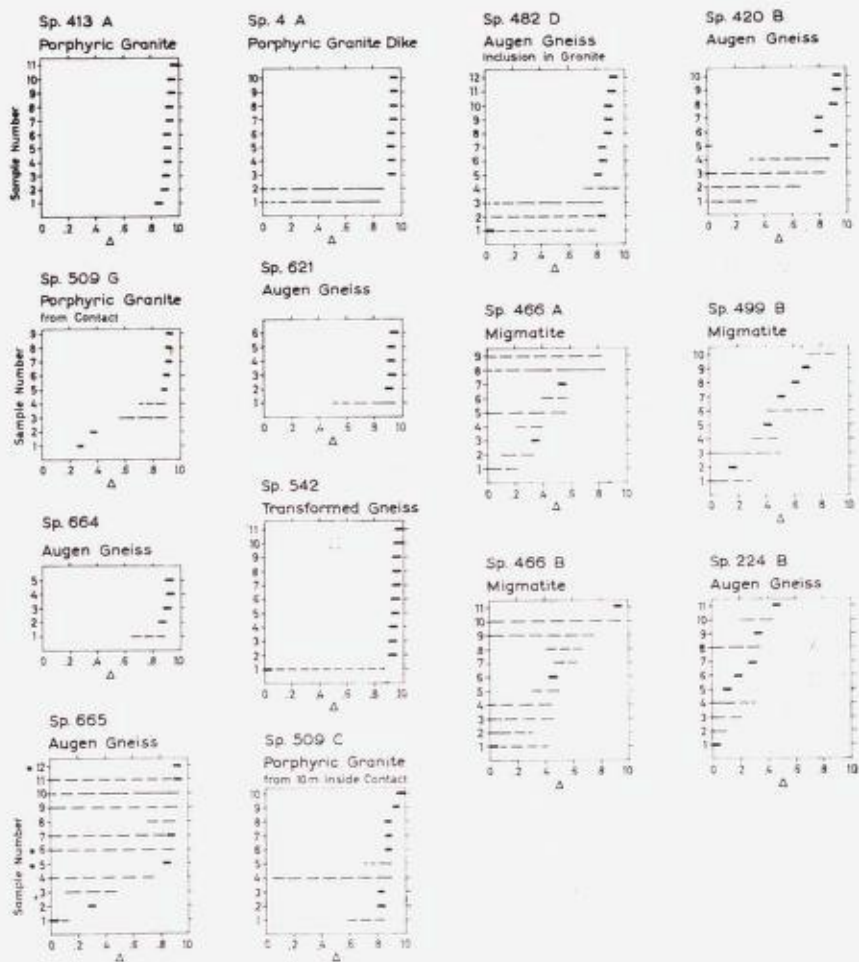


Fig. 61. Graphs showing the distribution of Δ among grains picked from a single hand specimen. — Sample with uniform obliquity (sharp reflection, Fig. 59 a, b and c). - - - Sample with variable obliquity increasing in frequency toward 1.0 (Fig. 59 d). ——— Sample with variable obliquity decreasing toward 1.0 ——— RD sample (Fig. 59 e). ——— Sample with dominantly uniform obliquity and some RD domains (Fig. 59 f).

Diagram som viser fordeling av Δ i korn plukket fra et enkelt håndstykke — Prøve med ensartet triklinitet (skarp refleks). - - - Prøve med varierende triklinitet, som øker mot 1,0. ——— Prøve med varierende triklinitet, som avtar mot 1,0. ——— RD prøve. ——— Prøve med overveiende uniform triklinitet og noen RD-områder.

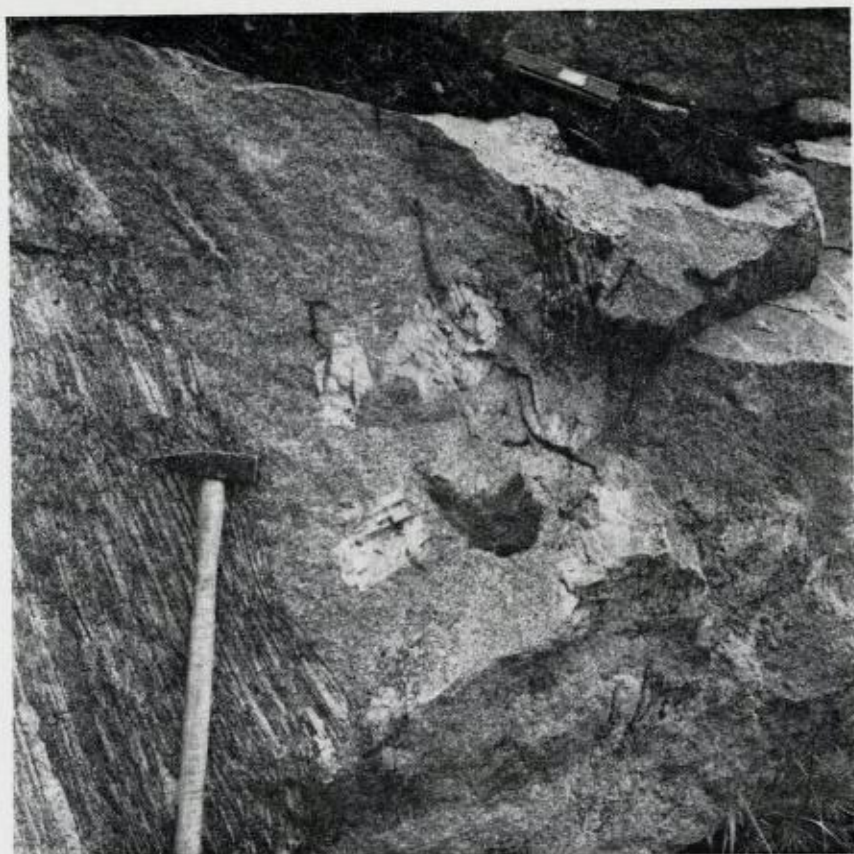


Fig. 62. Augen gneiss cut by fine grained granite. Inclusions of nonrotated augen gneiss grade into granite. Individual pegmatitic microcline crystals occur in the granite to the right of the hammer head. One of these pegmatitic microclines has the lowest obliquity ($\Delta = 0.85$) of any pegmatitic K-feldspar in the Flå area. K-feldspar from the granite dike is randomly disordered (max. $\Delta = 0.80$). Garthus (43,0, 1—01,4) at northeast contact of Hedal granite.

Oyegneis gjennomskåret av finkornet granitt. Inneslutninger av ikke rotert øyegneis går gradvis over i granitt. Isolerte pegmatitiske mikroklinkrystaller ses i granitten til høyre for hammerhodet. En av disse pegmatitiske mikrokliner har den laveste triklinitet ($\Delta = 0,85$) av alle pegmatitiske kalifeltspater i Flå-området. Kalifeltspat fra granittgangen er "randomly disordered" (max. $\Delta = 0,80$).

Garthus (43,0, 1—01,4) nær Hedal-granittens nordøstgrense.

Sp 665 were X-rayed. The Δ value was different in each of these, and one was an *RD* K-feldspar (Fig. 61). At least this *RD* crystal and probably many more are characterized by comparatively large (1—2 mm) domains that differ in obliquity from each other, a not uncommon phenomenon described previously by Goldsmith and Laves (1954 b) and Guitard and others (1960 a).

Two specimens, Sp 542 and Sp 665 (Fig. 61), show extreme ranges of obliquity. Of the 11 samples X-rayed from porphyroblasts of Sp 542, 10 of them were maximum microcline and the other was mainly orthoclase that had some variable domains. The orthoclase porphyroblast looked exactly like the microcline porphyroblasts (Fig. 63) in hand specimen. Sp 665 also contains crystals of both monoclinic and maximum microcline but the variability is great in this hand specimen; *i. e.*, 10 out of 12 samples produced X-ray patterns with diffuse $131/1\bar{3}1$ reflections. It seems reasonable that near-maximum microcline, which is the usual K-feldspar throughout the area, is the stable K-feldspar phase in both these specimens which are typified by metastable phases.

Conclusions.

This investigation demonstrates the following characteristics for an area composed of gneisses in the amphibolite facies and of the associated granites:

- (1) K-feldspars from granite and pegmatite have maximum obliquity except for the granite contact.
- (2) K-feldspars from gneisses may have either maximum obliquity or variable obliquity.
- (3) The K-feldspar from augen gneisses, migmatites, and inclusions, rocks that are obviously in a state of transformation, have peculiar obliquities that are typically variable but may be monoclinic.
- (4) Obliquity of K-feldspars in single hand specimens of augen gneisses and migmatites is highly variable from crystal to crystal as well as in single crystals and ranges continuously from $\Delta = 0$ to $\Delta = 1$.
- (5) The characteristic feature of the peculiar K-feldspar symmetry is blastesis in rocks that are undergoing either a chemical or textural transformation.



Fig. 63. Specimen of transformed biotite gneiss (Sp 542) that has approached the texture of the granite. Effects of shearing are visible through the middle of the specimen. Most of the K-feldspar porphyroblasts are near maximum microcline (Fig. 61). A single porphyroblast (1) is orthoclase with some domains that vary in obliquity. Scale in centimeters.

Prøve av omvandlet biotit gneis (Sp 542), hvis tekstur nærmer seg en granitts. Shearing-effekter er synlige gjennom midten av prøven. De fleste av K-feltspat porfyroblastene er nær maksimum mikroklin (Fig. 61). En enkelt porfyroblast er ortoklas med noen varierende områder. Målestokk i centimeter.

- (6) K-feldspar from the granite contact exhibits the same symmetry relations as K-feldspar from the augen gneisses and inclusions.

How can the petrogenic history of these rocks be interpreted in light of the symmetry relations of these alkali feldspars? It is generally recognized that monoclinic alkali feldspar may form in two fields:

- (1) Within the stability field of monoclinic feldspar over *ca.* 500° C. (Goldsmith and Laves, 1954 a).
- (2) Metastably within the stability field of microcline at less than *ca.* 500° C; *e. g.*, authigenic K-feldspars [Baskin (1956)].

Monoclinic alkali feldspars characterize granulite-facies rocks (Heier, 1957, 1960; Guitard and others, 1960). If the monoclinic alkali feldspars crystallized in the granulite facies above *ca.* 500° C, they were either formed in extremely restricted "hot spots" or represent the frozen relics of an earlier regional crystallization within the monoclinic stability field, but only amphibolite-facies mineral parageneses are found. Although hot fluids permeating these rocks might possibly raise the temperature considerably, both of the above possibilities seem unlikely in view of the restricted occurrence of the gneisses that show replacement features and transformation and of the lack of high-temperature parageneses. The only monoclinic alkali feldspar that can reasonably be ascribed to high temperature conditions is the one from the contact of the rhomb porphyry dike. Both the field occurrence and the textural features suggest that these augen gneisses are the product of at least a local metasomatism or redistribution and growth of the K-feldspar.

Crystallization of alkali feldspar under laboratory conditions always results in the formation of the monoclinic phase. Goldsmith and Laves (1954 b) stated that, although grid twinning in microcline indicates inversion from an original monoclinic phase, the monoclinic phase was not necessarily formed above 500° C. The structural relations of the alkali feldspars from augen gneisses are suggestive of the variable structure of adularia. Laves (1950) and Chaisson (1950) have noted the extremely variable structural character of adularia, which may be either monoclinic or triclinic. More recently, Bambauer and Laves (1960) have demonstrated that adularia is composed of domains that vary in optical properties and that these domains are caused by structural rather than chemical differences. They propose that adularia crystallizes as a monoclinic feldspar and then inverts to microcline by going through intermediate stages.

The occurrence of authigenic orthoclase and low-obliquity microcline within sedimentary rocks is well known (Baskin, 1956). These feldspars and the adularias from alpine veins have probably formed metastably within the stability field of maximum microcline (Ostwald Law). The metastable structural state of authigenic feldspar and of adularia must have been determined by the conditions of growth. The alkali feldspars from these augen gneisses, migmatites, inclusions, and the granite contact may have formed in a similar manner, although probably at a higher temperature.

The augen gneisses and the migmatites are commonly sheared as are the border facies of the Flå granite. This deformation can hardly be responsible for the unusual obliquities in K-feldspar of the augen gneisses. On the contrary, Eskola (1951) and Karamata (1960) believe that deformation catalyzes the ordering process in alkali feldspar. Deformation may have hastened the ordering process, and, in fact, some of the most highly sheared augen gneisses have the higher Δ -values.

The gneisses that contain K-feldspars with low to intermediate obliquity all exhibit a striking feature in common. *They have all recrystallized postkinematically.* The feldspars in one postkinematically recrystallized rock (Sp 224) are flattened into lenses; therefore, they must have been present before the recrystallization as K-feldspar and/or plagioclase. Apparently orthoclase was formed during the recrystallization. The augen gneisses whose K-feldspars show high but variable obliquity values are strongly sheared. These observations strongly suggest that deformation can assume a major role in facilitating the orthoclase-microcline inversion.

The composition of alkali feldspars from the augen gneisses and transformed rocks ranges from Or₇₈ to Or₉₂ (Fig. 57). The composition of the orthoclase perthites, however, lies near the lower values about Or₉₀; the highest of these is Or₈₅. A high plagioclase content in solid solution cannot have caused the low obliquity values.

Although the feldspar composition may not be applicable to indicate the temperature of formation for the monoclinic K-feldspars, their relatively low plagioclase content is highly suggestive. According to all our geological experience, the plagioclase content of an alkali feldspar varies directly with the temperature of formation. The monoclinic K-feldspars from these rocks contain the lowest amounts of plagioclase of all the rocks of the area; therefore, they were probably formed at a relatively low temperature (for a comparison with granulite facies rocks see Heier, 1960, p. 145—148).

Since the augen gneiss and migmatites generally follow the granite contacts, the low obliquity values from these rocks as well as from the granite contacts might be interpreted as thermal metamorphic phenomena. Rao (1960) has demonstrated an inversion from microcline to orthoclase in the gneisses adjacent to a Permian nordmarkite intrusive in the Oslo area. Nothing could be further from the case for the Flå area. There is no change in grain size at the contacts of the Flå

granite, no discoloration, and no baking of the adjacent gneisses. The only noticeable effect is a probable potassium metasomatism in some of the adjacent gneisses. The same mineral assemblages and even the same textural features that occur in gneiss and granite at the contact are found in the gneiss 10 km from the granite and in the granite 10 km inside the contact. The granite is in complete harmony with gneisses of the amphibolite facies; the low obliquity values are connected with a K-metasomatism at the granite contact.

A definite trend for the occurrence of low or variable obliquities in K-feldspar has become evident. These may be found in augen gneisses, migmatites, inclusions in the granite, and granite and gneiss at the granite contact. Variable-obliquity K-feldspar patches, which occur in plagioclase and seem to be a replacement phenomenon, occur commonly in all these rocks except for the granite. Antiperthite has never been observed in the granite. *These rocks are either undergoing a gross chemical change (inclusions, rocks at the granite contacts, and possibly augen gneisses) or a chemical redistribution without a change in mesoscopic composition (certainly augen gneisses and migmatites).*

The monoclinic K-feldspar has most likely crystallized metastably within the stability field of microcline during a potassium metasomatism or during a recrystallization accompanied by a chemical redistribution. That they have then attempted to invert to the stable form, microcline, is evidenced by the indistinct twinning observed along grain boundaries and particularly along slivers of groundmass plagioclase enclosed within the K-feldspar grain (Fig. 1, Plate 3; Fig. 1, Plate 12; Fig. 2, Plate 12). The plagioclase slivers are probably remnants of replaced plagioclase. These K-feldspars appear to be good examples of Laves' (1950) proposal that grid-twinned microcline has crystallized in the monoclinic form and then inverted.

Eskola (1952) described microclinization in granulites from Lapland. The orthoclases showed the same type of undulatory extinction and beginning twinning along strained areas. Goldsmith and Laves (1954 b) investigated these K-feldspars by X-ray methods and showed that the microclinization is accompanied by variable obliquity.

Since megacrysts of ordered K-feldspar occur in the granite, growth cannot be the only prerequisite for the retention of low- and variable-obliquity feldspars. Goldsmith (1953) has proposed a simplicity principle by which minerals will always tend to crystallize in the high temperature state, especially when crystallization is rapid. Bambauer and Laves (1960) have noted that in adularia the crystals

grow more slowly as they become larger so that the outer part grows more ordered than the center, and ordering progresses from the border to the center. Water is a most effective catalyst for the ordering process (Donnay and others, 1960). The obliquities of K-feldspars may depend on the amount of volatiles present, or, more likely, obliquities may depend on a delicate balance between growth rate, temperature, deformation, and available volatiles. If the growth occurs at a relatively low temperature, thermal energy may be too low to initiate ordering of the crystal lattice. The conditions must be quite variable from crystal to crystal for hand specimens to exhibit highly variable Δ -values.

Time may be an important factor in the inversion process. The last-formed K-feldspars could have a frozen-in low or variable obliquity in rocks that are partially transformed; *i. e.*, at the granite contact and in inclusions.

Water may be present as a variably adsorbed film that facilitates metasomatic transport, crystal growth, and ordering processes. Finitely spaced shear planes add further to the heterogeneity of the rock. Obviously these factors might tend to counteract each other somewhat; *i. e.*, greatest shearing, and most rapid chemical transport and crystal growth probably occur where water was most abundant. The effect of locally varying water content on K-feldspar obliquity has been stressed by several authors (Emeleus and Smith, 1959; Guitard and others, 1960). The effects of volatiles and deformation are probably the most important for promoting the ordering process in K-feldspar of the rocks studied.

As a result of this study, the author makes the following proposals:

- (1) In areas where different Δ -values are found, more than one sample is necessary from each hand specimen in order to determine a representative Δ -value.
- (2) Low- Δ and/or *RD* K-feldspars are characteristic of amphibolite-facies rocks undergoing transformation.
- (3) These unusual Δ -values are caused by a delicate interplay of growth rate, shear, temperature, time, and volatiles at temperatures within the stability field of microcline.
- (4) Amphibolite-facies gneisses are characterized by alkali feldspar with a wide range of obliquity but the granites usually contain microcline (see also Guitard and others 1960).
- (5) As already noted by Goldsmith and Laves (1954 a), alkali feldspars often form metastably; therefore, care must be exercised in interpreting low Δ -values as a function of high temperature.

Metamorphism and Metasomatism.

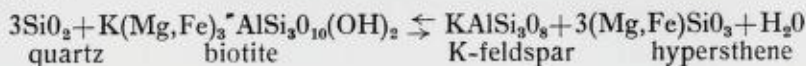
Metamorphic Facies.

The widespread occurrence of amphibolites interlayered in the gneisses provides the best indication of the metamorphic facies. Some typical mineral parageneses appear in Table I. Zoisite-minerals are lacking in the gneisses except as alteration products in chloritized biotite. Biotite is found in almost every rock, and muscovite occurs fairly commonly. The rocks are devoid of aluminosilicates and orthopyroxene. The plagioclase, which is typically An_{35-40} , ranges from An_{47} in amphibolites to An_{65} in orthoquartzites.

The gneisses exhibit two general mineral parageneses; quartz-plagioclase-K-feldspar-biotite and plagioclase-hornblende-biotite with or without considerable quartz (Table VIII). The only exceptions to this rule are the augen gneisses and migmatites that also contain *RD* and/or low-obliquity K-feldspar. The same compositional limitations appear in the modal analyses of Strand (1954, p. 17) for the granodioritic gneisses in the northern part of the area.

The lower boundary of the amphibolite facies has been placed at the P-T conditions where epidote is in equilibrium with plagioclase An_{30} (Ramberg, 1952, p. 150). Since no epidote occurs in the rocks including the amphibolites that contain calcic andesine, the mineral association must represent conditions considerably above the lower boundary of the amphibolite facies.

The upper boundary of the amphibolite facies is fixed by the reaction



which is displaced to the left under amphibolite facies conditions (*ibid.*, p. 152). The left hand side of the equation typifies the quartz-bearing rocks of the Flå area. This fact together with the widespread occurrence of epidote-free amphibolites in the mafic rocks demonstrates that the gneisses of the area achieved equilibrium under amphibolite facies conditions.

Three subdivisions of the amphibolite facies are recognized (Francis, 1956; Turner, 1958). These are the staurolite-quartz, kyanite-muscovite-quartz, and sillimanite-almandine subfacies. Since

Table VIII.

Mineral Paragenesis of the Gneisses in Relation to the Ab-Content of Plagioclase.

Plagioclase Ab Content	Quartz	Microcline	Biotite	Hornblende	Muscovite	Chlorite	Garnet	Diopside	Sphene	Opagues
95	×	—	—	—	+	+	—	—	—	—
90	×	×	—	—	+	+	—	—	+	—
83	×	×	+	—	—	—	—	—	—	+
76	×	×	+	—	+	+	—	—	—	+
70	—	+	×	—	+	+	—	—	+	—
68	×	×	×	—	—	+	—	—	+	+
68	×	×	×	—	—	+	—	—	+	+
68	×	×	×	—	+	+	—	—	+	+
63	×	—	+	×	—	+	—	—	+	+
54	+	—	×	×	—	+	—	—	+	+
53	+	—	+	×	—	—	×	×	—	+

× Present in major amounts.

+ Present in minor amounts.

— Not present.

neither staurolite nor any of the aluminosilicate minerals occur in these rocks, a corresponding subdivision is impossible here.

The typical mineral assemblage of quartz, feldspar, and mica is stable in both of the lower two subfacies. According to Francis (*op. cit.*, p. 356) the plagioclase in the pelitic assemblages of the kyanite-muscovite-quartz subfacies ranges up to An_{40} , but the maximum in the staurolite zone is An_{30} . Quartzo-feldspathic assemblages commonly contain plagioclase An_{32} . The variation in plagioclase composition among the rocks (Table VIII) appears to be largely controlled by the bulk composition of the rock and does not represent varying grades of metamorphism (Fig. 64). Amphibolites in the staurolite-quartz subfacies commonly carry epidote in equilibrium with a medium plagioclase (Turner, *op. cit.*, p. 229); this paragenesis is not found in the amphibolites of the Flå area. The mineral parageneses most likely correspond to the middle of the amphibolite facies (Barth, 1962, p. 323).

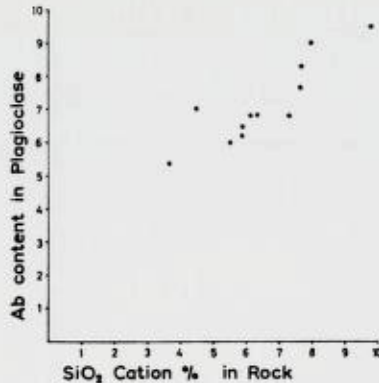
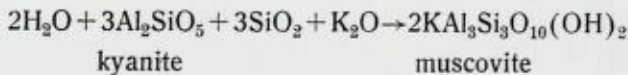


Fig. 64. Ab content in plagioclase plotted against SiO₂ content from the gneisses.
Ab-innholdet i plagioklas plottet mot SiO₂-innholdet i gneisene.

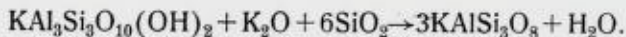
Metasomatism.

Except for the aureole of granitized rocks surrounding the granites, there are few occurrences of granitic rocks that cannot be explained by a local mobility of granitic material or even *in situ* recrystallization without a more detailed study. A coarsening of grain size, the appearance of K-feldspar, and sericitization of plagioclase along high-angle fractures indicate a movement of mobile constituents toward potential low-pressure areas. This may have been the process by which the numerous non-dilational pegmatites (Fig. 21) in Hallingdal were formed (Ramberg, 1956).

The fact that aluminosilicates have not been found may be implicit evidence for metasomatism since aluminous sediments could be expected to occur somewhere in the layered sequences. By introduction of K into aluminous sediments muscovite and/or K-feldspar would be formed according to the following reactions (Ramberg, 1925, p. 227):



and



These reactions may have taken place in gneisses along the east side of the area which is the only region where muscovite occurs commonly in the gneisses.

Numerous evidences indicate a syntectonic granitization that has outlasted the deformation and erased much of the folding in many places. Outside the immediate vicinity of the granite, these occurrences are best explained by the migration of locally derived material until more definitive field and compositional information is available.

Numerous concordant pegmatitic veins and augen of feldspar or quartz and feldspar are usually composed of plagioclase (\pm quartz) in mafic rocks and K-feldspar, plagioclase, and quartz in felsic rocks. Such occurrences suggest a local derivation. In the quartz-plagioclase gneiss (Sp 145 E), for example, the K-content may have migrated and recrystallized as an *RD* K-feldspar in the pegmatite vein.

The occurrence of quartzites containing plagioclase as the only other main mineral implies some material transfer. Quartz-rich sedimentary rocks are characterized by high ratios of K to Na (Pettijohn, 1957).

The layers of granitic gneiss and sills of gneissic granite exposed over a wide area along Sperillen present all gradations from gneiss to foliated granite. The granitic texture may have evolved by simple recrystallization, or material may have been introduced. The four modal analyses for these rocks approximate the minimum-melting composition of the granite system (Tuttle and Bowen, 1958). The granitic layers are so much thicker than the intercalated mafic layers that synkinematic intrusion without the complete disruption of the intervening layers seems impossible.

These granitic layers must have been shales or tuffs of a sedimentary succession if no metasomatism is assumed. The presence of undisturbed fragments of gneiss in the dikes and of granite permeating the folds suggests a certain amount of mobility. The sills may largely form by a recrystallization of the quartz-monzonitic gneiss coupled with the removal of some mafic material. If even a small amount of material was introduced to each granitic layer, the total amount of material transport within this area must have been tremendous. Possibly the fluid content of the rock promoted a moderate metasomatism and a recrystallization that generally outlasted the deformation.

The apparent incompatibility of hornblende and K-feldspar in the gneisses mentioned previously is found in adjacent layers; therefore, it cannot represent a change in facies. The low-obliquity K-feldspar, the flame perthite and the antiperthite that are usually found in rocks containing hornblende and K-feldspar have been interpreted as re-

placement features (p. 124). All gradations from hornblende gneisses in which all the K-feldspar is contained in antiperthite to augen gneisses containing a few fragments of hornblende can be observed on a regional scale and also on the scale of an outcrop in the augen gneiss shear zone at Bagn. Many of the gneisses containing both hornblende and K-feldspar have probably undergone a K-metasomatism that was arrested before the hornblende was completely replaced.

Granitic gneisses in the Telemark series contain hornblende but show no signs of transformation. The microcline in these rocks is evenly perthitic without showing any sign of corrosion and porphyroblastesis. These rocks belong to a much higher stratigraphic and structural level than the gneisses that appear to have undergone K-metasomatism. The gneisses represented by these two distinct behaviors of K-feldspar may be considered to be separated by the migmatite front (Wegmann, 1935), the zone which is transitional in this area and separates the metasomatic infrastructure from the superstructure.

Origin of the Metamorphosed Rocks.

The possible causes of banding in banded gneisses have been discussed by Dietrich (1960) who concluded that banding most likely represents an original sedimentary stratification. The composition of the strata may or may not have been subsequently altered.

In the Flå area, deformation has exerted profound effects on the layering. The more competent units are boudinaged on every scale; the less competent layers may be tightly folded. In some places, the fold hinges are sheared out and the limbs are sheared off. The extension of the layers may have been greater than 10 times. Although the banding in the gneiss resembles a relict sedimentary structure, certainly, the thickness of layers is greatly changed (Fig. 65), and mechanical differentiation (Wenk, 1937) may have been active to produce the present mineral composition of the banding. The banding is most likely inherited from a supracrustal layering but the original composition may have been altered during the extreme deformation.

The composition of the gneisses on the west side of the Flå granite is, nevertheless, highly indicative. The interlayered Telemark orthoquartzites and amphibolites are underlain by quartz-rich gneisses that contain varying proportions of plagioclase and K-feldspar. These

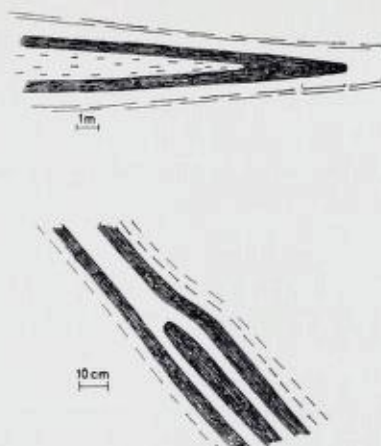


Fig. 65. *Folds in banded gneisses that illustrate the extreme extension in a that the gneisses have undergone.*

Folder i båndgneis som illustrerer den kraftige strekning i a, som gneisene har vært utsatt for.

grade into the banded granodioritic gneisses in which some quartz-rich layers are recognizable. The quartz content of all these rocks certainly points to a clastic sedimentary origin.

If isochemical metamorphism is assumed, the highest quartz-rich rocks were orthoquartzitic sandstones underlain by subgraywackes and finally graywackes. This appears to represent sedimentation changing from unstable to stable conditions; however, the orthoquartzites seem to be as strongly deformed as the banded gneisses.

Petrogenesis.

Introduction.

In the discussion of petrogenesis, the argument must be based on all the available information and on conclusions that are drawn from this information. It is expedient to compile a list of this data, and, in so doing, to distinguish between facts that cannot reasonably be doubted and other conclusions that could be disputed. Accordingly, the writer has set up Table IX in which facts and the resulting hypothesis are listed separately. The list also provides a summary of the main points covered in each chapter. The reader can use this list to construct his own petrogenesis according to his own experiences.

The evidence from the granite listed in Table IX shows features that are attributed to both magmatic and metasomatic granites; therefore, alternate hypotheses propounding a magmatic origin and a metasomatic origin will be developed. A discussion of the advantages and drawbacks of each hypothesis as applied to the Flå granite precedes the statement of the two hypotheses.

Comparison of Magmatic and Metasomatic Hypotheses with the Field Evidence.

The behavior of gneiss inclusions yields some puzzling features when compared with the way an inclusion should act in magma (Bowen, 1928). The inclusions, which are commonly more mafic than the granite, should react with the magma to form minerals with which the magma is in equilibrium (Bowen, *ibid.*). An amphibolite should, therefore, be transformed into a mass of biotite and more sodic plagioclase. These minerals are seen to be formed in the first stages of transformation, but the final product, regardless of its initial composition, is usually a rock whose composition approaches that of the granite, the minimum-melting composition.

According to Bowen (*ibid.*, p. 184), solution of an inclusion is not to be expected because the magma does not have superheat. The reactions that transform an inclusion commonly cause an increase in volume which may bring about the mechanical disintegration of an inclusion (Bowen, *ibid.*). Such scattered fragments and mineral grains of a hornfels are described by Goldsmith (1911, p. 107) from the contact zone of a nordmarkite in the Oslo magmatic province. The inclusions in the Flå granite, however, retain their form, often with angular outlines, right up to the point at which they can no longer be distinguished from the granite. Numerous delicate layers of biotite attest the presence of completed transformed inclusions. Other inclusions are sheared out in a plastic medium. Obviously at the final stages of the transformation, an area that was once an inclusion cannot be distinguished from the "true" granite (assuming the "true" granite was magmatic).

Inclusions that are found within tens of meters of each other and that appear to have been the same exhibit various stages of transformation. This fact is explained with difficulty by the magmatic hypothesis because they were probably incorporated into the granite

Table IX.

A List of Facts and Less-Certain Information Determined about the Granite.

Facts	Conclusions, Deductions, Hypotheses
The composition of the granite is near the minimum-melting composition in the granite system.	Crystal-liquid equilibrium <i>may</i> have determined the composition of the granite.
The 39 samples of the granite occupy a limited compositional range.	The composition of the granite is probably quite uniform; however, significant smaller variations cannot be excluded by so few samples.
The texture is granitic in places and granoblastic in others.	The granite may have undergone both magmatic and metasomatic stages.
The Hedal granite is fine-grained in the center and porphyric around the margin; the Adal granite is composed of porphyric granite that encloses smaller pieces of fine-grained granite.	The fine-grained granite generally appears to be older than the porphyric variety.
Oscillatory-zoned plagioclase porphyroblasts are found in inclusions but not in the granite.	Plagioclase porphyroblasts in the inclusions were subjected to a changing chemical environment which was repeated.
Oriented plagioclase grains are found in K-feldspar porphyroblasts of plagioclase lamellae in the perthite is exceedingly irregular.	The flame perthite is probably a replacement phenomenon; The evolutions is complex.
Oriented plagioclase grains are found in K-feldspar porphyroblasts from inclusions and K-feldspar megacrysts from the granite.	K-feldspar porphyroblasts that enclose oriented plagioclase grains can form in solid rock and <i>may</i> be indicative of formation in a solid or near-solid medium.

Facts	Conclusions, Deductions, Hypotheses
<p>Sericitized plagioclase interdigitates with fresh microcline; pockets and septa of plagioclase occur along the boundary of adjacent microcline grains.</p>	<p>Microcline has grown porphyroblastically and partially replaced plagioclase.</p>
<p>Rapakivi rims of plagioclase are found around a few microcline porphyroblasts within the inclusions.</p>	<p>Incomplete plagioclase rims are found within some microcline megacrysts in the granite and suggest that this rock <i>may</i> have been transformed.</p>
<p>Numerous inclusions that <i>appear</i> to have been the same kind of gneiss show all stages of transformation within a small area.</p>	<p>Inclusions that were incorporated within the granite almost simultaneously have been altered to varying degrees.</p>
<p>Reaction rims are never found surrounding inclusions.</p>	
<p>Folded biotite screens are found sporadically within most of the granite.</p>	<p>The rock immediately enclosing them was not molten.</p>
<p>The granite is foliated particularly at its border; the foliated granite is sheared.</p>	<p>The last movements took place in a solid medium to impart the present foliation to the granite.</p>
<p>The foliation generally conforms to the contacts of the granite; the shearing is partly contemporaneous with and partly older than the growth of the megacrysts.</p>	<p>The foliation was formed during the emplacement of the granite.</p>
<p>The mesoscopic deformation fabric of the gneisses in some small areas adjacent to the granites exhibits triclinic symmetry.</p>	<p>Earlier structures have probably been deformed around subvertical axes by the granite emplacement.</p>

Facts	Conclusions, Deductions, Hypotheses
<p>The regional deformation fabric, which is triclinic, is composed of north-to west-northwest-trending fold axes; the fabric is generally more complex near the granite contacts.</p>	<p>The position of granites has been determined by the structural geometry of the gneisses; movements that took place during the granite emplacement deformed the gneisses further.</p>
<p>The contacts between granite and gneiss are, with few exceptions, sharp.</p>	<p>The process that formed the granite must have been capable of producing a sharp contact.</p>
<p>No diminuation of grain size is found at the contacts.</p>	<p>The granite has attained equilibrium within the P-T conditions of the amphibolite facies.</p>
<p>Sills and subparallel dikes of granite pass into a contact zone of intermixed gneiss fragments and granite which form an eruptive breccia.</p>	<p>The contact breccia is a large scale agmatite formed by the coalescing of granite sills and dikes.</p>
<p>The orientation of K-feldspar megacrysts in a dike that has sharp contacts mirrors the fold pattern in the surrounding small-folded gneiss.</p>	<p>At least some of these dikes and sills which have sharp contacts are replacement features.</p>
<p>The S-surfaces of inclusions at the northwest contact of the Heddal granite define a north-northwest-plunging axis whose orientation approximates that of the axis outside the granite.</p>	<p>Most of these gneiss fragments have not been displaced since the regional deformation; the granite that encloses them was not fluid.</p>
<p>The foliation of some adjacent inclusions forms a "T"-intersection.</p>	<p>The inclusions must have been displaced relative to each other in highly mobile medium.</p>
<p>Inclusions and dark, biotite-rich shadows are found everywhere in the "tail" of the Adal granite.</p>	<p>Assimilation or metasomatism has been the dominant process in the development of the "tail".</p>

Facts	Conclusions, Deductions, Hypotheses
<p>The gravity anomalies over the granites are very small, <i>ca.</i> 4 to 6 mgal.</p>	<p>The granites are thin plates.</p>
<p>The maximum anomalies occur at the granite contact or in country rock over a granitized zone in the gneiss.</p>	<p>The maximum thickness of the granites is between 2.5 and 4 km.</p>
<p>The fresh modal plagioclase is considerably more calcic than the normative plagioclase.</p>	<p>The plagioclase has been sericitized and became more sodic under conditions that caused a sliding equilibrium.</p>
<p>Some K-feldspars from the contact zone of the granite and from inclusions show the same orthoclase symmetry as the K-feldspars from augen gneiss.</p>	<p>This phenomenon is attributed to the metastable formation of orthoclase within the stability field of microcline in rocks undergoing transformation.</p>
<p>Almost all the K-feldspar in the granite exhibits maximum obliquity (microcline).</p>	<p>Conditions within the granite favor the inversion to microcline.</p>

at approximately the same time. To say that some of the inclusions were derived at depth and others were derived locally as an explanation is to dodge the issue. This erratic transformation of neighboring inclusions is fully consistent with conventional transformist theories. The transformation of inclusions would depend on their position in respect to channels (shear planes) followed by metasomatizing solutions. Such a solution is, however, not much happier because the *apparent* uniformity of the granite formed by the presumed metasomatism is still inconsistent with the variable transformation of the inclusions.

The minimum-melting composition of the granite provides the strongest argument for a magmatic origin, and not without reason. According to Chayes (1952, p. 243), however, we shall never be able to prove any particular granite is magmatic *solely* because of its com-

position; it is only the bulk of granites that must be magmatic because of the concentration of compositions around the ternary minimum (Chayes, *ibid.*).

The difficulties of obtaining granitic magma by fractional crystallization of a basaltic magma have been discussed profusely (Waters, 1948) and do not seem to be in favor at present (Wyllie and Tuttle, 1960). We shall then form our magma anatectically; such a magma or one formed by fractional crystallization in a closed system can hardly have superheat (Bowen, 1928).

The task of this anatectic magma is formidable. This magma which is presumably of minimum-melting composition must react with a considerable volume of inclusions and surrounding country rocks and convert them to not only minerals with which the magma is in equilibrium but also to the same bulk composition. The felsic constituents, predominantly K, would be extracted from the magma; the magma would become poorer in K. The mafic materials were removed from the transformed rock and apparently disappeared. Finally as a last stage of the crystallization, a K-rich residual fluid would produce a general K-metasomatism including a rather extensive area at the peripheries of the granites. This process produces the K-feldspar porphyroblastesis and brings the composition of the granite back to the minimum-melting composition.

Since a large amount of K must be consumed in reacting with the inclusions, the residual solutions from the anatectic magma can hardly be enriched in K. The only way that this seems possible would be if a large amount of K were introduced into the magma by a metasomatic mechanism.

Certainly, a key point in evaluating the magmatic hypothesis is the amount of inclusions that have been made over by the magma. The writer cannot conceive of any rational means to estimate this short of very detailed mapping and sampling, which could not completely solve the problem.

The three chemical analyses would seem to form a differentiation series formed under increasing P_{H_2O} (Fig. 66). This impression is reinforced because Sp 413 A comes from the border and Sp 380 A comes from the center of the Heddal granite. Sp 380 A is, however, the most mafic of the three samples analyzed; furthermore, all the field relations indicate that the fine-grained granite (Sp 380 A) is older than the porphyric granite (Sp 413 A). The field relationships completely contradict the sequence given by the phase diagram.

The minimum-melting composition loses its significance as a criterion for a magmatic evolution. If a magma became somewhat basified by reaction with inclusions and then returned to a minimum melting composition during the K-metasomatism, caused by residual solutions which have somehow become K-rich, this uniform minimum-melt composition must have been caused by something other than crystal-liquid equilibrium.

The fine-grained granite has the same general composition as the porphyric granite; inclusions have approached the same composition. Processes which have produced the probable K-feldspar porphyroblastesis must have left behind a rock of this composition. If an influx of K took place, it has stopped within very definite compositional limits. Metasomatic processes are generally assumed to give rise to heterogeneous compositions; however, the experimental work of Orville (1962) demonstrates that almost the same feldspar solvus can be obtained by ion exchange as by crystal-melt equilibrium. Experimental confirmation is needed, but the field and petrographic observations suggest that a rather uniform minimum-melting granite can be formed by some sort of metasomatic process, which may or may not follow a magmatic crystallization.

Oscillatory-zoned plagioclase porphyroblasts in some inclusions suggest a magmatic history according to conventional thinking. This interpretation encounters difficulties because oscillatory zoned plagioclase is never found in the granite and because these inclusions are found in the "tail" of the Ådal granite where the granite appears to be the "most metasomatic" of the entire area. Some of the accompanying plagioclase grains are progressively zoned; most plagioclase grains in the groundmass are not zoned at all. The oscillatory zoned plagioclase porphyroblasts from an inclusion can hardly be indicative of a magmatic evolution when the supposed magmatic rock displays no traces of oscillatory zoned plagioclase. Emmons (1953) has ascribed a similar occurrence to locally varying (within the area of a large thin section) fluid content in rocks undergoing metasomatism. Although the mechanism remains unknown, the observations suggest that this oscillatory zoning is caused by extremely local chemical variations in rocks undergoing a change in their bulk chemistry.

The feldspars furnish clues to the evolution of the granite but may represent only the later stages of this evolution. Inclusions of plagioclase grains within the microcline megacrysts, screens and

pockets of corroded plagioclase between adjacent microclines, and the flame perthite are all interpreted as the products of a K-feldspar porphyroblastesis. This could be interpreted as the product of either a metasomatism that formed the granite or a deuteric stage that has somewhat altered the texture of a magmatic granite.

The composition of fresh plagioclase represents the composition of the plagioclase that crystallized from a magma or of some stage in the metasomatism, possibly of the original rock that was transformed. The sericitization of plagioclase occurred as the rock attempted to attain equilibrium during changing chemistry and/or P-T conditions; the sericitized plagioclase became more sodic. This sericitization is probably ascribed to lower temperature conditions during which the rock was solid. Al-poor solutions of alkali silicates would probably not react with the plagioclase to form sericite. Ca must have been removed from the rock during the sericitization because no other Ca-bearing minerals are commonly found in the granites.

The K-feldspar at the granite contact may show intermediate and variable obliquity. This feature may constitute a "frozen in" relic of the general metasomatic process that advanced through the country rocks and formed the granite; therefore, the metasomatism has been arrested as the process died out at the point where the contact is placed. The magmatic hypothesis relegates these intermediate K-feldspars to a deuteric stage or, more extremely, to thermal effects.

The K-feldspars in the granite are typified by their general high obliquity values ($\Delta = 0.9$). Although the effects of deformation and slow growth or longer time for inversion may be appreciable, the obliquity values imply a relatively high volatile content (Donnay and others, 1960).

The granitic texture is often interpreted as *per se* evidence of a magmatic history. According to Tuttle and Bowen (1958), Ca-poor granites will normally crystallize as a one-feldspar granite. A granitic texture in such a granite cannot demonstrate descent from a magma because the plagioclase and the alkali feldspar have probably unmixed in the solid state from a single alkali feldspar. If such a recrystallization can develop a granitic texture, so can a recrystallization in a metasomatic granite. The coexistence of granitic and granoblastic textures in the same rock may represent a deuterically produced granoblastic texture superimposed on a magmatically derived granitic texture, or it may indicate the diverse evolution of a metamorphic texture.

The cortege of dikes and sills that surrounds the granites can be interpreted equally well in terms magmatism or metasomatism. The metasomatic origin of many dikes and sills can hardly be doubted; however, replacement dikes and sills may surround magmatic granites (Compton, 1955). The sharp contacts of dikes, sills, and the granite itself could certainly be produced by magmatism, but knife-sharp contacts on metasomatic dikes within the area are an observed fact. The foliated crosscutting dikes are sheared as are many of the sills so that plastic and brittle deformation account for the foliation. The basic interpretive problem of the granite is whether these metasomatic features constitute the final stage and natural consequences of a magmatic history or the principal process of development during a metasomatic history.

The shape and the structural relations of the granite suggest a late-kinematic granite that has not intruded greatly. Deformation that is directly attributable to diapirism is lacking from much of the area. Horizontal lineations are found in the gneiss at the very contact of the granite; foliation in the granite is typically steep. The shearing in the granite and the surrounding dikes and sills indicates that a considerable amount of relative displacement has been accommodated by differential movements, but this movement is not easily distinguished from the regional deformation; *i. e.*, the extension in a that accompanies folding.

The strong shearing that has occurred in the granite and outlying sills and dikes and is not found in the gneiss has accommodated most of these late movements. The quartz content of the granites cannot be the only reason why these rocks have deformed so much. The shearing was probably localized in the granitic rocks by a pore solution, pore melt, or intergranular film. Flow into the west end of the Ådal granite has probably taken place.

The granite probably forms a sheet located in the crest of a broad arch. Whether the granite is magmatic or metasomatic, there is no reason to suspect that the granite has principally formed the arch. On the contrary, the regional structural geometry has probably localized the position of the granite. On a mesoscopic scale, granites, pegmatites, and porphyroblasts are seen to form in the crests of folds. They constitute occurrences in which the origin is very likely metasomatic; *i. e.* migration towards areas of potential low pressure. The same phenomenon may occur on a regional scale. If the granite formed from ana-

tetic magma, the magma or mush would flow into predetermined arches from which it might break through and move upward as a diapir (Wegman, 1930; Smithson, 1963). In either case, the structural geometry has determined the position of the granite, which may ultimately pierce and deform the overlying rocks.

The form of the granite is best described as a large plate which is classed as intermediate between stratiform sheets and batholiths (Raguin, 1957). The granite has many characteristics of a synkinematic intrusive, but it appears to have mainly recrystallized later than the main deformation. The position of the granite is placed in the upper catazone (Buddington, 1959).

A *basic front* (Reynolds, 1946) surrounding the granite would provide a happy supplement to the metasomatic hypothesis. The large amount of Mg, Fe, and Ca displaced by a metasomatic evolution had to go somewhere. Amphibolitic rocks are fairly common at the contacts of the granite, but the amphibolitic rocks that have been found are best explained in terms of the regional stratigraphy. Apparently, Mg, Fe, and Ca had to go down while K came up if the granite was formed metasomatically.

The problem is the same but much less acute for the magmatic hypothesis. The calcemic elements in the inclusions and the border zone had to go somewhere because all these rocks were transformed to the composition of the granite instead of simply reacting to form minerals with which the magma was in equilibrium.

An amphibolite layer would be expected to form both a mechanical and a chemical barrier for the advance of a granite irregardless of whether the granite was magmatic or metasomatic. Metzger (1947) proposed that marble and amphibolite layers in the Finnish Precambrian formed a resistant cover under which anatectic magma collected in domes. It should not be surprising to find many granites surrounded by mafic gneisses at their contacts.

The Magmatic Hypothesis.

Most petrologists believe that a granite composition corresponding to the "ternary" minimum in the granite system (Fig. 66) strongly suggests an origin by fractional crystallization or differential fusion (Chayes, 1952; Tuttle and Bowen, 1958; Barth, 1962). The three plotted compositions of the granite, particularly the mesonormal com-

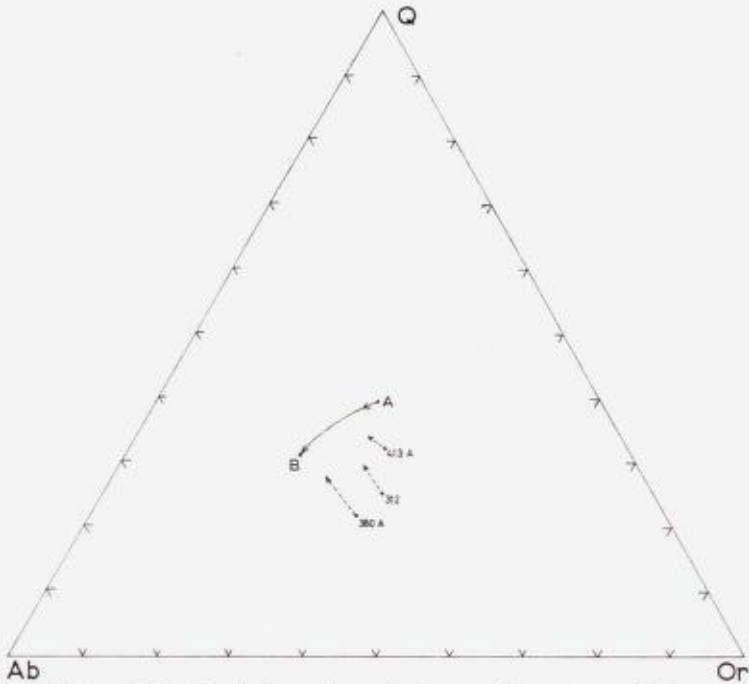


Fig. 66. Plots of the chemical analyses in the granite system. Circles represent cation norms and arrowheads represent mesonorms. The line AB is the locus of the minimum-melting compositions at P_{H_2O} between 500 and 4000 bars.

Pøtting av kjemiske analyser i granittsystemet. Ringer representerer katanorm c_n , pilespisser mesonorm. Linjen AB fremstiller minimum smeltepunkts sammensetninger mellom 500 og 4000 bar vanntrykk.

positions, are seen to fall so closely to the locus of the minimums at different pressure (line AB, Fig. 66) that a development by crystal-liquid equilibrium is likely. The modal analyses are mostly included within the spread of these chemical analyses so that all 39 analyses of the granite fall close to the minimum-melting composition.

The granite is, however, a calcalkaline granite whose composition cannot be represented so accurately in a ternary diagram. Accordingly, the compositions are plotted in a four component Ab-Or-An-Q diagram (Fig. 67) which shows how far the points are pulled out of the plane representing the Ab-Or-Q system by the An-content of the granite. Clearly the crystallization of the granite must be considered in terms of a four component system. Bowen has written in a letter to Eskola (Eskola, 1956):

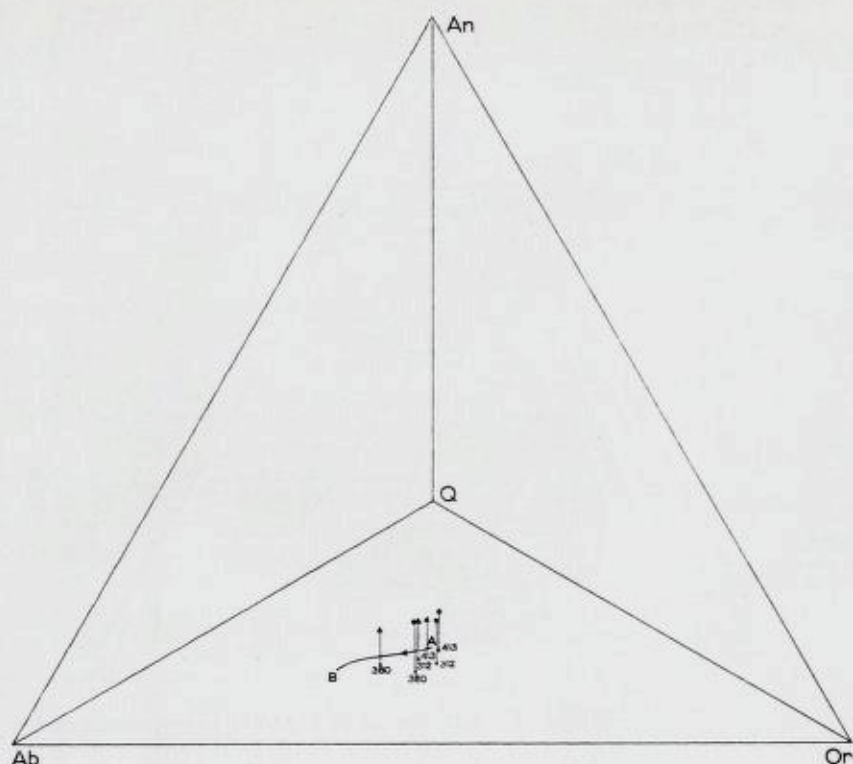


Fig. 67. Four-component plots of the catanorms (circles) and mesonorms (arrowheads) of the granite. The length of the vector indicates how far out the plane representing the granite system the rock is pulled by its An-content. Fire-komponent-plottinger av katanormer (ringer) og mesonormer (pilespisser) for granitten. Vektorlengden viser hvor langt ut av det plan som representerer granittsystemet, bergarten er trukket av sitt An-innhold.

" - - - We have found the peculiar fact that although water aids the crystallization of the purely alkali feldspars it does not aid much when some lime is added to the alkali feldspars, in fact, it even seems to have the opposite effect. Still the addition of An to alkali feldspars — cannot fail to push the low-melting liquids to Or-richer compositions since the "eutectic" between Or and An is practically at Or, whereas that between Or and Ab is richer in Ab than in Or."

The effect of An would be to displace the minimum-melting composition toward the Or-corner. The projection of this composition on the Ab-Or-Q plane would probably lie even closer to the composition of the granite (Fig. 66).

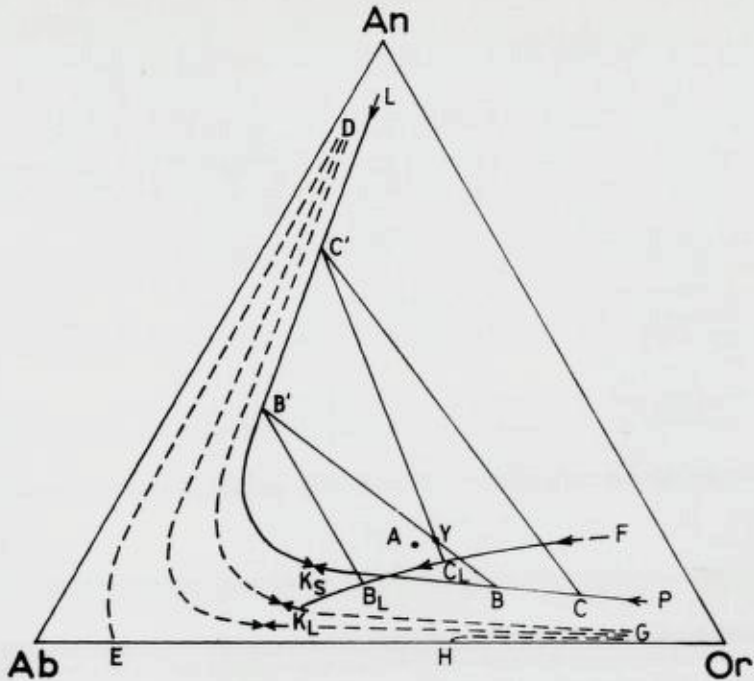


Fig. 68. The probable extent of solid solution at different temperatures in the Ab-Or-An system is represented by the family LK_sP to DE-HG. K_LF is the boundary between the fields of K-feldspar and plagioclase and represents the composition of liquids in equilibrium with two feldspars whose compositions lie along the curve LK_sP . (Adapted from Tuttle and Bowen, 1958.)

Den sannsynlige utstrekning av fast oppløsning ved forskjellige temperaturer i Ab-Or-An systemet fremstilles av kurvene LK_sP til DE-HG. K_LF er grensen mellom områdene for K-feltpat og plagioklas og representerer sammensetningen av smelte i likevekt med to feltpater, hvis sammensetning ligger langs kurven LK_sP . (Etter Tuttle og Bowen, 1958.)

The effect of adding CaO to a granitic magma is to cause the crystallization of two feldspars, a plagioclase and an alkali feldspar (Tuttle and Bowen, 1958). The probable extent of solid solution in the An-Or-Ab system varies directly with the temperature (Fig. 68). Curves GH and ED represent the probable extent of solid solution in a plutonic rock such as the Flå granite (Yoder and others, 1957). A liquid with the composition Y would first crystallize out a plagioclase with a composition somewhat more anorthite-rich than C'. As the temperature falls the liquid changes composition to toward the point

C_L , where a plagioclase of composition C' is joined by an alkali feldspar of composition C . Finally at B_L , all the liquid is consumed and a plagioclase of composition B' coexists with an alkali feldspar of composition B . Point A represents the composition of the Flå granite. A granitic melt of this composition would clearly crystallize a plagioclase and an alkali feldspar which would follow the path outlined above if fractionation or assimilation did not take place.

A magma from which the Flå granite was formed would thus be expected to crystallize out two feldspars, a plagioclase and an Or-rich alkali feldspar. A recrystallization and unmixing of a single alkali feldspar into a K-feldspar and an albitic plagioclase (Tuttle, 1952; Tuttle and Bowen, 1958) would not seem necessary.

The magma would probably be formed by anatexis deep in a sedimentary geosynclinal pile according to current thinking (Tuttle and Bowen, *op. cit.*; Wyllie and Tuttle, 1960; Barth, 1961). The magma is squeezed out of a mesh of mafic residuum by tectonic forces and flows into a structural clumination (Fig. 69). The residuum left behind is a thin layer. This suggestion agrees with the usual gravity profiles (Smithson, 1963, p. 108), and the magma does not have to come from a much deeper level than the present exposure.

The fractionation of the magma after emplacement must have been slight because of the small compositional range. The magma could have been formed at a greater depth and intruded to its present

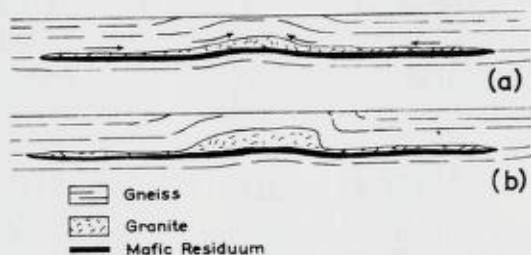


Fig. 69. Schematic diagram illustrating how the Flå granite might form by anatexis. (a) Anatectic melt separates from its mafic residuum and begins to flow into a structural high. (b) The melt forms a thin plate of granite and domes the country rocks further.

Skjematisk diagram som viser hvordan Flå-granitten kunne dannes ved anatekse. (a) Anatektiske smelte skilles fra sitt residuum av mørke mineraler og begynner å bevege seg oppover. (b) Smelten danner en tynn plate av granitt og får den opprinnelige bergart til å bøye seg videre oppover.

level or mainly formed in place. The fact that the granite appears to be in thermal equilibrium with its surroundings suggests a formation in place or, as suggested above, in a layer at a slightly deeper level. Because the composition of the gneisses is not favorable to the formation of sufficient magma, an anatectic formation in place must be accompanied by the metasomatic removal of calcic constituents, but the anatectic-layer concept overcomes this difficulty.

The magma congeals and leaves behind a pore fluid, possibly one rich alkali silicates (Tuttle and Bowen, 1958, p. 84) which are highly soluble in water. These alkali silicates react with the granite already formed and the country rocks to produce a K-metasomatism (Eskola, 1956). The granitic texture is retained in places; in others a granuloblastic texture and replacement features obtain. The solutions attack the plagioclase to form the sericite and plagioclase of variable composition. The residual solutions move along shear planes in the country rocks to metasomatically form the sills and dikes that mark the granite contact. These coalesce and envelope fragments of gneiss to give the appearance of a contact breccia. The sills and dikes attain the same (minimum melting) composition as the granite. Some inclusions within the granite are located along passages that determine the movement path of these solutions; these inclusions are more completely transformed. As the final act the granite is sheared to develop its foliation. The shearing takes place in solid material but is facilitated by a fluid film around the grains.

One dominant process has taken place in the area, the formation of a magma. The numerous replacement features and the shearing of the granite constitute the final act of a magmatic-crystallization history; they are deuteric effects.

The Metasomatic Hypothesis.

Until recently, metasomatic processes have lacked the experimental confirmation that is necessary to give them the required respectability. A possible mechanism for metasomatism has been discovered by Tuttle and Bowen (1958, p. 90), who write:

“Rapidly of transfer at high pressures was illustrated by one experiment - - -. A sample of Westerly granite (approximately 1 gm) was held in a cold-seal pressure vessel for 36 days at a temperature of 700°C and 4000 bars pressure. On quenching, the platinum-foil crucible contained only about 50 mg

of material which was largely monoclinic pyroxene and garnet with accessory alkali feldspar and apatite. The quartz and feldspar components had been almost completely abstracted from the liquid and deposited in the cooler portions of the pressure vessels - - -."

These results indicate that the felsic constituents should diffuse upward in the earth's crust.

Even more surprising results have come from the experiments of Orville (1962) which study cation exchange between the feldspars in the presence of chloride solutions. An alkali-feldspar solidus is obtained by cation exchange that resembles fairly closely the crystal-melt solvus determined by Bowen and Tuttle (1950). Orville also demonstrated that K^+ will diffuse toward the low-temperature side of a thermal gradient of only $30^\circ C$ in the presence of chloride solutions.

Solutions can clearly effect metasomatic reactions. There is even a suggestion that approximately the same equilibrium relations obtain from an exchange process as from crystal-liquid equilibrium. Solid diffusion is not considered to be effective over even moderate distances (Hedvall, 1952); however, diffusion through a fluid phase might account for a considerable amount of material transfer. Moreover, material transport by fluid flow through rocks may reach significant amounts (Rosenqvist, 1952) during geologic time. The fluid phase might be either a solution or a melt, but a solution would seem to be most compatible with temperatures indicated by amphibolite-facies conditions.

These solutions carry (or allow diffusion of) the necessary material, mainly K, up from below and deposit it at a site determined by the temperature, pressure, and chemistry. Shear surfaces provide the most likely path for this transfer. These shear surfaces are conformable or semi-conformable to the foliation in the gneiss; therefore, a sill or slightly crosscutting dike is formed along these shear planes. The same localization of K-feldspar can be observed along foliation planes on a microscopic scale. If the contact phenomena are extrapolated to the entire granite, the granite was formed by the coalescing of a series of sills to form a massive granite followed by a continued growth and incorporation of material at the margins. Finally the granite becomes sufficiently plastic to begin to flow upward diapirically facilitated by the pore solutions or absorbed fluid film and the dying orogenic stress.

Magma is not required for a granite to intrude its cover any more than it is required for a shale fold-core to intrude its cover or a salt layer to intrude its cover. Besides the lubricating effect of a fluid film, a considerable amount of movement may be taken up by the quartz which deforms internally, recrystallizes, and deforms again (Balk, 1949). Such componential movements would not be doubted in the gneisses that surround a granite emplaced in a regional-metamorphic terrain. If the scale of a body of granite deformed by solid flow is considered, it should be no more surprising to find rotated inclusions in the granite than to find biotite flakes that differ from the maximum concentration in the thin section of a tectonite. Sander (1948, p. 187) points out the need for both caution and petrofabric analysis in the interpretation of contact breccias as magmatic effects. Berthelsen (1960, p. 212—14) proposes that intrusive-appearing relations between granitic layers and the surrounding gneisses may arise from double folding. Intrusive-looking granites in regionally metamorphosed rocks may have intruded by solid flow or be produced by complicated folding.

A granite body of minimum-melting composition has thus been formed metasomatically and has risen a moderate distance diapirically. What will happen if this granite body attains a higher temperature somewhat over 600° C? It must then melt to form an anatectic magma and rise even higher into the arch that has already been formed. It may even break through to the higher levels in the crust and form a discordant magmatic granite body.

The above hypothesis may seem a bit fanciful to the reader. It is, however, no more unreasonable than the magmatic hypothesis; and it does suit the field evidence, which according to the magmatic hypothesis, must be completely written off as the last somewhat accidental act of a magmatic evolution.

Conclusions.

Both hypotheses will explain the origin of the Flå granite, but both hypotheses leave much unexplained as we might well expect when dealing with natural phenomena. The magmatic hypothesis enjoys the benefits of considerable experimental research (Tuttle and Bowen, 1958; Wyart and Sabatier, 1959; Wyllie and Tuttle, 1961;

Winkler, 1961) and is generally regarded as being the "most scientific". We must admit, however, that if the magmatic hypothesis is adopted most of the field and petrographic observations are ascribed to "deuteric processes". In other words, the geologic and petrographic observations are disregarded and the word, "granite", becomes truly genetic because not even the significance of the minimum-melting composition withstands a deductive testing of the magmatic hypothesis.

The writer prefers a metasomatic hypothesis involving either a pore solution or pore melt because it is in better harmony with the observations. Unfortunately, we are in no position to judge the quantitative participation of metasomatic reactions facilitated by intergranular solutions or melts because their action has been only moderately investigated in the laboratory. As Winkler (1961, p. 362—63) has remarked, the importance of metasomatic processes cannot be excluded and awaits experimental confirmation. The metasomatic hypothesis, nevertheless, encounters the traditional difficulties in the source of the introduced material and the destination of the removed material. Although Orville (1962) has demonstrated that ion exchange processes may produce almost the same equilibrium assemblages as crystal-liquid equilibrium, another even greater hurdle is how a metasomatic process can produce such a uniform rock with sharp contacts. Finally the metasomatic hypothesis meets with danger because it interprets features such as rotated inclusions and foliated crosscutting dikes that could be igneous as the result of shearing in solid or near-solid rock.

Irregardless of whether the dominant process was magmatic or metasomatic, the writer strongly objects to the use of this granite in a statistic representing the minimum-melting composition. *Any granite that exhibits such marked metamorphic features can hardly be used to demonstrate that all or most granites have formed by crystal-liquid equilibrium.* The writer would prefer a granite-by-granite evaluation of which granites are even suitable to be included in such a statistic.

The formation of an anatectic pore magma rich in volatiles could be expected to promote considerable metasomatism before the pore fluid comprised enough of the entire rock to separate into a homogeneous magma (Eskola, 1948). The intruding magma itself may provide a medium for the large scale transfer of material. On the other hand, the low melting components may become concentrated in one place by metasomatic processes before the melting point is reached;

as the temperature rises, an anatectic melt would form in the already metasomatized area.

The transformation of inclusions and country rock into typical granite and the sericitization of plagioclase with concomitant loss of Ca demand a significant amount of material transfer. Irregardless of whether the granite was predominantly formed by crystallization from a melt or by granitization of solid rock, metasomatic processes were involved and a considerable amount of calcic material has disappeared to parts unknown. One of the most certain conclusions is that *the system was open*.

The actual process that formed the granite is certainly complicated, and the attempt to force its evolution into one scheme or the other can only encounter difficulties. These very difficulties imply that the petrologist must proceed carefully with an open mind and be on the lookout for some heretofore unrecognized explanation.

The diverse development of the fine-grained- and porphyric-granite facies may be ascribed to variable water content of the two rock types. A higher water content around the margins of the granite body may promote K-feldspar porphyroblastesis. Shearing would be facilitated by a liquid film along the grain surfaces. The sheared granite always contains K-feldspar megacrysts; this shearing is found in the granites, predominantly at the contacts, and in dikes and sills surround the granites. The well foliated (and sheared) Ådal granite is almost entirely composed of porphyric granite, and the part with the biggest megacrysts is the most highly sheared. Kennedy (1955) has suggested that water might concentrate in the cooler roof and sides of a magma chamber. The same principles should hold for solid rock if the water were free to migrate. The field evidence demonstrates that shearing and K-feldspar porphyroblastesis accompany each other; the fluid content is a likely cause of both.

Although the fine-grained granite is uniform on a large scale, significant small scale variations in color index occur. Biotite gneiss that is in an obvious stage of transformation passes into a homogeneous granitic-appearing rock where it is sheared (Sp 542 in petrographic description, in Tables VII and XII, and in Fig. 64). Small darker bodies of fine-grained granite (Sp 380 A in Table II and III) may represent remnants of inclusions that have undergone a dissimilar path of transformation.

The room problem for the Flå granite is greatly diminished

because of its plate-like form, which has also been interpreted to be the original shape of the granite. Although the approximate amount is uncertain, much of the granite has been emplaced by replacement. If an anatectic magma were involved, it has most likely formed at almost the same level as the present position of the granite. Some space has been acquired by buckling aside the country rocks, especially at the west end of the Ådal granite. The space provided by the combined effects of two or three of these processes seems adequate to explain the emplacement of the plate-like granite.

Age of the Flå Granite and Comparison with Other Southern Norwegian Granites.

Five K-Ar age determinations on mica from the Flå granite and a related pegmatite give ages that range from 852 to 977 m.y. (Neumann, 1960). The mean value is 930 m.y. which corresponds to the mean age of 930 m.y. for the Herefoss (Birkeland) granite in Sörlandet. Although the elongate Flå granite is strongly contrasted in form with the round Herefoss granite, the two granites are probably coeval. The Flå granite was probably emplaced earlier with respect to the cessation of regional deformation.

The Flå granite resembles the Östfold (Iddefjord) granite in megascopic appearance, shape, and contact phenomena. In addition, the granites define a granite axis if an eastward deflection through the Ådal granite is considered. The apparent age of the Östfold granite, however, is placed at *ca.* 800 m.y. (Neumann, 1960). A striking similarity is provided by a comparison of the gravity fields of the two granites. Preliminary results (Smithson, unpublished) indicate that the gravity anomaly caused by the Östfold granite is small so that this granite must also be regarded as a thin plate which is the interpretation proposed by Swedish geologists (Magnusson and others, 1957) for the Swedish extension of the Östfold granite.

General Remarks.

Considerable attention is paid to the "normal" granites that can easily be related to the minimum-melting composition of the granite system. "Contaminated granites" might just as well represent the expected result of a magma formed anatectically. Approximately 20 per

cent of a graywacke may become molten within 5°C of the initial melting temperature (Winkler, 1961). A rock layer in such a condition would behave much more plastically than the surrounding rocks. If tangential forces were applied or if domes had already been formed, the partially melted layer would tend to flow as a layer into the structural highs and eventually form diapir granites. The solid material could be dragged along and swept into the diapir. The interesting result would be that, even though the granite was magmatic (in the sense that a melt was involved), most of the granite was never molten and the composition of the intrusion was determined by the gross composition of a sedimentary layer or layers (Barth, 1961) not by crystal-liquid equilibrium. If the tectonic mobility of a partially melted layer is considered, the near perfect separation of melt and residuum would be a remarkable accomplishment.

Barth (1961) has accounted for the diversity of igneous rocks by the melting of geosynclinal sedimentary rocks; Wyllie and Tuttle (1960) and Wyart and Sabatier (1959) have suggested that melting is common at great depths within geosynclines. Tuttle and Bowen (1958) have proposed that beginning melting may occur in geosynclines at depths between 13 and 21 km according to which geothermal gradient is used. Crustal thickness of from 50 to 60 km are found under young mountain ranges (Gutenberg, 1954; Woollard, 1959) and of the 30 to 40 km under the Precambrian shields. If uniformitarian principles are applied, the old mountain ranges had roots about 60 km deep. These roots have slowly risen as isostatic compensation because of the loss of material by erosion. If the roots have risen from an initial depth of 60 km under a young mountain range to a present depth of 40 km under a deeply eroded shield, 20 km of material must have been eroded. The zone of beginning anatexis would therefore be exposed over much of the shields. Anatexis was first described from the Fenno-scandian shield by Sederholm (1907).

Gravity profiles of granites are just as characteristic as the petrography of granites but perhaps more puzzling because the gravity profiles do not give any indication of the presence of the missing country rock (Bott, 1956; Smithson, 1963). In other words, the gravity anomalies do not reflect the presence of a mass surplus represented by the missing country rock at depth; the country rock displaced by the granite has disappeared.

The problem is not acute for a granite like the Flå granite in

which the emplacement of a plate-shaped body was probably accomplished by formation "on the spot" (whatever the process) followed by some deformation of the country rocks. The gravity-profile problem would also be negligible for a granite emplaced by doming the country rocks and uplifting them along fractures (de Waard, 1949). The disposition of the missing country rocks becomes most inexplicable for the most magmatic-appearing granites, the epizonal granites that have thermal aureoles and chilled margins.

The fact that these granites have simply "replaced" (traded places with) the country rocks impressed Daly (1933) and led him to champion a stoping mode of emplacement. The stoped blocks have neither been observed at lower levels in a granite nor detected gravimetrically. The whereabouts of this missing country rock constitutes an important aspect of the petrology of the rocks concerned.

In contrast to the great thickness of epi- and mesozonal granites (Bott, 1956, 1960), the six catazonal granites investigated by the writer in the Norwegian Precambrian have proved to be thin, plate- or disc-like bodies. According to Buddington (1959), such thin bodies typify catazonal granites.

Considering how much has been written about granites, remarkably little is really known about them. If the complicated evolution that a granite has followed is to be deciphered, much more detailed information will be required. The study of any rock is a field problem, and the key to the field relations is a detailed map. Only when the spatial and temporal relations of the rock types of a granite are known, will the chemical relations achieve real significance. The problem of how much assimilation or reaction with inclusions a granite has undergone is of paramount importance for determining the course of crystallization (or transformation). Numerous modal analyses are required to determine the composition and variation in composition of a granite (Whitten, 1961). Structural studies are a necessity to ascertain how and why a granite was emplaced. Petrographic and X-ray studies of the rock suggest the reactions and inversions that the minerals have undergone. Gravity interpretation can reveal how much granite was emplaced and the possible disposition of the missing country rock. By combining the chemical and field evidence of assimilation with the mass of the emplaced granite determined by the gravity study, semiquantitative calculations of the energy and material requirements for the granite emplacement may be carried out and compared with the experimental

data. Obviously such studies will demand considerable effort, but only through such studies will the complicated genesis of granites be disentangled.

Sammendrag.

Granitt studier: II. Den prekambriske Flå granitten, en geologisk og geofysisk undersøkelse.

Flågranitten består av to elliptiske granittmassiver som støter opp til hverandre, den større nordre Hedalsgranitt og Ådalsgranitten. Granittene er omgitt av båndete granodioritiske gneiser. Migmatiter og øyegneiser er vanlige like utenfor granittkontaktene. Båndete kvarts-monzonitiske gneiser finnes på østsiden. Telemarks suprakrustal-bergarter som består av vekslende lag av kvartsiter og amfiboliter, finnes på vestsiden og båndete kvartsdioritiske gneiser på nordsiden av området. Variasjoner i granitten begrenser seg til porfyrisk granitt, som omfatter mesteparten av blotningene, og til finkornet granitt som omfatter de sentrale deler av Hedalsgranitten. Den porfyriske granitt synes å være yngre enn den finkornete granitt. K-feldspat-megakrystaller i den porfyriske granitt er antagelig porfyroblaster. Sammensetningen av granitten faller innen området for kvartsmonzoniter og stemmer ganske godt med minimums-smeltepunktssammensetningen i granittsystemet.

Foliasjon, linjestrukturer og β -akser i gneisen stryker stort sett mot nord til nordvest. De lineære strukturers fall varierer fra svakt til middels. I stor målestokk er den generelle symmetri triklin. Steilt fallende β -akser nær granitten tilskrives deformasjonen som ledsaget granittens fremtreden. Foliasjon finnes ofte i granitten og er parallell med granittkontaktene. Lineasjon i granitten er lite observert. Granitt som viser orienterte strukturer er alltid granulert. Denne påvirkning representerer sene diapiriske bevegelser i en stort sett fast granitt. Granittens form og beliggenhet er i stor utstrekning bestemt av den regionale struktur-geometri, som igjen i sin tur er blitt lokalt deformert av granittens fremtredning. Granittene er i alminnelighet konkordante, konforme senkinematiske plutoner som viser noen av de synkinematiske plutoners egenskaper.

Granittens grenser er markert ved en gradvis overgang fra granitt med tallrike gneis-bruddstykker til gneis gjennomskåret av tallrike

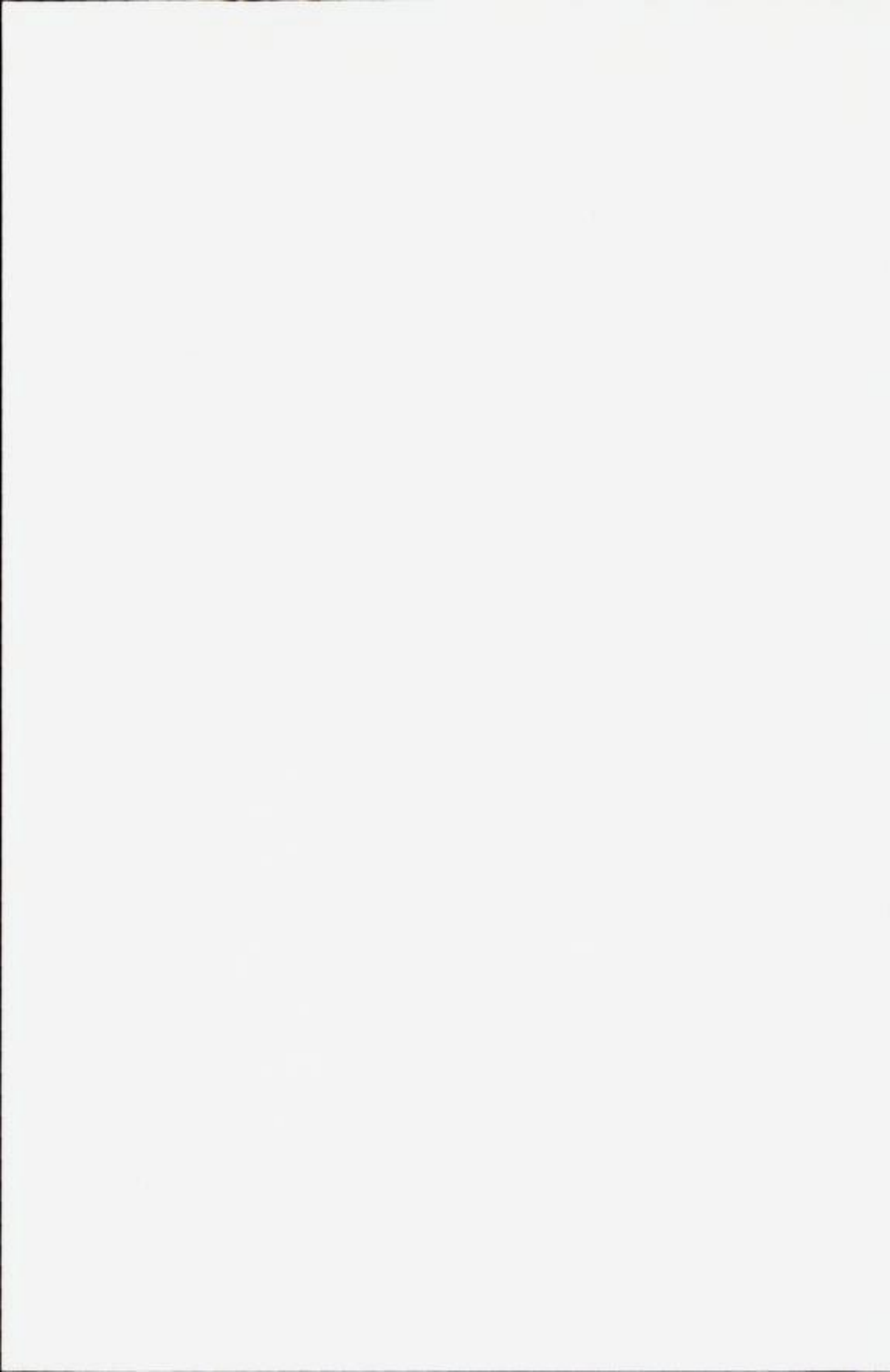
granitiske ganger. Gneisbruddstykkene er uforstyrret noen steder og er tydelig rotert på andre. Grensesonen er en agmatit i stor målestokk.

Tyngdemålinger viser residuelle Bouguer anomalier fra 4 til 6 mgal over granittene. Disse anomalier svarer til tykkelser fra 1.7 til 2.5 km. En 6 mgal anomali sydøst for Ådalsgranitten forekommer over en sone med granitisert gneis og er tolket som en skjult 2.5 km tykk utløper av Ådalsgranitten. Granittenes maksimale tykkelse antas å være omtrent 2.5 km.

Antiperthiter, som er vanlige i øyegneiser tolkes som et «replacement»-fenomen. Orienterte plagioklaskorn i K-feldspat megakrystaller forekommer i inneslutninger såvel som i granitt. Denne utvikling tyder på en porfyroblastisk vekst av K-feltspaten. Sammensetningen av plagioglas og K-feldspat fra granitten viser en del variasjon innenfor et enkelt håndstykke; feltspat termometri kan derfor ikke anvendes på denne granitt. En undersøkelse av K-feldspat trikliniteter viser at K-feldspat fra granitt, gneis og pegmatit er nær maksimum mikroklin, mens de fra øyegneiser, migmatiter, inneslutninger og fra granitt-kontakten viser lav og/eller varierende triklinitet. K-feltspater med lav og/eller varierende triklinitet finnes i bergarter som har vært utsatt for rekrystallasjon eller kjemisk omvandling. K-feldspat i disse siste bergarter er antagelig dannet metastabilt som ortoklas og er «frosset» på forskjellige stadier i ortoklas-mikroklin inversjonen.

Gneisene er fra midtre del av amfibolit-facies. Granittenes mineralsammensetning er den samme som i de granitiske gneiser.

Granittens petrogenese er betraktet ut fra anatektiske og metasomatiske hypoteser. Inneslutningenes opptreden tyder på at en betydelig volum-for-volum utbytning har funnet sted. Dette indisium sammen med granittens metamorfe (eller endometamorfe) tekstur leder til den slutning at granittens minimums-smeltepunkts-sammensetning ikke er avgjørende for en dannelse ved fraksjonert krystallasjon eller oppsmelting. Skjønt både anatektiske og metasomatiske hypoteser forklarer enkelte egenskaper hos granitten og ikke kan forklare andre, må systemet ha vært åpent uansett hovedprosessen: D.v.s. metasomatose har vært et virksomt middel.



Appendix

Table X.
Modal Analyses of Gneisses.

Specimen Number	Rock Type	Plagioclase	K-Feldspar	Quartz	Biotite	Hornblende	Muscovite	Chlorite	Accessories	Area cm ²	Counts
224A	Augen gneiss	% 30.8	% 19.9	% 28.3	% 15.0	% 5.0	% —	% —	% 1.0	36	1022
420B	Augen gneiss	34.5	29.5	23.7	6.5	5.3	—	—	0.5	46	1600
420C	Quartz-dioritic gneiss	46.6	4.4	25.8	13.2	8.6	—	—	1.3	22	787
528A	Orthoquartzite	1.0	—	96.9	+	—	2.0	+	—	19	681
G224	Orthoquartzite	1.5	2.6	95.2	0.6	—	+	—	—	25	726
612B	Granitic gneiss	5.2	40.6	52.7	—	—	+	1.3	0.2	25	937
612B	Dioritic gneiss	68.3	1.2	—	28.9	—	+	+	1.6	6	246
145E	Quartz-plagioclase gneiss	38.0	0.5	59.4	2.1	—	+	+	+	30	848
145E	Pegmatitic felsic layer in above gneiss	32.9	34.2	27.8	4.9	—	+	+	—	16	425
145E	Total composition of above										
	2 analyses	36.3	11.8	48.9	3.1	—	+	+	—	46	1273
211C	Banded granodioritic gneiss	36.6	8.0	47.0	8.3	—	—	+	0.2	41	1486
211D	Quartzite	2.4	15.5	79.9	1.0	—	—	0.6	0.5	22	792
219A	Quartz-dioritic gneiss	43.0	3.3	30.0	22.3	0.3	—	+	1.2	15	574
8	Veined granodioritic gneiss	43.2	17.8	25.8	9.4	2.9	—	—	0.8	22	616
639B	Foliated quartz-diorite	59.6	4.0	27.4	7.8	—	+	—	1.2	19	720
639C	Veined granodioritic gneiss	35.9	12.4	41.5	6.0	—	+	—	0.7	44	1231
590A	Veined quartz-monzonitic gneiss	21.6	37.7	22.5	12.4	—	5.1	+	0.7	25	703

590B	Foliated quartz monzonite	26.7	30.1	33.8	3.1	—	5.5	—	0.8	25	705
593A	Veined quartz-monzonitic gneiss	32.8	19.0	35.0	12.6	—	+	+	0.6	68	1904
264	Granodioritic Gneiss	40.2	10.7	27.0	—	—	+	20.9	1.1	22	626
701	Quartz-monzonitic gneiss	21.5	38.8	33.2	0.6	—	5.7	+	0.3	15	615
454	Quartz-monzonitic gneiss	28.4	17.2	36.2	10.9	—	6.3	+	1.0	30	838
595A	Granitic gneiss	16.3	49.4	30.4	3.6	—	—	—	0.2	24	894
642	Granodioritic gneiss	31.9	17.1	31.0	19.1	—	—	+	0.8	27	765
528B*	Amphibolite	20.7	—	0.7	14.1	60.0	—	+	4.7	8	1817
10*	Quartz-dioritic gneiss	45.9	3.7	20.5	13.0	15.8	—	—	1.2	7	752
208A*	Quartz-dioritic gneiss	38.7	—	28.5	4.5	28.2	—	—	0.1	8	850
3B*	Amphibolite	24.6	—	12.0	13.3	39.4	—	—	11.9	7	707
103A*	Quartz-dioritic gneiss	27.0	1.9	24.9	5.8	—	—	28.8	11.6	4.5	482
103B*	Quartz-dioritic gneiss	49.6	+	28.8	18.1	1.3	—	+	2.2	6	629
104*	Quartz-dioritic gneiss	37.6	+	31.7	29.5	—	—	—	1.2	9	907
192A*	Quartz-dioritic gneiss	52.0	—	26.3	—	—	+	19.0	2.8	6	657
674C	Quartz-monzonitic gneiss	23.3	21.2	36.3	9.0	9.0	—	—	1.2	13	490
682	Granitic gneiss	14.6	35.5	47.1	0.7	—	—	—	2.2	20	733
266	Banded quartz-monzonitic gneiss	40.2	19.3	31.4	7.9	—	—	0.5	0.6	102	3076
266A	Quartz-monzonitic gneiss	35.1	27.8	30.8	5.7	—	—	+	0.7	31	878
266B	Quartz-monzonitic gneiss	28.2	30.3	33.7	7.3	—	—	+	0.5	26	730
266C	Quartz-monzonitic gneiss	32.4	37.9	25.6	3.8	—	—	+	0.3	18	680

* Analyzed in thin section.

Table XI.

Modal Analyses of Fine-grained Quartz Monzonites.

Specimen Number	Plagioclase	Microcline	Quartz	Biotite	Chlorite	Accessories	Area cm ²	Counts	I C Number
	%	%	%	%	%	%			
514E	30.8	40.1	22.8	4.9	—	1.4	26	966	62
G326*	28.3	33.8	33.8	2.4	1.5	0.3	25	710	29
399A*	40.1	27.4	27.6	4.3	—	0.6	24	678	29
443A*	31.8	33.0	28.0	6.4	+	0.8	29	832	28
393*	35.6	30.0	25.5	8.1	—	0.9	21	793	54
315	31.0	34.4	31.7	2.4	+	0.5	21	777	41
399B*	32.9	35.7	23.2	6.7	—	1.5	18	686	35
380A	38.3	29.5	21.8	9.3	—	1.1	28	1000	55
506*	33.7	34.5	26.6	4.7	+	0.5	23	849	29
383*	29.8	37.8	27.7	3.7	+	1.0	15	573	33
379*	38.7	29.7	23.7	7.1	—	0.8	25	903	28
262*†	32.3	35.7	26.1	5.3	—	0.5	20	750	37
479*	29.9	37.3	28.7	3.7	+	0.4	19	708	46
524A	31.4	34.4	26.3	5.6	+	2.2	31	1080	32
395	28.6	36.4	29.9	4.8	—	0.3	19	692	32
486*	30.7	38.0	26.7	3.4	+	1.1	20	737	38
595C†	29.7	33.4	32.4	4.0	+	0.5	14	560	35
377†	31.2	34.2	25.6	8.1	+	0.9	18	695	40
105B†	33.8	35.6	26.3	4.0	—	0.3	24	669	35
149†	30.1	34.3	29.4	6.0	+	0.2	29	814	34
509A††	43.9	39.0	17.0	—	—	—	14	539	36

* Foliated

† Dike or sill

†† Aplite Dike

Table XII.

Modal Analyses of Porphyric Quartz Monzonites.

Specimen Number	Plagioclase	Microcline	Quartz	Biotite	Chlorite	Accessories	Area counted cm ²	I C Number
	%	%	%	%	%	%		
174	36.0	29.8	28.5	5.1	+	0.6	63	26
200A	26.0	40.7	28.1	+	4.6	0.4	56	23
183A	35.6	30.4	24.3	+	9.4	0.3	44	28
93D	43.6	29.7	21.7	2.4	2.2	0.4	44	22
321*	36.4	27.6	29.3	6.0	+	0.6	47	27
51*	30.8	35.0	29.0	4.6	—	0.6	67	24
85	27.7	35.9	32.3	0.5	3.4	0.2	46	26
373A*	34.0	27.9	32.4	4.6	+	1.1	36	28
357	28.2	36.6	28.5	5.9	+	0.8	48	30
509C	31.2	32.2	27.2	8.3	—	1.0	46	21
413A*	31.5	33.4	29.6	5.0	+	0.5	63	19
248	28.7	35.3	28.3	6.4	—	1.3	31	18
492*	33.1	31.0	29.8	5.4	+	0.6	25	28
312*	39.3	32.6	22.1	4.2	1.2	0.6	49	21
369	33.8	27.9	23.9	5.6	—	0.6	39	29
156	34.5	30.5	27.9	6.7	—	0.5	56	22
9†*	39.5	25.9	24.6	9.2	—	0.8	41	24
456C†*	34.0	35.5	25.5	4.3	—	0.6	75	17
4A†*	32.0	32.3	26.4	8.4	—	0.8	43	27

* Foliated

† Dike or sill

Table XIII.

Modal Analyses of Inclusions in Granite.

Specimen Number	Plagioclase	Microcline	Quartz	Biotite	Chlorite	Hornblende	Accessories	Area cm ²	Counts
248	37.8	17.0	33.2	10.7	—	—	1.3	14	394
482D	37.9	30.8	23.4	7.3	+	—	0.7	50	1807
240B	30.2	31.2	32.0	6.3	+	—	0.3	26	953
95	40.1	20.2	32.1	7.2	—	—	0.3	32	1151
359	40.6	17.0	14.8	17.0	—	5.7	4.8	18	660
175A	37.3	23.9	30.6	6.4	+	—	1.8	23	840
542A	54.6	14.9	15.6	14.4	—	—	0.5	25	912
153	57.6	—	27.6	14.7	—	—	0.3	21	776
256A	40.7	15.3	16.8	24.4	+	—	2.7	15	619
256B	36.2	22.0	21.5	15.7	+	—	4.5	18	687

Table XIV.

Partial Chemical Analyses of Granitic Rocks.

Specimen No.	% Na ₂ O	% K ₂ O	% CaO
542A	4.49	3.20	3.24
492	3.26	5.00	1.30
262	2.93	5.58	1.66
377	3.00	5.25	1.61
315	3.38	5.17	0.93
393	3.35	4.93	2.28
59A	3.18	5.43	2.36
380B	3.06	5.52	1.01

Analyst: K. Haugen, Norges geologiske undersøkelse.

Sp 542 A. Transformed biotite gneiss. 2 km W of Øvstevann.
(23.9, 1-02.0).

Sp 492. Porphyric quartz monzonite. Fløytesæter (42.8, 1-14.3).

Sp 262. Fine-grained quartz monzonite. Faasteinodden (32.7, 0-40.4).

Sp 377. Fine-grained quartz monzonite. Nedre Kolsjøen
(20.4, 0-49.0).

Sp 315. Fine-grained quartz monzonite. Gullknappen (21.4, 0-43.5).

Sp 393. Fine-grained quartz monzonite. Sørbølnatten (27.3, 1-04.8).

Sp 59 A. Porphyric quartz monzonite. Killingstrømmen
(21.3, 0-38.1).

Sp 380 B. Porphyric quartz monzonite. Ørneflag (29.1, 1-01.5).

Gravity Procedure.

Station Net.

A pre-existing station net, which was established by the Geographical Survey of Norway (Norges geografiske oppmåling) follows the main valleys and consists of 173 stations. Since the granite largely occupies the upland region between the valleys, a number of profiles that cross the upland area and tie into the valley net was required.

To a large extent, private logging roads covered most parts of the area so that stations were located along these roads whenever possible. Some important areas, however, were accessible only on foot. The gravity meter was carried on 10 traverses in order to obtain the necessary coverage over parts of the granite and its contacts.

The writer occupied 332 gravity stations. Stations G 150 to G 165 which are located in Slidre do not appear on the gravity map, but they are included in the station data so that they will be available. The station data appear in Table XV in the Appendix.

Elevations.

Elevations were determined from barometric readings and from spot elevations given on topographic maps (quadrangle map, 1 : 100,000). Although some elevations were determined solely from barometric readings, the map elevations constitute a most important basis for the elevations. Many of the traverses, particularly the ones on foot, were necessarily of such long duration that relatively stable barometric conditions could not be expected.

The original field data used to construct the topographic maps were made available for which the writer is indebted to Mr. G. Hagene of the Geographical Survey of Norway. The spot elevations employed from these maps were those given on lakes, farms, mountain tops, and triangulation points. The average error of these points should not exceed ± 3.5 m; however, larger errors may exceptionally be encountered for some of the uncontrolled points (G. Hagene, written communication).

Another important source of elevation control is provided by the levelling of the Watershed Commission (Vassdragsvesenet). They

have carried out continuous levelling along the major valleys that parallel the granites and along the Vassfaret and Höljera watershed that cut across the middle of the Hedal granite. The elevations along the watersheds were used for gravity stations and for check points with the barometers.

The stations of the Geographical Survey are located on precision-levelled bench marks along traverses that follow the major valleys. These bench marks were a major source of control for the barometric determinations.

Elevation differences up to 5 m were observed between barometric elevations and levelled elevations on the same point; therefore, barometric elevations errors up to 5 m should be expected. Some elevations are better than this, and as is always the case with barometric elevations, larger errors can enter in without being detected.

Terrain Corrections.

In the Flå area, the terrain correction constitutes the largest single source of error. The usual relief along the valleys that dissect the area is from 200 to 300 m, but in Hallingdal the relief is as great as 800 to 900 m. Terrain corrections were computed by means of the chart of Hammer (1939) and the 2-dimensional profiles of Hubbert (1948 b). The 2-dimensional method was used where it most closely approximated the terrain and where the correction was least critical. Terrain corrections were applied to all of the stations.

Terrain corrections of from 3 to 5 mgal were applied to many stations in the Flå area. The corrections in Hallingdal attain values as great as 15 mgal.

Obviously, anomalies of 4 to 5 mgal lose much of their significance if the terrain corrections are very large. Fortunately the terrain also offers the opportunity to locate stations where the terrain effect is practically zero. The terrain on the upland erosion surface varies from rolling to almost flat. By locating stations on this upland surface, terrain effects are greatly diminished, even near the rims of valleys, and the corrections that were applied to stations in the adjacent valleys are controlled.

Terrain corrections should normally not be in error by more than 1 mgal. The corrections in Hallingdal at a distance from the granite, however, may be in error by several mgal.

Observed Gravity.

Base stations were established throughout the area in order to check the drift of the gravity meter. Normally, the gravity meter was returned to a base station at least twice daily; however, this was impossible for five of the traverses during which the gravity meter was carried on foot. A drift of up to 1 mgal could be distributed among the stations on these traverses.

A Worden standard model gravity meter (No. 178) was used for the gravity measurements. The instrument has a dial constant of 0.0902 mgal.

Bouguer Correction.

The Bouguer correction accounts for the attraction of the material between sea level, which is the common datum for the reductions, and the station elevation. The density chosen for this material should approximate the true mean density of the rocks found between sea level and the gravity station as closely as possible. Since many of the station elevations are situated between 1000 and 1200 m, an error of 0.05 gm/cm³ in the Bouguer density could introduce an error in the Bouguer anomalies of slightly over 2 mgal. Densities of 2.65 gm/cm³ for the granite, 2.74 gm/cm³ for the eastern gneiss and 2.78 gm/cm³ for the western and southern gneiss are used for the Bouguer correction.

Accuracy.

A 5-m error in the elevation will cause an error of 1 mgal in the Bouguer anomaly. In addition, errors up to 1 mgal can be expected in the larger terrain corrections. These errors will be additive in some cases; therefore, errors up to 2 mgal can be expected in the Bouguer anomalies.

The application of an incorrect Bouguer density could introduce errors that vary linearly with elevation. These errors would be uniform over a given area and would probably not exceed 1 mgal at the higher elevations in the gneiss.

That the error probably does not commonly attain such great values is shown by the values of the stations plotted on the map. Most of the stations in a given area show approximately the same gravity values and trends.

The terrain correction for the stations in Hallingdal is so huge that errors greater than 2 mgal may occur even though the error introduced by the elevation is negligible. The useful Bouguer anomalies along Hallingdal are found at the stations located up over the valley rim.

Table XV.
Gravity Station Data.

Sta No.	Lat. N	Long. W. of Oslo	Elev. mtr	Obs. Grav. mgal.	Free Air & Boug. Corr. mgal.	Boug. Grav. Anom. mgal.
G 1	60 34.3	0 44.3	160.14	981 878.7	+ 31.8	—57.9
2	33.5	46.4	155	875.6	32.1	—59.7
3	33.3	49.1	201	861.8	43.0	—62.3
4	33.4	51.0	240	851.2	50.5	—65.6
5	32.7	53.4	301	837.2	62.0	—68.2
6	32.8	54.2	330	830.3	68.8	—67.4
7	32.9	55.8	398	814.6	83.1	—68.9
8	33.1	57.5	370	816.8	77.5	—72.6
9	33.5	0 59.1	343	820.4	71.8	—75.2
10	32.2	1 01.9	536	781.5	108.8	—75.4
11	32.3	03.7	540	776.4	111.2	—78.2
12	32.3	07.0	544	772.2	113.0	—80.6
13	32.1	09.1	544	770.3	112.0	—82.3
14	32.0	11.2	544	769.5	113.0	—83.0
15	31.7	13.0	564	766.6	117.0	—81.5
16	31.7	14.2	575	765.0	119.2	—80.9
17	38.8	57.3	197.41	852.8	45.5	—75.9
18	38.6	57.7	351	823.3	74.6	—76.1
19	38.3	59.0	552	786.0	113.9	—73.7
20	37.5	59.4	554	784.7	111.4	—76.5
21	37.3	01.6	512	790.5	102.9	—78.9
22	38.2	03.8	665	760.4	132.5	—80.6
23	37.9	06.3	678	754.0	136.5	—82.6
24	38.1	08.9	677	751.8	136.1	—85.4
25	38.4	10.7	758	735.6	151.5	—86.6
26	38.6	13.2	866	714.8	172.0	—87.2
27	38.8	14.6	958	696.6	189.4	—88.2
28	39.2	16.3	938	700.8	186.2	—87.8
29	38.8	19.9	836	719.4	164.5	—90.3
30	39.1	18.7	864	714.2	171.6	—88.8
31	38.8	21.1	838	719.4	164.5	—90.3
32	39.2	23.4	847	717.1	166.1	—91.6
33	38.9	25.2	839	719.2	164.7	—90.5
34	38.8	27.3	847	718.6	164.7	—90.9
35	38.0	29.4	847	718.9	164.5	—89.8

Sta No.	Lat. N. ° ' "	Long. W. of Oslo ° ' "	Elev. mtr	Obs. Grav. mgal.	Free Air & Boug. Corr. mgal	Boug. Grav. Anom. mgal
G 36	60 37.3	1 30.6	813	981 725.7	+158.2	—88.4
37	36.8	32.6	682	752.1	133.9	—85.6
38	36.8	33.2	556	775.8	109.8	—86.0
39	34.6	33.9	513	784.0	101.6	—83.2
40	34.2	1 34.8	328	814.6	70.1	—83.6
41	15.3	0 46.9	179	877.6	35.7	—30.5
42	15.9	46.5	170	878.0	34.7	—31.9
43	17.2	47.4	193	872.8	39.7	—33.8
44	17.8	48.7	211	865.2	43.2	—38.7
45	18.6	49.2	213	862.8	43.6	—41.6
46	20.5	52.9	255	848.8	52.7	—49.1
47	22.1	53.1	252	846.1	53.7	—52.8
48	22.9	54.2	292	835.4	60.6	—57.7
49	19.8	51.8	219	856.6	44.1	—49.0
50	20.7	50.6	331	838.1	66.0	—46.7
51	19.1	51.4	216	858.4	43.6	—46.8
52	19.6	50.0	279	849.0	55.6	—44.8
53	19.2	48.1	324	844.6	63.9	—40.4
54	19.6	46.5	392	833.0	76.2	—40.2
55	19.8	48.5	396	830.5	77.0	—42.2
56	20.1	47.8	421	825.5	81.3	—43.3
57	20.9	48.5	482	813.4	93.5	—44.2
58	14.7	49.9	145	878.8	28.3	—35.9
59	15.7	52.2	208	863.4	42.8	—38.1
60	16.1	54.9	238.7	852.4	46.9	—45.6
61	16.9	56.6	212	850.4	41.3	—53.2
62	19.3	59.3	339	817.4	68.0	—63.6
63	18.2	57.9	278	833.8	55.0	—59.2
64	16.8	51.3	441	818.1	88.8	—38.9
65	17.6	51.9	405	823.0	81.2	—42.6
66	18.3	53.3	453	809.5	91.6	—46.6
67	12.4	59.1	324	830.4	63.5	—46.2
68	13.5	1 00.7	354	823.2	71.8	—46.5
69	11.5	0 58.8	274	840.0	53.3	—45.6
70	16.3	45.3	187	875.4	38.7	—31.0
71	16.6	43.7	252	864.8	50.9	—29.8
72	16.8	40.7	249	868.2	51.1	—26.5
73	17.5	42.1	277	861.9	54.7	—30.1
74	18.0	43.0	300	856.6	58.9	—31.8
75	18.8	43.3	352	845.9	70.5	—32.0

Sta No.	Lat. N.	Long. W. of Oslo	Elev. mtr	Obs. Grav. mgal	Free Air & Boug. Corr. mgal	Boug. Grav. Anom. mgal
G 76	60 19.7	0 44.0	509	981 811.2	+101.1	—37.3
77	13.4	41.0	138	898.3	27.7	—15.4
78	14.3	41.2	198	880.3	38.7	—23.5
79	15.6	42.0	306	858.6	59.5	—26.0
80	16.8	39.2	294	861.7	56.9	—26.2
81	16.5	37.7	318	859.5	61.3	—24.6
82	15.9	37.0	303	862.5	58.4	—23.7
83	16.9	36.5	275	869.7	52.3	—23.9
84	16.3	34.4	160	892.4	31.0	—21.7
85	18.7	33.0	181	884.7	36.3	—27.2
86	19.0	32.2	184	885.2	37.6	—25.8
87	19.6	31.7	187	884.5	37.6	—27.3
88	20.6	31.8	205	880.0	42.2	—28.5
89	21.9	34.7	423	835.9	85.0	—31.5
90	21.4	33.7	390	843.0	78.6	—30.1
91	23.6	39.0	150	882.4	31.5	—40.7
92	23.8	37.2	403	837.8	78.9	—38.1
93	24.2	35.3	373	845.9	73.1	—36.4
94	24.8	34.4	319	857.2	62.4	—36.6
95	25.9	37.4	150	885.3	31.6	—40.7
96	24.8	38.0	150	883.8	31.6	—40.8
97	22.4	38.3	150	882.4	35.2	—34.4
98	20.5	36.7	140	889.2	31.7	—29.7
99	27.1	40.9	160	883.0	33.5	—42.6
100	26.7	39.9	150	885.5	32.5	—40.6
101	27.7	41.8	209	870.5	43.7	—45.7
102	25.1	39.7	179	880.2	37.1	—39.2
103	23.8	40.0	186	875.7	41.5	—37.6
104	23.3	40.1	173	877.0	40.0	—37.2
105	22.2	39.4	162	880.3	37.0	—35.5
106	21.2	37.9	150	886.2	33.6	—31.7
107	20.4	37.8	164	882.9	36.4	—31.1
108	19.7	37.5	164	885.0	35.7	—28.9
109	19.2	36.1	166	886.1	34.6	—28.2
110	18.8	34.8	157	893.3	32.2	—22.9
111	19.3	37.9	278	863.8	55.5	—29.7
112	19.5	40.5	474	822.2	92.0	—35.1
113	19.6	42.2	556	803.8	108.9	—36.7
114	18.6	38.0	373	849.7	72.5	—25.9
115	16.2	20.6	134	908.3	27.8	— 8.0

Sta No.	Lat. N °	Long. W. of Oslo °	Elev. mtr	Obs. Grav. mgal	Free Air & Boug. Corr. mgal.	Boug. Grav. Anom. mgal.
G 116	60 18.4	0 22.1	149	981 904.4	+ 32.1	—11.4
117	19.9	22.4	134	907.6	30.6	—11.6
118	19.9	24.8	394	855.7	77.5	—16.6
119	19.9	26.0	389	854.3	76.0	—19.5
120	22.0	21.4	133	911.8	29.0	—11.7
121	26.8	19.6	133	916.2	28.8	—13.7
122	29.8	20.2	133	913.8	28.5	—20.3
123	31.0	25.2	133	909.2	27.9	—27.1
124	30.5	28.8	202	891.8	40.5	—31.2
125	31.1	31.0	202	888.2	40.4	—35.7
126	31.9	33.0	223	882.2	45.3	—37.8
127	32.4	35.5	232	876.5	46.6	—42.9
128	31.3	36.0	232	876.5	45.6	—42.5
129	31.7	37.7	150	888.0	30.8	—46.3
130	32.6	54.4	337	827.1	70.2	—68.9
131	34.0	54.9	508	794.3	102.6	—71.1
132	35.3	55.2	568	785.4	113.9	—70.4
133	36.5	55.8	669	765.7	133.5	—72.1
134	34.6	58.6	450	801.2	91.4	—76.2
135	35.9	58.4	478	798.0	96.9	—75.6
136	40.1	49.8	319	844.0	64.3	—67.5
137	42.2	42.4	643	792.8	124.8	—61.0
138	43.1	40.6	668	790.8	129.8	—59.2
139	43.9	37.6	552	818.3	107.4	—55.1
140	44.5	34.8	595	813.2	115.7	—52.6
141	44.6	32.2	500	835.9	97.9	—47.9
142	44.3	30.7	452	846.4	90.3	—44.6
143	52.3	1 04.9	482	820.0	96.7	—74.9
144	53.2	04.5	331	848.6	68.5	—75.6
145	53.9	04.8	334	848.9	70.2	—74.5
146	54.9	04.8	371	842.5	78.2	—74.2
147	56.2	05.3	383	844.7	80.1	—71.8
148	58.1	05.8	433	835.0	88.7	—75.3
149	59.0	08.6	468	839.8	95.1	—65.3
150	61 00.4	10.3	553	828.1	109.5	—64.4
151	01.5	13.0	656	815.3	130.3	—57.8
152	02.2	14.9	699	814.2	137.2	—52.9
153	03.3	20.1	699	826.6	136.0	—43.1
154	02.0	21.6	869	796.0	167.4	—40.6
155	00.9	23.3	831	798.8	160.1	—43.7

Sta No.	Lat. N ° ' "	Long. W. of Oslo ° ' "	Elev. mtr	Obs. Grav. mgal	Free Air & Boug. Corr. mgal.	Boug. Grav. Anom. mgal.
G 156	60 59.5	1 25.8	712	981 814.7	+139.4	-46.7
157	59.6	27.9	614	833.3	121.3	-45.7
158	61 01.7	30.4	602	855.4	120.8	-28.0
159	04.1	31.8	725	841.7	145.8	-19.2
160	04.7	28.8	849	810.7	165.4	-31.3
161	05.2	26.2	924	793.0	179.0	-36.1
162	06.1	24.0	918	788.0	177.2	-44.0
163	07.3	21.4	975	772.3	187.9	-50.6
164	07.9	19.4	964	769.7	186.0	-55.9
165	08.6	18.9	971	762.7	188.3	-61.4
166	60 49.8	13.6	526	818.1	106.5	-63.8
167	49.5	15.8	679	791.3	135.4	-81.3
168	50.3	18.3	773	775.1	150.1	-63.8
169	49.2	20.9	792	765.3	154.3	-68.0
170	48.4	1 24.1	1007	719.2	193.9	-73.5
171	40.3	0 59.0	197	856.0	43.7	-76.5
172	40.7	1 00.2	328	832.3	69.8	-75.5
173	41.1	0 02.0	446	808.8	91.2	-77.2
174	41.3	04.1	512	791.3	104.1	-82.1
175	41.4	05.9	604	775.7	121.0	-80.9
176	46.2	05.9	379	826.2	78.1	-79.4
177	45.3	05.0	507	803.4	102.4	-76.8
178	44.6	07.5	691	766.4	135.7	-79.6
179	44.5	09.2	681	766.1	133.7	-81.8
180	44.0	11.1	710	757.9	140.8	-82.2
181	42.9	14.3	776	740.5	153.6	-85.4
182	42.0	14.5	868	720.1	172.1	-86.2
183	42.5	16.0	780	736.8	154.4	-87.8
184	41.9	18.5	784	734.0	155.2	-89.0
185	41.4	19.8	803	727.9	158.9	-90.8
186	41.1	20.9	795	729.0	157.4	-90.8
187	40.7	22.1	817	724.2	161.8	-90.7
188	40.4	23.3	846	719.0	166.1	-91.2
189	39.9	24.0	838	719.8	164.8	-91.0
190	43.1	17.8	827	727.8	163.5	-88.5
191	44.3	17.2	877	721.2	173.4	-86.7
192	45.0	16.4	827	734.6	163.6	-84.0
193	46.8	13.3	829	743.9	161.4	-79.2
194	48.2	10.7	574	793.0	115.3	-78.0
195	47.4	12.0	699	771.6	136.8	-77.1

Sta No.	Lat. N	Long. W. of Oslo	Elev. mtr	Obs. Grav. mgal	Free Air & Boug. Corr. mgal.	Boug. Grav. Anom. mgal.
G 196	60 45.8	1 10.4	842	981 738.6	+163.6	—81.0
197	45.9	15.2	823	741.7	159.9	—81.8
198	45.6	16.5	792	744.3	155.4	—83.3
199	44.3	19.7	926	710.8	181.5	—89.0
200	44.1	20.5	925	709.8	181.8	—89.4
201	43.5	22.2	962	700.0	189.0	—91.3
202	43.0	24.6	1003	690.4	197.4	—91.8
203	42.9	26.0	917	708.6	180.2	—90.7
204	41.8	26.7	917	707.2	180.9	—90.0
205	43.8	27.5	1003	694.3	195.5	—90.9
206	43.7	31.2	900	719.3	177.3	—83.9
207	43.2	33.5	856	727.5	166.7	—85.7
208	42.9	35.0	852	727.4	165.7	—86.4
209	42.6	36.8	762	742.9	149.0	—87.2
210	42.4	38.1	570	779.3	112.5	—87.1
211	42.0	40.8	444	801.7	90.6	—86.1
212	33.4	38.4	263	818.7	65.1	—83.5
213	33.7	41.7	360	804.4	75.7	—87.5
214	33.3	44.0	477	777.5	96.3	—93.3
215	32.4	46.7	591	753.0	117.1	—95.9
216	31.1	48.6	727	730.0	141.5	—92.8
217	29.9	50.4	818	712.5	158.5	—91.8
218	29.2	54.1	838	709.0	161.6	—91.2
219	26.9	56.4	727	723.2	140.8	—94.9
220	32.6	31.3	451	789.6	93.3	—83.3
221	33.5	30.0	771	733.4	153.0	—81.0
222	33.0	28.3	887	713.7	170.8	—82.3
223	33.5	26.4	975	696.4	189.6	—81.4
224	33.6	25.1	998	687.4	194.3	—85.8
225	33.9	24.2	983	692.4	191.0	—84.5
226	34.5	23.7	971	692.7	189.3	—86.7
227	34.7	22.4	993	685.7	192.7	—90.5
228	24.6	19.6	348	805.5	72.2	—78.2
229	27.4	15.8	454	787.0	92.0	—80.5
230	28.4	15.9	595	761.9	117.4	—81.5
231	29.1	16.7	620	756.4	121.2	—84.1
232	29.5	18.4	734	735.5	142.4	—84.3
233	30.0	14.6	803	722.0	156.5	—84.4
234	29.7	15.5	742	733.5	146.0	—82.0
235	27.4	30.8	530	776.6	105.1	—77.8

Sta No.	Lat. N. ° ' "	Long. W. of Oslo ° ' "	Elev. mtr	Obs. Grav. mgal	Free Air & Boug. Corr. mgal	Boug. Grav. Anom. mgal
G 236	60 26.9	1 32.4	695	981 743.6	+135.6	-79.7
237	26.1	33.7	839	717.1	162.2	-78.5
238	26.8	35.8	906	704.1	175.0	-79.6
239	26.5	36.9	931	696.6	180.1	-81.7
240	26.6	31.1	635	755.4	123.8	-79.3
241	25.4	31.4	715	738.9	138.7	-79.3
242	24.3	32.2	838	715.2	162.1	-78.2
243	23.4	31.6	884	704.4	171.1	-78.8
244	21.8	31.9	862	706.1	167.8	-78.4
245	22.4	09.2	157	842.2	35.8	-75.0
246	22.1	09.5	268	821.1	56.4	-75.1
247	21.2	11.1	563	767.8	111.3	-73.4
248	23.7	06.2	396	800.3	81.5	-72.9
249	24.7	06.1	532	775.6	107.8	-72.6
250	25.7	06.2	631	757.3	127.8	-72.2
251	26.6	06.9	694	743.6	141.4	-73.5
252	27.1	07.5	684	742.3	140.7	-76.1
253	22.9	04.7	273	826.4	55.6	-71.7
254	23.4	04.0	381	808.8	76.0	-69.5
255	23.9	02.6	441	798.0	87.4	-69.6
256	24.4	1 01.2	420	800.1	85.2	-70.3
257	24.4	0 59.9	427	801.8	87.4	-66.4
258	24.2	56.3	375	815.9	77.0	-62.5
259	23.2	55.4	292	831.4	61.0	-61.7
260	24.3	57.9	375	813.4	77.0	-65.1
261	25.2	56.3	475	795.1	99.1	-62.5
262	24.9	53.7	547	786.0	110.2	-60.1
263	26.5	53.1	571	781.8	117.3	-59.3
264	27.8	53.4	585	776.4	124.1	-59.5
265	28.8	53.5	573	778.3	122.6	-60.4
266	30.1	54.1	536	785.8	112.5	-64.7
267	31.2	54.4	360	819.8	75.7	-68.9
268	38.9	1 05.5	668	758.2	132.4	-83.8
269	39.6	05.8	694	755.1	137.6	-82.6
270	39.7	07.4	801	733.6	158.7	-83.1
271	40.4	09.3	894	715.4	176.7	-84.2
272	40.3	11.9	820	727.3	162.9	-86.0
273	39.8	13.0	921	706.7	182.4	-86.4
274	38.4	11.8	849	718.0	169.1	-86.6
275	37.8	15.0	968	693.7	192.5	-86.7

Sta No.	Lat. N. ° ' "	Long. W. of Oslo ° ' "	Elev. mtr	Obs. Grav. mgal	Free Air & Boug. Corr. mgal	Boug. Grav. Anom. mgal
G 276	60 37.1	0 16.1	820	981 720.7	+163.1	—88.2
277	35.8	16.9	747	732.6	149.5	—88.3
278	37.4	11.2	841	720.5	166.6	—85.3
279	36.3	10.4	939	700.5	186.0	—84.5
280	34.9	11.9	1011	684.6	200.4	—84.2
281	33.6	13.4	994	687.0	198.4	—82.1
282	33.9	09.9	1007	683.4	200.4	—84.1
283	34.4	09.7	1016	682.7	201.6	—84.3
284	35.1	09.9	1012	683.8	200.6	—85.1
285	30.7	0 46.8	531	802.1	104.3	—57.4
286	31.7	47.4	493	808.1	98.2	—58.8
287	32.4	46.7	344	837.8	69.9	—58.3
288	17.9	42.8	298	856.1	58.5	—32.6
289	19.8	43.1	532	806.6	106.2	—36.9
290	22.0	43.8	944	720.2	190.6	—41.7
291	22.5	43.0	1010	705.7	204.9	—42.6
292	22.9	43.3	1005	707.5	204.0	—42.2
293	23.3	43.8	921	726.0	185.8	—42.4
294	23.8	44.4	877	734.0	177.3	—43.5
295	23.5	47.3	953	714.8	192.9	—46.6
296	23.2	46.5	855	735.6	172.9	—45.6
297	22.6	46.0	760	756.6	152.9	—43.8
298	22.1	46.2	682	773.6	136.1	—42.9
299	21.0	45.2	703	770.5	140.3	—40.4
300	20.2	44.7	772	753.5	157.3	—39.4
301	29.2	42.7	286	855.0	59.6	—47.2
302	29.5	44.8	508	811.7	99.7	—50.8
303	26.9	45.7	674	777.9	132.4	—48.6
304	27.8	47.1	966	714.8	193.4	—51.8
307	26.2	47.7	773	758.1	150.2	—49.7
308	25.4	48.1	816	745.0	160.1	—51.8
309	25.1	47.7	732	761.8	142.7	—52.0
310	24.5	46.2	776	757.0	151.0	—47.8
311	25.2	46.2	774	757.8	150.4	—48.5
312	25.1	45.0	737	767.3	143.4	—45.8
313	24.8	43.3	680	780.8	133.3	—42.1
314	26.2	45.3	666	784.6	129.5	—43.9
315	26.5	44.8	620	791.4	120.7	—46.3
316	25.8	41.9	414	834.5	82.7	—40.2
317	31.5	1 00.7	563	773.2	114.9	—76.7

Sta No.	Lat. N. ° /	Long. W. of Oslo ° /	Elev. mtr	Obs. Grav. mgal	Free Air & Boug. Corr. mgal	Boug. Grav. Anom. mgal
G 318	60 31.0	1 00.7	628	981 760.4	+127.8	-76.0
319	30.4	00.7	681	749.3	138.9	-75.2
320	29.8	1 00.3	891	709.7	180.5	-72.4
321	28.6	0 59.6	1116	665.7	222.1	-73.3
322	27.5	0 58.3	991	690.9	196.8	-71.9
323	29.2	1 03.2	1084	670.3	215.9	-75.6
324	29.2	05.4	1172	649.7	232.3	-79.8
325	28.6	06.3	1220	639.6	242.1	-79.4
326	28.4	1 07.0	1285	623.1	258.3	-79.4
395	13.1	0 29.5	157.0	901.3	30.7	-9.0
396	13.8	28.5	198	893.9	38.3	-9.7
397	14.7	28.1	214	890.2	42.2	-10.6
398	15.6	27.5	249	879.6	49.1	-15.5
399	16.7	26.7	338	861.1	65.6	-18.9
400	17.5	26.2	340	860.7	65.6	-20.4
401	18.2	26.5	340	860.3	65.6	-21.6
402	18.6	26.5	341	859.8	65.9	-22.3

Table XVI.

Composition of Feldspars from Gneisses.

Sp.No.	Rock Type	Alkali Feldspar Parts Plagioclase	Plagioclase Parts Ab	k
647A	Quartz-monzonitic gneiss	18	65	0.28
105C	Quartz-dioritic gneiss	15	64	0.23
102A	Augen gneiss	12	65	0.18
420B	Augen gneiss	14	64	0.22
224A	Augen gneiss	10	60	0.17
292A	Augen gneiss	22	58	0.38
595A	Augen gneiss	14	67	0.21
45	Augen gneiss	11	64	0.17
488C	Augen gneiss	8	67	0.12
665	Augen gneiss	15	67	0.22
Ho	Augen gneiss	10	65	0.15
Sö55	Augen gneiss	14	60	0.23
675	Augen gneiss	8	61	0.13
466A	Migmatite	13	60	0.22
499B	Migmatite	15	61	0.25
642	Granodioritic gneiss	11	68	0.16
590A	Veined quartz-monzonitic gneiss	13	68	0.19
639C	Veined granodioritic gneiss	13	77	0.17
266	Banded quartz- monzonitic gneiss	16.5	68	0.24
661	Granodioritic gneiss	22	63	0.35
145E	Quartz-plagioclase gneiss	19	76	0.25
612A	Meta-conglomerate	17	93	0.18
264	Granodioritic gneiss	15	67	0.22

Table XVII.

Composition of Feldspars from Fine-Grained Granite.

Sp. No.	Alkali Feldspar Parts Plagioclase	Plagioclase Parts Ab	k
227	10	70	0.14
379	14.5	69	0.21
77	13	70	0.18
177B	12	80	0.15
61	11	70	0.16
180B	12	67	0.18
524B	13	72	0.18
292B	12	63	0.19
80	14	75	0.18
262	14	61	0.23
377	21	63	0.33
393	9	65	0.29
399B	11	75	0.15
443A	10	74	0.14
486	15	72	0.20
149	15	75	0.19
315	15	80	0.18

Table XVIII.

Composition of Feldspars from Porphyric Granite.

Sp. No.	Alkali Feldspar Parts Plagioclase	Plagioclase Parts Ab	k
59	19	65	0.29
26	16	78	0.21
229A	18	76	0.24
312	16	73	0.22
271A	16	80	0.20
514A	11	72	0.15
248	14	70	0.20
456C	12	66	0.18
357	13	72	0.18
163	12	70	0.17
200A	12	84	0.14
297B	14	65	0.22
413A	12	72	0.17
12	15	86	0.17
373A	11	77	0.14
157	21	70	0.30
36	12	63	0.19
51	15	65	0.23
239	18	72	0.25
258	15	62	0.24
509C	14	63	0.22
4A	17	66	0.26
55A	13	75	0.17
108	11	67	0.16
85	18	84	0.21
93B	16	74	0.22

Table XIX.

Compositions of Feldspars from Pegmatites.

Sp. No.	Alkali Feldspar Parts Plagioclase	Plagioclase Parts Ab	k
414A	20	80	0.25
88C	15	76	0.20
524B	19	78	0.24
259	18	88	0.20
229E	20	86	0.23
425B	20	80	0.25
211B	21	92	0.23
145C	19	98	0.19
488D*	8	84	0.10
373B	19	89	0.21
41	13	80	0.16
219C	19	82	0.23
499A	17	90	0.19
456D	22	77	0.29
434A	24	84	0.29
341	17	86	0.20
105A	15	67	0.22
207D	16	—	—
650	14	—	—
489A	20	—	—
448C	16	—	—

* Gradational with augen gneiss.

Table XX.

Compositions of Feldspars from Inclusions.

Sp. No.	Alkali Feldspar Parts Plagioclase	Plagioclase Parts Ab	k
95	22	75	0.29
95	14.5	75	0.19
95	17	75	0.23
55B	13	80	0.16
177A	16	80	0.20
240B	17	78	0.22
482D	17	72	0.24
542F	16	63	0.25

References.¹

- Akaad, M. K.*, 1956. The Ardara granitic diapir of County Donegal, Ireland. Geol. Loc. London Quart. Jour., V. 112, pp. 263—90.
- Alling, H. L.*, 1932. Perthites: Amer Min., V. 17, p. 43—65.
- Andersen, O.*, 1921. En kort meddelelse om geologiske iakttagelser på kartbladet Flå. Norsk geol. tidsskr., Bd. 6, pp. 227—78.
- 1928. The genesis of some types of feldspar from granite pegmatites. Norsk geol. tidsskr. Bd. 10, pp. 116—207.
- Bailey, E. H. and Stevens, R. E.*, 1960. Selective staining of K-feldspar and plagioclase on rock slabs and thin sections. Amer. Min. V. 45, pp. 1020—25.
- Balk, R.*, 1937. Structural behavior of igneous rocks. Geol. Soc. Amer. Mem. 5, 177 p.
- 1953. Faltenachsen in Überschiebungszonen. Geol. Rund. Bd. 41, pp. 90—103.
- Bambauer, H. and Laves, F.*, 1960. Zum Adularproblem. Schweiz. Min. petr. Mitt. Bd. 40, p. 177—205
- Barth, T. F. W.*, 1955. Presentation of rock analyses. Jour. Geol. V. 63, pp. 348—63.
- 1959. Principles of classification and norm calculations of metamorphic rocks. *Ibid.* V. 67, pp. 135—52.
- 1962. Theoretical petrology. 2nd Edition, New York, Wiley. 416 p.
- Baskin, Y.*, 1956. A study of authigenic feldspars. Jour. Geol. V. 64, pp. 132—55.
- Bayly, M. B.*, 1960. Modal analyses by point counting — The choice of sample area. Jour. Geol. Soc. Australia. V. 6. p. 2.
- Berthelsen, A.*, 1960. Structural studies in the Pre-Cambrian of Western Greenland. Medd. om Grönland. Bd. 123, h. 1, 223 p.
- Bowen, N. L.*, 1928. The evolution of the igneous rocks. New York, Dover. 332 p.
- and *Tuttle, O. F.*, 1950. The system $\text{NaAlSi}_3\text{O}_8$ — KAISi_3O_8 — H_2O . Jour. Geol. V. 58, pp. 485—511.
- Brögger, W. C.*, 1933 a. Essexitrekkenes erupsjoner. Norges geol. undersøk. no. 138, 103 p.
- 1933 b. Om rombeporfyrangene og de dem ledsagende forkastninger i Oslofeltet. *Ibid.* no. 139, 51 p.

¹ References listed in the first publication of this series, Norges geol. undersøk. no. 214 B, are not repeated here.

- Carey, S. W.*, 1953. The Rheid concept in geotectonics. *Jour. Geol. Soc. Australia*. V. 1, pp. 67—118.
- Chaisson, U.*, 1950. The optics of triclinic adularia. *Jour. Geol.* V. 58, pp. 537—47.
- Chayes, F.*, 1952. The finer-grained calcalkaline granites of New England. *Jour. of Geol.* V. 60, pp. 207—54.
- 1956. Petrographic modal analysis. New York, Wiley. 113 p.
- Christie, O. H. J.*, 1962. Discussion; Feldspar structure and the equilibrium between plagioclase and epidote. *Amer. Jour. Sci.* V. 260, pp. 149—53.
- Cloos, E.*, 1946. Lineation. *Geol. Soc. Amer. Mem.* 18, 122 p.
- 1947. Tectonic transport and fabric in a Maryland granite: *Bull. Comm. geol. Finl.* no. 140, pp. 1—13.
- Cloos, H.*, 1925. Einführung in die tektonische Behandlung magmatischer Erscheinungen, pt. 1, Das Riesengebirge. Berlin, Gebr. Borntraeger. 194 p.
- 1928. Zur Terminologie der Plutone. *Fennia*. V. 50, pp. 1—11.
- 1936. Einführung in die Geologie. Berlin, Gebr. Borntraeger. 498 p.
- Compton, R. R.*, 1955. Trondhjemite batholith near Bidwell Bar, California. *Geol. Soc. Amer. Bull.* V. 66, pp. 9—44.
- Crump, R. M. and Ketner, K. B.*, 1953. Feldspar optics: in Emmons, R. C., *Editor*, Selected petrogenic relationships of plagioclase. *Geol. Soc. Amer. Mem.* 52, pp. 23—40.
- Daly, R. A.*, 1933. Igneous rocks and the depths of the earth. New York, McGraw-Hill. 598 p.
- Dietrich, R. V.*, 1954. Fish Creek phacolith, northwestern New York. *Amer. Jour. Sci.* V. 252, pp. 513—31.
- and *Mehnert, K. R.*, 1961. Proposal for the nomenclature of migmatites and associated rocks: in Sørensen, H., *Editor*, Symposium on migmatite nomenclature: Report of twenty-first session. Norden, Int'l Geol. Congr. Pt. 26, pp. 56—78.
- Donnay, G., Wyart, J. and Sabatier, G.*, 1960. The catalytic nature of high-low feldspar transformations. *Ann. Rpt. Dir. Geophys. Lab.* pp. 173—74.
- Drescher-Kaden, F.*, 1948. Die Feldspat-Quartz-Reaktionsgefüge der Granite und Gneise. Berlin, Springer. 259 p.
- Emeleus, C. H. and Smith, J. V.*, 1959. Alkali feldspars: VI, Sanidine and orthoclase perthites from Northern Ireland. *Amer. Min.* V. 44, pp. 1187—1209.
- Emerson, D. D.*, 1960. Structure and composition of potassium feldspar from the Inyo batholith, California — Nevada (abstract). *Program 1960 Ann. Meetings Geol. Soc. Amer.* p. 90.
- Emmons, R. C.*, 1953. The argument: in Emmons, R. C., *Editor*. Selected petrogenic relationship of plagioclase. *Geol. Soc. Amer. Mem.* 52, pp. 111—18.
- Eskola, P.*, 1948. The nature of metasomatism in the process of granitization. *Rpt. of 18th Session, Int'l Geol. Congress.* Pt. III, pp. 5—13.
- 1951. Around Pitkäranta. *Ann. Acad. Scien. Fennicæ. Ser. A.* III. 90 p.
- 1952. On the granulites of Lapland. *Amer. Jour. Sci.*, Bowen Vol. pp. 133—71.

- 1956. Postmagmatic potash metasomatism of granite. *Bull. Comm. geol. Finl.* no. 172, pp. 85—100.
- Francis, G. H.*, 1956. Facies boundaries in pelites at the middle grades of regional metamorphism. *Geol. Mag.* V. 93, pp. 353—68.
- Frasl, G.*, 1954. Anzeichen schmelzflüssigen und hochtemperierten Wachstums an den grossen Kaliefeldspaten einiger Porphyrrgranite, Porphyrrgranitgneise und Augengneise Österreichs. *Jahrb. geol. Bundesanstalt, Wien.* Bd. 97. H. 1, pp. 71—134.
- Fyfe, W. S., Turner, F. J. and Verhoogen, J.*, 1958. Metamorphic reactions and metamorphic facies. *Geol. Soc. Amer. Mem.* 73, 259 p.
- Gates, R. M.*, 1953. Petrogenic significance of perthite: in Emmons, R. C., *Editor*. Selected petrogenic relationships of plagioclase. *Geol. Soc. Amer. Mem.* 52, pp. 55—70.
- Goldich, S. S. and Kinser, J. H.*, 1939. Perthite from Tory Hill, Ontario. *Amer. Min.* V. 24, pp. 407—27.
- Goldschmidt, V. M.*, 1911. Die Kontaktmetamorphose im Kristianiagebiet. *Oslo Vidensk. Skr. I. Mat.-Naturv. Kl. No.* 11, 405 p.
- Goldsmith, J. R.*, 1953. A "simplicity principle" and its relation to "ease" of crystallization. *Jour. Geol.* V. 61, pp. 439—51.
- and *Laves, F.*, 1954 a. The microcline-sanidine stability relations. *Geochim. Cosmochim. Acta.* V. 5, pp. 1—19.
- — 1954 b. Potassium feldspars structurally intermediate between microcline and sanidine. *Ibid.* V. 6, pp. 100—18.
- — 1961. The sodium content of microclines and the microcline-albite series. *Instituto Lucas Mallada, Cursos y Conferencias.* Fasc. 8. Madrid. pp. 81—96.
- Grout, F. J.*, 1932. *Petrography and petrology.* New York. McGraw-Hill.
- Grønhaug, A.*, 1963. Some notes on a compiled gravimetric map of southern Scandinavia. *Norges geol. undersøk.* no. 215, p. 22—29.
- Guitard, G., Raguin, E. and Sabatier, G.*, 1960. La symétrie des feldspaths potassique dans les gneiss et les granites des Pyrénées orientales. *Bull. Soc. franc. Minér. Crist.* T. 83, pp. 48—62.
- Gustafson, J. K., Buerell, H. C. and Garretty, M. D.*, 1950. Geology of the Broken Hill ore deposit. Broken Hill, N. S. W. Australia. *Geol. Soc. Amer. Bull.* V. 61, pp. 1369—1438.
- Haller, J.*, 1958. Probleme der Tiefentektonik. Bauformen im Migmatit Stockwerk der ostgrönländischen Kalidonien. *Geol. Rund.* Bd. 45, pp. 159—67.
- Härme, M.*, 1954. Structure and stratigraphy of the Mustio area, southern Finland. *Bull. Comm. geol. Finl.* no. 166, pp. 29—48.
- Hedvall, J. A.*, 1952. Einführung in die Festkörperchemie. Braunschweig. Vieweg. 292 p.
- Heier, K. S.*, 1957. Phase relations of potash feldspar in metamorphism. *Jour. Geol.* V. 65, pp. 468—79.
- 1960. Petrology and geochemistry of high-grade metamorphic and igneous rocks on Langøy, Northern Norway. *Norges geol. undersøk.* no. 207, 246 p.

- 1961. Estimation of the chemical composition of rocks. *Amer. Min.* V. 46, pp. 728—33.
- Heiskanen, W. A. and Vening Meinesz, F. A.*, 1958. The earth and its gravity field. New York, McGraw-Hill. 470 p.
- Holtedah, O. and Schetelig, J.*, 1923. Kartbladet Gran. Norges geol. undersøk. no. 97, 46 p.
- Howell, J. V.*, 1957. Glossary of geology. Washington Amer. Geol. Inst. 325 p.
- Isachsen, F.*, 1942. Permiske gangspalter i grunnfjellet vest for Randsfjorden og deres betydelse for utformingen av reliefet. Svensk geogr. årsbok, Lund. Pp. 15—23.
- Karamato, St.*, 1961. Einfluss des geologischen Alters und des tektonischen Drucks auf die Art der Alkalifeldspäte. Instituto Lucas Mallada, Cursos y Conferencias. Fasc. 8, Madrid. pp. 127—30.
- Kennedy, G. C.*, 1955. Some aspects of the role of water in rock melts. In Poldervaart, A., *Editor*. Crust of the Earth. Geol. Soc. Amer. Sp. Paper 62, pp. 489—504.
- Kjerulf, Th.*, 1879. Udsigt over det sydlige Norges geologi. Christiania.
- Kranck, E. H.*, 1957. On folding movements in the zone of the basement. Geol. Rund. Bd. 46, pp. 261—82.
- Kvale, A.*, 1948. Petrologic and structural studies in the Bergsdalen Quadrangle, Western Norway. Part 2. Bergens Museums Arbok. Naturvit. rk. no. 1, 255 p.
- 1953. Linear structures and their relation to movement in the Caledonides of Scandinavia and Scotland. Geol. Soc. London Quart. Jour. V. 107, pp. 51—74.
- Lafitte, P.*, 1953. Étude de la précision des analyses des roches. Bull. Soc. geol. France. Ser. 6. T. 3, pp. 723—45.
- Laves, F.*, 1950. Lattice and twinning of microcline and other potash feldspars. Jour. Geol. V. 58, pp. 548—72.
- Lindström, M.*, 1961. On the significance of B-Intersections in superposed deformation fabrics. Geol. Mag. V. 98, pp. 33—40.
- Magnusson, N., Lundqvist, G. and Granlund*, 1957. Sveriges geologi. Stockholm. Norstedt. 556 p.
- Martin, N. R.*, 1952. The structure of the granite massif of Flamanville, Manche, North-West France. Geol. Soc. London Quart. Jour. V. 108, pp. 311—39.
- Maucher, A.*, 1943. Über geregelte Plagioclaseinschlüsse in Orthoklas (Sanidin). Zeit. Krist. Bd. 105, pp. 82—90.
- Metzger, A.*, 1947. Zum tektonischer Stil von Palingengranit und Marmor in den Svekofenniden in Finland. Bull. Comm. geol. Finl. no. 140, pp. 183—88.
- Neumann, H.*, 1960. Apparent ages of Norwegian minerals and rocks. Norsk geol. tidsskr. Bd. 40, pp. 173—92.
- Nilssen, B.*, 1961. Noen geologiske undersøkelser av Herefossgraniten. University of Oslo thesis.
- Orville, P. M.*, 1960. Powder x-ray method for determination of (Ab-An) content of microcline (abstract). Program 1960 Ann. Meeting Geol. Soc. Amer. p. 171.

- 1962. Alkali ion exchanged between vapor and feldspar phases. *Amer. Jour. Sci.* (in press).
- Pettijohn, F. J.*, 1957. *Sedimentary rocks*. 2nd edition. New York, Harper, 718 p.
- Poldervaart, A.*, 1955. Zircons in rocks. I. *Sedimentary rocks. Amer. Jour. Sci.* V. 253, pp. 33—61.
- Ramberg, H.*, 1952. *The origin of metamorphic and metasomatic rocks*. Chicago. U. of Chicago Press. 317 p.
- 1955. Natural and experimental boudinage and pinch-and-swell structures. *Jour. Geol.* V. 63, pp. 512—26.
- 1956. Pegmatites in West Greenland. *Geol. Soc. Amer. Bull.* V. 67, pp. 185—214.
- Ramsay, J. G.*, 1960. The deformation of early linear structures in areas of repeated folding. *Jour. Geol.* V. 68, pp. 75—93.
- 1962. Geometry and mechanics of formation of "similar" type folds. *Ibid.* V. 70, pp. 309—27.
- Rao, S. V. L.*, 1960. X-ray study of potash feldspar of the contact metamorphic zones at Gjelleråsen, Oslo. *Norsk geol. tidsskr.* Bd. 40, pp. 1—12.
- Reynolds, D. L.*, 1946. The sequence of geochemical changes leading to granitization. *Quart. Jour. Geol. Soc. London.* V. 102, pp. 389—446.
- Rosenqvist, I. Th.*, 1950. Some investigations in the crystal chemistry of silicates. II. The orientation of perthite lamellae in feldspars. *Norsk Geol. Tidsskr.* Bd. 28, pp. 192—98.
- 1952. The metamorphic facies and the feldspar minerals. Bergen museums yearbook, *Naturvid.* no. 1—5, 108 p.
- Sander, B.*, 1948. Einführung in die Gefügekunde der geologischen Körper, Teil I. Vienna, Springer. 215 p.
- Schermerhorn, L. J. G.*, 1956. Petrogenesis of a porphyritic granite east of Oporto (Portugal). *Tschermaks. Min. petr. Mitt.*, F. 3. Bd. 4, pp. 73—115.
- Sederholm, J. J.*, 1907. Om granit och gneis. *Bull. Comm. geol. Finl.* no. 23, 110 p.
- 1923. On migmatites and associated pre-Cambrian rocks. Part I: The Pelling region. *Ibid.* no. 58, 153 p.
- Sen, S. K.*, 1959. Potassium content of natural plagioclases and the origin of antiperthites. *Jour. Geol.* V. 67, pp. 479—95.
- Shand, S. J.* 1950 a. Rock-magma and rock-species. *Amer. Min.* V. 35, pp. 922—30.
- 1950 b. *Eruptive rocks*. London, Murphy. 488 p.
- Sitter, L. U. de*, 1958. Boudins and parasitic folds in relation to cleavage and folding. *Geologie en Mijnbouw.* V. 20, pp. 277—86.
- Smithson, S. B.*, 1962. Symmetry relations in alkali feldspars of some amphibolite-facies rocks from the Southern Norwegian Precambrian. *Norsk geol. tidsskr.* Bd 42 A, Feldspar supplement.
- 1963. Granite studies: I. A gravity investigation of two Precambrian granites in South Norway. *Norges geol. undersøk.* no. 214 b, pp. 53—140.
- Strand, T.*, 1943. Et gneiss-amfibolitt-kompleks i grunnfjellet i Valdres. *Norges geol. undersøk.* no. 159, 56 p.

- 1944. Structural petrology of the Bygdin conglomerate. *Norsk geol. tidsskr.* Bd. 24, pp. 14—31.
- 1949. On the gneisses from a part of the north-western gneiss area of Southern Norway. *Norges geol. undersøk.* no. 173, 45 p.
- 1954. Aurdal, beskrivelse til det geologiske gradteigskart. *Ibid.* no. 185 70 p.
- Turner, F. J.*, 1957. Lineation, symmetry, and internal movement in monoclinic tectonite fabrics. *Geol. Soc. Amer. Bull.* V. 68, pp. 1—18.
- Tuttle, O. F.*, 1952. Origin of the contrasting mineralogy of extrusive and salic plutonic rocks. *Jour. Geol.* V. 60, pp. 107—24.
- and *Bowen, N.*, 1958. Origin of granite in the light of experimental studies in the system $\text{NaAlSi}_3\text{O}_8\text{-KAlSi}_3\text{O}_8\text{-SiO}_2\text{-H}_2\text{O}$. *Geol. Soc. Amer. Mem.* 74, 152 p.
- Waard, D. de*, 1949. Tectonics of the Mt. Aigoual pluton in the southern Cevennes, France. Pt. I and II. *Kon. Nederlandsche Akad. van Wetenschapen.* V. 52, pp. 389—402 and 539—50.
- Waters, A. C.*, 1948. Discussion. In Gilluly, J., *Editor*. Origin of granite. *Geol. Soc. Amer. Mem.* 28, pp. 104—08.
- and *Krauskopf, K.*, 1941. Protoclastic border of the Colville batholith. *Geol. Soc. Amer. Bull.* V. 52, pp. 1355—1417.
- Wegmann, C. E.*, 1929. Beispiele tektonischer Analysen des Grundgebirges in Finnland. *Bull. Comm. geol. Finl.* no. 87, pp. 98—127.
- Weiss, L. E.*, 1954. A study in tectonic style. California Univ., Dept. Geol. Sci. *Publ.* V. 30, pp. 1—102.
- 1955. Fabric analysis of a triclinic tectonite and its bearing on the geometry of flow in rocks. *Amer. Jour. Sci.* V. 253, pp. 225—36.
- 1959. Geometry of superposed folding. *Geol. Soc. Amer. Bull.* V. 70, pp. 91—106.
- and *McIntyre, D. B.*, 1957. Structural geometry of Dalradian rocks at Loch Seven, Scottish Highlands. *Jour. Geol.* V. 65, pp. 575—602.
- Wenk, E.*, 1937. Zur Genese der Bändergneiss von Ornö Huvud. *Bull. Geol. Inst. Upsala.* V. 26, pp. 53—90.
- Whitten, E. H. J.*, 1961. Quantitative areal modal analysis of granitic complexes. *Geol. Soc. Amer. Bull.* V. 72, pp. 1331—60.
- Winkler, H. G. F.*, 1961. Genesen von Graniten und Migmatiten auf Grund neuer Experimente. *Geol. Rund.* Bd. 51, pp. 347—64.
- Yoder, H. S., Stewart, D. B. and Smith, J. R.*, 1957. Ternary feldspars. *Geophys. Lab. Ann. Rpt. Director for 1956—57*, pp. 206—214.

PLATES

2—12

Plate 2.

Fig. 1. *Metaconglomerate (Sp 612 A) showing rounded grains of microcline perthite in a groundmass of quartz. Microcline grains have dusty borders that suggest alteration (weathering?). A composite grain of microcline and plagioclase appears in the left center. Austvoll, Hallingdal (25.8, 1—19.8). $\times 25$. All microphotographs are with crossed nicols.*

Metakonglomerat (Sp 612 A), som viser rundete korn av mikroklin perthit i en kvartsgrunnmasse. Mikroklin-korn har uklare grenser, som tyder på omvandling. Et sammensatt korn av mikroklin og plagioklas kan ses i midten til venstre. Austvoll, Hallingdal (25.8, 1—19.83 $\times 25$. Alle mikrofotografier tatt, er med kryssete nicoler.

Fig. 2. *Plagioclase porphyroblast containing K-feldspar. The K-feldspar patches tend to follow the (010) cleavage. The K-feldspar is indistinctly twinned. X-ray patterns and optic angles indicate that this K-feldspar is of intermediate and/or variable obliquity. The section through the K-feldspar patches is oblique. Quartz-dioritic gneiss (Sp 10). Simensrud farm, Ådal (28.8, 0—41.4). $\times 78$.*

Plagioklas porfyroblaster med K-feltspat. K-feltspatflekkene har en tendens til å følge (010) spaltbarheten. K-feltspaten har utydelig tvillingdannelse. Røntgen-diagrammer og optiske vinkler tyder på at denne k-feltspat er av interdemiær og/eller varierende triklinitet. Snittet gjennom K-feltspatflekkene er skjevt. Kvartsdioritsk gneis (Sp 10). Simensrud gård, Ådal (28.8, 0—41.4. $\times 78$.

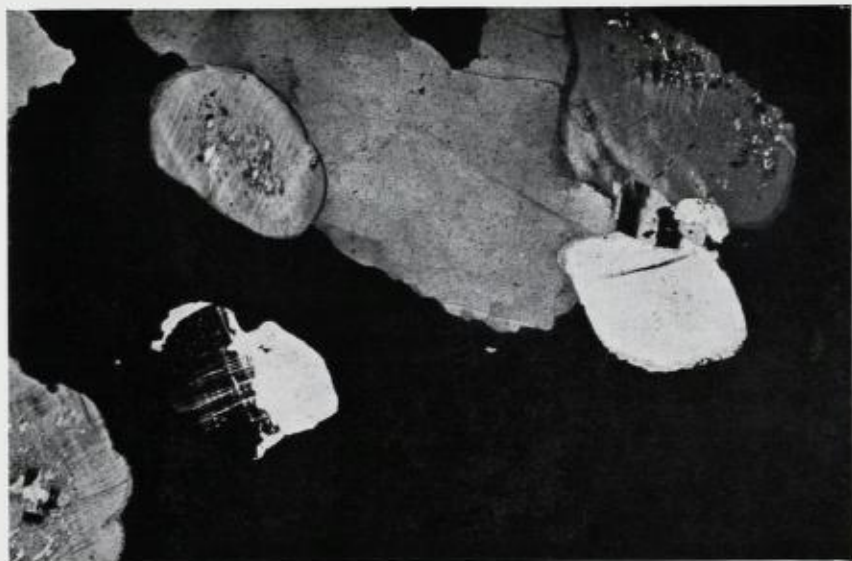


Plate 3.

Fig. 1. *K-feldspar porphyroblast from the same augen gneiss as below (Sp 224 A). Orthoclase and slightly ordered K-feldspar occur in this rock. Incipient twinning is visible along zones and around the borders in the porphyroblast. These zones appear to be fractures, but they were recognizable as plagioclase septa in another rock from a similar occurrence (Fig. 2, Plate 12). K-feldspar is microperthitic. Signs of deformation are lacking. $\times 25$.*

K-feltpat porfyroblast fra samme øyegneis som nedenfor (Sp 224 a). Ortoklas og svakt ordnet K-feltpat forekommer i denne bergart. Begynnende tvillingdannelse er synlig langs soner og rundt kantene i porfyroblastene. Disse soner ser ut til å være sprekker, men de kunne identifiseres som tynne plagioklasplater i en annen prøve fra en lignende forekomst (Fig. 2, Plate 12). K-feltpaten er mikroperthitisk. Tegn på deformering mangler. $\times 25$.

Fig. 2. *Antiperthitic plagioclase porphyroblast (right center) from an augen gneiss (Sp 224 A). K-feldspar in the patches exhibits orthoclase optics ($2V^\circ = 58^\circ$). K-feldspar comprises a larger proportion of the plagioclase grain than in Fig. 2, Plate 1. Note the unstrained appearance of the quartz grains (q). Near Gulsvik, Hallingdal (23.2, 1—04.0). $\times 25$.*

Antiperthitisk plagioklas porfyroblast (i midten til høyre) fra en øyegneis (Sp 224 A). K-feltpaten i flekkene viser ortoklas optikk. ($2V^\circ = 58^\circ$). K-feltpaten omfatter en større del av plagioklaskornet enn i Fig. 2, Plate 1. Legg merke til kvartskornenes upåvirkete utseende (q). Nær Gulsvik, Hallingdal (23.2, 1—04.0). $\times 25$.





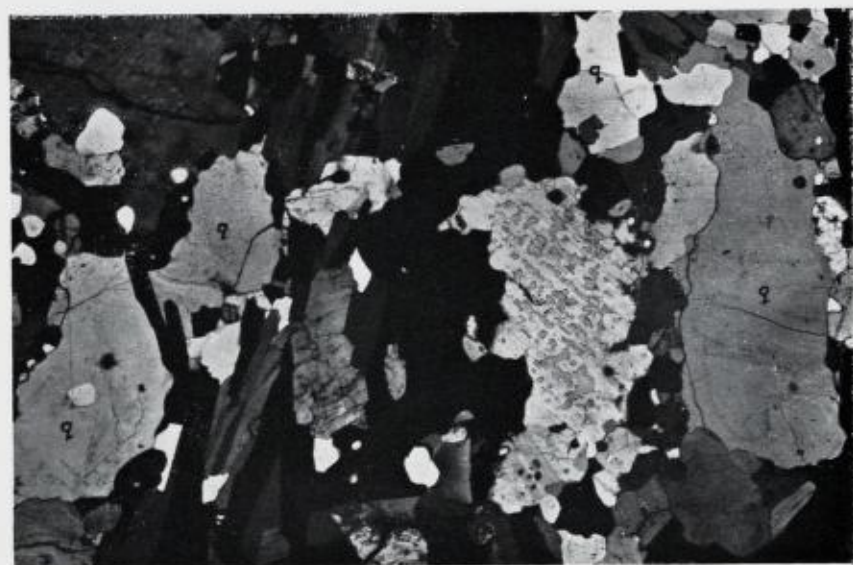


Plate 4.

Fig. 1. *Augen gneiss (Sp 102 A) showing different types of K-feldspar (3 grains in the center). (1) has two perpendicular directions of perthite films and is untwinned. (2) has no visible perthite and is indistinctly twinned. Plagioclase is heavily sericitized in places. Lindelia, Hedalen (32.8, 0-53.2). $\times 25$.*

Oyegneis (Sp 102 A) viser forskjellige typer K-feltspat (3 korn i midten). (1) har filmperthiter i to retninger loddrett på hverandre og ingen tvillingdannelse. (2) har en filmperthitretning og ikke tvillinger. (3) har ingen synlig perthit og har utydelig tvillingdannelse. Plagioklasen er noen steder sterkt sericitisert. Lindelia, Hedalen (32.8, 0-53.2). $\times 25$.

Fig. 2. *Feldspar augen from the same augen gneiss (Sp 102 A). Mesoperthitic intergrowth is interpreted as an advanced stage of the process represented by the antiperthites on the previous two plates. Plagioclase is heavily sericitized in scattered patches including some in the mesoperthitic augen. $\times 25$.*

Feltspatøye fra den samme øyegneis (Sp 102 A). Mesoperthitisk sammenvoksing av plagioklas (An 35) og K-feltspat. Denne sammenvoksing er tolket som en videre utvikling av den prosess som er representert ved antiperthitene på de to foregående plater. Plagioklasen er sterkt sericitisert i spredte flekker, innbefattet noen steder i de mesoperthitiske øyne. $\times 25$.

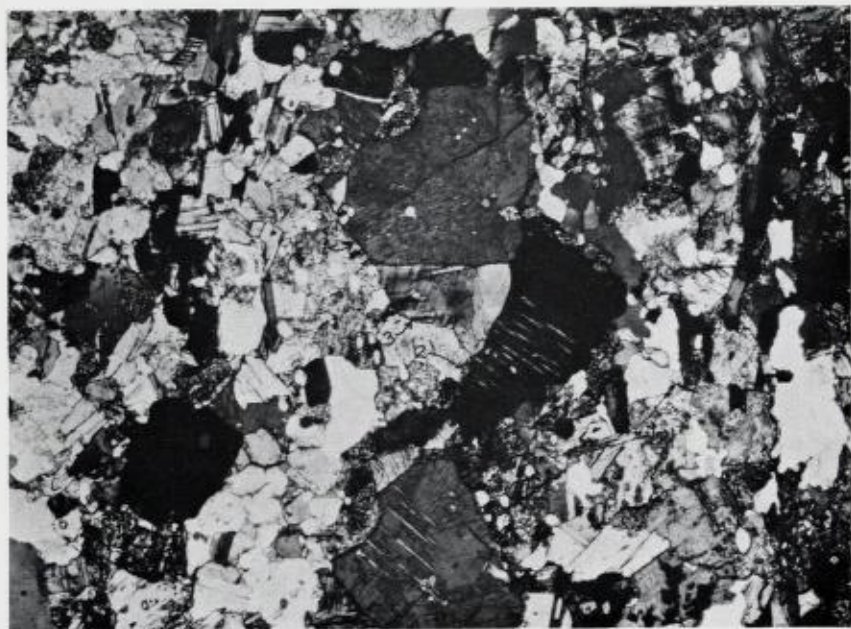


Plate 5.

Fig. 1. *Megacryst of Carlsbad-twinned microcline perthite in porphyric granite (Sp 413 A). Plagioclase inclusions in the megacryst are oriented parallel to or normal to (010) of the host. Lower twin individual shows grid twinning where there are no perthite films and no twinning where there are films (at both ends of the individual). Quartz sheared and plagioclase sericitized. Near Sandvatn (26.1, 0—52.5). × 25.*

Megakrystall av mikroklin perthit med Karlsbader-tvillinger i porfyrisk granitt (Sp 413 A). Plagioklasinneslutninger i megakrystallen er orientert parallelt med eller normalt på vertens (010). Den nedre tvilling viser rutenett-tvillinger, hvor det ikke er perthitfilm, og ingen tvillinger hvor det er filmer (i begge ender av krystallen). Kvartsen er utgnidd og plagioklasen sericitisert. Nær Sandvatn (26.1, 0—52.5). × 25.

Fig. 2. *Heavy unevenly distributed flame perthite in microcline from porphyric granite (Sp 413 A). Straight border of flame perthite (upper right center) suggests that two microcline grains may have coalesced here. This configuration would be produced if two microcline grains forming flame perthite grew together (similar to Fig. 2, Plate 7). Other flame perthite is adjacent to a heavily sericitized plagioclase grain. Intented borders between plagioclase and microcline. × 78.*

Grov, ujevnt fordelt flammepertit i mikroklin fra porfyrisk granitt (Sp 413 A). Flammepertitenes rette grense (øverst til høyre i midten) tyder på at to mikroklinkorn kan ha smeltet sammen her. Dette bilde ville oppstå hvis to mikroklinkorn med flammepertit vokste sammen (på samme måte som fig. 2, plate 7). Andre flammepertit hiter støter opp til en sterkt sericitisert plagioklas. Sagtakkete grenser mellom plagioklas og mikroklin. × 78.



Plate 6.

Fig. 1. *Granitic texture in fine-grained granite (Sp 399 B). Subhedral, sericitized plagioclase, subhedral to anhedral microcline, and interstitial, anhedral quartz. Some clear sodic rims on the plagioclase (upper left). Near Fisketjern, Storrustefjell (28.2, 0—58.3). × 25.*

Granitisk tekstur i finkørnet granitt (Sp 399 B). Subhedral, sericitisert plagioklas, subhedral til anhedral mikroklin og anhedral kvarts i mellomrommene. Noen klare, natriumrike kanter på plagioklasen (øverst til venstre). Nær Fisketjern, Storrustefjell (28.2, 0—58.3). × 25.

Fig. 2. *Heavy, unevenly developed flame perthite in a microcline megacryst. The heaviest plagioclase "flames" occur next to plagioclase grain (upper right). The plagioclase "flames" follow and are continuous with a train of groundmass plagioclase inclusions (p) running through the microcline megacryst. The plagioclase inclusions and the perthitic plagioclase extinguish simultaneously. × 78.*

Grov, ujevnt utviklet flammepertit i en mikroklin megakrystall. De groveste plagioklas-"flammer" finnes nær en plagioklas (øverst til høyre). Plagioklas-"flammene" følger og står i forbindelse med en rekke inneslutninger av grunnmasseplagioklas (B), som går gjennom mikroklinkrystallen. Plagioklas-inneslutningene og den perthitiske plagioklas slukker likt. × 78.



Plate 7.

Fig. 1. *Plagioclase inclusions (p) in microcline that are continuous with the plagioclase films. Plagioclase in the inclusions extinguishes simultaneously with the plagioclase in the perthite films. Perthite appears to be intermediate between film perthite and flame perthite. Trevaskollen (35.2, 1—39.8). × 78.*

Plagioklaseinneslutninger (p) i mikroklin, som går over i plagioklasfilmperthit. Plagioklasen i inneslutningene har samme utslukning som plagioklasen i perthitfilmene. Perthiten ser ut til å være en mellomting mellom filmperthit og flammepertthit. Trevasskollen (35.2, 1—39.8). × 78.

Fig. 2. *Flame perthite strongly developed next to a sericitized plagioclase grain. Sharply indented border between the plagioclase and microcline perthite. The same fine-grained granite (Sp 399 B) that has a granitic texture. (Fig. 1, Plate 6). × 78.*

Flammepertthit, sterkt utviklet, nær en sericitisert plagioklas. Skarpt sagtakket grense mellom plagioklas og mikroklinperthit. Den samme finkornete granitt (Sp 399 B), som har en granittisk tekstur. (Fig. 1, plate 6). × 78.



Plate 8.

Fig. 1. *L-shaped plagioclase inclusion in microcline megacryst in porphyric Adal granite (Sp 271 A). An irregular plagioclase appendage on the L-shaped inclusion just inside the border of the megacryst (lower right corner) is in optical continuity with this inclusion. The L-shaped inclusion forms a major part of an incomplete plagioclase rim that is now enclosed within the megacryst. The quartz (q) is sheared. Holmtjern (19.5, 0—41.6). × 25.*

L-formet plagioklasinneslutning i mikroklin megakrystall i porfyrisk Adalsgranitt (Sp 271 A). En uregelmessig plagioklas utvekst like innenfor megakrystallens grense (nedre høyre hjørne) stemmer optisk overens med denne inneslutning. Den L-formete inneslutning utgjør en større del av en ukomplet plagioklas-rand, som nå er innesluttet i megakrystallen. Kvartsen (q) er knust. Holmtjern (19.5, 0—41.6). × 25.

Fig. 2. *Incomplete rim of plagioclase inclusions in a microcline megacryst in porphyric Adal granite (Sp 312). A plagioclase grain from the groundmass projects through the rim of inclusions. Huskebudalen (21.8, 0—45.2). × 25.*

Ufullstendig rand av plagioklasinneslutninger i en mikroklin megakrystall i porfyrisk Adalsgranitt (Sp 312). Et plagioklaskorn fra grunnmassen stikker frem gjennom randen av inneslutninger. Huskebudalen (21.8, 0—45.2). × 25.



Plate 9.

Fig. 1. *Sheared porphyric Heddal granite (Sp 175 A) from near the center of the granite. Quartz (q) is sheared and granulated; plagioclase is bent and fractured. Quartz-filled fractures in plagioclase grain (lower center). Åslibru, Hedalen (38.2, 1—08.0). × 25.*

Knaust porfyrisk Heddal-granitt (Sp 175 A) fra nær granittens sentrum. Kwarts (q) er utgnidd og granulert; plagioklasen er bøyd og oppsprukket. Kwartsfylte sprekker i plagioklas (nederst til høyre). Åslibru, Hedalen (38.2, 1—08.0). × 25.

Fig. 2. *Oscillatory zoned plagioclase porphyroblast in a biotite-gneiss inclusion (Sp 514 D) from the "tail" of the Adal granite. At least 8 zones, which follow the euhedral crystal outlines, can be counted. The porphyroblast has an irregular poikiloblastic border. Bergsund, Adal (19.6, 0—34.2). × 25.*

Plagioklas porfyroblast med oscillerende soning i en biotitgneisneslutning (Sp 5141) fra Adal-granittens "hale". Minst 8 soner som følger den euhedrale krystallbegrensning, kan telles. Porfyroblastene har en uregelmessig poikiloblastisk grense. Bergsund, Adal (19.6, 0—34.2). × 25.



Plate 10.

Fig. 1. *Plagioclase mantling a microcline grain in a biolite gneiss inclusion (Sp 514 D) — Rapakivi texture. This is from the same inclusion as Fig. 2, Plate 9. × 25.*

Plagioklas som omgir et mikroklinskorn i en biotitgneisneslutning — Rapakivitekstur. Fra samme inneslutning som fig. 2, plate 9. × 25.

Fig. 2. *A microcline porphyroblast in the same inclusion (Sp 514 D) which appears to be incorporating plagioclase grains from the groundmass (arrows point to plagioclase grains). These plagioclase grains are oriented so that their longest dimension is parallel with the adjacent microcline face and so that their (010) face is either parallel to or normal to (010) of the microcline porphyroblast. Completely enclosed oriented plagioclase inclusions are visible. The numerous plagioclase grains in and adjacent to the porphyroblast extinguish simultaneously. × 25.*

En mikroklin porfyroblast i samme inneslutning (Sp 514 D), som ser ut til å oppta i seg plagioklaskorn fra grunnmassen (pilene peker på plagioklaskorn). Disse plagioklaskorn er orientert slik at deres lengderetning er parallell med den tilstøtende mikroklinflate, og slik at deres (010) flate enten er parallell med eller normal på mikroklinporfyroblastens (010). Fullstendig innesluttede, orienterte plagioklaskorn kan sees. De tallrike plagioklaskorn i porfyroblasten og like utenfor den har samme utslukning. × 25.

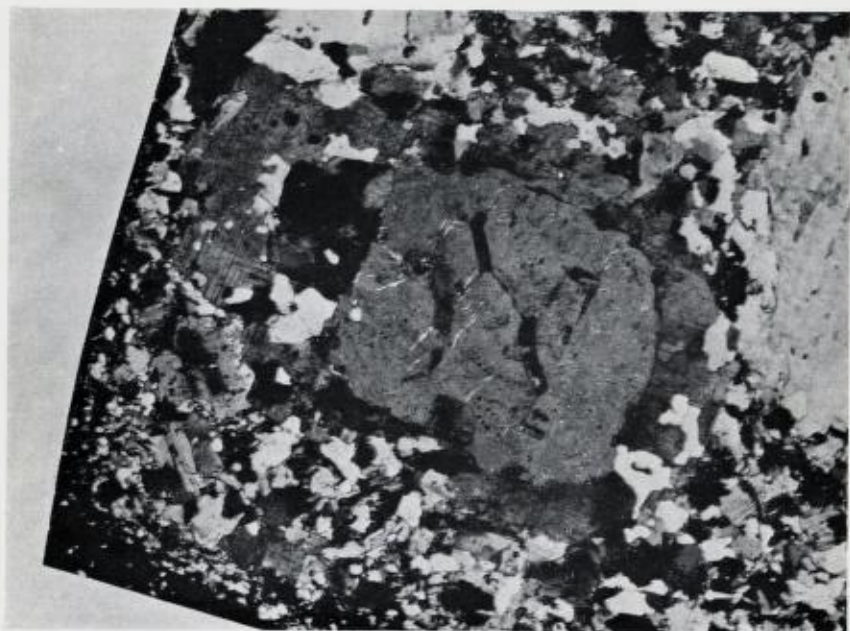


Plate 11.

Fig. 1. *Fine-grained Heddal granite (Sp 80) that exhibits a granoblastic texture. Screens and pockets of sericitized plagioclase between microcline grains are marked by arrows. Quartz is granulated in places and strained. Vidalen (31.4, 55.4). × 25.*

Finkornet Heddal-granitt (Sp 80), som viser granoblastisk tekstur. Nett og lommer av sericitisert plagioklas mellom mikroklinkorn er merket med piler. Kvartsen er granulert enkelte steder og presset. Vidalen (31.4, 55.4). × 25.

Fig. 2. *Sill of sheared medium-grained granite (Sp 292 B). Feldspar grains are drawn out and fractured; quartz (q) is granulated and drawn out into leaves. Vikertjell (28.5, 45.7). × 25.*

Gang av middelskornet "sheared" granitt (Sp 292 B). Feltspatkornene er dradd ut og oppsprukket, kvartsen (q) er granulert og dradd ut til blad. Vikertjell (28.5, 0—45.7). × 25.

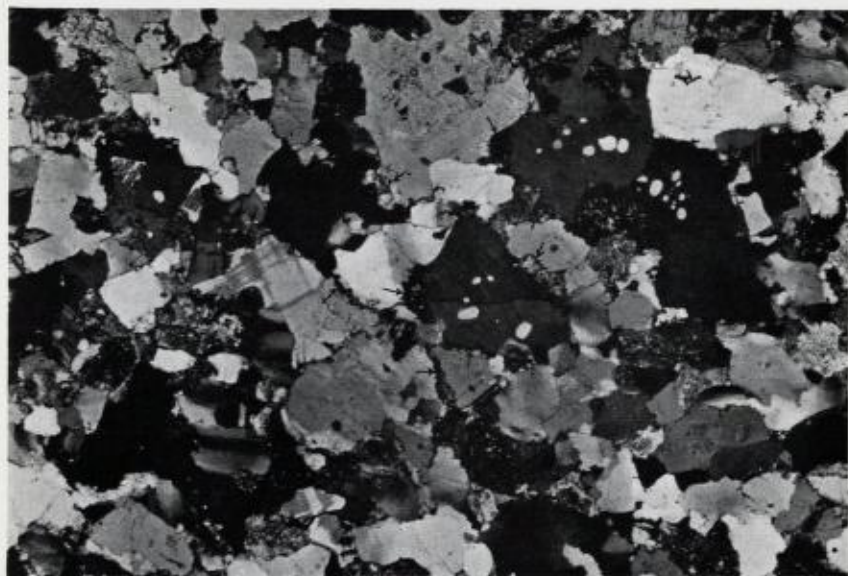


Plate 12.

Fig. 1. *K-feldspar megacrysts in porphyric granite (Sp 509 C) from 10 m inside the north contact of the Ådal granite. Grain (1) exhibits microcline optics ($Z \wedge b = 15^\circ$, $2V_x = 83^\circ$). Grain (2) exhibits the optics of an intermediate microcline of variable obliquity (highly undulatory extinction, $2V_x = 64^\circ$ and 72°). Plagioclase seams mark the boundary between the two grains. The faint twinning in the center of grain 2 (arrows) occurs along thin films of sericitized plagioclase. Quartz is sheared out and granulated. Near Sperillen, Ådal (22.6, 0—38.1). $\times 25$.*

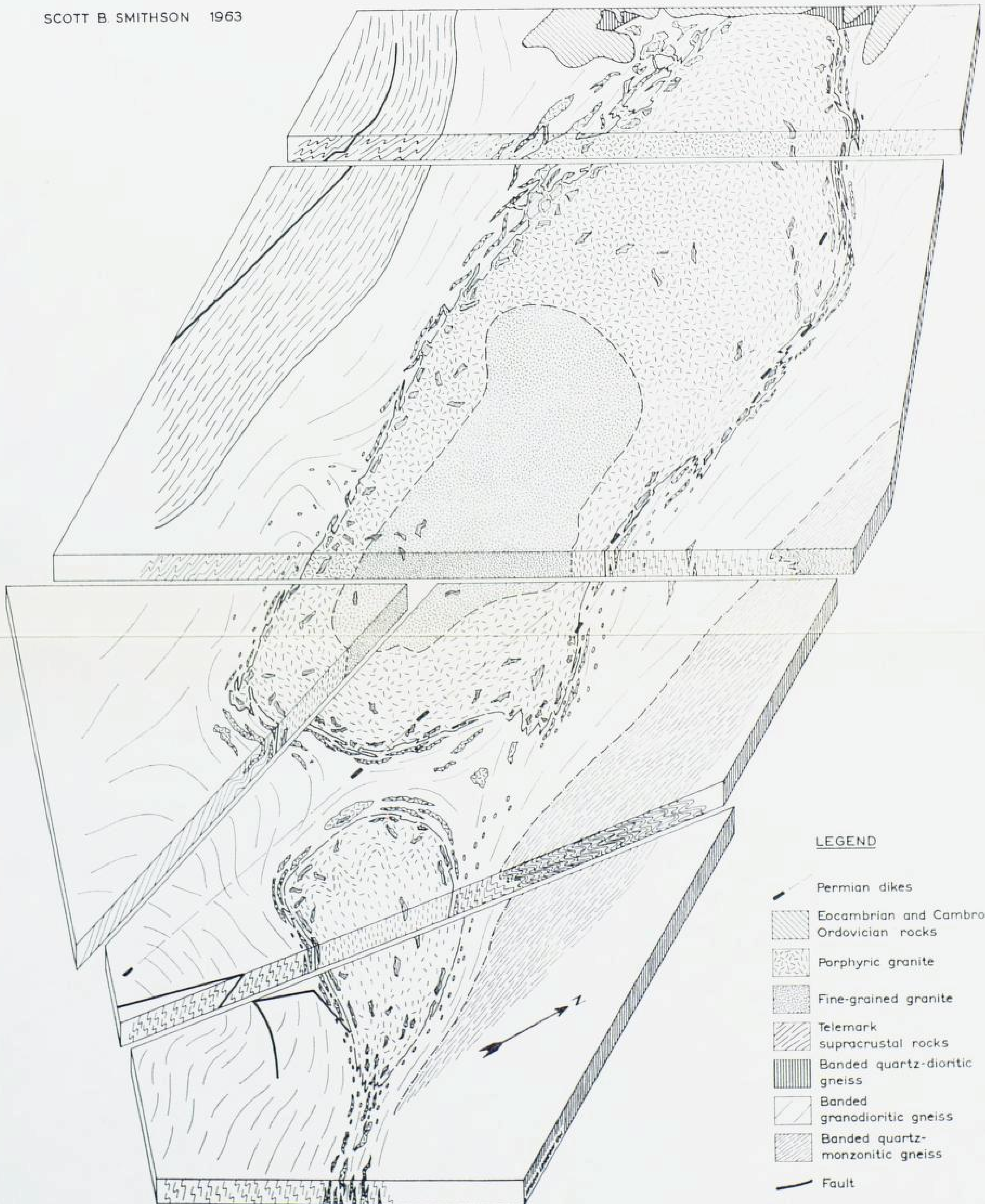
K-feltspat megakrystaller i porfyrisk granitt (Sp 509 C) fra 10 m innenfor Adalgranittens nordgrense. Korn (1) viser mikroklinoptikk ($Z \wedge b = 15^\circ$, $2V_x = 83^\circ$). Korn (2) viser optiske egenskaper som er intermediær mikroklin med varierende triklinitet (sterkt undulerende utslukning, $2V_x = 64^\circ$ og 72°). Plagioklas markerer grensen mellom de to korn. Den svake tvillingdannelse i midten av korn (2) (pil) forekommer langs tynne filmer av sericitisert plagioklas. Kvartsen er utgnidd og granulert. Nær Sperillen, Ådal (22.6, 0—38.1). $\times 25$.

Fig. 2. *Orthoclase porphyroblast from an augen gneiss enclosing quartz (q) and plagioclase (p). Beginning twinning in the orthoclase is localized along slivers of plagioclase which are commonly contiguous with larger plagioclase inclusions. Hornnes near Evje in Sørlandet. $\times 25$.*

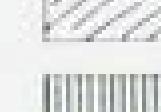


Ortoklas porfyroblast fra en øyegneis med kvarts (q) og plagioklas (p) inneslutninger. Begynnende tvillingdannelse i ortoklasen finnes langs tynne plagioklasårer, som i alminnelighet har forbindelse med større plagioklasinneslutninger. Hornnes ved Evje, Sørlandet. $\times 25$.

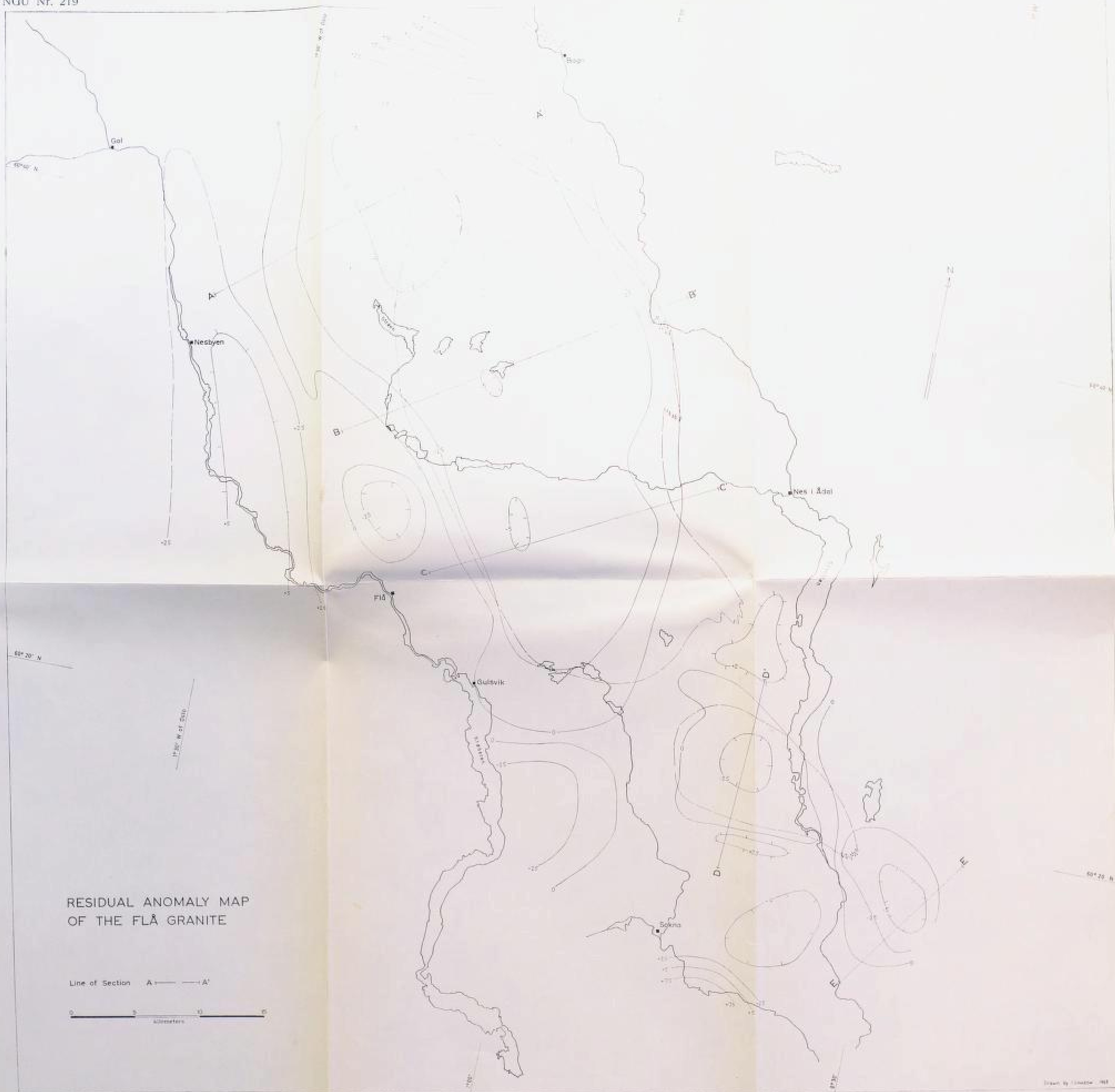
Block Diagram of the Flå Granite

SCOTT B. SMITHSON 1963



LEGEND

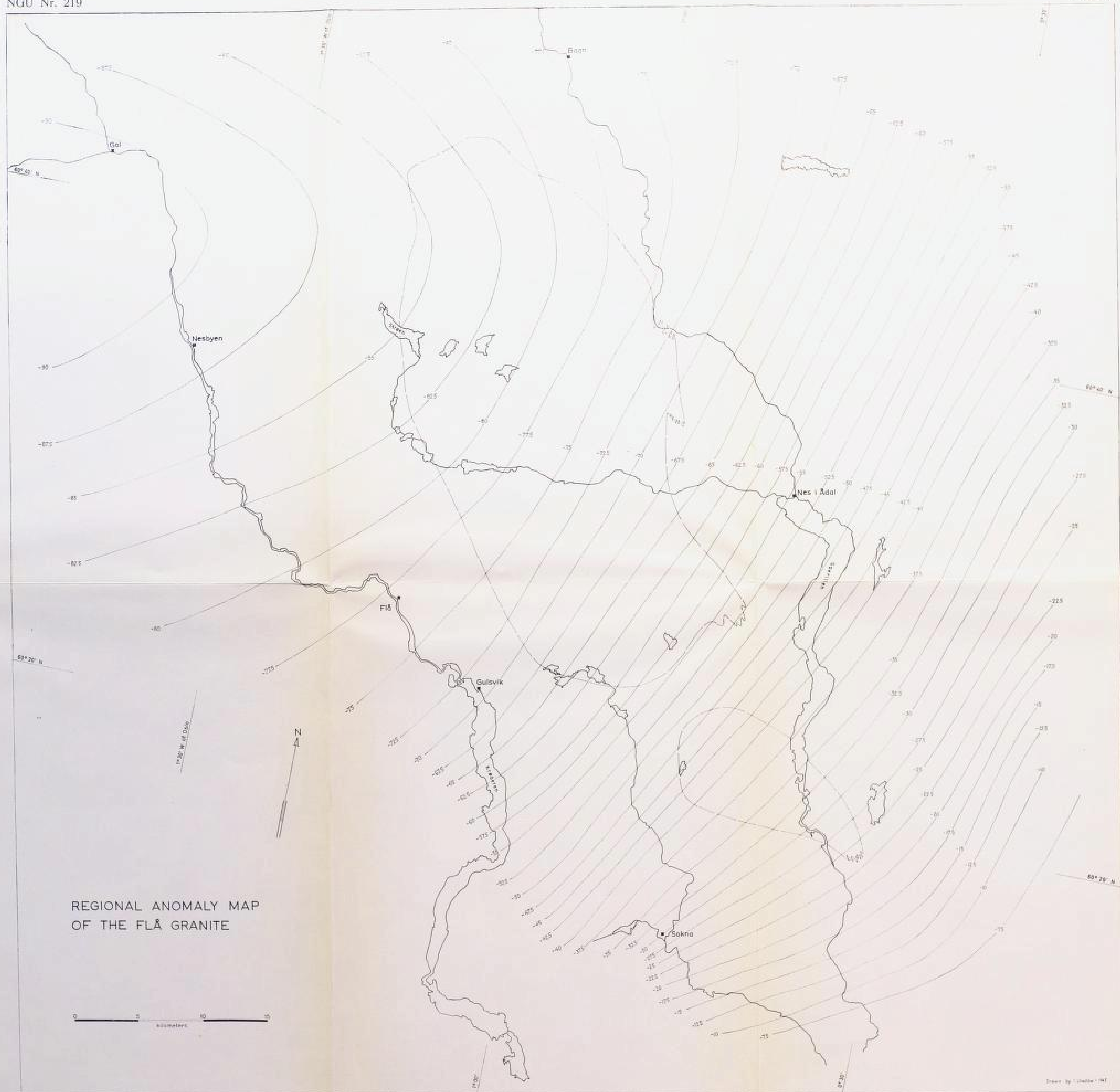
-  Permian dikes
-  Eocambrian and Cambro-Ordovician rocks
-  Porphyritic granite
-  Fine-grained granite
-  Telemark supracrustal rocks
-  Banded quartz-dioritic gneiss
-  Banded granodioritic gneiss
-  Banded quartz-monzonitic gneiss
-  Fault

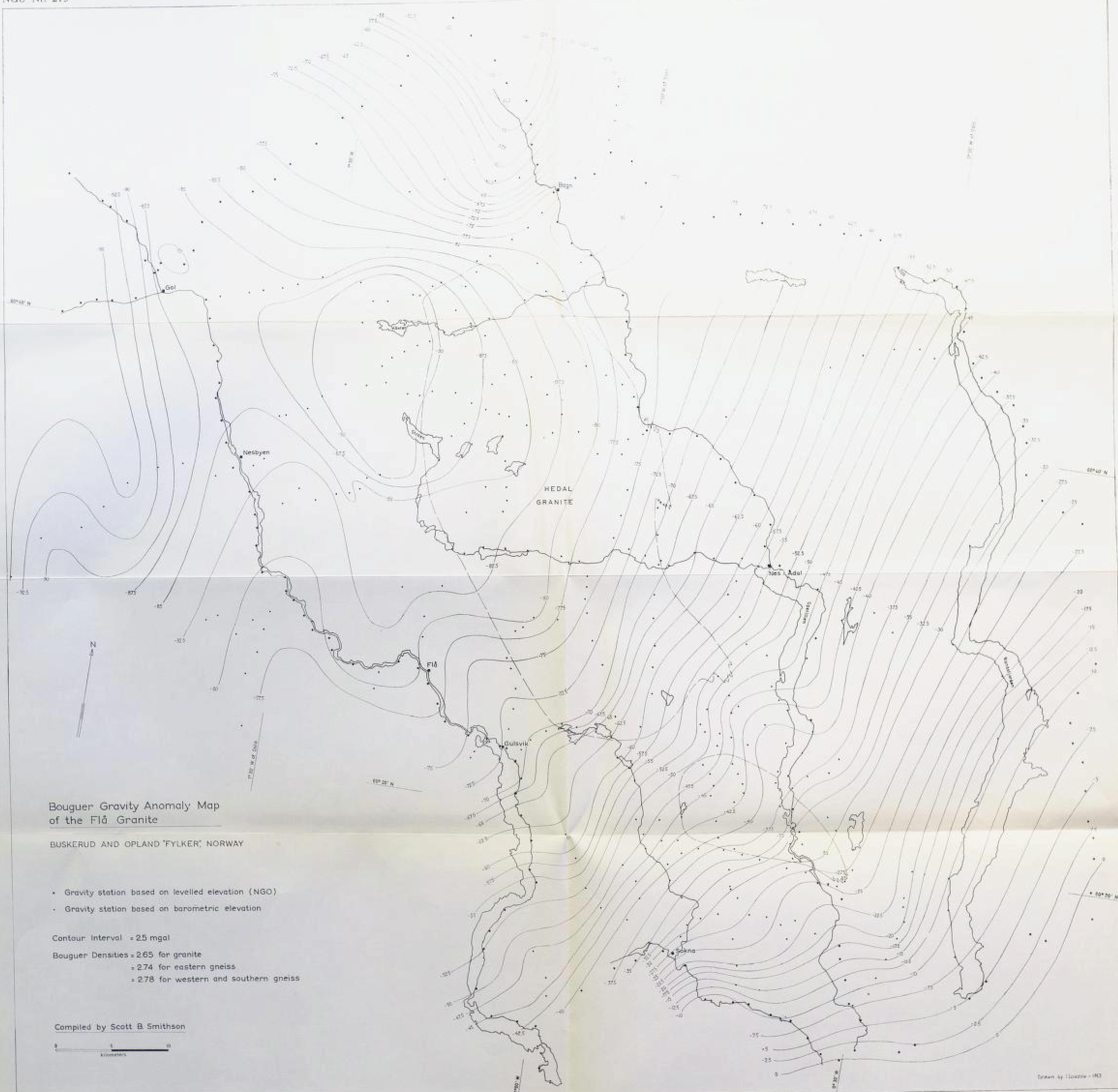


RESIDUAL ANOMALY MAP
OF THE FLÅ GRANITE

Line of Section A — A'

0 5 10 15
kilometers





Bouguer Gravity Anomaly Map
of the Flå Granite

BUSKERUD AND OPLAND "FYLKER" NORWAY

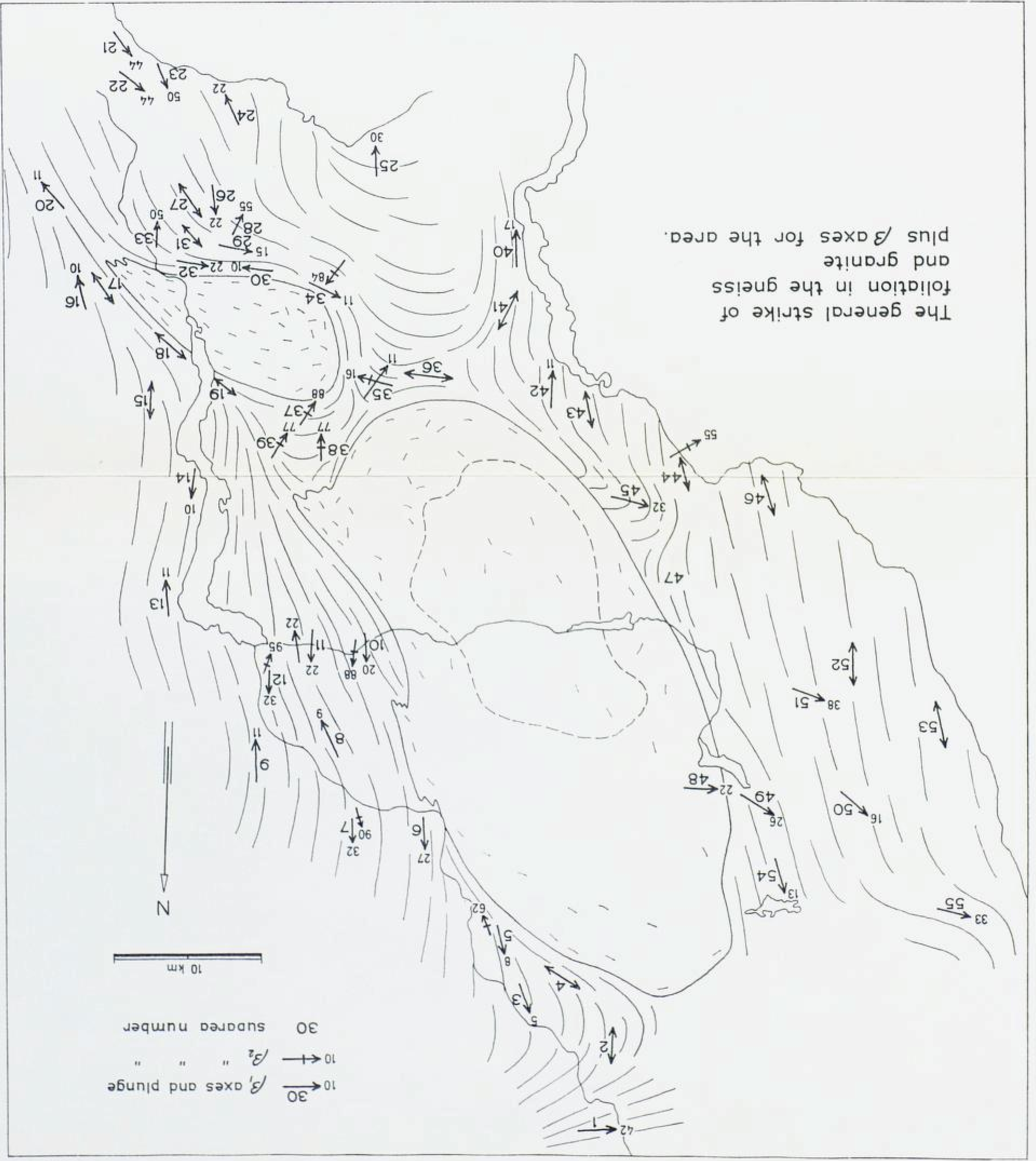
- Gravity station based on levelled elevation (NGO)
- Gravity station based on barometric elevation

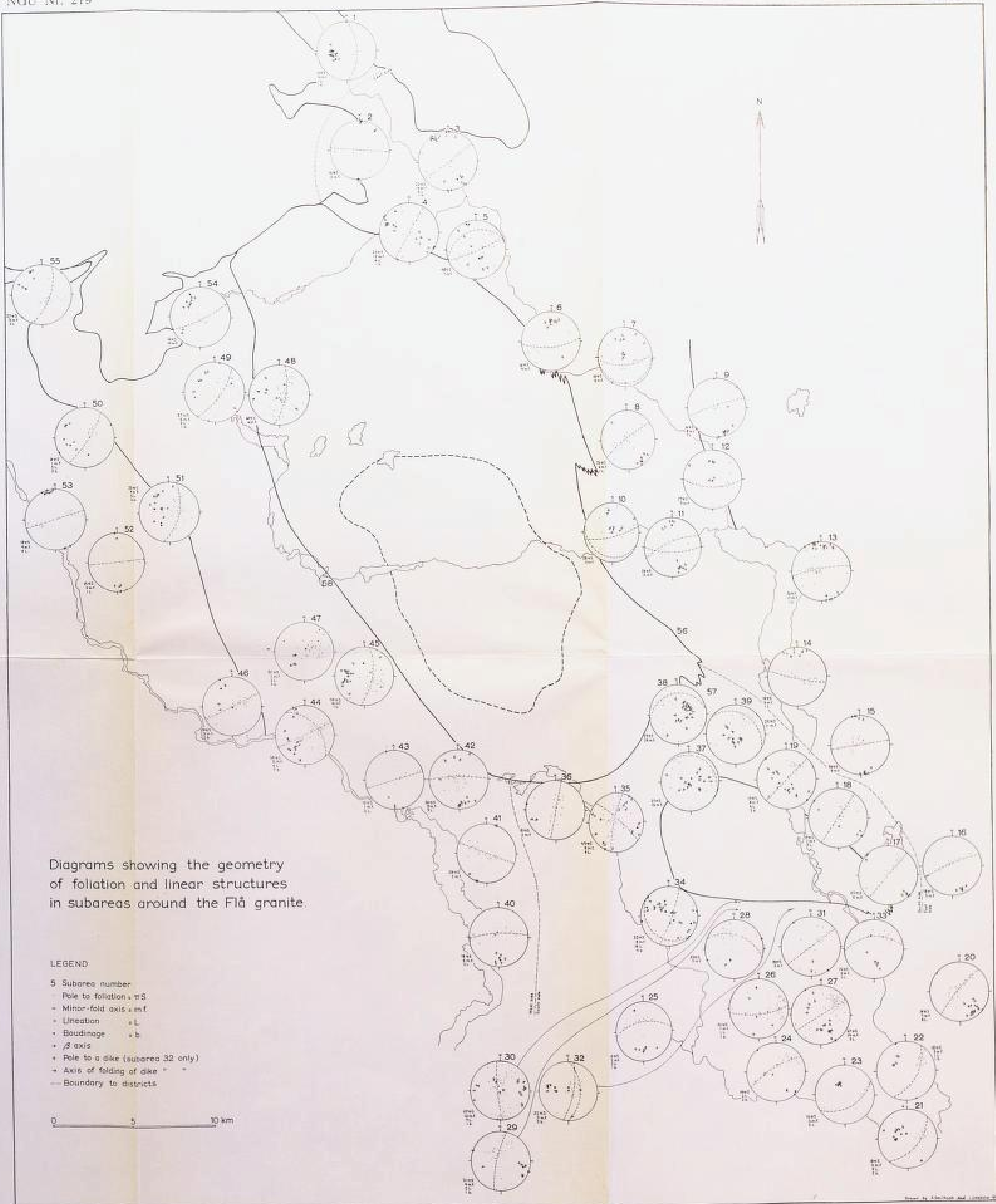
Contour Interval = 25 mgal

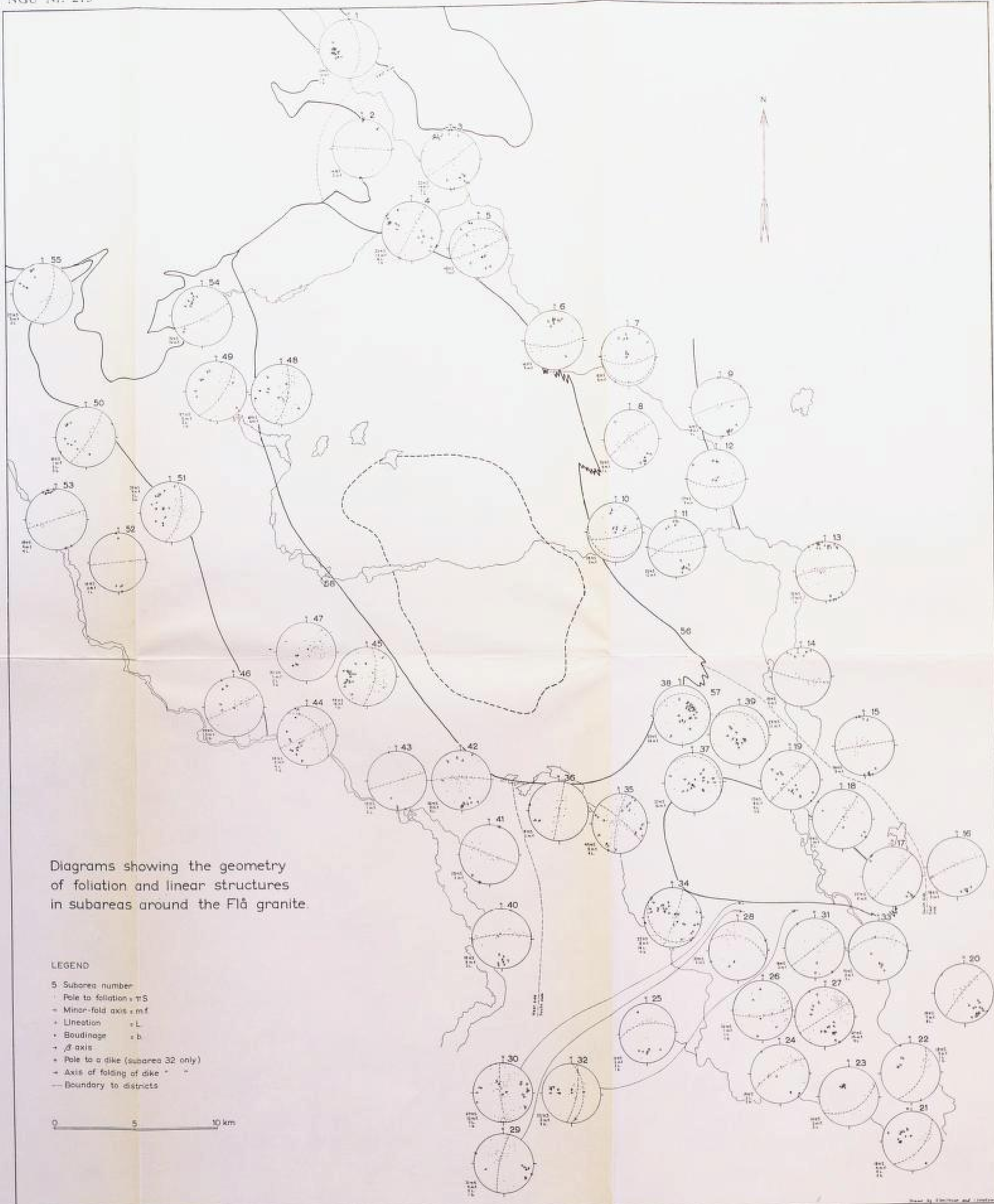
Bouguer Densities = 2.65 for granite
= 2.74 for eastern gneiss
= 2.78 for western and southern gneiss

Compiled by Scott B. Smithson

0 5 10
kilometers







Diagrams showing the geometry of foliation and linear structures in subareas around the Flå granite.

LEGEND

- S Subarea number
- Pole to foliation = S
- Minor-fold axis = mf
- Lineation = L
- Boudinage = b
- β axis
- Pole to a dike (subarea 32 only)
- Axis of folding of dike
- - - Boundary to districts

0 5 10 km

